
Two-Loop Corrections to Electroweak Precision Observables in Two-Higgs-Doublet-Models

Stephan Hossenberger



Max-Planck-Institut für Physik
(Werner-Heisenberg-Institut)



Technischen Universität München
Max-Planck-Institut für Physik
(Werner-Heisenberg-Institut)

Two-Loop Corrections to Electroweak Precision Observables in Two-Higgs-Doublet-Models

Stephan Hessenberger

Vollständiger Abdruck der von der Fakultät für Physik
der Technischen Universität München zur Erlangung des
akademischen Grades
eines **Doktors der Naturwissenschaften (Dr. rer. nat.)**
genehmigten Dissertation.

Vorsitzender: Prof. Dr. Stefan Schönert

Prüfer der Dissertation: 1. Hon.-Prof. Dr. Wolfgang F. L. Hollik
2. Prof. Dr. Alejandro Ibarra

Die Dissertation wurde am 29.11.2017
bei der Technischen Universität München eingereicht und
durch die Fakultät für Physik am 23.01.2018 angenommen.

This thesis is based on the author's work conducted at the Max Planck Institute for Physics (Werner-Heisenberg-Institut) in Munich from December 2013 until November 2017. Parts of this work have already been published or are in preparation for publication:

- S. Hossenberger and W. Hollik. „*Two-loop corrections to the ρ parameter in Two-Higgs-Doublet Models*“. Eur. Phys. J. C77.3 (2017), p. 178. DOI: 10.1140/epjc/s10052-017-4734-8. arXiv: 1607.04610 [hep-ph]
- S. Hossenberger and W. Hollik. „*Two-loop improved predictions of the W boson mass and the effective leptonic mixing angle in Two-Higgs-Doublet Models*“. in preparation (2017)

Abstract

The topic of this thesis is the calculation and the analysis of electroweak precision observables including quantum corrections up to the two-loop order in extensions of the Standard Model (SM) by an additional scalar doublet in the Higgs sector. These *Two-Higgs-Doublet Models* (THDM) contain in general a large number of additional parameters. The loop corrections to precision observables incorporate also non-standard contributions from the extended Higgs-sector, in addition to the already known contributions of the SM. The comparison of the theoretical prediction with the experimental values of the precision observables leads therefore to indirect constraints on the free parameters of the THDM. These parameters are the masses of the Higgs bosons and additional independent couplings of the scalar self-interaction.

After the discovery of a scalar particle at the Large-Hadron-Collider with the properties of the Higgs boson in the SM, one of the neutral scalars in the THDM can be identified with the observed particle. This allows a separation of standard and non-standard contributions in the loop corrections. The dominant one-loop contributions are related to the corrections to the ρ parameter from the top-Yukawa interaction and the self-interaction of the non-standard scalars. These contributions constitute the leading process-independent corrections to many precision observables and the first step for the improvement of the theoretical prediction requires the calculation of the corresponding corrections at the two-loop order. In this thesis, the non-standard two-loop corrections to the ρ parameter from the top-Yukawa interaction and the scalar self-interaction are calculated and their influence on various precision observables is analysed. The results of the corrections are implemented in Fortran routines, which allow a numerical evaluation of the precision observables.

The first part of the thesis describes the details of the calculation. The masses of the light fermions are negligible. In order to obtain the leading two-loop contributions, the gauge-couplings can also be neglected, which leads to the two-loop contributions from the top-Yukawa interaction and the scalar self-interaction. A numerical investigation shows regions of the parameter space in which the two-loop corrections are important and the calculation at the one-loop order is insufficient. Specific parameter configurations exist, for which the non-standard top-quark contribution can become comparable to the corresponding contribution in the SM. The scalar two-loop corrections increase with the mass-splitting between the non-standard scalars, a feature that is already present in the non-standard one-loop corrections. In addition, the two-loop contributions can be enhanced by free parameters from the Higgs potential, which enter for the first time at the two-loop level.

The second part of the thesis investigates the influence of the two-loop corrections on the W - Z mass interdependence, the effective leptonic mixing angle and the width of the Z boson, as important examples for precision observables. The non-standard two-loop corrections are combined with the complete one-loop contribution and the known higher-order corrections from the SM. The new sensitivity on parameters of the Higgs potential gives additional indirect constraints on the Higgs-self couplings of the THDM. Numerical studies of representative parameter configurations demonstrate the dependence on the mass difference between the non-standard scalars and the additional modification from the Higgs-potential parameters. Different phenomenological scenarios are presented in which the two-loop contributions can become significant.

Zusammenfassung

Diese Doktorarbeit befasst sich mit der Berechnung und Auswertung von elektroschwachen Präzisionsobservablen mit Quantenkorrekturen bis zur Zweischleifenordnung in Erweiterungen des Standardmodells (SM) mit einem zusätzlichen skalaren Dublett im Higgs-Sektor. Solche Erweiterungen, bezeichnet als *Two-Higgs-Doublet Models* (THDM), enthalten im Allgemeinen eine große Anzahl an zusätzlichen Parametern. Die Schleifenbeiträge zu den Präzisionsobservablen enthalten zusätzlich zu den bekannten Beiträgen aus dem SM auch die nicht-standard Beiträge vom erweiterten Higgs-Sektor. Der Vergleich der theoretischen Vorhersage mit den experimentell bestimmten Werten der Präzisionsobservablen liefert somit indirekte Einschränkungen der freien Parameter des THDM. Zu diesen Parametern gehören die Massen der Higgsbosonen und weitere unabhängige Kopplungen in der Higgs-Selbstwechselwirkung.

Nach der Entdeckung eines skalaren Teilchens am Large-Hadron-Collider mit den Eigenschaften des Higgsbosons im SM lässt sich eines der neutralen Skalare im THDM mit dem beobachteten Teilchen identifizieren. Dadurch können die standard und nicht-standard Beiträge in den Schleifenkorrekturen separiert werden. Die dominanten Einschleifenbeiträge sind gegeben durch die Korrekturen zum ρ Parameter von der top-Yukawa Wechselwirkung und der Selbstwechselwirkung der nicht-standard Skalare. Da diese Beiträge die führenden prozessunabhängigen Korrekturen zu vielen Präzisionsobservablen liefern, besteht der erste Schritt zur Verbesserung der theoretischen Vorhersage in der Berechnung der entsprechenden Beiträge auf der Zweischleifenordnung. In dieser Arbeit werden die nicht-standard Zweischleifenbeiträge zum ρ Parameter von der top-Yukawa Wechselwirkung und der skalaren Selbstwechselwirkung im CP -erhaltenden THDM berechnet und ihr Einfluss auf verschiedene elektroschwache Präzisionsobservablen untersucht. Die Ergebnisse der Korrekturen sind in Fortran Routinen implementiert, welche eine numerische Auswertung der Präzisionsobservablen ermöglichen.

Der erste Teil der Doktorarbeit beschreibt die Details der Berechnung. Die Massen der leichten Fermionen sind vernachlässigbar. Um die führenden Zweischleifenbeiträge zu erhalten, können die Eichkopplungen ebenfalls vernachlässigt werden, sodass nur noch die Beiträge von der top-Yukawa Kopplung und den skalaren Selbstkopplungen verbleiben. Eine numerische Auswertung der Ergebnisse zeigt Regionen des Parameterraumes, in denen die Zweischleifenkorrekturen signifikant sind und eine Berechnung auf der Einschleifenordnung nicht ausreicht. Der nicht-standard top-Yukawa Beitrag ist für bestimmte Parameterwerte vergleichbar mit dem entsprechenden Beitrag im SM. Der skalare Zweischleifenbeitrag wächst mit dem Massenunterschied zwischen den nicht-standard Skalaren, eine Eigenschaft, die bereits von der entsprechenden Einschleifenkorrektur bekannt ist. Durch die freien Parameter der Higgs-Selbstkopplungen, welche zum ersten Mal auf der Zweischleifenordnung auftreten, können die skalaren Beiträge zusätzlich verstärkt werden.

Der zweite Teil der Doktorarbeit beschäftigt sich mit dem Einfluss der Zweischleifenkorrekturen auf die W - Z Massenkorelation, den effektiven leptonischen Mischungswinkel und die Zerfallsbreite des Z Bosons als wichtige Beispiele für Präzisionsobservablen. Die nicht-standard Zweischleifenkorrekturen werden mit den kompletten Einschleifenbeiträgen und den bekannten Korrekturen höherer Ordnung aus dem SM kombiniert. Die zusätzliche Abhängigkeit von den Parametern des Higgspotentials kann genutzt werden, um die Higgs-Selbstkopplungen im THDM indirekt einzuschränken. Numerische Untersuchungen von einer repräsentativen Auswahl an Parametern zeigen den Einfluss der Massendifferenzen der nicht-standard Skalare und eine Modifikation der Korrekturen durch die Parameter der Higgs-Selbstkopplungen. Verschiedene phänomenologische Szenarien werden präsentiert, in denen die Zweischleifenkorrekturen signifikante Beiträge liefern.

Contents

1	Introduction	1
2	The Two-Higgs-Doublet Model	5
2.1	Yang-Mills part and gauge-fermion interaction	5
2.2	Higgs potential	7
2.3	Higgs-boson interaction with gauge bosons	12
2.4	Yukawa interaction	13
2.5	The alignment limit	16
2.6	The Inert-Higgs-Doublet Model	17
2.7	Theoretical constraints	19
3	Higher-order corrections	21
3.1	Dimensional regularization	21
3.2	Gauge-boson self-energies	21
3.2.1	One-loop integrals for self-energies	22
3.2.2	Two-loop integrals for self-energies	23
3.3	Technical evaluation of higher-order corrections	24
4	Renormalization	27
4.1	Renormalized perturbation theory	27
4.2	On-shell renormalization scheme	28
4.2.1	Renormalization of the gauge-boson sector	28
4.2.2	Renormalization of the fermion sector	32
4.2.3	Renormalization of the Higgs sector	33
5	The ρ parameter in the THDM	39
5.1	Custodial symmetry in the SM and the THDM	39
5.1.1	Custodial symmetry in the SM	39
5.1.2	Custodial symmetry in the THDM potential	41
5.1.3	Custodial symmetry in the Yukawa sector of the THDM	43
5.1.4	Custodial symmetry in the IHDM	44
5.2	Corrections to the ρ parameter from quantum loops	45
5.2.1	One-loop corrections in the SM and the THDM	46
5.2.2	Approximations for the two-loop contributions	47
5.2.3	Higher-order corrections in the THDM	48
5.2.4	Corrections to the ρ parameter in the IHDM	56
5.3	Numerical analysis	57
5.3.1	Results for the top-Yukawa contribution	57
5.3.2	Quality of the top-Yukawa approximation	58
5.3.3	Results for the non-standard scalar contribution	58
5.3.4	Results for the mixed scalar contribution	61
5.3.5	Results in the IHDM	62

6	The M_W–M_Z interdependence	63
6.1	Corrections in the SM	63
6.2	Non-standard corrections in the THDM	67
6.3	Non-standard corrections in the IHDM	69
6.4	Incorporation of non-standard corrections	69
7	Precision observables at the Z pole	71
7.1	The width of the Z boson	72
7.1.1	QED and QCD corrections in radiation factors	73
7.1.2	Electroweak corrections in effective couplings	75
7.1.3	Partial Z widths	78
7.2	The effective leptonic weak mixing angle	81
8	Numerical Results	85
8.1	Input parameters	85
8.2	Influence of reducible two-loop corrections	86
8.3	Results in the aligned THDM	88
8.3.1	Results for a light pseudoscalar	92
8.3.2	Results in the CP -overlap scenario	95
8.3.3	Results in the exotic decay scenario	98
8.4	Results in the IHDM	100
9	Conclusions	105
A	Feynman Rules of the THDM	109
B	Loop integrals	121
B.1	One-loop integrals	121
B.2	Two-loop integrals	123
C	Analytic results	127
C.1	Non-standard one-loop corrections to the gauge boson selfenergies	127
C.2	Two-loop corrections to the ρ parameter	128
C.2.1	Non-standard corrections from the top-Yukawa coupling	128
C.2.2	Scalar corrections from the interaction of the non-standard scalars	130
C.2.3	Scalar corrections from the interactions of the SM scalars with the non-standard scalars	133

Chapter 1

Introduction

A long history of accurate theoretical predictions and successful validation by various experiments has established the Standard Model (SM) [3–5] as the fundamental theory of strong and electroweak interactions. The most recent example for these exceptional achievements is the discovery of a scalar particle at the Large Hadron Collider (LHC) by ATLAS [6] and CMS [7] with properties resembling those of the Higgs boson as predicted in the SM for electroweak symmetry breaking [8–12]. The precisely measured mass of $M_H = 125.09 \pm 0.24$ GeV [13] completes the input parameters of the SM. Before the discovery of the scalar particle, the mass of the SM Higgs boson was constrained by comparing accurate theoretical predictions with precise measurements of electroweak observables. These electroweak precision observables are, among others, the masses of the gauge bosons, M_W and M_Z , the width of the Z boson and the various asymmetries measured in electron-positron collisions, which determine the effective electroweak mixing angle of the leptons, $\sin^2 \theta_{\text{eff}}^l$. The theoretical predictions of the electroweak precision observables depend also on the parameters of the virtual particles, which enter the loop corrections in higher-order calculations. This dependence can be used to obtain indirect constraints on the parameters by performing global fits to the precision observables [14], as it was done for the mass of the SM Higgs boson or the mass of the top quark before its discovery at the Tevatron. With the meanwhile complete input, the electroweak precision observables provide stringent tests of the SM. Only few deviations between predictions and data are found. For example the anomalous magnetic moment of the muon is measured to differ from the SM prediction by 3.6σ [15]. Nevertheless, the global fit leads to a remarkably good agreement between theory and experiments [16, 17].

The unique SM prediction of the precision observables can be used for getting constraints on extended models, provided that the accuracy of the theoretical calculation is comparable to the precision of the measurements. Such extensions are motivated by several unsolved issues for which the SM provides no explanations, like the nature of dark matter, the origin of neutrino masses or the matter-antimatter asymmetry in the universe. Since the scalar sector is the least investigated part of the SM, possible extensions with extended Higgs sectors are very appealing. In the SM, the minimal version of the Higgs sector incorporates all scalar degrees of freedom in one doublet of the gauge group $SU(2)_L \times U(1)_Y$. Although the properties of the Higgs boson in the SM are consistent with the current measurements at the LHC, the possibility of additional scalar particles is not ruled out.

A very important constraint that has to be fulfilled by possible extensions arises from the electroweak ρ parameter, which is defined as the ratio between the effective coupling strengths of the neutral and charged currents in four-fermion interactions at low momentum. Experimentally ρ is determined to be close to unity. The minimal version of the scalar sector in the SM leads to $\rho = 1$ at tree-level, and deviations from unity arise only through higher-order corrections. These corrections $\Delta\rho$ play a very prominent role in the calculation of precision observables, since they constitute the leading process-independent loop corrections. In the SM, the dominant non-QED contributions to $\Delta\rho$ originate from the top-Yukawa interaction. The large top mass enters quadratically in the one-loop contribution. The high sensitivity to this parameter was essential for its indirect constraints by electroweak precision observables. On the other hand, one-loop corrections quadratic in the Higgs mass are absent, since the ρ parameter is protected from corrections of the scalar sector in the SM by a global custodial symmetry

of the Higgs potential [18–20]. Over the years corrections in the SM were calculated at the one-loop [21–23], two-loop [24–31], three-loop [32–35] and even at the four-loop order [36–38].

The tree-level relation $\rho = 1$ is preserved if the Higgs sector is extended by additional doublets [39]. An even simpler extension with ρ equal to unity adds just a scalar singlet [40–42] and provides a natural dark matter candidate or a portal to an additional hidden sector. In contrast to the afore mentioned models, extensions with scalar triplets will in general lead to $\rho \neq 1$ at the tree-level. Historically these models gained interest as the source of neutrino masses [43, 44]. In order to achieve $\rho = 1$ for triplet extensions additional assumptions are necessary, like for example additional global symmetries [45, 46]. For a recent review of these different scalar extensions see [47].

In this thesis we consider the extension of the SM by a second Higgs doublet, labelled as the Two-Higgs-Doublet Model (THDM). This simple extension already exhibits very interesting phenomena, for example charged scalars. The most popular motivation for a second doublet is probably supersymmetry. In supersymmetric theories one Higgs doublet is insufficient to provide the masses for the up- and the down-type quarks simultaneously. Moreover an additional doublet is required for the cancellation of anomalies. For these reasons two doublets are contained in the Minimal Supersymmetric Standard Model (MSSM). If all the masses of the supersymmetric partners are very heavy, the effective theory below the supersymmetric mass scale is described by a THDM [48–52]. In contrast to the MSSM, where supersymmetry relates the parameters of the Higgs potential with the gauge couplings, the Higgs potential of a general THDM contains a large number of free parameters. Originally proposed as a source of CP -violation [53, 54], the THDM could also explain the matter-antimatter asymmetry in the universe since it can lead to a strong first-order electroweak phase transition [55–57], as it is required in electroweak baryogenesis. Usually discrete symmetries are imposed in the THDM, in order to avoid tree-level flavour-changing neutral currents from the Yukawa-couplings. The resulting different versions of the THDM are labelled as type-I, type-II, type-Z and type-Y. A survey about the THDM with additional details and references is given in [58].

An especially interesting version of a THDM, the Inert-Higgs-Doublet Model (IHDM), is obtained by imposing a discrete Z_2 symmetry under which one of the doublets transforms odd and all the other fields transform even [59]. The IHDM has received attention in the context of radiative neutrino masses [60] or as a solution to the naturalness problem [61]. Moreover, since the Z_2 symmetry stays unbroken, the lightest particle in the inert doublet can provide a dark matter candidate [62]. The phenomenology of the IHDM has been studied in large detail during the last years, see for example [63–66].

The simple scalar sector in the SM is parameterized by a single free parameter, the scalar self-coupling or equivalently the mass of the SM Higgs boson. Adding the second doublet in the THDM increases the numbers of free parameters substantially. The additional degrees of freedom result in multiple massive scalars. Especially striking is a pair of charged scalars H^\pm , a novel feature which is completely absent in the SM. Furthermore, three massive neutral scalars are present. In a CP -conserving THDM the neutral scalars are two CP -even states h^0 and H^0 and a CP -odd scalar A^0 . One of the neutral scalars can be identified with the resonance found at the LHC. The mass of this scalar is therefore fixed at 125 GeV. The couplings are constrained by the overall agreement of the measured properties with the SM expectations. SM-like couplings of the chosen scalar to the gauge bosons or fermions are obtained for example in the *decoupling limit*, in which the masses of the remaining scalars are very heavy [67]. A more general way to arrange SM-like couplings is the *alignment limit*, which adjusts the mixing angle of the CP -even scalars [68, 69].

There are several possibilities to restrict the scalar masses and additional free parameters of the THDM. The most obvious way are direct collider constraints from LEP and LHC. A combined analysis of the LEP searches gives a lower bound on the mass of the charged scalar [70]. The implications of the Higgs discovery and direct searches for heavy Higgs states on the THDM parameters are investigated in many publications, for example in [71–74]. Detailed analyses in scenarios with an alignment limit of a CP -even Higgs state are given in [75, 76]. The possibility of a light scalar with a mass below 60 GeV is investigated in [77]. In the absence of a direct signal of new physics, loop corrections to precisely measured observables provide indirect information on the free parameters of the THDM. One example are flavour observables which are very sensitive to corrections from the charged Higgs [78–82]. Recent limits on the charged Higgs boson mass from a combination of direct searches and flavour observables can be found

in [83]. Another example are the aforementioned electroweak precision observables, which have been exploited so successfully in the past for the indirect determination of the masses of the SM Higgs boson and the top quark.

The calculation of electroweak precision observables in the general THDM has a long history [84–95]. The non-standard corrections are obtained in most cases at the one-loop order. Only [93] contains some higher-order terms by means of effective couplings. The dominant non-standard contribution at the one-loop order can be identified with the scalar corrections to the ρ parameter. In difference to the SM, these scalar corrections arise since $\rho = 1$ is not protected by an custodial symmetry of the Higgs potential. The parameters of the potential enter through the loop corrections and lead to scalar contributions to $\Delta\rho$. A custodial symmetry can be restored for equal masses of charged and neutral scalars. The non-standard one-loop corrections to $\Delta\rho$ are therefore very sensitive to the mass splitting between charged and neutral scalars, which leads to potentially important contributions to electroweak precision observables.

The status of the non-standard corrections in the THDM is not comparable in accuracy to the SM, where most of the precision observables are calculated at the full two-loop order [29–31, 96–112] with additional leading three- and four-loop corrections from $\Delta\rho$ [32–38, 113–115]. The prediction in the MSSM is also more advanced, since the non-standard one-loop corrections to precision observables have been supplemented with the leading two-loop corrections to $\Delta\rho$ from the strong and Yukawa interactions [116–119].

As an improvement of the theoretical predictions in the CP -conserving THDM, this thesis presents the two-loop corrections to the ρ parameter and to precision observables which result from the top-Yukawa interaction and the self-interaction of the Higgs bosons. Since these sectors lead to sizable contributions already at the one-loop level, the corresponding two-loop corrections can be expected to be dominant. Moreover, the two-loop contribution originating from the scalar self-couplings are sensitive to additional parameters of the Higgs potential, which are completely absent in the one-loop corrections. Technically, this class of two-loop corrections is obtained in the gauge-less limit, in which the effect of the gauge-couplings are neglected. Furthermore, the lighter CP -even Higgs is identified with the scalar discovered at the LHC and the alignment limit is applied. In this way, a clear separation between non-standard and SM contributions is possible. In a similar manner, the scalar corrections to $\Delta\rho$ in the IHDM are calculated, where no further assumptions are required for a separation between non-standard and SM contributions.

The first part of this thesis describes the calculation of the two-loop contributions to the ρ parameter. The second part discusses the impact of these corrections on several precision observables, namely the M_W – M_Z correlation, the effective leptonic mixing angle and the width of the Z boson. The non-standard two-loop corrections from the top-Yukawa interaction and the scalar self-interaction are combined with the complete one-loop corrections and the known higher-order corrections from the SM.

The structure of this thesis is as follows. Chapter 2 introduces the THDM. In order to give an overview over the notation and the particle content, the gauge-boson self-interaction and the gauge-fermion interaction is reviewed in the beginning. Afterwards the scalar potential, the resulting Higgs boson spectrum and the interaction of the scalars with the gauge bosons are discussed. The Yukawa-interaction is presented for the different versions of the THDM (type-I, type-II, type-X and type-Y). The special characteristics of the IHDM are also described. Theoretical constraints on the parameters of the THDM and the IHDM are discussed at the end of Chapter 2.

Chapter 3 outlines technical aspects for the evaluation of self-energy corrections, introduces the required loop integrals and describes the method of the calculation with the help of various computer programs. Chapter 4 discusses the renormalization of the THDM, with an particular focus on the renormalization of the scalar sector.

Chapter 5 presents the calculation of the two-loop corrections to the ρ parameter in the THDM and the IHDM. In the beginning the possible realizations of the custodial symmetry in the THDM are described, which provide a deeper understanding of the various higher-order contributions to $\Delta\rho$. The approximations for the two-loop corrections are explained. The conceptual description of the calculation together with a classification in terms of distinct, UV-finite two-loop corrections is given. At the end of Chapter 5 the dependence of the various classes of contributions on the THDM parameters is analyzed.

The subsequent chapters describe the calculation of the precision observables in the THDM.

The one-loop corrections and the higher-order SM predictions are reviewed for completeness before explaining the incorporation of the two-loop contributions. Chapter 6 focuses on the prediction of the W boson mass from M_Z , the Fermi-constant G_F and the electromagnetic fine structure constant α_{em} via the decay width of the muon. Chapter 7 describes the calculation of Z observables in terms of the width of the Z boson and the effective leptonic mixing angle.

Chapter 8 presents the numerical results for the precision observables. For the general THDM in the alignment limit, different parameter configurations are investigated as representative examples for the influence of the various two-loop contributions. Afterwards scenarios which are motivated by different phenomenological aspects are considered. It is shown that in these scenarios the two-loop corrections can give large modification for the prediction of precision observables. At the end of Chapter 8, results in the IHDM are presented.

Conclusions are given in Chapter 9. The Appendix contains the Feynman rules of the THDM with counter-terms, the expressions for the scalar loop integrals and the analytic results for the non-standard two-loop corrections to the ρ parameter from the top-Yukawa interaction and the scalar self-interaction.

Chapter 2

The Two-Higgs-Doublet Model

The electroweak Standard Model (SM) [3–5] is a non-Abelian gauge theory based on the product $SU(2)_L \times U(1)_Y$ of the unitary hypercharge gauge group $U(1)_Y$ and the special unitary weak-isospin group $SU(2)_L$.

Fermion masses are forbidden in the symmetric theory, since the SM is chiral, meaning that left- and right-handed fermions transform according to different representations of the gauge group. The masses of the gauge bosons and fermions are introduced via spontaneous symmetry breaking of the electroweak gauge group down to the electromagnetic gauge group $U(1)_{\text{EM}}$ as proposed by [8–12]. In the SM, electroweak symmetry breaking is realized by introducing a complex scalar doublet with a non-vanishing vacuum expectation value. Three degrees of freedom are absorbed by the longitudinal components of the massive gauge bosons. The remaining degree of freedom corresponds to a massive scalar particle H_{SM} , the Higgs boson in the SM. Yukawa interaction terms between the scalar doublet and the fermions together with the spontaneous symmetry breaking lead to the masses of the fermions.

The Two-Higgs-Doublet Model (THDM) [53, 54, 59, 120–124] is one of the simplest possible extensions of the SM which preserves its fundamental properties. The electroweak interaction is also described by the gauge group $SU(2)_L \times U(1)_Y$, which is spontaneously broken to the $U(1)_{\text{EM}}$. However the scalar sector, which is responsible for the electroweak symmetry breaking is extended to two scalar doublets under the $SU(2)_L$. This results into a larger spectrum of massive scalar eigenstates and a more complicated Yukawa interaction between scalars and fermions.

2.1 Yang-Mills part and gauge–fermion interaction

In the THDM no additional degrees of freedom are added to the gauge boson or the fermionic sector of the SM. For simplicity we also discard the possibility of right-handed neutrino states, which could explain the observed oscillations of solar and atmospheric neutrinos [125–127]. The kinetic parts and the interaction terms in the Lagrangian, which contain solely the gauge bosons and the fermions, are therefore identical to the minimal version of the SM. The corresponding parts of the classical Lagrangian are reviewed here, in order to introduce the particle content and to provide an overview over the notation.

The Abelian group $U(1)_Y$ is generated by the hypercharge Y . The associated gauge field B_μ transforms in the adjoint representation with the hypercharge coupling g_1 . The gauge group of the $SU(2)_L$ is generated by the weak isospin generators $I_a = \sigma_a/2$, with the usual Pauli-matrices σ_a . The associated vector fields are grouped in the isotriplet W_μ^a ($a = 1, 2, 3$) and transform in the adjoint representation of the $SU(2)_L$ with the gauge coupling g_2 . The pure gauge field Lagrangian

$$\mathcal{L}_{YM} = -\frac{1}{4}W_{\mu\nu}^a W^{\mu\nu,a} - \frac{1}{4}B_{\mu\nu}B^{\mu\nu} \quad (2.1)$$

with the field strength tensors

$$W_{\mu\nu}^a = \partial_\mu W_\nu^a - \partial_\nu W_\mu^a + g_2 \epsilon_{abc} W_\mu^b W_\nu^c, \quad (2.2)$$

$$B_{\mu\nu} = \partial_\mu B_\nu - \partial_\nu B_\mu, \quad (2.3)$$

is invariant under the gauge transformations. The structure constant ϵ_{abc} is the totally anti-symmetric Levi-Civita tensor with $\epsilon_{123} = 1$.

Fermion field	Isospin I_3	Hypercharge Y
ν'_l ($l = e, \mu, \tau$)	$+\frac{1}{2}$	-1
l'_L ($l = e, \mu, \tau$)	$-\frac{1}{2}$	-1
l'_R ($l = e, \mu, \tau$)	0	-2
$u'_{j,L}$ ($u_j = u, c, t$)	$+\frac{1}{2}$	$\frac{2}{6}$
$d'_{j,L}$ ($d_j = d, s, b$)	$-\frac{1}{2}$	$\frac{2}{6}$
$u'_{j,R}$ ($u_j = u, c, t$)	0	$\frac{4}{3}$
$d'_{j,R}$ ($d_j = d, s, b$)	0	$-\frac{2}{3}$

Table 2.1: Quantum numbers of the fermion fields

In the SM (and in the THDM) the fundamental fermions of the different lepton and quark generations are arranged in $SU(2)_L$ doublets for the left-handed states

$$L_j^{\prime L} = \begin{pmatrix} \nu'_e \\ e'_L \end{pmatrix}, \quad \begin{pmatrix} \nu'_\mu \\ \mu'_L \end{pmatrix}, \quad \begin{pmatrix} \nu'_\tau \\ \tau'_L \end{pmatrix}, \quad (2.4)$$

$$Q_j^{\prime L} = \begin{pmatrix} u'_L \\ d'_L \end{pmatrix}, \quad \begin{pmatrix} c'_L \\ s'_L \end{pmatrix}, \quad \begin{pmatrix} t'_L \\ b'_L \end{pmatrix}, \quad (2.5)$$

and into singlet representations (with $I_a = 0$) for the right-handed states

$$l_j^{\prime R} = e'_R, \quad \mu'_R, \quad \tau'_R, \quad (2.6)$$

$$u_j^{\prime R} = u'_R, \quad c'_R, \quad t'_R, \quad (2.7)$$

$$d_j^{\prime R} = d'_R, \quad s'_R, \quad b'_R. \quad (2.8)$$

The index j represents the different generations. The states of left- and right-handed chirality are obtained by applying the projectors

$$\omega_\pm = \frac{1 \pm \gamma_5}{2}, \quad (2.9)$$

on a full fermion spinor ψ_f , such that

$$f^L = \omega_- \psi_f, \quad (2.10)$$

$$f^R = \omega_+ \psi_f. \quad (2.11)$$

An explicit colour index for the left- and right-handed quark states is omitted for the sake of clarity.

The hypercharges of the left- and right-handed fermions have to fulfill the Gell-Mann–Nishijima relation

$$Q = I_3 + \frac{Y}{2} \quad (2.12)$$

in order to produce the right quantum number of the electric charge operator Q . The resulting quantum numbers of the fermion fields are given in Table 2.1.

Gauge-invariant kinetic terms of the fermions are obtained by replacing the ordinary derivatives with the covariant derivative

$$D_\mu = \partial_\mu + ig_2 I_a W_\mu^a + ig_1 \frac{Y}{2} B_\mu. \quad (2.13)$$

With the fermion multiplets in (2.4), (2.5), (2.6), (2.7) and (2.8) the fermionic part of the Lagrangian reads

$$\begin{aligned} \mathcal{L}_F = & \sum_j \left[\bar{L}_j'^L i\gamma^\mu D_\mu L_j'^L + \bar{l}_j'^R i\gamma^\mu D_\mu l_j'^R \right] \\ & + \sum_j \left[\bar{Q}_j'^L i\gamma^\mu D_\mu Q_j'^L + \bar{u}_j'^R i\gamma^\mu D_\mu u_j'^R + \bar{d}_j'^R i\gamma^\mu D_\mu d_j'^R \right]. \end{aligned} \quad (2.14)$$

The index j runs over the different generations for the quark and leptons. The summation of the quark states runs also over the additional colour index, which has been omitted for brevity.

In this notation the primed fermion states are defined to be eigenstates of the electroweak interaction. These states are not necessarily identical to the mass eigenstates, which are obtained by the Yukawa interaction in Section 2.4.

2.2 Higgs potential

The THDM Higgs sector consists of two complex $SU(2)_L$ doublet scalar fields with hypercharge $Y = 1$:

$$\Phi_1 = \begin{pmatrix} \phi_1^+ \\ \phi_1^0 \end{pmatrix}, \quad \Phi_2 = \begin{pmatrix} \phi_2^+ \\ \phi_2^0 \end{pmatrix}. \quad (2.15)$$

The most general gauge-invariant and renormalizable potential can be written as follows [58, 67],

$$\begin{aligned} V(\Phi_1, \Phi_2) = & m_{11}^2 \Phi_1^\dagger \Phi_1 + m_{22}^2 \Phi_2^\dagger \Phi_2 - \left(m_{12}^2 \Phi_1^\dagger \Phi_2 + \text{h.c.} \right) \\ & + \frac{1}{2} \Lambda_1 \left(\Phi_1^\dagger \Phi_1 \right)^2 + \frac{1}{2} \Lambda_2 \left(\Phi_2^\dagger \Phi_2 \right)^2 + \Lambda_3 \left(\Phi_2^\dagger \Phi_2 \right) \left(\Phi_1^\dagger \Phi_1 \right) + \Lambda_4 \left(\Phi_1^\dagger \Phi_2 \right) \left(\Phi_2^\dagger \Phi_1 \right) \\ & + \left[\frac{1}{2} \Lambda_5 \left(\Phi_1^\dagger \Phi_2 \right)^2 + \left(\Lambda_6 \Phi_1^\dagger \Phi_1 + \Lambda_7 \Phi_2^\dagger \Phi_2 \right) \Phi_1^\dagger \Phi_2 + \text{h.c.} \right]. \end{aligned} \quad (2.16)$$

The parameters m_{11}^2 , m_{22}^2 and $\Lambda_{1,2,3,4}$ are real due to the hermicity of the potential. In general the parameters m_{12}^2 , $\Lambda_{5,6,7}$ can be complex. Since the two doublets carry the same quantum numbers, one can rewrite the potential in terms of new doublets Φ'_a , which are obtained from the original ones by

$$\Phi'_a = \sum_{b=1}^2 U_{ab} \Phi_b \quad (2.17)$$

where U is a unitary 2×2 matrix (see for example [58, 128, 129]). This basis transformation can be used to eliminate some of the degrees of freedom of the potential.

Usually a specific basis is defined by the discrete Z_2 symmetry

$$\Phi_1 \rightarrow \Phi_1; \quad \Phi_2 \rightarrow -\Phi_2. \quad (2.18)$$

As discussed in Section 2.4 this discrete symmetry prevents flavour-changing neutral currents in the Yukawa-sector. In the scalar potential, the symmetry forbids the Z_2 -breaking terms of mass-dimension four, resulting in

$$\Lambda_6 = \Lambda_7 = 0. \quad (2.19)$$

Conventionally, one allows a soft-violation by dimension-two terms and keeps $m_{12}^2 \neq 0$, since this results in a richer phenomenology of the model.

In this thesis we are assuming a CP -conserving potential in which all of the parameters are real. In the discussions about the alignment limit in Section 2.5 and the custodial symmetry in Section 5.1 we keep $\Lambda_{6,7} \neq 0$. In this way, we can highlight differences that arise from the corresponding terms in the potential. However, in our phenomenological study of the results will be done for $\Lambda_{6,7} = 0$, since the model with soft Z_2 -violation already covers the main characteristics of the two-loop corrections.

Under the requirement that the minimum of the potential respects the $U(1)_{\text{EM}}$ symmetry, the vacuum expectation values of the scalar fields are

$$\langle \Phi_i \rangle = \begin{pmatrix} 0 \\ \frac{v_i}{\sqrt{2}} \end{pmatrix}, \quad i = 1, 2. \quad (2.20)$$

Expanding the scalar fields around the vacuum expectation values,

$$\Phi_1 = \begin{pmatrix} \phi_1^+ \\ \frac{1}{\sqrt{2}}(v_1 + \eta_1 + i\chi_1) \end{pmatrix}, \quad \Phi_2 = \begin{pmatrix} \phi_2^+ \\ \frac{1}{\sqrt{2}}(v_2 + \eta_2 + i\chi_2) \end{pmatrix}, \quad (2.21)$$

and inserting this decomposition in the potential leads to the following terms, which are linear and quadratic in the field components

$$\begin{aligned} V = & -T_1\eta_1 - T_2\eta_2 + \begin{pmatrix} \phi_1^- & \phi_2^- \end{pmatrix} \tilde{\mathbf{M}}^\phi \begin{pmatrix} \phi_1^+ \\ \phi_2^+ \end{pmatrix} \\ & + \frac{1}{2} \begin{pmatrix} \chi_1 & \chi_2 \end{pmatrix} \tilde{\mathbf{M}}^\chi \begin{pmatrix} \chi_1 \\ \chi_2 \end{pmatrix} + \frac{1}{2} \begin{pmatrix} \eta_1 & \eta_2 \end{pmatrix} \tilde{\mathbf{M}}^\eta \begin{pmatrix} \eta_1 \\ \eta_2 \end{pmatrix} + \dots \end{aligned} \quad (2.22)$$

The coefficients of $\eta_{1,2}$ are

$$T_1 = -v_1 m_{11}^2 + v_2 m_{12}^2 - \frac{1}{2} \Lambda_1 v_1^3 - \frac{1}{2} \Lambda_{345} v_2^2 v_1 - \frac{3}{2} \Lambda_6 v_2 v_1^2 - \frac{1}{2} \Lambda_7 v_2^3, \quad (2.23)$$

$$T_2 = -v_2 m_{22}^2 + v_1 m_{12}^2 - \frac{1}{2} \Lambda_2 v_2^3 - \frac{1}{2} \Lambda_{345} v_2 v_1^2 - \frac{1}{2} \Lambda_6 v_1^3 - \frac{3}{2} \Lambda_7 v_2^2 v_1. \quad (2.24)$$

with

$$\Lambda_{345} = \Lambda_3 + \Lambda_4 + \Lambda_5. \quad (2.25)$$

The mass matrices can be written as

$$\tilde{\mathbf{M}}^X = \mathbf{M}^X + \mathbf{M}^T; \quad X = \phi, \chi, \eta, \quad (2.26)$$

with

$$\mathbf{M}^T = \begin{pmatrix} -\frac{T_1}{v_1} & 0 \\ 0 & -\frac{T_2}{v_2} \end{pmatrix} \quad (2.27)$$

and

$$\mathbf{M}^\eta = \begin{pmatrix} m_{12}^2 \frac{v_2}{v_1} + v_1^2 \Lambda_1 + \frac{3}{2} v_1 v_2 \Lambda_6 - \frac{v_2^3}{2v_1} \Lambda_7 & -m_{12}^2 + v_1 v_2 \Lambda_{345} + \frac{3}{2} v_1^2 \Lambda_6 + \frac{3}{2} v_2^2 \Lambda_7 \\ -m_{12}^2 + v_1 v_2 \Lambda_{345} + \frac{3}{2} v_1^2 \Lambda_6 + \frac{3}{2} v_2^2 \Lambda_7 & m_{12}^2 \frac{v_1}{v_2} + v_2^2 \Lambda_2 - \frac{v_1^3}{2v_2} \Lambda_6 + \frac{3}{2} v_2 v_1 \Lambda_7 \end{pmatrix}, \quad (2.28)$$

$$\mathbf{M}^\chi = \begin{pmatrix} m_{12}^2 \frac{v_2}{v_1} - \Lambda_5 v_2^2 - \frac{1}{2} v_1 v_2 \Lambda_6 - \frac{v_2^3}{2v_1} \Lambda_7 & -m_{12}^2 + v_1 v_2 \Lambda_5 + \frac{1}{2} v_1^2 \Lambda_6 + \frac{1}{2} v_2^2 \Lambda_7 \\ -m_{12}^2 + v_1 v_2 \Lambda_5 + \frac{1}{2} v_1^2 \Lambda_6 + \frac{1}{2} v_2^2 \Lambda_7 & m_{12}^2 \frac{v_1}{v_2} - \Lambda_5 v_1^2 - \frac{v_1^3}{2v_2} \Lambda_6 - \frac{1}{2} v_2 v_1 \Lambda_7 \end{pmatrix}, \quad (2.29)$$

$$\mathbf{M}^\phi = \begin{pmatrix} m_{12}^2 \frac{v_2}{v_1} - \frac{1}{2} v_2^2 \Lambda_{45} - \frac{1}{2} v_1 v_2 \Lambda_6 - \frac{v_2^3}{2v_1} \Lambda_7 & -m_{12}^2 + \frac{1}{2} v_1 v_2 \Lambda_{45} + \frac{1}{2} v_1^2 \Lambda_6 + \frac{1}{2} v_2^2 \Lambda_7 \\ -m_{12}^2 + \frac{1}{2} v_1 v_2 \Lambda_{45} + \frac{1}{2} v_1^2 \Lambda_6 + \frac{1}{2} v_2^2 \Lambda_7 & m_{12}^2 \frac{v_1}{v_2} - \frac{1}{2} v_1^2 \Lambda_{45} - \frac{v_1^3}{2v_2} \Lambda_6 - \frac{1}{2} v_2 v_1 \Lambda_7 \end{pmatrix}. \quad (2.30)$$

In the last matrix the abbreviation

$$\Lambda_{45} = \Lambda_4 + \Lambda_5 \quad (2.31)$$

is introduced.

The requirements that the tadpoles in (2.23) and (2.24) must vanish results in the minimum conditions

$$m_{11}^2 = -\frac{1}{2}\Lambda_1 v_1^2 + \frac{v_2}{v_1} m_{12}^2 - \frac{1}{2}\Lambda_{345} v_2^2 - \frac{3}{2}\Lambda_6 v_1 v_2 - \frac{v_2^3}{2v_1} \Lambda_7, \quad (2.32a)$$

$$m_{22}^2 = -\frac{1}{2}\Lambda_2 v_2^2 + \frac{v_1}{v_2} m_{12}^2 - \frac{1}{2}\Lambda_{345} v_1^2 - \frac{v_1^3}{2v_2} \Lambda_6 - \frac{3}{2}\Lambda_7 v_2 v_1. \quad (2.32b)$$

Applying the minimum conditions to the quadratic terms in (2.22) eliminates \mathbf{M}^T . The diagonalization of the remaining mass matrices results in the physical mass eigenstates.

In each of the mass matrices \mathbf{M}^ϕ and \mathbf{M}^χ one eigenvalue is equal to zero. The corresponding scalar states are the unphysical Goldstone bosons G^0 and G^\pm , which are absorbed by the longitudinal degrees of freedom of the gauge bosons.¹ The rotations

$$\begin{pmatrix} G^\pm \\ H^\pm \end{pmatrix} = \mathbf{R}(\beta) \begin{pmatrix} \phi_1^\pm \\ \phi_2^\pm \end{pmatrix}, \quad \begin{pmatrix} G^0 \\ A^0 \end{pmatrix} = \mathbf{R}(\beta) \begin{pmatrix} \chi_1 \\ \chi_2 \end{pmatrix} \quad (2.33)$$

with

$$\mathbf{R}(x) = \begin{pmatrix} \cos x & \sin x \\ -\sin x & \cos x \end{pmatrix} \quad (2.34)$$

diagonalize \mathbf{M}^ϕ and \mathbf{M}^χ . The mixing angle is given by

$$\cos \beta = \frac{v_1}{v}, \quad \sin \beta = \frac{v_2}{v}, \quad \tan \beta = \frac{v_2}{v_1} \quad (2.35)$$

with

$$v^2 = v_1^2 + v_2^2. \quad (2.36)$$

In addition to the Goldstone bosons, (2.33) gives a charged pair H^\pm with mass

$$m_{H^\pm}^2 = \frac{m_{12}^2}{c_\beta s_\beta} - v^2 \left(\frac{\Lambda_{45}}{2} + \frac{\Lambda_6}{2t_\beta} + \frac{\Lambda_7 t_\beta}{2} \right), \quad (2.37)$$

and a CP -odd scalar A^0 with mass

$$m_{A^0}^2 = \frac{m_{12}^2}{c_\beta s_\beta} - \frac{1}{2}v^2 \left(2\Lambda_5 + \frac{\Lambda_6}{t_\beta} + \Lambda_7 t_\beta \right). \quad (2.38)$$

The mass matrix \mathbf{M}^η of the fields $\eta_{1,2}$ has the two eigenvalues,

$$m_{h^0}^2 = \frac{1}{2} \left[\mathbf{M}_{11}^\eta + \mathbf{M}_{22}^\eta - \sqrt{(\mathbf{M}_{11}^\eta - \mathbf{M}_{22}^\eta)^2 + 4(\mathbf{M}_{12}^\eta)^2} \right], \quad (2.39)$$

$$m_{H^0}^2 = \frac{1}{2} \left[\mathbf{M}_{11}^\eta + \mathbf{M}_{22}^\eta + \sqrt{(\mathbf{M}_{11}^\eta - \mathbf{M}_{22}^\eta)^2 + 4(\mathbf{M}_{12}^\eta)^2} \right]. \quad (2.40)$$

The two corresponding CP -even mass eigenstates h^0 and H^0 are obtained by the rotation

$$\begin{pmatrix} H^0 \\ h^0 \end{pmatrix} = \mathbf{R}(\alpha) \begin{pmatrix} \eta_1 \\ \eta_2 \end{pmatrix}. \quad (2.41)$$

The mixing angle α of the CP -even scalars is given by

$$\sin 2\alpha = \frac{2\mathbf{M}_{12}^\eta}{\sqrt{(\mathbf{M}_{11}^\eta - \mathbf{M}_{22}^\eta)^2 + 4(\mathbf{M}_{12}^\eta)^2}}, \quad (2.42a)$$

$$\cos 2\alpha = \frac{\mathbf{M}_{11}^\eta - \mathbf{M}_{22}^\eta}{\sqrt{(\mathbf{M}_{11}^\eta - \mathbf{M}_{22}^\eta)^2 + 4(\mathbf{M}_{12}^\eta)^2}}. \quad (2.42b)$$

¹As usual mass terms of the Goldstone bosons arise solely from the gauge-fixing part of the Lagrangian. In the 't Hooft-Feynman gauge, which is used in this thesis, the resulting masses of the Goldstone-bosons are given by the masses of the corresponding gauge bosons.

Restricting the mixing angle to

$$-\frac{\pi}{2} \leq \alpha < \frac{\pi}{2} \quad (2.43)$$

fixes the sign of the mass eigenstates h^0 and H^0 .

From now on we will use the short notation

$$\sin x = s_x, \quad \cos x = c_x, \quad \tan x = t_x \quad (2.44)$$

for all the appearances of the mixing angles.

The parameters m_{11}^2 and m_{22}^2 can be eliminated by the minimum conditions. Five of the remaining parameters can be traded for the scalar masses, the sum of the vacuum expectation values v^2 and the mixing angles α and β , resulting in

$$\Lambda_1 = -\frac{m_{12}^2 t_\beta}{v^2 c_\beta^2} + \frac{c_\alpha^2 m_{H^0}^2 + m_{h^0}^2 s_\alpha^2}{v^2 c_\beta^2} + \frac{1}{2} \Lambda_7 t_\beta^3 - \frac{3\Lambda_6 t_\beta}{2}, \quad (2.45)$$

$$\Lambda_2 = -\frac{m_{12}^2}{v^2 s_\beta^2 t_\beta} + \frac{c_\alpha^2 m_{h^0}^2 + m_{H^0}^2 s_\alpha^2}{v^2 s_\beta^2} + \frac{\Lambda_6}{2t_\beta^3} - \frac{3\Lambda_7}{2t_\beta}, \quad (2.46)$$

$$\Lambda_3 = -\frac{m_{12}^2}{v^2 c_\beta s_\beta} + \frac{2m_{H^\pm}^2}{v^2} - \frac{c_\alpha s_\alpha (m_{h^0}^2 - m_{H^0}^2)}{v^2 c_\beta s_\beta} - \frac{\Lambda_6}{2t_\beta} - \frac{\Lambda_7 t_\beta}{2}, \quad (2.47)$$

$$\Lambda_4 = \frac{m_{12}^2}{v^2 c_\beta s_\beta} + \frac{m_{A^0}^2 - 2m_{H^\pm}^2}{v^2} - \frac{\Lambda_6}{2t_\beta} - \frac{\Lambda_7 t_\beta}{2}, \quad (2.48)$$

$$\Lambda_5 = \frac{m_{12}^2}{v^2 c_\beta s_\beta} - \frac{m_{A^0}^2}{v^2} - \frac{\Lambda_6}{2t_\beta} - \frac{\Lambda_7 t_\beta}{2}. \quad (2.49)$$

In addition v^2 is fixed by the electric charge and the masses of the gauge bosons (see Section 2.3). The remaining free parameters are m_{12}^2 , Λ_6 and Λ_7 . As discussed before we will use $\Lambda_{6,7} = 0$ in the examination of the two-loop corrections to electroweak precision observables. Moreover we will use the dimensionless parameter

$$\lambda_5 = \frac{2m_{12}^2}{v^2 s_\beta c_\beta}. \quad (2.50)$$

This combination is used in the THDM modelfile of **FeynArts** [130], a Mathematica program for the automatic generation of Feynman diagrams. In this modelfile, the Feynman rules of the THDM are derived from the Higgs potential with the conventions from [131], which contains the parameter λ_5 . Since the two-loop corrections are obtained with the help of **FeynArts**, the parameter λ_5 is used instead of m_{12}^2 in the discussion of the results.

The field rotations in (2.33) and (2.41) together with the minimum conditions in (2.32) result in diagonal propagators and vanishing Goldstone-boson masses at the tree-level. At higher-orders the propagators receive off-diagonal corrections since the scalars with identical quantum numbers (neutral CP -even, neutral CP -odd and charged scalars) can mix. Identifying the off-diagonal mass-terms at tree-level is advantageous for the renormalization of the mixing terms and the Goldstone-boson masses in Chapter 4. Therefore the original fields in (2.22) are rotated by

$$\begin{pmatrix} G^\pm \\ H^\pm \end{pmatrix} = \mathbf{R}(\beta_c) \begin{pmatrix} \phi_1^\pm \\ \phi_2^\pm \end{pmatrix}, \quad \begin{pmatrix} G^0 \\ A^0 \end{pmatrix} = \mathbf{R}(\beta_n) \begin{pmatrix} \chi_1 \\ \chi_2 \end{pmatrix}, \quad \begin{pmatrix} H^0 \\ h^0 \end{pmatrix} = \mathbf{R}(\alpha) \begin{pmatrix} \eta_1 \\ \eta_2 \end{pmatrix}, \quad (2.51)$$

before imposing the minimum condition, leading to

$$\begin{aligned} V = & -T_h h^0 - T_H H^0 + \begin{pmatrix} G^- & H^- \end{pmatrix} \tilde{\mathbf{M}}_{G^\pm H^\pm} \begin{pmatrix} G^+ \\ H^+ \end{pmatrix} \\ & + \frac{1}{2} \begin{pmatrix} G^0 & A^0 \end{pmatrix} \tilde{\mathbf{M}}_{G^0 A^0} \begin{pmatrix} G^0 \\ A^0 \end{pmatrix} + \frac{1}{2} \begin{pmatrix} H^0 & h^0 \end{pmatrix} \tilde{\mathbf{M}}_{H^0 h^0} \begin{pmatrix} H^0 \\ h^0 \end{pmatrix} + \dots \end{aligned} \quad (2.52)$$

The mixing angles of the CP -odd and the charged scalars are denoted by β_n and β_c to distinguish them from the angle β , which is defined by the ratio of v_2 and v_1 in (2.35). The terms linear in $\eta_{1,2}$ are translated into the tadpoles

$$T_h = c_\alpha T_2 - s_\alpha T_1 \quad (2.53a)$$

$$T_H = c_\alpha T_1 + s_\alpha T_2 \quad (2.53b)$$

of h^0 and H^0 . The matrices for the quadratic terms are given by

$$\tilde{\mathbf{M}}_{H^0 h^0} = \begin{pmatrix} \tilde{m}_{H^0}^2 & \tilde{m}_{H^0 h^0}^2 \\ \tilde{m}_{H^0 h^0}^2 & \tilde{m}_{h^0}^2 \end{pmatrix} = \mathbf{R}(\alpha) [\mathbf{M}^n + \mathbf{M}^T] \mathbf{R}(\alpha)^{-1}, \quad (2.54a)$$

$$\tilde{\mathbf{M}}_{G^0 A^0} = \begin{pmatrix} \tilde{m}_{G^0}^2 & \tilde{m}_{G^0 A^0}^2 \\ \tilde{m}_{G^0 A^0}^2 & \tilde{m}_{A^0}^2 \end{pmatrix} = \mathbf{R}(\beta_n) [\mathbf{M}^x + \mathbf{M}^T] \mathbf{R}(\beta_n)^{-1}, \quad (2.54b)$$

$$\tilde{\mathbf{M}}_{G^\pm H^\pm} = \begin{pmatrix} \tilde{m}_{G^\pm}^2 & \tilde{m}_{G^\pm H^\pm}^2 \\ \tilde{m}_{G^\pm H^\pm}^2 & \tilde{m}_{H^\pm}^2 \end{pmatrix} = \mathbf{R}(\beta_c) [\mathbf{M}^\phi + \mathbf{M}^T] \mathbf{R}(\beta_c)^{-1}. \quad (2.54c)$$

The elements of the last two matrices can be expressed very simply in terms of the tadpoles T_{h^0} , T_{H^0} and the masses m_{H^\pm} and m_{A^0} defined by (2.37) and (2.38). For the CP -odd scalars they take the form

$$\tilde{m}_{G^0}^2 = m_{A^0}^2 s_{\beta-\beta_n}^2 + T_h \frac{(c_{\alpha-\beta} c_{2\beta_n} - c_{\alpha+\beta})}{v s_{2\beta}} + T_H \frac{(c_{2\beta_n} s_{\alpha-\beta} - s_{\alpha+\beta})}{v s_{2\beta}}, \quad (2.55)$$

$$\tilde{m}_{A^0}^2 = m_{A^0}^2 c_{\beta-\beta_n}^2 - T_h \frac{(c_{\alpha+\beta} + c_{\alpha-\beta} c_{2\beta_n})}{v s_{2\beta}} - T_H \frac{(c_{2\beta_n} s_{\alpha-\beta} + s_{\alpha+\beta})}{v s_{2\beta}}, \quad (2.56)$$

$$\tilde{m}_{G^0 A^0} = -\frac{1}{2} m_{A^0}^2 s_{2\beta-2\beta_n} - T_h \frac{c_{\alpha-\beta} s_{2\beta_n}}{v s_{2\beta}} - T_H \frac{s_{2\beta_n} s_{\alpha-\beta}}{v s_{2\beta}}. \quad (2.57)$$

The matrix-elements for the charged sectors are given by

$$\tilde{m}_{G^\pm}^2 = s_{\beta-\beta_c}^2 m_{H^\pm}^2 + T_h \frac{(c_{2\beta_c} c_{\alpha-\beta} - c_{\alpha+\beta})}{v s_{2\beta}} + T_H \frac{(c_{2\beta_c} s_{\alpha-\beta} - s_{\alpha+\beta})}{v s_{2\beta}}, \quad (2.58)$$

$$\tilde{m}_{H^\pm}^2 = c_{\beta-\beta_c}^2 m_{H^\pm}^2 - T_h \frac{(c_{\alpha+\beta} + c_{2\beta_c} c_{\alpha-\beta})}{v s_{2\beta}} - T_H \frac{(c_{2\beta_c} s_{\alpha-\beta} + s_{\alpha+\beta})}{v s_{2\beta}}, \quad (2.59)$$

$$\tilde{m}_{G^\pm H^\pm} = -\frac{1}{2} s_{2\beta-2\beta_c} m_{H^\pm}^2 - T_h \frac{c_{\alpha-\beta} s_{2\beta_c}}{v s_{2\beta}} - T_H \frac{s_{2\beta_c} s_{\alpha-\beta}}{v s_{2\beta}}. \quad (2.60)$$

The minimums-conditions are then equivalent to the requirement that the tadpoles vanish,

$$T_h = 0, \quad T_H = 0, \quad (2.61)$$

and the off-diagonal matrix-elements are equal to zero. This yields

$$\beta_n = \beta_c = \beta \quad (2.62)$$

and fixes the mixing-angle α according to (2.42).

2.3 Higgs-boson interaction with gauge bosons

The two doublets couple to the gauge bosons via the kinetic term

$$\mathcal{L}_{\text{kin}} = \sum_{i=1,2} (D_\mu \Phi_i)^\dagger (D^\mu \Phi_i) \quad (2.63)$$

with the covariant derivative from (2.13). Inserting the vacuum expectation values from (2.20) leads to the quadratic terms

$$\frac{g_2^2 v^2}{8} (W_\mu^1 + iW_\mu^2) (W^{1\mu} - iW^{2\mu}) + \frac{v^2}{8} (W_\mu^3, B_\mu) \begin{pmatrix} g_2^2 & -g_1 g_2 \\ -g_1 g_2 & g_1^2 \end{pmatrix} \begin{pmatrix} W^{3\mu} \\ B^\mu \end{pmatrix}. \quad (2.64)$$

To obtain diagonal mass terms, the fields W_μ^a and B_μ have to be transformed to the physical fields

$$W_\mu^\pm = \frac{1}{\sqrt{2}} (W_\mu^1 \mp iW_\mu^2) \quad (2.65)$$

and

$$\begin{pmatrix} Z_\mu \\ A_\mu \end{pmatrix} = \begin{pmatrix} \cos \theta_W & -\sin \theta_W \\ \sin \theta_W & \cos \theta_W \end{pmatrix} \begin{pmatrix} W_\mu^3 \\ B_\mu \end{pmatrix}, \quad (2.66)$$

with the electroweak mixing angle θ_W and

$$\cos \theta_W = c_W = \frac{g_2}{\sqrt{g_1^2 + g_2^2}}, \quad \sin \theta_W = s_W = \frac{g_1}{\sqrt{g_1^2 + g_2^2}}. \quad (2.67)$$

With the physical fields the mass terms in (2.64) become

$$M_W^2 W_\mu^- W^{+\mu} + \frac{1}{2} (Z_\mu, A_\mu) \begin{pmatrix} M_Z^2 & 0 \\ 0 & 0 \end{pmatrix} \begin{pmatrix} Z^\mu \\ A^\mu \end{pmatrix}. \quad (2.68)$$

Here the physical masses are

$$M_W^2 = \frac{g_2^2 v^2}{4} \quad (2.69)$$

and

$$M_Z^2 = \frac{(g_1^2 + g_2^2) v^2}{4}. \quad (2.70)$$

Therefore we obtain for the weak mixing angle the relation

$$c_W = \frac{M_W}{M_Z}. \quad (2.71)$$

The massless field A_μ is identified with the photon field and its coupling to the electron with the electric charge $e = \sqrt{4\pi} \alpha_{em}$, where α_{em} is the electromagnetic fine structure constant. For the gauge couplings this yields

$$e = \frac{g_1 g_2}{\sqrt{g_1^2 + g_2^2}}, \quad (2.72)$$

or

$$g_1 = \frac{e}{c_W}, \quad g_2 = \frac{e}{s_W}. \quad (2.73)$$

The parameter v^2 can be expressed in terms of the electric charge and the gauge boson masses via

$$v^2 = v_1^2 + v_2^2 = \frac{4M_W^2 s_W^2}{e^2}, \quad (2.74)$$

such that

$$v_1 = \frac{2M_W s_W}{e} \cos \beta \quad (2.75)$$

and

$$v_2 = \frac{2M_W s_W}{e} \sin \beta. \quad (2.76)$$

The Feynman rules for the interaction of the gauge bosons to the Higgs fields are given in Appendix A.

Model	u^R	d^R	l^R
type-I	-1	-1	-1
type-II	-1	+1	+1
type-X	-1	-1	+1
type-Y	-1	+1	-1

Table 2.2: Transformations of the right-handed fermion singlets under the discrete Z_2 symmetry in the different versions of the THDM

Model	Φ_u	Φ_d	Φ_l
type-I	Φ_2	Φ_2	Φ_2
type-II	Φ_2	Φ_1	Φ_2
type-X	Φ_2	Φ_2	Φ_1
type-Y	Φ_2	Φ_1	Φ_2

Table 2.3: Doublet-assignment in the different Z_2 symmetric versions of the THDM

2.4 Yukawa interaction

The possible interaction between scalars and fermions are restricted strongly by the experimental limits on tree-level flavour-changing neutral currents (FCNCs) obtained for example from the meson decays or meson mixing. In the SM, the diagonalization of the fermion mass matrix diagonalizes also the interaction of the Higgs boson with the fermions and FCNC processes are automatically absent at the tree-level.

In extensions with more than one scalar doublet, each of the doublets can couple to the quarks or leptons with its own Yukawa matrix. In general these matrices cannot be simultaneously diagonalized and introduce flavour changing couplings for the neutral scalars.

It has been shown in [132] and [133] that a necessary and sufficient condition to avoid the FCNCs by neutral Higgs exchange at the tree-level is that not more than one of the doublets couples to right-handed fermions of a given charge. In the THDM, this requirement can be enforced by imposing a discrete Z_2 symmetry on the doublets and the right-handed fermions. Depending on the charge-assignment to the right-handed lepton or quark states, the Z_2 symmetry can be imposed in four different ways, which are usually classified as type-I, type-II, type-X or type-Y. The possible realization differ in the transformation of the right-handed fermion singlets under the Z_2 symmetry. Whether the right-handed fermion singlets transform even ($f^R \rightarrow f^R$) or odd ($f^R \rightarrow -f^R$) under the Z_2 symmetry in the different models is summarized in Table 2.2. Denoting the doublet which couples to the right-handed fermion-states f ($f = u, d, l$) by Φ_f , the Yukawa-part of the Lagrangian can be written in the general form

$$\mathcal{L}_Y = - \sum_{i,j=1}^3 \left[(Y'_l)_{ij} \bar{L}_i^{\prime L} \Phi_l l_j^{\prime R} + (Y'_d)_{ij} \bar{Q}_i^{\prime L} \Phi_d d_j^{\prime R} + (Y'_u)_{ij} \bar{Q}_i^{\prime L} \tilde{\Phi}_u u_j^{\prime R} + \text{h.c.} \right] \quad (2.77)$$

with $\tilde{\Phi}_i \equiv i\sigma_2 \Phi_i^*$. The assignment of Φ_f ($f = u, d, l$) in the different models is given in Table 2.3. The diagonalization of the Yukawa-matrices transforms the fermion-states from the weak-interaction basis into the mass eigenstates.

For the leptons the bi-unitary transformation

$$U_l^{L\dagger} Y'_l U_l^R = Y_l = \begin{pmatrix} y_e & 0 & 0 \\ 0 & y_\mu & 0 \\ 0 & 0 & y_\tau \end{pmatrix}, \quad (2.78)$$

gives the field redefinitions

$$L_i^L = (U_l^{L\dagger})_{ij} L_j'^L = \begin{pmatrix} \nu_i \\ l_i^L \end{pmatrix}, \quad (2.79)$$

$$l_i^R = (U_l^{R\dagger})_{ij} l_j'^R. \quad (2.80)$$

Since we are discarding right-handed neutrino states, the neutrino fields can be redefined such that the matrix U_l^L is canceled in the interaction of the leptons with the charged Higgs states or the W bosons. The masses of the unprimed states are given by

$$\frac{v_l}{\sqrt{2}} Y_l = \begin{pmatrix} m_e & 0 & 0 \\ 0 & m_\mu & 0 \\ 0 & 0 & m_\tau \end{pmatrix} \quad (2.81)$$

where v_l denotes the vacuum expectation value of the doublet, which is assigned to Φ_l in Table 2.3.

The Yukawa-coupling matrices of the quarks are diagonalized by the bi-unitary transformations

$$U_u^{L\dagger} Y_u' U_u^R = Y_u = \begin{pmatrix} y_u & 0 & 0 \\ 0 & y_c & 0 \\ 0 & 0 & y_t \end{pmatrix} \quad (2.82)$$

and

$$U_d^{L\dagger} Y_d' U_d^R = Y_d = \begin{pmatrix} y_d & 0 & 0 \\ 0 & y_s & 0 \\ 0 & 0 & y_t \end{pmatrix}. \quad (2.83)$$

The resulting quark mass states are given by the field redefinitions

$$\begin{aligned} d_i^R &= (U_d^{R\dagger})_{ij} d_j'^R, & d_i^L &= (U_d^{L\dagger})_{ij} d_j'^L, \\ u_i^R &= (U_u^{R\dagger})_{ij} u_j'^R, & u_i^L &= (U_u^{L\dagger})_{ij} u_j'^L. \end{aligned} \quad (2.84)$$

Due to unitarity, the matrices $U_q^{L,R}$ cancel themselves in the interaction of the quark fields with the neutral components of the scalar doublets. This leads to the diagonal mass-matrix

$$\frac{v_u}{\sqrt{2}} Y_u = \begin{pmatrix} m_u & 0 & 0 \\ 0 & m_c & 0 \\ 0 & 0 & m_t \end{pmatrix}, \quad (2.85)$$

$$\frac{v_d}{\sqrt{2}} Y_d = \begin{pmatrix} m_d & 0 & 0 \\ 0 & m_s & 0 \\ 0 & 0 & m_b \end{pmatrix}, \quad (2.86)$$

and a flavour-diagonal interaction between the quarks and the neutral scalars. The up-type quarks receive their mass in all of the different version of the THDM by the doublet Φ_2 such that $v_u = v_2$. For the down-type quarks v_d denotes the vacuum expectation value, which is assigned to the doublet Φ_d in Table 2.3. In the interaction of the quark with the charged component of the doublets, the different field-redefinitions of the up- and down-type quarks introduce the CKM-matrix

$$V = U_u^{L\dagger} U_d^L, \quad (2.87)$$

	ξ_h^u	ξ_h^d	ξ_h^l	ξ_H^u	ξ_H^d	ξ_H^l	ξ_A^u	ξ_A^d	ξ_A^l
type-I	$\frac{c_\alpha}{s_\beta}$	$\frac{c_\alpha}{s_\beta}$	$\frac{c_\alpha}{s_\beta}$	$\frac{s_\alpha}{s_\beta}$	$\frac{s_\alpha}{s_\beta}$	$\frac{s_\alpha}{s_\beta}$	$\frac{1}{t_\beta}$	$-\frac{1}{t_\beta}$	$-\frac{1}{t_\beta}$
type-II	$\frac{c_\alpha}{s_\beta}$	$-\frac{s_\alpha}{c_\beta}$	$-\frac{s_\alpha}{c_\beta}$	$\frac{s_\alpha}{s_\beta}$	$\frac{c_\alpha}{c_\beta}$	$\frac{c_\alpha}{c_\beta}$	$\frac{1}{t_\beta}$	t_β	t_β
type-X	$\frac{c_\alpha}{s_\beta}$	$\frac{c_\alpha}{s_\beta}$	$-\frac{s_\alpha}{c_\beta}$	$\frac{s_\alpha}{s_\beta}$	$\frac{s_\alpha}{s_\beta}$	$\frac{c_\alpha}{c_\beta}$	$\frac{1}{t_\beta}$	$-\frac{1}{t_\beta}$	t_β
type-Y	$\frac{c_\alpha}{s_\beta}$	$-\frac{s_\alpha}{c_\beta}$	$\frac{c_\alpha}{s_\beta}$	$\frac{s_\alpha}{s_\beta}$	$\frac{c_\alpha}{c_\beta}$	$\frac{s_\alpha}{s_\beta}$	$\frac{1}{t_\beta}$	t_β	$-\frac{1}{t_\beta}$

 Table 2.4: Proportionality factors of the couplings of the fermions to the scalars in the different versions of the Z_2 symmetric THDM

which enters also the interaction of the quarks with the W boson, if the electroweak eigenstates of the quarks in the kinetic part in (2.14) are expressed in terms of the mass eigenstates defined via (2.84).

With the mass eigenstates of the Higgs bosons the Yukawa-part of the Lagrangian can be written as follows,

$$\begin{aligned}
 \mathcal{L}_Y = & - \sum_l \left[(\bar{\psi}_l \psi_l) m_l + \frac{\xi_h^l m_l}{v} (\bar{\psi}_l \psi_l) h^0 + \frac{\xi_H^l m_l}{v} (\bar{\psi}_l \psi_l) H^0 \right. \\
 & + \frac{im_l}{v} (\bar{\psi}_l \gamma_5 \psi_l) G^0 - \frac{i\xi_A^l m_l}{v} (\bar{\psi}_l \gamma_5 \psi_l) A^0 \\
 & + \frac{\sqrt{2}m_l}{v} \left((\bar{\psi}_l \omega_- \psi_{\nu_l}) G^- + (\bar{\psi}_{\nu_l} \omega_+ \psi_l) G^+ \right) \\
 & \left. - \frac{\sqrt{2}\xi_A^l m_l}{v} \left((\bar{\psi}_l \omega_- \psi_{\nu_l}) H^- + (\bar{\psi}_{\nu_l} \omega_+ \psi_l) H^+ \right) \right] \\
 & - \sum_j \left[(\bar{\psi}_{d_j} \psi_{d_j}) m_{d_j} + (\bar{\psi}_{u_j} \psi_{u_j}) m_{u_j} \right. \\
 & - G^0 \left(\frac{im_{u_j}}{v} (\bar{\psi}_{u_j} \gamma_5 \psi_{u_j}) - \frac{im_{d_j}}{v} (\bar{\psi}_{d_j} \gamma_5 \psi_{d_j}) \right) \\
 & - A^0 \left(\frac{im_{d_j} \xi_A^d}{v} (\bar{\psi}_{d_j} \gamma_5 \psi_{d_j}) + \frac{im_{u_j} \xi_A^u}{v} (\bar{\psi}_{u_j} \gamma_5 \psi_{u_j}) \right) \\
 & + h^0 \left(\frac{m_{d_j} \xi_h^d}{v} (\bar{\psi}_{d_j} \psi_{d_j}) + \frac{m_{u_j} \xi_h^u}{v} (\bar{\psi}_{u_j} \psi_{u_j}) \right) \\
 & \left. + H^0 \left(\frac{m_{d_j} \xi_H^d}{v} (\bar{\psi}_{d_j} \psi_{d_j}) + \frac{m_{u_j} \xi_H^u}{v} (\bar{\psi}_{u_j} \psi_{u_j}) \right) \right] \\
 & + \sum_{j,i} \left[G^+ \left(\frac{\sqrt{2}m_{u_i} V_{ij}}{v} (\bar{\psi}_{u_i} \omega_- \psi_{d_i}) - \frac{\sqrt{2}m_{d_j} V_{ij}}{v} (\bar{\psi}_{u_i} \omega_+ \psi_{d_j}) \right) \right. \\
 & + G^- \left(\frac{\sqrt{2}m_{u_i} V_{ij}^*}{v} (\bar{\psi}_{d_j} \omega_+ \psi_{u_i}) - \frac{\sqrt{2}m_{d_j} V_{ij}^*}{v} (\bar{\psi}_{d_j} \omega_- \psi_{u_j}) \right) \\
 & + H^+ \left(\frac{\sqrt{2}m_{d_j} V_{ij} \xi_A^d}{v} (\bar{\psi}_{u_i} \omega_+ \psi_{d_j}) + \frac{\sqrt{2}m_{u_i} V_{ij} \xi_A^u}{v} (\bar{\psi}_{u_i} \omega_- \psi_{d_i}) \right) \\
 & \left. + H^- \left(\frac{\sqrt{2}m_{d_j} V_{ij}^* \xi_A^d}{v} (\bar{\psi}_{d_j} \omega_- \psi_{u_j}) + \frac{\sqrt{2}m_{u_i} V_{ij}^* \xi_A^u}{v} (\bar{\psi}_{d_j} \omega_+ \psi_{u_i}) \right) \right]. \quad (2.88)
 \end{aligned}$$

The factors ξ_s^f for the different versions of the Z_2 -symmetric THDM are specified in Table 2.4. The resulting Feynman rules for the Yukawa-interaction are given in Appendix A.

If the discrete symmetries are not imposed in the Yukawa sector each of the doublets is in principle allowed to couple to all fermions and a different mechanism has to be considered

in order to suppress the FCNCs. For example in the (flavour-)aligned model [134, 135] one assumes that the Yukawa-coupling matrices of the two doublets are proportional to each other. The diagonalization of the fermion mass matrices eliminates then all the tree-level FCNC. This flavour-aligned model contains three arbitrary proportionality constants and the four different realization of the Z_2 symmetric Yukawa sector are contained as specific choices of the proportionality constants. Another example is known as the type-III models [136–139], in which the the flavour-changing couplings are proportional to $\sqrt{m_i m_j}/v$, where m_i and m_j are the masses of the fermions interacting with the neutral scalars. This so-called Cheng-Sher ansatz [136] suppresses the Yukawa-couplings of the first two generations, from which the most strict bounds on the FCNCs arise. More details on these and other models with flavour-changing interactions of the neutral scalars can be found in [58] and references therein. In this work we will restrict ourselves on the Z_2 symmetric versions of the THDM.

2.5 The alignment limit

Due to the fact that a scalar particle with a mass of approximately 125 GeV has been observed at the LHC [6, 7] we have to identify one of the CP -even scalars with the observed resonance. Choosing h^0 (without loss of generality) corresponds to setting

$$m_{h^0} = 125 \text{ GeV}. \quad (2.89)$$

Furthermore the analysis of the Higgs couplings by ATLAS [140] and CMS [141] indicate no significant deviations from the couplings of the Higgs boson in the SM. Therefore we choose to work in the alignment limit [68, 69, 75], in which the angles are correlated via

$$\alpha = \beta - \frac{\pi}{2} \quad (2.90)$$

and the couplings of h^0 to the vector bosons and fermions are identical to the corresponding couplings of the Higgs boson in the SM. In this limit the CP -even Higgs states are obtained by

$$\begin{pmatrix} H^0 \\ h^0 \end{pmatrix} = \begin{pmatrix} s_\beta & -c_\beta \\ c_\beta & s_\beta \end{pmatrix} \begin{pmatrix} \eta_1 \\ \eta_2 \end{pmatrix} \quad (2.91)$$

and the two doublets can be rewritten as

$$\Phi_1 = c_\beta \Phi_{\text{SM}} - s_\beta \Phi_{\text{NS}}, \quad (2.92)$$

$$\Phi_2 = s_\beta \Phi_{\text{SM}} + c_\beta \Phi_{\text{NS}} \quad (2.93)$$

with

$$\Phi_{\text{SM}} = \begin{pmatrix} G^+ \\ \frac{1}{\sqrt{2}} (v + h^0 + iG^0) \end{pmatrix}, \quad (2.94)$$

$$\Phi_{\text{NS}} = \begin{pmatrix} H^+ \\ \frac{1}{\sqrt{2}} (-H^0 + iA^0) \end{pmatrix}. \quad (2.95)$$

Moreover, the relations for Λ_1 , Λ_2 and Λ_3 are given by

$$\Lambda_1 = \frac{1}{v^2} \left(m_{h^0}^2 + m_{H^0}^2 t_\beta^2 - \frac{m_{12}^2 t_\beta}{c_\beta^2} \right) + \frac{1}{2} \Lambda_7 t_\beta^3 - \frac{3\Lambda_6 t_\beta}{2}, \quad (2.96)$$

$$\Lambda_2 = \frac{1}{v^2} \left(m_{h^0}^2 + \frac{m_{H^0}^2}{t_\beta^2} - \frac{m_{12}^2}{s_\beta^2 t_\beta} \right) + \frac{\Lambda_6}{2t_\beta^3} - \frac{3\Lambda_7}{2t_\beta}, \quad (2.97)$$

$$\Lambda_3 = \frac{1}{v^2} \left(m_{h^0}^2 - m_{H^0}^2 + 2m_{H^\pm}^2 - \frac{m_{12}^2}{c_\beta s_\beta} \right) - \frac{\Lambda_6}{2t_\beta} - \frac{\Lambda_7 t_\beta}{2}. \quad (2.98)$$

The potential can be rewritten in terms of the doublets given in (2.94) and (2.95). For the classification with respect to the custodial symmetry in Chapter 5, we split it in the four parts:

$$V = V_I + V_{II} + V_{III} + V_{IV}; \quad (2.99)$$

$$V_I = \frac{m_{h^0}^2}{2v^2} \left(\Phi_{SM}^\dagger \Phi_{SM} \right)^2 - \frac{1}{2} m_{h^0}^2 \left(\Phi_{SM}^\dagger \Phi_{SM} \right), \quad (2.99a)$$

$$V_{II} = \left[\frac{1}{2v^2} \left(m_{h^0}^2 + \frac{4}{t_{2\beta}^2} \left(m_{H^0}^2 - \frac{m_{12}^2}{s_\beta c_\beta} \right) \right) + \frac{\Lambda_6 (2c_{2\beta} - 1)}{4c_\beta s_\beta^3} - \frac{\Lambda_7 (2c_{2\beta} + 1)}{4c_\beta^3 s_\beta} \right] \left(\Phi_{NS}^\dagger \Phi_{NS} \right)^2 + \left(\frac{m_{12}^2}{c_\beta s_\beta} - \frac{m_{h^0}^2}{2} \right) \left(\Phi_{NS}^\dagger \Phi_{NS} \right), \quad (2.99b)$$

$$V_{III} = \left(\frac{m_{A^0}^2}{v^2} - \frac{2m_{H^\pm}^2}{v^2} + \frac{m_{H^0}^2}{v^2} \right) \left(\Phi_{SM}^\dagger \Phi_{NS} \right) \left(\Phi_{NS}^\dagger \Phi_{SM} \right) + \left(\frac{m_{H^0}^2}{2v^2} - \frac{m_{A^0}^2}{2v^2} \right) \left(\left(\Phi_{NS}^\dagger \Phi_{SM} \right)^2 + \left(\Phi_{SM}^\dagger \Phi_{NS} \right)^2 \right) + \left(\Phi_{NS}^\dagger \Phi_{NS} \right) \left(\Phi_{SM}^\dagger \Phi_{SM} \right) \left(\frac{2m_{H^\pm}^2}{v^2} + \frac{m_{h^0}^2}{v^2} - \frac{2m_{12}^2}{v^2 c_\beta s_\beta} \right), \quad (2.99c)$$

$$V_{IV} = \left(\frac{2}{v^2 t_{2\beta}} \left(m_{H^0}^2 - \frac{m_{12}^2}{c_\beta s_\beta} \right) - \frac{\Lambda_7}{2c_\beta^2} + \frac{\Lambda_6}{2s_\beta^2} \right) \left(\Phi_{NS}^\dagger \Phi_{NS} \right) \left(\Phi_{NS}^\dagger \Phi_{SM} + \Phi_{SM}^\dagger \Phi_{NS} \right). \quad (2.99d)$$

We see that only the parts V_{II} and V_{IV} depend on the parameters Λ_6 and Λ_7 . The part V_{II} gives the quartic couplings between four non-standard scalars. As we will see in Chapter 5 the non-standard corrections to the ρ parameter are independent of these couplings. The part V_{IV} gives the coupling between three non-standard scalars, when the vacuum expectation value

$$\langle \Phi_{SM} \rangle = \frac{1}{\sqrt{2}} \begin{pmatrix} 0 \\ v \end{pmatrix} \quad (2.100)$$

is inserted for the doublet Φ_{SM} . The only dependence on Λ_6 and Λ_7 in $\Delta\rho$ follows from these triple non-standard scalar couplings. For the THDM without a hard Z_2 violation, the term V_{IV} is simply given by

$$V_{IV} = \frac{1}{t_{2\beta}} \left(\frac{2m_{H^0}^2}{v^2} - \lambda_5 \right) \left(\Phi_{NS}^\dagger \Phi_{NS} \cdot \Phi_{NS}^\dagger \Phi_{SM} + \Phi_{NS}^\dagger \Phi_{NS} \cdot \Phi_{SM}^\dagger \Phi_{NS} \right), \quad (2.101)$$

where we replaced m_{12}^2 by λ_5 with the help of (2.50).

By imposing (2.90) on the Yukawa-couplings given in Table 2.4 one finds that the resulting coupling between the SM-like scalar h^0 and the fermions are identical to the Yukawa couplings in the SM. The couplings of the non-standard Higgs states A^0 , H^0 and H^\pm to the top-quark receive an additional factor of t_β^{-1} in all of the different models. The couplings of the non-standard Higgs bosons to the bottom quark is model dependent: in the models of type-I and type-X they are proportional to t_β^{-1} , whereas in the THDM of type-II or type-Y they are proportional to t_β .

2.6 The Inert-Higgs-Doublet Model

The Inert-Higgs-Doublet Model (IHDM) is a version of a THDM with an exact, unbroken Z_2 symmetry [59]. Under this symmetry all the fermions and gauge boson as well as the doublet Φ_1 transform even, whereas Φ_2 transforms like $\Phi_2 \rightarrow -\Phi_2$. The potential of the IHDM is therefore given by (2.16) with

$$m_{12}^2 = 0, \quad (2.102)$$

$$\Lambda_6 = 0, \quad (2.103)$$

$$\Lambda_7 = 0. \quad (2.104)$$

Since the Z_2 symmetry should not be spontaneously broken, only the doublet Φ_1 is allowed to develop a non-vanishing vacuum expectation value

$$\langle \Phi_1 \rangle = \begin{pmatrix} 0 \\ \frac{v}{\sqrt{2}} \end{pmatrix}, \quad \langle \Phi_2 \rangle = \begin{pmatrix} 0 \\ 0 \end{pmatrix}, \quad (2.105)$$

which fulfills the minimum condition

$$v^2 = -\frac{2m_{11}^2}{\Lambda_1}. \quad (2.106)$$

With the expansion around the vacuum state, the SM-like doublet Φ_1 and the so-called inert doublet Φ_2 are written as

$$\Phi_1 = \begin{pmatrix} G^\pm \\ \frac{1}{\sqrt{2}}(v + h^0 + iG^0) \end{pmatrix}, \quad \Phi_2 = \begin{pmatrix} H^\pm \\ \frac{1}{\sqrt{2}}(H^0 + iA^0) \end{pmatrix}, \quad (2.107)$$

where G^0 and G^\pm are the Goldstone bosons and h^0 , H^0 , A^0 and H^\pm are already mass eigenstates. The scalar h^0 is identical to the Higgs boson in the SM and its mass is given by

$$m_{h^0}^2 = -2m_{11}^2 = \Lambda_1 v^2. \quad (2.108)$$

The inert doublet gives four massive particles: two neutral scalars A^0 and H^0 and a pair of charged states H^\pm . Their masses are

$$m_{H^0}^2 = m_{22}^2 + \frac{1}{2}(\Lambda_3 + \Lambda_4 + \Lambda_5)v^2, \quad (2.109)$$

$$m_{A^0}^2 = m_{22}^2 + \frac{1}{2}(\Lambda_3 + \Lambda_4 - \Lambda_5)v^2, \quad (2.110)$$

$$m_{H^\pm}^2 = m_{22}^2 + \frac{1}{2}\Lambda_3 v^2. \quad (2.111)$$

The couplings of the scalar h^0 to the fermions and gauge bosons are identical to the corresponding couplings of the Higgs boson in the SM and we can identify it with the resonance observed at the LHC, which results again in (2.89). Due to the Z_2 symmetry the additional scalars H^0 , A^0 and H^\pm do not couple to the fermions in the IHDM. Moreover these scalars can only appear in pairs in their interaction vertices and the lightest of these non-standard scalars will be stable. If this stable particle is one of the neutral states H^0 or A^0 , the IHDM provides a good dark matter candidate.

Since the non-standard scalars do not couple to the fermions, a clear assignment which of the neutral scalars is CP -even and which is CP -odd is not possible. From the coupling to the gauge-bosons we can only deduce that H^0 and A^0 have opposite CP -properties. The two possible CP -transformations, $H^0 \rightarrow H^0$, $A^0 \rightarrow -A^0$ or $H^0 \rightarrow -H^0$, $A^0 \rightarrow A^0$, get interchanged by the transformation of the doublet $\Phi_2 \rightarrow i\Phi_2$, which exchanges the role of H^0 and A^0 . Moreover, the sign of Λ_5 is also phenomenologically irrelevant, since the replacement $\Lambda_5 \rightarrow -\Lambda_5$ interchanges just the masses and couplings of H^0 and A^0 . In this sense the scalars H^0 and A^0 are indistinguishable in the IHDM and we can assume without loss of generality

$$m_{H^0} < m_{A^0} \quad (2.112)$$

and

$$\Lambda_5 > 0. \quad (2.113)$$

With this choice the parameter

$$\Lambda_{345} = \Lambda_3 + \Lambda_4 + \Lambda_5, \quad (2.114)$$

is of special interest, since it describes the size of the coupling of the SM-like Higgs to the dark matter candidate.

The vacuum expectation value v is again fixed by electroweak symmetry breaking and one parameter of the potential is eliminated by the minimums condition. For the remaining

free parameters we choose the masses of the scalar particles, the quartic coupling of the non-standard scalars Λ_2 and the parameter Λ_{345} . With these parameters the potential of the IHDM is expressed by

$$V^{\text{IHDM}} = V_{\text{I}}^{\text{IHDM}} + V_{\text{II}}^{\text{IHDM}} + V_{\text{III}}^{\text{IHDM}}, \quad (2.115)$$

$$V_{\text{I}}^{\text{IHDM}} = \frac{m_{h^0}^2}{2v^2} \left(\Phi_1^\dagger \Phi_1 \right)^2 - \frac{1}{2} m_{h^0}^2 \left(\Phi_1^\dagger \Phi_1 \right), \quad (2.115a)$$

$$V_{\text{II}}^{\text{IHDM}} = \frac{1}{2} \Lambda_2 \left(\Phi_2^\dagger \Phi_2 \right)^2 + \frac{1}{2} \left(\Phi_2^\dagger \Phi_2 \right) \left(2m_{H^0}^2 - \Lambda_{345} v^2 \right), \quad (2.115b)$$

$$\begin{aligned} V_{\text{III}}^{\text{IHDM}} = & \frac{(m_{A^0}^2 - 2m_{H^\pm}^2 + m_{H^0}^2)}{v^2} \left(\Phi_2^\dagger \Phi_1 \right) \left(\Phi_1^\dagger \Phi_2 \right) \\ & + \frac{(m_{H^0}^2 - m_{A^0}^2)}{2v^2} \left(\left(\Phi_1^\dagger \Phi_2 \right)^2 + \left(\Phi_2^\dagger \Phi_1 \right)^2 \right) \\ & + \left(\Phi_1^\dagger \Phi_1 \right) \left(\Phi_2^\dagger \Phi_2 \right) \left(\Lambda_{345} - \frac{2(m_{H^0}^2 - m_{H^\pm}^2)}{v^2} \right). \end{aligned} \quad (2.115c)$$

2.7 Theoretical constraints

The parameters of the potential in (2.16) are subject to various restrictions. For example a stable vacuum requires the potential to be bounded from below such that it does not tend to $-\infty$ for large field values. In the THDM this requirement has to be fulfilled for all possible directions along which the component fields of $\Phi_{1,2}$ go to large values. In the THDM with $\Lambda_6 = \Lambda_7 = 0$ the conditions

$$\Lambda_1 > 0 \quad (2.116)$$

$$\Lambda_2 > 0 \quad (2.117)$$

$$\Lambda_3 + \sqrt{\Lambda_1 \Lambda_2} > 0 \quad (2.118)$$

$$\Lambda_3 + \Lambda_4 - |\Lambda_5| > -\sqrt{\Lambda_1 \Lambda_2} \quad (2.119)$$

are necessary and sufficient to ensure that the quartic terms in the potential stay positive along all directions [59, 142, 143]. These requirements should be taken with some caution, since they are very constraining and may exclude interesting scenarios (see the discussion in [58]).² Moreover, improved conditions should also consider higher-order corrections of the potential. For example a recent analysis for the THDM of type-II showed that many parameter points which are excluded by the tree-level conditions are revived if the loop-corrected, effective potential is used instead [144].

Additional constraints on the potential parameters arise from the requirement that the unitarity of the scattering matrix is not violated in scattering processes between physical scalars. Moreover, due to the Goldstone boson equivalence theorem the scattering of longitudinal gauge bosons can be calculated as scalar-scalar scattering by replacing the gauge boson with the corresponding Goldstone bosons. Due to the optical theorem, the s-wave scattering length a_0 is restricted to $|a_0| \leq 1/2$. For scalar-scalar scattering processes in the high-energy limit a_0 is directly proportional to the scalar couplings. In the SM, this has lead to an upper bound on the Higgs mass [145, 146]. The application of the analysis in the THDM [147–153] is more complicated due to the larger number of possible scattering processes and the more complex structure of the scalar quartic couplings. The scattering matrix of the coupled scalar-scalar channels can be simplified by using the original fields ϕ_i^+ , η_i and χ_i instead of the mass eigenstates with the help of unitary transformation. In the THDM with $\Lambda_6 = \Lambda_7 = 0$ the restriction on the s-wave scattering length constraints the eigenvalues of the scattering matrix

²Softer requirements allow also directions in which the quartic terms go to zero for large values of the component fields, as long as the quadratic terms do not go to negative values in this direction.

at tree-level (see [58, 151, 152]), given by

$$e_{1,2} = \frac{3}{2}(\Lambda_1 + \Lambda_2) \pm \sqrt{\frac{9}{4}(\Lambda_1 - \Lambda_2)^2 + (2\Lambda_3 + \Lambda_4)^2}, \quad (2.120)$$

$$e_{3,4} = \frac{1}{2}(\Lambda_1 + \Lambda_2) \pm \frac{1}{2}\sqrt{(\Lambda_1 - \Lambda_2)^2 + 4\Lambda_4^2}, \quad (2.121)$$

$$e_{5,6} = \frac{1}{2}(\Lambda_1 + \Lambda_2) \pm \frac{1}{2}\sqrt{(\Lambda_1 - \Lambda_2)^2 + 4\Lambda_5^2}, \quad (2.122)$$

$$e_7 = \Lambda_3 + 2\Lambda_4 - 3\Lambda_5, \quad (2.123)$$

$$e_8 = \Lambda_3 - \Lambda_5, \quad (2.124)$$

$$e_9 = \Lambda_3 + 2\Lambda_4 + 3\Lambda_5, \quad (2.125)$$

$$e_{10} = \Lambda_3 + \Lambda_5, \quad (2.126)$$

$$e_{11} = \Lambda_3 + \Lambda_4, \quad (2.127)$$

$$e_{12} = \Lambda_3 - \Lambda_4, \quad (2.128)$$

to fulfill $|e_i| \leq 8\pi$. The constraints in THDM with Z_2 violation are more complicated and were studied in [153]. For more accurate restrictions higher-order corrections need to be considered in the scattering processes. A one-loop analysis of the unitarity bounds can be found in [154, 155].

An additional constraint arises in the the THDM, due to the possibility that the potential can have several minima of different depth. In addition to charge- and CP -conserving vacua in the form of (2.20), also charge-breaking or CP -violating minima can exist. A specific set of parameters determined in terms of masses and couplings together with the requirement that the electroweak symmetry is broken selects a specific vacuum. If the selected vacuum is not the global minimum it will be metastable and can decay into the deeper minimum via tunneling. In [156, 157] it has been shown that if a neutral, CP -conserving minima exists, all the possible charge-breaking or CP -violating stationary points are automatically saddle points. However it is possible that two neutral minima can coexist in the tree-level potential of the THDM [158, 159]. Simple methods were developed in [160–162] in order to test whether the selected vacuum is the global minimum. In the CP -conserving THDM with a softly broken Z_2 symmetry, it is sufficient to check the sign of the discriminant

$$D = m_{12}^2 (m_{11}^2 - k^2 m_{22}^2) (t_\beta - k) \quad (2.129)$$

with

$$k = \left(\frac{\Lambda_1}{\Lambda_2} \right)^{\frac{1}{4}}. \quad (2.130)$$

The selected vacuum is the global minimum if and only if $D > 0$ [161]. If $D < 0$, the selected vacuum is a local minimum, which is metastable. In this case, the corresponding parameters should be excluded if the tunneling time is smaller than the age of the universe. The calculation of the vacuum lifetime is however a very complicated task. An estimation in [161] showed that for a scan over parameter points with two co-existing minima the vacuum lifetime is shorter than the age of the universe in most cases. However, the estimation relies on specific assumptions and the result might change for different assumptions.

The constraints from the stability of the vacuum and the unitarity of the scattering matrix are identical in the aligned THDM and the IHDM. In the IHDM the parameters are further constrained by

$$\frac{\mu_1^2}{\sqrt{\Lambda_1}} < \frac{\mu_2^2}{\sqrt{\Lambda_2}} \quad (2.131)$$

to ensure that the configuration in (2.105) is the global minimum of the potential [163].

Chapter 3

Higher-order corrections

The evaluation of Feynman diagrams for the calculation of higher order corrections in perturbative quantum field theories involves integrals over the momenta of particles in closed loops. The denominator of the integrand consists of the squared masses and momenta from the propagators of the particles running in the loop. If the numerator contains a Lorentz index which is originating from the integration momenta, the integral is called a tensor integral. Otherwise the integral is called a scalar integral. This chapter outlines the techniques used in the calculation of gauge-boson self-energy corrections.

3.1 Dimensional regularization

For large loop momenta the loop integrals are in general divergent. For a consistent treatment of the divergences, the integrals are redefined in a procedure called regularization. In this thesis the popular method of *dimensional regularization* is used, which preserves Lorentz and gauge invariance [164–167]. In dimensional regularization, the integrals are evaluated in a generic number of dimensions D instead of four dimensions:

$$\int d^4q \rightarrow \mu_D^{4-D} \int d^Dq. \quad (3.1)$$

In order to keep the couplings dimensionless the regularization mass parameter μ_D with mass dimension one is introduced. The integrals in D dimensions are convergent. The result can be expanded in $\delta = (D - 4)/2$ and the divergences appear as poles in δ for $\delta \rightarrow 0$.

3.2 Gauge-boson self-energies

The dominant non-standard corrections to electroweak precision observables in the THDM are given in terms of the gauge-boson self-energies. The self-energies describe the higher-order contributions in the two-point vertex functions. In the 't Hooft-Feynman gauge, which is used in this thesis, the two-point functions for the gauge bosons are given by

$$\Gamma_{\mu\nu}^{ab}(p) = -ig_{\mu\nu}(k^2 - M_a^2)\delta_{ab} - i\Sigma_{\mu\nu}^{ab}(p), \quad (3.2)$$

where p is the external momentum and $a, b = \gamma, Z$ for the neutral gauge bosons (with $M_\gamma = 0$) and $a = b = W$ for the W boson. The two-point functions are decomposed in the tree-level contributions, which are equivalent to the inverse of the tree-level gauge-boson propagator, and the self-energies $\Sigma_{\mu\nu}^{ab}$. These gauge-boson self-energies can be written in terms of scalar quantities with the help of the tensor-decomposition

$$\Sigma_{\mu\nu}^{ab}(p) = \left(g_{\mu\nu} - \frac{p_\mu p_\nu}{p^2}\right) \Sigma_T^{ab}(p^2) + \frac{p_\mu p_\nu}{p^2} \Sigma_L^{ab}(p^2). \quad (3.3)$$

The transverse and longitudinal parts are obtained by projection operators of the form

$$\Sigma_T^{ab}(p^2) = \frac{1}{D-1} \left(g^{\mu\nu} - \frac{p^\mu p^\nu}{p^2}\right) \Sigma_{\mu\nu}^{ab}(p), \quad (3.4)$$

and

$$\Sigma_L^{ab}(p^2) = \frac{p^\mu p^\nu}{p^2} \Sigma_{\mu\nu}^{ab}(p). \quad (3.5)$$

For processes with light external fermions the contributions from the longitudinal parts of the gauge-boson self-energies are suppressed by the light fermion masses and can be neglected. The transverse part, which is extracted with the help of (3.4), can be expressed just in terms of scalar loop integrals by the methods described in [168] for the one-loop case and in [169] for the two-loop case. For processes with zero external momentum, which are considered in this thesis, all the scalar loop integrals can be reduced to two types of scalar one- and two-loop integrals, which are specified in the next section.

3.2.1 One-loop integrals for self-energies

The reduction of one-loop tensor integrals was first discussed in [168]. At the one-loop order, all the tensor integrals can be reduced to a set of scalar n -point integrals, which correspond to the scalar one-loop diagrams with n external legs that are connected to the loop only by three-vertices. For $n \leq 4$ the scalar n -point integrals are denoted by A_0 , B_0 , C_0 and D_0 . The integrals for $n > 4$ can be reduced to a linear combination of the box integrals D_0 [170]. Therefore all the one-loop amplitudes can be expressed in terms of the basis integrals A_0 , B_0 , C_0 and D_0 , for which analytic results were derived in [171]. More details can be found in [172, 173]. In the following, only the necessary expression for the calculation of one-loop self-energies are reviewed.

The only one-loop scalar integrals which are needed for the evaluation of the self-energies are

$$A_0(m^2) = \int \frac{d^D q}{i\pi^2 (2\pi\mu)^{D-4}} \frac{1}{(q^2 - m^2 + i\epsilon)}, \quad (3.6)$$

$$B_0(p^2, m_1^2, m_2^2) = \int \frac{d^D q}{i\pi^2 (2\pi\mu)^{D-4}} \frac{1}{(q^2 - m_1^2 + i\epsilon)((p+q)^2 - m_2^2 + i\epsilon)}. \quad (3.7)$$

The analytic expressions up to terms of the order δ^0 can be found in [172]. Two-loop calculations contain also products of these one-loop integrals and an expansion up to the order δ^1 is necessary, which can be found in [174, 175].

The following two tensor integrals appear in the calculation of one-loop two-point functions,

$$B_\mu(p^2, m_1^2, m_2^2) = \int \frac{d^D q}{i\pi^2 (2\pi\mu)^{D-4}} \frac{q_\mu}{(q^2 - m_1^2 + i\epsilon)((p+q)^2 - m_2^2 + i\epsilon)}, \quad (3.8)$$

$$B_{\mu\nu}(p^2, m_1^2, m_2^2) = \int \frac{d^D q}{i\pi^2 (2\pi\mu)^{D-4}} \frac{q_\mu q_\nu}{(q^2 - m_1^2 + i\epsilon)((p+q)^2 - m_2^2 + i\epsilon)}. \quad (3.9)$$

Since these integrals are Lorentz covariant, they can be expressed in terms of Lorentz tensors constructed from the external momentum and the metric tensor $g_{\mu\nu}$:

$$\begin{aligned} B_\mu(p^2, m_1^2, m_2^2) &= p_\mu B_1(p^2, m_1^2, m_2^2), \\ B_{\mu\nu}(p^2, m_1^2, m_2^2) &= g_{\mu\nu} B_{00}(p^2, m_1^2, m_2^2) + p_\mu p_\nu B_{11}(p^2, m_1^2, m_2^2). \end{aligned} \quad (3.10)$$

The scalar coefficient functions B_1 and B_{00} can be obtained by inverting (3.10),

$$B_1(p^2, m_1^2, m_2^2) = \frac{1}{p^2} p^\mu B_\mu(p^2, m_1^2, m_2^2), \quad (3.11)$$

$$B_{00}(p^2, m_1^2, m_2^2) = \frac{1}{2(D-1)} \left(g^{\mu\nu} - \frac{p^\mu p^\nu}{p^2} \right) B_{\mu\nu}(p^2, m_1^2, m_2^2). \quad (3.12)$$

The resulting scalar products in the numerator can be expressed in terms of the squared momenta via

$$2p \cdot q = (p+q)^2 - p^2 - q^2. \quad (3.13)$$

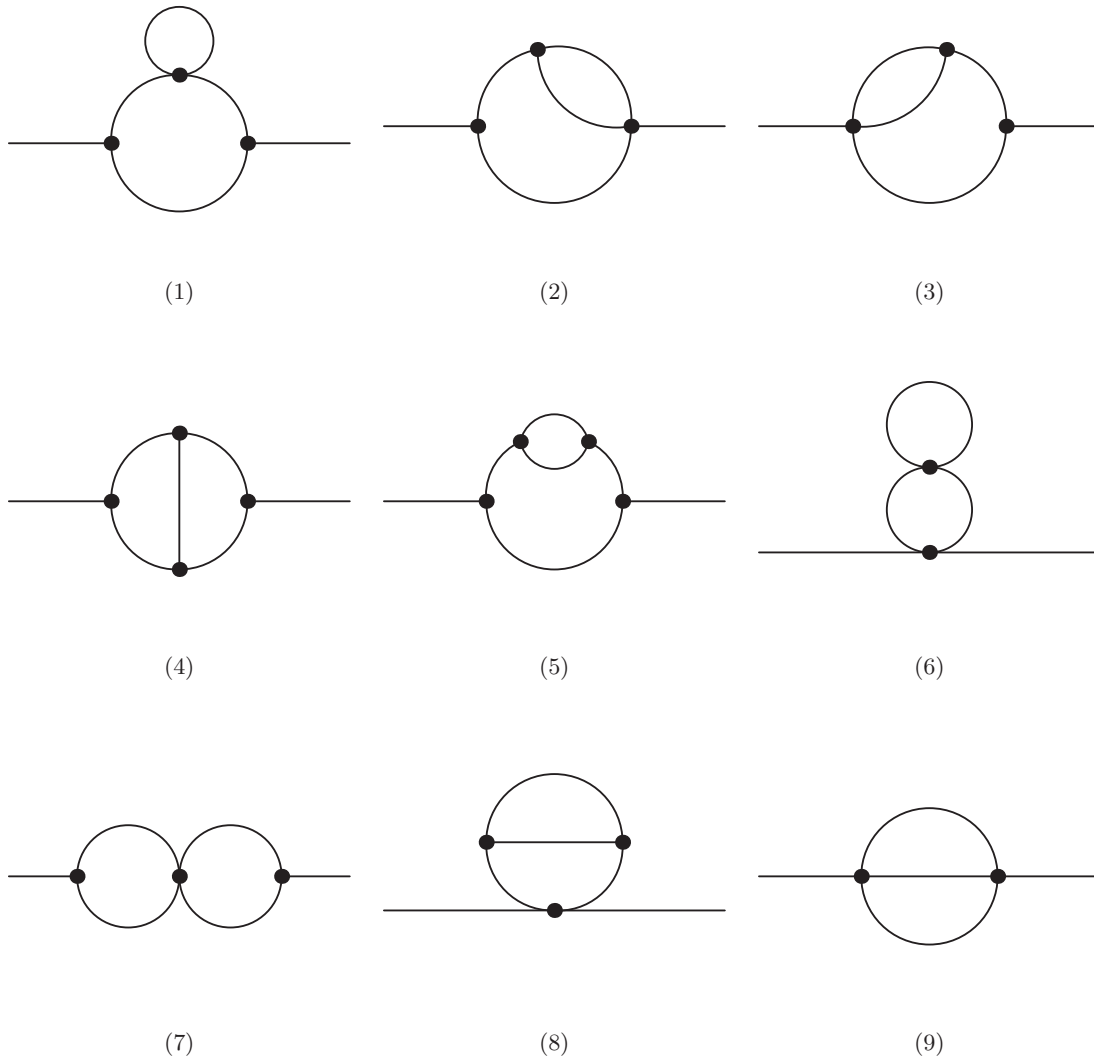


Figure 3.1: Topologies for the two-loop self-energy diagrams

The squared momenta can be canceled by the propagators, resulting in the scalar coefficient functions

$$B_1(p^2, m_1^2, m_2^2) = \frac{1}{2p^2} \left[A_0(m_1^2) - A_0(m_2^2) - (p^2 + m_1^2 - m_2^2) B_0(p^2, m_1^2, m_2^2) \right], \quad (3.14)$$

$$B_{00}(p^2, m_1^2, m_2^2) = \frac{1}{2(D-1)} \left[A_0(m_1^2) + 2m_1^2 B_0(p^2, m_1^2, m_2^2) + (p^2 + m_1^2 - m_2^2) B_1(p^2, m_1^2, m_2^2) \right]. \quad (3.15)$$

3.2.2 Two-loop integrals for self-energies

For two-loop self-energy diagrams the reduction of tensor integrals to scalar integrals is described in [169]. It was shown, with the help of a generalization of the Passarino-Veltman-techniques [168] together with symmetry properties of the resulting scalar integrals, that every two-loop self-energy amplitude can be written in terms of a small number of two-loop scalar integrals as well as products of the one-loop integrals A_0 and B_0 . The routines for the tensor decomposition and the reduction of the scalar integrals are implemented in the Mathematica program `TwoCalc` [169, 176]. In the following the conventions for the two-loop scalar integrals are reviewed.

All of the needed two-loop self-energy diagrams are related to one of the topologies shown in Figure 3.1. The tensor reduction and the symmetry properties of the scalar integrals are derived in [169], where it was shown that the self-energy amplitudes can be expressed in terms

of a class of scalar two-loop integrals

$$T_{i_1 i_2 \dots i_n}(m_1^2, m_2^2, \dots, m_n) = \int \int \frac{d^D q_1 d^D q_2}{(i\pi^2 (2\pi\mu)^{D-4})^2} \frac{1}{[k_{i_1}^2 - m_1^2][k_{i_2}^2 - m_2^2] \dots [k_{i_n}^2 - m_n^2]}, \quad (3.16)$$

with $i_j \in \{1, 2, 3, 4, 5\}$. k_{i_j} and m_j denote the momenta and the mass of the j -th propagator. Thereby the internal momenta are expressed by the integration momenta q_1 and q_2 and the external momentum p as

$$k_1 = q_1, \quad k_2 = q_1 + p, \quad k_3 = q_2 - q_1, \quad k_4 = q_2, \quad k_5 = q_2 + p. \quad (3.17)$$

Extracting the transverse part of the self-energy with the help of (3.4) results in scalar products of the momenta $(k_i \cdot k_j)$, $(k_i \cdot p)$, p^2 in the numerator. By using momentum conservation and (3.17), all scalar products can be expressed as sums of k_i^2 and p^2 (in an analogous way to the one-loop case in (3.13)). If all the k_i^2 appearing in the numerator are also contained in the denominator, they can be canceled against the corresponding propagator via

$$k_i^2 = (k_i^2 - m_i^2) + m_i^2, \quad (3.18)$$

and the loop integral can be written in the form of (3.16). If one of the squared momenta in the numerator is not contained in the denominator, one can perform a decomposition of a subloop by expressing it in terms of tensors build by the external momentum of the subloop and scalar coefficient functions (similar to the decomposition (3.10) of the tensor integrals in the one-loop case). In [169] it is explicitly shown, that the scalar products resulting from this decomposition are canceled and that all the loop integrals can be expressed in terms of scalar integrals of the form of (3.16).

Additional relations between the T -integrals exist, which can be used to reduce the number of occurring integrals. For example all the scalar integrals are invariant under the permutations

$$k_1 \leftrightarrow k_2, \quad k_4 \leftrightarrow k_5; \quad (3.19a)$$

$$k_1 \leftrightarrow k_4, \quad k_2 \leftrightarrow k_5; \quad (3.19b)$$

$$k_1 \leftrightarrow k_5, \quad k_2 \leftrightarrow k_4; \quad (3.19c)$$

which results from the definition in (3.17) and the invariance of the integrals under a shift in the integration momenta. If one of the five momenta from (3.17) is absent in the loop integrals, further symmetries can be found. For example, if k_1 is absent, then the integral is invariant under

$$k_2 \leftrightarrow k_3. \quad (3.20)$$

Additional relations between the scalar integrals can be derived by integration by parts methods or partial fractioning (for details see Appendix B).

For self-energies evaluated at vanishing external momentum, the only remaining kinematic variables from (3.17) are k_1 , k_3 and k_4 . In this case all the scalar loop integrals appearing in the Feynman amplitudes after the tensor decomposition, can be expressed in terms of one scalar two-loop integral

$$T_{134}(m_1^2, m_2^2, m_3^2) = \int \int \frac{d^D q_1 d^D q_2}{(i\pi^2 (2\pi\mu)^{D-4})^2} \frac{1}{[k_1^2 - m_1^2][k_3^2 - m_2^2][k_4^2 - m_3^2]} \quad (3.21)$$

and products of one-loop integrals A_0 . For the basis-integral T_{134} an analytic expression is known [177, 178]. A compact form can be found in [175], which is repeated in Appendix B for the sake of completeness.

For the massive two-loop integral with non-vanishing external momentum an analytic expression is in general not possible [179] and numerical techniques are needed for the evaluation.

3.3 Technical evaluation of higher-order corrections

All needed diagrams and amplitudes are generated with the help of the Mathematica package `FeynArts` [130]. The evaluation of the one-loop amplitudes and the calculation of the

renormalization constants is done with the help of the package `FormCalc` [180], which is also employed to generate a Fortran expression of the result. For the numerical evaluation the program `LoopTools` [180] is used.

The package `TwoCalc` [169, 176] is applied to deal with the Lorentz and Dirac algebra of the two-loop amplitudes and to reduce the tensor integrals to scalar integrals. In the gaugeless limit the external momenta of all the two-loop diagrams are equal to zero and the result depends only on the one-loop functions A_0 and B_0 (see Appendix B.1) and on the two-loop function T_{134} (see Appendix B.2).

The calculation cannot be done in a single Mathematica session due to conflicts between the different packages. Therefore, the intermediate results have to be saved externally and reloaded in a new session. For the implementation of the two-loop Higgs-mass corrections at $\mathcal{O}(\alpha_t^2)$ in `FeynHiggs`, this procedure was automated by dividing the calculation into different working steps which are implemented as shell scripts [181]. These scripts run the Mathematica Kernel internally as described in [182] and load just the packages required in the specific step. In addition, a lot of sophisticated techniques were developed, leading to a very compact Fortran code for the result. The scripts from [181] were used as a template and adapted for the calculation of the two-loop corrections to the ρ parameter in the THDM. This allows a repetition of the calculation in different versions of the THDM or different SM extensions in a fairly straightforward way.

For the evaluation of the one-loop corrections to electroweak precision observables in the THDM, a Fortran code was developed in [94]. These routines are now supplemented with the two-loop corrections to the self-energies. For the numerical evaluation of the two-loop integral T_{134} we use the Fortran routine encoded in the program `FeynHiggs` [183, 184].

Chapter 4

Renormalization

As discussed in the previous chapter, loop integrals lead to divergences in the higher-order prediction of physical processes. These higher-order contributions modify also the relations between the theory parameters and the measurable observables. In order to obtain physical predictions, the original parameters of the Lagrangian, the bare parameters, have to be redefined in the renormalization of the theory. The renormalized parameters are then finite and can be related to measurable observables by a set of renormalization conditions.

4.1 Renormalized perturbation theory

In the framework of *renormalized perturbation theory*, the bare masses m_0 and couplings g_0 are divided into the renormalized parameters m and g and the renormalization constants δm and δg (also called counterterms)

$$m_0 = m + \delta m, \quad (4.1)$$

$$g_0 = g + \delta g. \quad (4.2)$$

The divergences from loop corrections to the S -matrix elements are then absorbed by the renormalization constants. The radiative corrections modify also the normalization of the external fields, resulting in UV-divergent Green functions. If the external fields are renormalized, by expanding the bare fields

$$\phi_0 = Z_\phi^{1/2} \phi = \left(1 + \frac{1}{2} \delta Z_\phi\right) \phi, \quad (4.3)$$

the Green functions are also finite.

In a renormalizable quantum-field-theory, as for example quantum electrodynamics (QED), only a finite number of counterterms is necessary to cancel all the UV-divergences in the calculation of physical processes. This is a consequence of the Bogoliubov-Parasiuk-Hepp-Zimmermann theorem [185–187]. The renormalizability of non-Abelian gauge theories with spontaneous symmetry breaking, such as the SM or the THDM, was proven by 't Hooft in 1971 [188, 189].

The definition of the renormalized parameters is specified in the renormalization scheme. The divergent parts of the renormalization constants are independent of the renormalization scheme, since they are required to compensate the divergences from the loop integrals. The finite part of the counterterms differ in different renormalization schemes, resulting in a renormalization scheme dependence of finite-order calculations in perturbation theory. Equivalent results of physical quantities in different results would only be obtained in an exact (all-order) calculation. Popular renormalization schemes are:

- the on-shell renormalization scheme, in which the renormalized parameters are equal to physical parameters in all orders of perturbation theories. For example, the renormalized masses are identified with the poles of the propagators, which correspond to the physical masses. Another example is the electric charge, which is defined by the Thomson cross section in the on-shell renormalization of QED. The extension of the on-shell scheme to electroweak theories was first proposed by Ross and Taylor [190] and has been used for many calculations in the SM (see for example [172]). More details are given in Section 4.2.

- the minimal subtraction scheme (MS-scheme), in which the renormalization constants contain only divergent parts and the renormalized parameters are defined at the arbitrary mass scale μ_D . In the modified minimal subtraction scheme ($\overline{\text{MS}}$ -scheme) the counterterms absorb also the finite parts $\log(4\pi)$ and γ_e , which are a by-product of the loop integrals in dimensional regularization (see Appendix B). The $\overline{\text{MS}}$ -scheme is often used in the definition of the light quark masses, for which a direct measurement is not possible due to the strong interaction.

4.2 On-shell renormalization scheme

In this thesis we use the on-shell renormalization scheme, following the conventions from [100, 172]. The renormalized parameters for the gauge bosons and fermions are the particle masses and the electric charge. The corresponding renormalization conditions together with the field renormalization are given in Section 4.2.1 for the gauge bosons and in Section 4.2.2 for the fermions.

The Higgs potential can be renormalized in terms of the original parameters of the potential and the vacuum expectation values. The resulting counterterms can be traded for tadpole and mass counterterms, which are fixed by the renormalization conditions given in Section 4.2.3. More details about the renormalization of the Higgs sector in the THDM can be found in [191–197].

4.2.1 Renormalization of the gauge-boson sector

The renormalized parameters for the gauge bosons are the masses M_W and M_Z as well as the electric charge. The expansion of the bare parameter into renormalized parameters and counterterms is given at the two-loop order by

$$e_0 = Z_e e = (1 + \delta^{(1)} Z_e + \delta^{(2)} Z_e) e, \quad (4.4)$$

$$M_{W,0}^2 = M_W^2 + \delta^{(1)} M_W^2 + \delta^{(2)} M_W^2, \quad (4.5)$$

$$M_{Z,0}^2 = M_Z^2 + \delta^{(1)} M_Z^2 + \delta^{(2)} M_Z^2. \quad (4.6)$$

The two-loop counterterms are used in Chapter 6 and Chapter 7 to identify the universal corrections to the precision observables.

Following the conventions from [172] the physical fields W^\pm , Z and γ are renormalized.¹ We restrict ourselves to field renormalization at the one-loop order. For the bare field of the W boson it is given by

$$W_{\mu,0}^\pm = (Z_W)^{1/2} W_\mu^\pm = (1 + \frac{1}{2}\delta^{(1)} Z_W) W_\mu^\pm. \quad (4.7)$$

Since the photon and the Z boson carry the same quantum numbers, the two fields mix at higher orders. In order to define the renormalized fields as mass eigenstates also at the one-loop order, a matrix-valued field renormalization is introduced. The field renormalization of the photon and the Z boson at one-loop order is therefore given by

$$\begin{pmatrix} Z_{\mu,0} \\ A_{\mu,0} \end{pmatrix} = \begin{pmatrix} 1 + \frac{1}{2}\delta^{(1)} Z_{ZZ} & \frac{1}{2}\delta^{(1)} Z_{Z\gamma} \\ \frac{1}{2}\delta^{(1)} Z_{\gamma Z} & 1 + \frac{1}{2}\delta^{(1)} Z_{\gamma\gamma} \end{pmatrix} \begin{pmatrix} Z_\mu \\ A_\mu \end{pmatrix}. \quad (4.8)$$

The renormalization conditions for the mass and field counterterms are fixed via the renormalized one-particle irreducible two-point functions. In the 't Hooft-Feynman gauge the two-

¹Alternatively the Lagrangian can be renormalized in its original, symmetric form, such that one field renormalization constant is introduced for the field B_μ and just one renormalization constant for the fields in the triplet W_μ^a . This minimal field renormalization is used for example in [198].

point vertex functions of the gauge bosons are given by

$$\hat{\Gamma}_{\mu\nu}^W(p) = -ig_{\mu\nu}(p^2 - M_W^2) - i\left(g_{\mu\nu} - \frac{p_\mu p_\nu}{p^2}\right)\hat{\Sigma}_W(p^2), \quad (4.9)$$

$$\hat{\Gamma}_{\mu\nu}^Z(p) = -ig_{\mu\nu}(p^2 - M_Z^2) - i\left(g_{\mu\nu} - \frac{p_\mu p_\nu}{p^2}\right)\hat{\Sigma}_Z(p^2), \quad (4.10)$$

$$\hat{\Gamma}_{\mu\nu}^\gamma(p) = -ig_{\mu\nu}p^2 - i\left(g_{\mu\nu} - \frac{p_\mu p_\nu}{p^2}\right)\hat{\Sigma}_\gamma(p^2), \quad (4.11)$$

$$\hat{\Gamma}_{\mu\nu}^{\gamma Z}(p) = -i\left(g_{\mu\nu} - \frac{p_\mu p_\nu}{p^2}\right)\hat{\Sigma}_{\gamma Z}(p^2), \quad (4.12)$$

where we kept only the transversal part of the gauge-boson self-energies. The renormalized self-energies are denoted by $\hat{\Sigma}$. At the one-loop order these are related to the unrenormalized self-energies via

$$\hat{\Sigma}_W^{(1)}(p^2) = \Sigma_W^{(1)}(p^2) + p^2\delta^{(1)}Z_W - M_W^2\delta^{(1)}Z_W - \delta^{(1)}M_W^2, \quad (4.13)$$

$$\hat{\Sigma}_Z^{(1)}(p^2) = \Sigma_Z^{(1)}(p^2) + p^2\delta^{(1)}Z_{ZZ} - M_Z^2\delta^{(1)}Z_{ZZ} - \delta^{(1)}M_Z^2, \quad (4.14)$$

$$\hat{\Sigma}_\gamma^{(1)}(p^2) = \Sigma_\gamma^{(1)}(p^2) + p^2\delta^{(1)}Z_{\gamma\gamma}, \quad (4.15)$$

$$\hat{\Sigma}_{\gamma Z}^{(1)}(p^2) = \Sigma_{\gamma Z}^{(1)}(p^2) + p^2\frac{1}{2}\left(\delta^{(1)}Z_{\gamma Z} + \delta^{(1)}Z_{Z\gamma}\right) - M_Z^2\frac{1}{2}\delta^{(1)}Z_{Z\gamma}. \quad (4.16)$$

where the number i in the parentheses of a self-energy $\Sigma^{(i)}$ indicates the loop order. In the on-shell scheme the renormalized masses are identified with the physical masses. For the W boson, the physical mass at one-loop order is equivalent to the pole of the real part of the propagators, which correspond to the zero of the one-particle irreducible two-point functions. In order to use this on-shell mass renormalization also for the Z boson, diagonal two-point functions for on-shell photons or Z bosons are defined with the help of the matrix-valued field renormalization. This fixes the off-diagonal element of the field renormalization matrix. The diagonal elements (and the field counterterm of the W boson) are determined by the condition that the residues of the renormalized propagators are equal to one and no external wave function corrections need to be considered. The resulting one-loop renormalization conditions are

$$\begin{aligned} \operatorname{Re}\hat{\Sigma}_W^{(1)}(M_W^2) &= 0; \\ \operatorname{Re}\hat{\Sigma}_Z^{(1)}(M_Z^2) &= 0; & \operatorname{Re}\hat{\Sigma}_\gamma^{(1)}(0) &= 0; \\ \operatorname{Re}\hat{\Sigma}_{\gamma Z}^{(1)}(0) &= 0; & \operatorname{Re}\hat{\Sigma}_{\gamma Z}^{(1)}(M_Z^2) &= 0; \\ \operatorname{Re}\left.\frac{\partial\hat{\Sigma}_W^{(1)}(p^2)}{\partial p^2}\right|_{p^2=M_W^2} &= 0; & & \\ \operatorname{Re}\left.\frac{\partial\hat{\Sigma}_Z^{(1)}(p^2)}{\partial p^2}\right|_{p^2=M_Z^2} &= 0; & \operatorname{Re}\left.\frac{\partial\hat{\Sigma}_\gamma^{(1)}(p^2)}{\partial p^2}\right|_{p^2=0} &= 0. \end{aligned} \quad (4.17)$$

The condition that the photon self-energy vanishes for zero external momentum is automatically fulfilled due to a Ward identity. The remaining conditions determine the one-loop mass counterterms

$$\delta^{(1)}M_W^2 = \operatorname{Re}\Sigma_W^{(1)}(M_W^2), \quad \delta^{(1)}M_Z^2 = \operatorname{Re}\Sigma_Z^{(1)}(M_Z^2), \quad (4.18)$$

and field renormalization constants

$$\begin{aligned} \delta^{(1)}Z_W &= -\operatorname{Re}\left.\frac{\partial\Sigma_W^{(1)}(p^2)}{\partial p^2}\right|_{p^2=M_W^2}, \\ \delta^{(1)}Z_{ZZ} &= -\operatorname{Re}\left.\frac{\partial\Sigma_Z^{(1)}(p^2)}{\partial p^2}\right|_{p^2=M_Z^2}, & \delta^{(1)}Z_{\gamma\gamma} &= -\operatorname{Re}\left.\frac{\partial\Sigma_\gamma^{(1)}(p^2)}{\partial p^2}\right|_{p^2=0}, \\ \delta^{(1)}Z_{\gamma Z} &= -2\frac{\operatorname{Re}\Sigma_{\gamma Z}^{(1)}(M_Z^2)}{M_Z^2}, & \delta^{(1)}Z_{Z\gamma} &= 2\frac{\Sigma_{\gamma Z}^{(1)}(0)}{M_Z^2}. \end{aligned} \quad (4.19)$$

For the renormalization of the electric charge the $ee\gamma$ vertex is used. The renormalized electric charge is defined as the coupling of the electron to the photon for on-shell external particles and vanishing photon momentum. Due to the gauge-boson field renormalization, no photon- Z -mixing or external wave-function corrections have to be considered. The counterterm of the electric charge has to absorb the additional vertex corrections. The resulting expression can be simplified by a generalization of the QED Ward identity. At one-loop order this results in the counterterm²

$$\delta^{(1)} Z_e = -\frac{1}{2}\delta^{(1)} Z_{\gamma\gamma} - \frac{s_W}{c_W} \frac{1}{2}\delta^{(1)} Z_{\gamma Z} = \frac{1}{2}\Pi_\gamma^{(1)}(0) + \frac{s_W}{c_W} \frac{\Sigma_{\gamma Z}^{(1)}(0)}{M_Z^2} \quad (4.20)$$

where

$$\Pi_\gamma^{(1)}(0) = \left. \frac{\partial \Sigma_\gamma^{(1)}(p^2)}{\partial p^2} \right|_{p^2=0} \quad (4.21)$$

denotes the one-loop photon vacuum polarization

$$\Pi_\gamma^{(1)}(p^2) = \frac{\Sigma_\gamma^{(1)}(p^2)}{p^2} \quad (4.22)$$

for vanishing momentum. The contribution to the photon vacuum polarization from the light fermions does not depend on the details of the electroweak theory and gives a dominant, universal correction to many precision observables (see the discussion in Chapter 6).

In the on-shell scheme, the relation between the weak mixing angle and the gauge-boson masses,

$$s_W^2 = 1 - \frac{M_W^2}{M_Z^2} \quad (4.23)$$

is valid to all orders of perturbation theory. The bare parameters are related via

$$s_{W,0}^2 = 1 - c_{W,0}^2 = 1 - \frac{M_{W,0}^2}{M_{Z,0}^2}. \quad (4.24)$$

Inserting the bare masses from (4.5) and (4.6) and expanding the ratio up to the one-loop order leads to the counterterm

$$\frac{\delta^{(1)} s_W^2}{s_W^2} = -\frac{c_W^2}{s_W^2} \frac{\delta^{(1)} c_W^2}{c_W^2} = \frac{c_W^2}{s_W^2} \left(\frac{\delta^{(1)} M_Z^2}{M_Z^2} - \frac{\delta^{(1)} M_W^2}{M_W^2} \right). \quad (4.25)$$

The definition of the renormalized mass as the pole of the real part of the propagators results in a gauge-dependent mass parameter at the two-loop order, since the W and the Z boson are unstable particles [199]. For a gauge-independent definition at the two-loop order, the masses of the W and the Z boson have to be defined according to the real part of the complex pole of the propagator (see [100] and references therein). For the two-loop mass counterterms this definition yields

$$\delta^{(2)} M_W^2 = \text{Re } \Sigma_W^{(2)}(M_W^2) - \delta^{(1)} M_W^2 \delta^{(1)} Z_W + \text{Im } \Sigma_W^{(1)'}(M_W^2) \text{Im } \Sigma_W^{(1)}(M_W^2), \quad (4.26)$$

$$\begin{aligned} \delta^{(2)} M_Z^2 &= \text{Re } \Sigma_Z^{(2)}(M_Z^2) - \delta^{(1)} M_Z^2 \delta^{(1)} Z_{ZZ} + \frac{M_Z^2}{4} \left(\delta^{(1)} Z_{\gamma Z} \right)^2 + \frac{\left(\text{Im } \Sigma_{\gamma Z}^{(1)}(M_Z^2) \right)^2}{M_Z^2} \\ &\quad + \text{Im } \Sigma_Z^{(1)'}(M_Z^2) \text{Im } \Sigma_Z^{(1)}(M_Z^2), \end{aligned} \quad (4.27)$$

where $\Sigma_V^{(1)'}(k^2)$ denotes the derivative of the self-energy with respect to k^2 . In the mass-definition according to the pole of the real part of the propagator the terms with the imaginary part of the one-loop self-energies are absent.

The two-loop self-energy contains also contributions from the subloop renormalization. These are one-loop diagrams which contain one-loop counterterms in a vertex or in a propagator. For the discussion of the two-loop corrections to electroweak precision observables in

²More details can be found for example in [172].

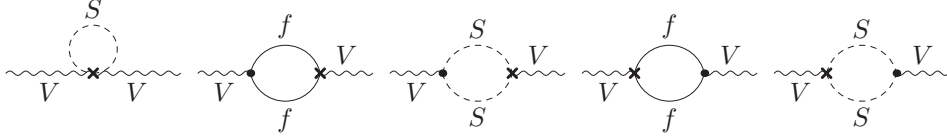


Figure 4.1: Generic diagrams of the gauge-boson self-energies with vertex counterterm insertions for internal scalars or fermions.

Chapter 6 and Chapter 7 it will be useful to describe them in more detail. The field counterterms of the internal particles drop out in the final result. The remaining contribution of the subloop renormalization can be divided into the part with the mass counterterms of the internal particles and the remaining renormalization constants from the counterterm insertions in the vertices. For self-energies which contain only internal scalars or fermions, the diagrams with vertex counterterm insertions are depicted in Figure 4.1. The contributions from these diagrams can be rewritten in a universal way as products of one-loop counterterms and self-energies. With the vertex counterterms given in Appendix A, the gauge-boson self-energies which contain only scalars or fermions as internal particles can be decomposed as follows,

$$\Sigma_W^{(2)}(p^2) = \left(2\delta^{(1)}Z_e - \frac{\delta^{(1)}s_W^2}{s_W^2} + \delta^{(1)}Z_W \right) \Sigma_W^{(1)}(p^2) + \tilde{\Sigma}_W^{(2)}(p^2), \quad (4.28)$$

$$\begin{aligned} \Sigma_Z^{(2)}(p^2) &= \left(2\delta^{(1)}Z_e - \frac{c_W^2 - s_W^2}{c_W^2} \frac{\delta^{(1)}s_W^2}{s_W^2} + \delta^{(1)}Z_{ZZ} \right) \Sigma_Z^{(1)}(p^2) \\ &+ \left(\delta^{(1)}Z_{\gamma Z} - 2\frac{s_W}{c_W} \frac{\delta^{(1)}s_W^2}{s_W^2} \right) \Sigma_{\gamma Z}^{(1)}(p^2) + \tilde{\Sigma}_Z^{(2)}(p^2), \end{aligned} \quad (4.29)$$

$$\Sigma_\gamma^{(2)}(p^2) = \left(2\delta^{(1)}Z_e + \delta^{(1)}Z_{\gamma\gamma} \right) \Sigma_\gamma^{(1)}(p^2) + \delta^{(1)}Z_{Z\gamma} \Sigma_{\gamma Z}^{(1)}(p^2) + \tilde{\Sigma}_\gamma^{(2)}(p^2), \quad (4.30)$$

$$\begin{aligned} \Sigma_{\gamma Z}^{(2)}(p^2) &= \left(2\delta^{(1)}Z_e + \frac{1}{2}\delta^{(1)}Z_{ZZ} + \frac{1}{2}\delta^{(1)}Z_{\gamma\gamma} - \frac{1}{2} \frac{c_W^2 - s_W^2}{c_W^2} \frac{\delta^{(1)}s_W^2}{s_W^2} \right) \Sigma_{\gamma Z}^{(1)}(p^2) \\ &+ \left(\frac{1}{2}\delta^{(1)}Z_{\gamma Z} - \frac{s_W}{c_W} \frac{\delta^{(1)}s_W^2}{s_W^2} \right) \Sigma_\gamma^{(1)}(p^2) + \frac{1}{2}\delta^{(1)}Z_{Z\gamma} \Sigma_Z^{(1)}(p^2) + \tilde{\Sigma}_{\gamma Z}^{(2)}(p^2). \end{aligned} \quad (4.31)$$

The contribution of the genuine two-loop diagrams and the part of the subloop renormalization from the mass counterterms of the internal particles are contained in $\tilde{\Sigma}_V^{(2)}(p^2)$ with $V = W, Z, \gamma, \gamma Z$.

The term in (4.28) which is proportional to the one-loop self-energy of the W boson can be understood by looking at the vertex counterterms given in Appendix A. The vertex counterterms with the W boson contain the field counterterm $\delta^{(1)}Z_W$ from the expansion of the bare field and the counterterms following from the expansion

$$g_{2,0} = \frac{e_0}{s_{W,0}} = \frac{e}{s_W} \left(1 + \delta^{(1)}Z_e - \frac{1}{2} \frac{\delta^{(1)}s_W^2}{s_W^2} \right). \quad (4.32)$$

of the bare gauge coupling. The corresponding parts in the vertex counterterms are directly proportional to the tree-level coupling and lead therefore to the first term in (4.28).

The decompositions of the photon and the Z boson self-energy are more complicated due to the photon- Z -mixing. For a better understanding we write the bare covariant derivative of a generic field ϕ (which corresponds to the internal scalar or fermion) as

$$D^\mu \phi = \dots + i \frac{e_0}{s_{W,0} c_{W,0}} (I_\phi^3 - s_{W,0}^2 Q_\phi) Z_0^\mu \phi + i e_0 Q_\phi A_0^\mu \phi + \dots \quad (4.33)$$

Expanding the bare parameters up to the first order leads to the following part in the coun-

terterm Lagrangian

$$\begin{aligned}
 & i \frac{e}{s_W c_W} (I_\phi^3 - s_W^2 Q_\phi) \left(\delta^{(1)} Z_e + \frac{1}{2} \delta^{(1)} Z_{ZZ} - \frac{1}{2} \frac{c_W^2 - s_W^2}{c_W^2} \frac{\delta^{(1)} s_W^2}{s_W^2} \right) Z_\mu \phi \\
 & + i e Q_\phi \left(\frac{1}{2} \delta^{(1)} Z_{\gamma Z} - \frac{s_W}{c_W} \frac{\delta^{(1)} s_W^2}{s_W^2} \right) Z_\mu \phi \\
 & + i e Q_\phi \left(\delta^{(1)} Z_e + \frac{1}{2} \delta^{(1)} Z_{\gamma\gamma} \right) A_\mu \phi + i \frac{e}{s_W c_W} (I_\phi^3 - s_W^2 Q_\phi) \frac{1}{2} \delta^{(1)} Z_{Z\gamma} A_\mu \phi. \tag{4.34}
 \end{aligned}$$

We see that the counterterm vertex of the Z boson has one part which is proportional to the electric coupling to the photon and the vertex counterterm from the photon receives a part which is proportional to the tree-level coupling to the Z boson. This explains the terms in the subloop renormalization which contains the photon- Z -mixing at the one-loop order.

Inserting the decompositions (4.28) and (4.29) into the two-loop renormalization condition in (4.26) and (4.27) leads to the following parts in the two-loop mass counterterms of the gauge bosons,

$$\delta^{(2)} M_W^2 = \left(2\delta^{(1)} Z_e - \frac{\delta^{(1)} s_W^2}{s_W^2} \right) \delta^{(1)} M_W^2 + \text{Im} \Sigma_W^{(1)'} (M_W^2) \text{Im} \Sigma_W^{(1)} (M_W^2) + \dots \tag{4.35}$$

$$\begin{aligned}
 \delta^{(2)} M_Z^2 &= \left(2\delta^{(1)} Z_e - \frac{c_W^2 - s_W^2}{c_W^2} \frac{\delta^{(1)} s_W^2}{s_W^2} \right) \delta^{(1)} M_Z^2 + \frac{M_Z^2}{2} \frac{s_W}{c_W} \frac{\delta^{(1)} s_W^2}{s_W^2} \delta^{(1)} Z_{\gamma Z} - \frac{M_Z^2}{4} \left(\delta^{(1)} Z_{\gamma Z} \right)^2 \\
 &+ \frac{\left(\text{Im} \Sigma_{\gamma Z}^{(1)} (M_Z^2) \right)^2}{M_Z^2} + \text{Im} \Sigma_Z^{(1)'} (M_Z^2) \text{Im} \Sigma_Z^{(1)} (M_Z^2) + \dots \tag{4.36}
 \end{aligned}$$

For the two-loop counterterm of s_W^2 , the expansion of the ratio of the bare masses in (4.24) up to two-loop order results in

$$\begin{aligned}
 \frac{\delta^{(2)} s_W^2}{s_W^2} &= - \frac{c_W^2}{s_W^2} \frac{\delta^{(2)} c_W^2}{c_W^2} \\
 &= \frac{c_W^2}{s_W^2} \left(- \frac{\delta^{(1)} M_Z^2}{M_Z^2} \left(\frac{\delta^{(1)} M_Z^2}{M_Z^2} - \frac{\delta^{(1)} M_W^2}{M_W^2} \right) + \left(\frac{\delta^{(2)} M_Z^2}{M_Z^2} - \frac{\delta^{(2)} M_W^2}{M_W^2} \right) \right). \tag{4.37}
 \end{aligned}$$

For the two-loop renormalization of the electric charge, the generalization of the QED Ward identity at the two-loop order gives [100]

$$\delta^{(2)} Z_e = - \frac{1}{2} \delta^{(2)} Z_{\gamma\gamma} - \frac{1}{2} \frac{s_W}{c_W} \delta^{(2)} Z_{Z\gamma} + \left(\delta^{(1)} Z_e \right)^2 + \frac{1}{8} \left(\delta^{(1)} Z_{\gamma\gamma} \right)^2 - \frac{1}{4} \frac{s_W}{c_W^3} \delta^{(1)} Z_{Z\gamma} \frac{\delta^{(1)} s_W^2}{s_W^2}. \tag{4.38}$$

Analogous to the one-loop renormalization condition, the two-loop field counterterm of the photon is given by

$$\delta^{(2)} Z_{\gamma\gamma} = - \text{Re} \left. \frac{\partial \Sigma_\gamma^{(2)}(p^2)}{\partial p^2} \right|_{p^2=0}. \tag{4.39}$$

4.2.2 Renormalization of the fermion sector

The renormalization of the fermion masses and fields are needed up to the one-loop order. The expansion of the bare masses gives

$$m_{f,0} = m_f + \delta^{(1)} m_f. \tag{4.40}$$

Independent field renormalization constants are introduced for the left- and right-handed fermion fields. The CKM matrix is approximated by the unity matrix, since the off-diagonal elements of the CKM matrix have a negligible influence on the calculations in this thesis. Therefore, no mixing between different fermion generations has to be considered and the field

renormalization up to the one-loop order is given by

$$f_0^L = (Z_f^L)^{1/2} f_i^L = \left(1 + \frac{1}{2}\delta^{(1)} Z_f^L\right) f^L, \quad (4.41)$$

$$f_0^R = (Z_f^R)^{1/2} f_i^R = \left(1 + \frac{1}{2}\delta^{(1)} Z_f^R\right) f^R. \quad (4.42)$$

With the decomposition of the fermion self-energy

$$\Sigma_f(p^2) = \not{p}\omega_- \Sigma_f^L(p^2) + \not{p}\omega_+ \Sigma_f^R(p^2) + m_f \Sigma_f^S(p^2), \quad (4.43)$$

the two-point vertex function can be written as

$$\hat{\Gamma}_f(p) = i(\not{p} - m_f) + i \left[\not{p}\omega_- \hat{\Sigma}_f^L(p^2) + \not{p}\omega_+ \hat{\Sigma}_f^R(p^2) + m_f (\omega_- + \omega_+) \hat{\Sigma}_f^S(p^2) \right]. \quad (4.44)$$

The renormalized self-energy is related to the unrenormalized self-energy by

$$\hat{\Sigma}_f^L(p^2) = \Sigma_f^L(p^2) + \delta^{(1)} Z_f^L, \quad (4.45)$$

$$\hat{\Sigma}_f^R(p^2) = \Sigma_f^R(p^2) + \delta^{(1)} Z_f^R, \quad (4.46)$$

$$\hat{\Sigma}_f^S(p^2) = \Sigma_f^S(p^2) - \frac{1}{2} \left(\delta^{(1)} Z_f^L + \delta^{(1)} Z_f^R \right) - \frac{\delta^{(1)} m_f}{m_f}. \quad (4.47)$$

The renormalization constants are again fixed by the conditions that the renormalized mass is equal to the real part of the pole of the renormalized propagator and that the residues of the renormalized propagators are equal to one. These renormalization conditions yield for the different components of the renormalized self-energy

$$m_f \left[\text{Re} \hat{\Sigma}_f^L(m_f^2) + \text{Re} \hat{\Sigma}_f^S(m_f^2) \right] = 0, \quad (4.48)$$

$$m_f \left[\text{Re} \hat{\Sigma}_f^R(m_f^2) + \text{Re} \hat{\Sigma}_f^S(m_f^2) \right] = 0, \quad (4.49)$$

$$\text{Re} \hat{\Sigma}_f^L(m_f^2) + m_f^2 \frac{\partial}{\partial p^2} \text{Re} \left[\Sigma_f^L(p^2) + \Sigma_f^R(p^2) + 2\Sigma_f^S(p^2) \right] \Big|_{p^2=m_f^2} = 0, \quad (4.50)$$

$$\text{Re} \hat{\Sigma}_f^R(m_f^2) + m_f^2 \frac{\partial}{\partial p^2} \text{Re} \left[\Sigma_f^L(p^2) + \Sigma_f^R(p^2) + 2\Sigma_f^S(p^2) \right] \Big|_{p^2=m_f^2} = 0. \quad (4.51)$$

The resulting fermion mass counterterm and field renormalization constants are

$$\delta^{(1)} m_f = \frac{1}{2} m_f \left[\text{Re} \Sigma_f^L(m_f^2) + \text{Re} \Sigma_f^R(m_f^2) + 2 \text{Re} \Sigma_f^S(m_f^2) \right], \quad (4.52)$$

$$\delta^{(1)} Z_f^L = - \text{Re} \Sigma_f^L(m_f^2) - m_f^2 \frac{\partial}{\partial p^2} \text{Re} \left[\Sigma_f^L(p^2) + \Sigma_f^R(p^2) + 2\Sigma_f^S(p^2) \right] \Big|_{p^2=m_f^2}, \quad (4.53)$$

$$\delta^{(1)} Z_f^R = - \text{Re} \Sigma_f^R(m_f^2) - m_f^2 \frac{\partial}{\partial p^2} \text{Re} \left[\Sigma_f^L(p^2) + \Sigma_f^R(p^2) + 2\Sigma_f^S(p^2) \right] \Big|_{p^2=m_f^2}. \quad (4.54)$$

4.2.3 Renormalization of the Higgs sector

Most of the counterterm vertices of the Higgs sector have been implemented in the **FeynArts** modelfile of the THDM as part of this work and are now available for further calculations. In order to provide an overview, the renormalization of the Higgs sector is discussed here in more detail, although the renormalization of the Higgs masses is in principle sufficient for the calculations of this thesis.

The Higgs sector can be renormalized by introducing counterterms

$$m_{ii,0}^2 = m_{ii}^2 + \delta m_{ii}^2, \quad (i = 1, 2), \quad (4.55a)$$

$$m_{12,0}^2 = m_{12}^2 + \delta m_{12}^2, \quad (4.55b)$$

$$\Lambda_{i,0} = \Lambda_i + \delta \Lambda_i, \quad (i = 1, \dots, 7), \quad (4.55c)$$

for the original potential parameters. Following [192, 200] the fields are renormalized by introducing field renormalization constants Z_{Φ_i} for the two doublets Φ_i , resulting in bare doublets

$$\Phi_{i,0} = \sqrt{Z_{\Phi_i}} \begin{pmatrix} \phi_i^+ \\ \frac{1}{\sqrt{2}}(v_i + \delta v_i + \eta_i + i\chi_i) \end{pmatrix}; \quad i = 1, 2. \quad (4.56)$$

In addition to the field renormalization the counterterms δv_i ($i = 1, 2$) are introduced. These counterterms cancel radiative corrections in the minimum of the Higgs potential, such that the renormalized vacuum expectation values are the actual minimum of the effective potential. This condition is equivalent to the requirement that the renormalized tadpoles vanish. With the additional counterterms the renormalized t_β is defined by the ratio

$$\sqrt{\frac{Z_{\Phi_2} v_2 + \delta v_2}{Z_{\Phi_1} v_1 + \delta v_1}} = t_{\beta,0} = t_\beta + \delta t_\beta. \quad (4.57)$$

Expanding the bare vacuum expectation values results in

$$\frac{\delta t_\beta}{t_\beta} = \frac{\delta v_2}{v_2} - \frac{\delta v_1}{v_1} + \frac{1}{2}(\delta Z_{\Phi_2} - \delta Z_{\Phi_1}). \quad (4.58)$$

Imposing the renormalization condition [192, 200–202]

$$\frac{\delta v_1}{v_1} = \frac{\delta v_2}{v_2} \quad (4.59)$$

leads to

$$\frac{\delta t_\beta}{t_\beta} = \frac{1}{2}(\delta Z_{\Phi_2} - \delta Z_{\Phi_1}). \quad (4.60)$$

In an analogous manner to (2.22) the bare potential can be decomposed in the linear and quadratic terms

$$\begin{aligned} V_0 = & -T_{1,0}\eta_{1,0} - T_{2,0}\eta_{2,0} + \begin{pmatrix} \phi_{1,0}^- & \phi_{2,0}^- \end{pmatrix} \tilde{\mathbf{M}}_0^\phi \begin{pmatrix} \phi_{1,0}^+ \\ \phi_{2,0}^+ \end{pmatrix} \\ & + \frac{1}{2} \begin{pmatrix} \chi_{1,0} & \chi_{2,0} \end{pmatrix} \tilde{\mathbf{M}}_0^\chi \begin{pmatrix} \chi_{1,0} \\ \chi_{2,0} \end{pmatrix} + \frac{1}{2} \begin{pmatrix} \eta_{1,0} & \eta_{2,0} \end{pmatrix} \tilde{\mathbf{M}}_0^\eta \begin{pmatrix} \eta_{1,0} \\ \eta_{2,0} \end{pmatrix} + \dots \end{aligned} \quad (4.61)$$

with the bare field components

$$\eta_{i,0} = \left(1 + \frac{1}{2}\delta Z_{\Phi_i}\right)\eta_i, \quad (4.62a)$$

$$\chi_{i,0} = \left(1 + \frac{1}{2}\delta Z_{\Phi_i}\right)\chi_i, \quad (4.62b)$$

$$\phi_{i,0}^\pm = \left(1 + \frac{1}{2}\delta Z_{\Phi_i}\right)\phi_i^\pm. \quad (4.62c)$$

The bare tadpoles and mass matrices are obtained by replacing the parameters in the corresponding expressions in Section 2.2 with the bare counterparts. Expanding the bare parameters and fields in (4.61) results in the counterterm potential in the original fields with

$$T_{i,0} = T_i + \delta T_i, \quad (i = 1, 2) \quad (4.63)$$

$$\tilde{\mathbf{M}}_0^X = \tilde{\mathbf{M}}^X + \delta\tilde{\mathbf{M}}^X, \quad (X = \phi, \chi, \eta). \quad (4.64)$$

However, the potential expressed in the mass-eigenstates and physical parameters is more suitable for the definition of on-shell renormalization conditions. In the following part, the mixing angles in (2.51) are defined to diagonalize the tree-level mass matrices \mathbf{M}^X ($X = \phi, \eta, \chi$), resulting in (2.42) for the CP -even angle α and in

$$\beta = \beta_n = \beta_c \quad (4.65)$$

where β is defined via the ratio of the renormalized vacuum expectation values, according to (4.57). Applying the rotations on the bare fields gives

$$\begin{pmatrix} G_0^\pm \\ H_0^\pm \end{pmatrix} = \mathbf{R}(\beta) \begin{pmatrix} \phi_{1,0}^\pm \\ \phi_{2,0}^\pm \end{pmatrix} = \begin{pmatrix} 1 + \frac{1}{2}\delta Z_{G^\pm} & \frac{1}{2}\delta Z_{G^\pm H^\pm} \\ \frac{1}{2}\delta Z_{G^\pm H^\pm} & 1 + \frac{1}{2}\delta Z_{H^\pm} \end{pmatrix} \begin{pmatrix} G^\pm \\ H^\pm \end{pmatrix}, \quad (4.66)$$

$$\begin{pmatrix} G_0^0 \\ A_0^0 \end{pmatrix} = \mathbf{R}(\beta) \begin{pmatrix} \chi_{1,0} \\ \chi_{2,0} \end{pmatrix} = \begin{pmatrix} 1 + \frac{1}{2}\delta Z_{G^0} & \frac{1}{2}\delta Z_{A^0 G^0} \\ \frac{1}{2}\delta Z_{A^0 G^0} & 1 + \frac{1}{2}\delta Z_{A^0} \end{pmatrix} \begin{pmatrix} G^0 \\ A^0 \end{pmatrix}, \quad (4.67)$$

$$\begin{pmatrix} H_0^0 \\ h_0^0 \end{pmatrix} = \mathbf{R}(\alpha) \begin{pmatrix} \eta_{1,0} \\ \eta_{2,0} \end{pmatrix} = \begin{pmatrix} 1 + \frac{1}{2}\delta Z_{H^0} & \frac{1}{2}\delta Z_{h^0 H^0} \\ \frac{1}{2}\delta Z_{h^0 H^0} & 1 + \frac{1}{2}\delta Z_{h^0} \end{pmatrix} \begin{pmatrix} H^0 \\ h^0 \end{pmatrix}, \quad (4.68)$$

with

$$\delta Z_{h^0} = s_\alpha^2 \delta Z_{\Phi_1} + c_\alpha^2 \delta Z_{\Phi_2}, \quad (4.69)$$

$$\delta Z_{H^0} = c_\alpha^2 \delta Z_{\Phi_1} + s_\alpha^2 \delta Z_{\Phi_2}, \quad (4.70)$$

$$\delta Z_{A^0} = \delta Z_{H^\pm} = s_\beta^2 \delta Z_{\Phi_1} + c_\beta^2 \delta Z_{\Phi_2}, \quad (4.71)$$

$$\delta Z_{G^0} = \delta Z_{G^\pm} = c_\beta^2 \delta Z_{\Phi_1} + s_\beta^2 \delta Z_{\Phi_2}, \quad (4.72)$$

$$\delta Z_{h^0 H^0} = s_\alpha c_\alpha (\delta Z_{\Phi_2} - \delta Z_{\Phi_1}), \quad (4.73)$$

$$\delta Z_{A^0 G^0} = \delta Z_{H^\pm G^\pm} = s_\beta c_\beta (\delta Z_{\Phi_2} - \delta Z_{\Phi_1}), \quad (4.74)$$

as the field renormalization of the mass eigenstates.

The counterterms of the original parameters can be related to counterterms of the tadpoles and the physical masses. The expansion of the bare tadpoles in (4.61) gives

$$-\delta T_1 \eta_1 - \delta T_2 \eta_2 = -\delta T_h h^0 - \delta T_H H^0 \quad (4.75)$$

with

$$\delta T_h = c_\alpha \delta T_2 - s_\alpha \delta T_1, \quad (4.76a)$$

$$\delta T_H = c_\alpha \delta T_1 + s_\alpha \delta T_2, \quad (4.76b)$$

as tadpole-counterterms for the states h^0 and H^0 . The counterterm expansion in the quadratic terms gives

$$\frac{1}{2} \begin{pmatrix} \eta_1 & \eta_2 \end{pmatrix} \delta \tilde{\mathbf{M}}^\eta \begin{pmatrix} \eta_1 \\ \eta_2 \end{pmatrix} = \frac{1}{2} \begin{pmatrix} H^0 & h^0 \end{pmatrix} \begin{pmatrix} \delta m_{H^0}^2 & \delta m_{h^0 H^0}^2 \\ \delta m_{h^0 H^0}^2 & \delta m_{h^0}^2 \end{pmatrix} \begin{pmatrix} H^0 \\ h^0 \end{pmatrix}, \quad (4.77)$$

$$\frac{1}{2} \begin{pmatrix} \chi_1 & \chi_2 \end{pmatrix} \delta \tilde{\mathbf{M}}^\chi \begin{pmatrix} \chi_1 \\ \chi_2 \end{pmatrix} = \frac{1}{2} \begin{pmatrix} G^0 & A^0 \end{pmatrix} \begin{pmatrix} \delta m_{G^0}^2 & \delta m_{A^0 G^0}^2 \\ \delta m_{A^0 G^0}^2 & \delta m_{A^0}^2 \end{pmatrix} \begin{pmatrix} G^0 \\ A^0 \end{pmatrix}, \quad (4.78)$$

$$\begin{pmatrix} \phi_1^- & \phi_2^- \end{pmatrix} \delta \tilde{\mathbf{M}}^\phi \begin{pmatrix} \phi_1^+ \\ \phi_2^+ \end{pmatrix} = \frac{1}{2} \begin{pmatrix} G^- & H^- \end{pmatrix} \begin{pmatrix} \delta m_{G^\pm}^2 & \delta m_{G^\pm H^\pm}^2 \\ \delta m_{G^\pm H^\pm}^2 & \delta m_{H^\pm}^2 \end{pmatrix} \begin{pmatrix} G^+ \\ H^+ \end{pmatrix}, \quad (4.79)$$

as counterterms in the mass eigenstate basis. In addition to the mass counterterms on the diagonal entries, mixing counterterms are obtained in the off-diagonal elements. This is a consequence of the definition of the mixing angles via the diagonalization of the tree-level mass matrix. A diagonal mass matrix at higher-orders can be obtained by introducing additional counterterms for the mixing angles, which remove the off-diagonal counterterms. A detailed discussion can be found for example in [197]. In the following the mass counterterms δm_S^2 ($S = h^0, H^0, A^0, H^\pm$) and the mixing counterterm $\delta m_{h^0 H^0}$ are kept as free renormalization constant. The remaining mixing counterterms and the mass counterterms of the Goldstone-

bosons are related to the tadpole counterterms and δt_β by

$$\delta m_{G^0} = -c_{\alpha-\beta} \frac{\delta T_H}{v} + s_{\alpha-\beta} \frac{\delta T_h}{v}, \quad (4.80)$$

$$\delta m_{A^0 G^0} = -m_{A^0}^2 c_\beta^2 \delta t_\beta - c_{\alpha-\beta} \frac{\delta T_h}{v} - s_{\alpha-\beta} \frac{\delta T_H}{v}, \quad (4.81)$$

$$\delta m_{G^\pm} = -c_{\alpha-\beta} \frac{\delta T_H}{v} + s_{\alpha-\beta} \frac{\delta T_h}{v}, \quad (4.82)$$

$$\delta m_{G^\pm H^\pm} = -m_{H^\pm}^2 c_\beta^2 \delta t_\beta - c_{\alpha-\beta} \frac{\delta T_h}{v} - s_{\alpha-\beta} \frac{\delta T_H}{v}. \quad (4.83)$$

These relations can also be derived from the tree-level expressions of the Goldstone-masses in (2.55) and (2.58) and the mixing-terms in (2.57) and (2.60), if the bare tadpoles

$$T_{h,0} = T_h + \delta T_h, \quad (4.84)$$

$$T_{H,0} = T_H + \delta T_H, \quad (4.85)$$

are introduced and β is replaced by the bare angle β_0 defined in (4.57). The expansion of the bare parameters results then in the counterterms as stated above. Note that the angles β_n and β_c , which originate only from the rotation to the mass-eigenstates receive no additional counterterm.

The renormalized tadpoles

$$\hat{T}_H = T_H^{(1)} + \delta T_H, \quad (4.86)$$

$$\hat{T}_h = T_h^{(1)} + \delta T_h, \quad (4.87)$$

contain the counterterms $\delta T_{h,H}$ together with the sum of the respective one-loop tadpole graphs, denoted by $T_{h,H}^{(1)}$. The tadpole counterterms are fixed by the conditions, that the renormalized tadpoles vanish, resulting in

$$\delta T_h = -T_h^{(1)}, \quad (4.88)$$

$$\delta T_H = -T_H^{(1)}. \quad (4.89)$$

These renormalization conditions fix also the mass counterterms of the Goldstone bosons. Moreover, they have the advantage, that Feynman diagrams with tadpoles as subgraphs can be discarded in higher-order calculations.

The renormalized one-particle irreducible two-point functions for the scalars are

$$\hat{\Gamma}^{ab}(p^2) = i\delta_{ab}(p^2 - m_a^2) + i\hat{\Sigma}_{ab}^{(1)}(p^2) \quad (4.90)$$

with $a, b = h^0, H^0, A^0, G^0, H^\pm, G^\pm$. The renormalized diagonal self-energies are

$$\hat{\Sigma}_{h^0}^{(1)}(p^2) = \Sigma_{h^0}^{(1)}(p^2) - \delta m_{h^0}^2 + (p^2 - m_{h^0}^2) \delta Z_{h^0}, \quad (4.91)$$

$$\hat{\Sigma}_{H^0}^{(1)}(p^2) = \Sigma_{H^0}^{(1)}(p^2) - \delta m_{H^0}^2 + (p^2 - m_{H^0}^2) \delta Z_{H^0}, \quad (4.92)$$

$$\hat{\Sigma}_{A^0}^{(1)}(p^2) = \Sigma_{A^0}^{(1)}(p^2) - \delta m_{A^0}^2 + (p^2 - m_{A^0}^2) \delta Z_{A^0}, \quad (4.93)$$

$$\hat{\Sigma}_{H^\pm}^{(1)}(p^2) = \Sigma_{H^\pm}^{(1)}(p^2) - \delta m_{H^\pm}^2 + (p^2 - m_{H^\pm}^2) \delta Z_{H^\pm}, \quad (4.94)$$

$$\hat{\Sigma}_{G^0}^{(1)}(p^2) = \Sigma_{G^0}^{(1)}(p^2) - \delta m_{G^0}^2 + p^2 \delta Z_{G^0}, \quad (4.95)$$

$$\hat{\Sigma}_{G^\pm}^{(1)}(p^2) = \Sigma_{G^\pm}^{(1)}(p^2) - \delta m_{G^\pm}^2 + p^2 \delta Z_{G^\pm}. \quad (4.96)$$

The renormalized mixing self-energies are

$$\hat{\Sigma}_{h^0 H^0}^{(1)}(p^2) = \Sigma_{h^0 H^0}^{(1)}(p^2) - \delta m_{h^0 H^0}^2 + \left(p^2 - \frac{1}{2}(m_{h^0}^2 + m_{H^0}^2) \right) \delta Z_{h^0 H^0}, \quad (4.97)$$

$$\hat{\Sigma}_{A^0 G^0}^{(1)}(p^2) = \Sigma_{A^0 G^0}^{(1)}(p^2) - \delta m_{A^0 G^0}^2 + \left(p^2 - \frac{1}{2}m_{A^0}^2 \right) \delta Z_{A^0 G^0}, \quad (4.98)$$

$$\hat{\Sigma}_{H^\pm G^\pm}^{(1)}(p^2) = \Sigma_{H^\pm G^\pm}^{(1)}(p^2) - \delta m_{H^\pm G^\pm}^2 + \left(p^2 - \frac{1}{2}m_{H^\pm}^2 \right) \delta Z_{H^\pm G^\pm}. \quad (4.99)$$

The renormalized masses are identified again with the zeros of the renormalized two-point functions, such that

$$\text{Re } \hat{\Sigma}_S^{(1)}(m_S^2) = 0, \quad (S = h^0, H^0, A^0, H^\pm). \quad (4.100)$$

The corresponding conditions for the mass counterterms reads

$$\delta m_S^2 = \text{Re } \Sigma_S(m_S^2), \quad (S = h^0, H^0, A^0, H^\pm). \quad (4.101)$$

These renormalization conditions are sufficient to obtain finite results in Chapter 5. The field renormalization constants drop out, since the scalars appear only as internal particles. Moreover, no mass-mixing counterterms are needed due to the alignment limit.

The renormalization of the Yukawa interaction and the kinetic part of the Higgs-Lagrangian results in the counterterm vertices of the scalars with the gauge bosons or fermions. The bare vacuum expectation values are related to the bare gauge-boson masses and the bare electric charge via

$$v_0^2 = v_{1,0}^2 + v_{2,0}^2 = \frac{4M_{W,0}^2 s_{W,0}^2}{e_0^2}. \quad (4.102)$$

Expanding the bare parameters leads to

$$v_0^2 = v^2 + \delta v^2 \quad (4.103)$$

with

$$\frac{\delta v^2}{v^2} = -2\delta^{(1)}Z_e + \frac{\delta^{(1)}M_W^2}{M_W^2} + \frac{\delta^{(1)}s_W^2}{s_W^2}. \quad (4.104)$$

Reexpressing $v_{1,0}$ and $v_{2,0}$ in terms of

$$v_{1,0} = v_0 c_{\beta,0} \quad (4.105)$$

$$v_{2,0} = v_0 s_{\beta,0} \quad (4.106)$$

with

$$c_{\beta,0} = c_\beta - s_\beta c_\beta^2 \delta t_\beta \quad (4.107)$$

$$s_{\beta,0} = s_\beta - c_\beta^3 \delta t_\beta \quad (4.108)$$

gives the renormalized kinetic Higgs-Lagrangian expressed in the renormalized parameters M_W , s_W , e and t_β . In a similar manner, the renormalized Yukawa-interaction is expressed in terms of the renormalized fermion masses m_f and M_W , s_W , e and t_β . The resulting counterterm vertices are stated in Appendix A.

The vertex counterterms for the interaction of the scalars with the gauge bosons or fermions were implemented in the `FeynArts` modelfile for the THDM of type-I and type-II and UV-finiteness was tested for all the vertices. In addition also the counterterm vertices of the triple scalar interaction for the THDM with a softly broken Z_2 symmetry were implemented and tested. For the test of the UV-finiteness the renormalization conditions for $\delta m_{h^0 H^0}^2$ and the scalar field counterterms δZ_{Φ_i} were taken from [192].³

³The vertices between three scalars contain an additional counterterm for the parameter λ_5 . For the test of UV-finiteness this counterterm was fixed as the divergent part from the one-loop correction to the vertex between three h^0 .

Chapter 5

The ρ parameter in the THDM

The dominant process-independent higher-order contributions to many precision observables can be identified with the loop corrections to the so-called ρ parameter. The ρ parameter is defined in the effective four-fermion interaction at low-energies as the ratio between the strengths of the charged and neutral currents (see Section 5.2). In electroweak theories these currents are mediated by the exchange of massive gauge bosons. The SM and its extensions by an additional number of scalar doublets fulfill the relation $\rho = 1$ at the tree-level, due to a global custodial symmetry of the kinetic part of the scalar Lagrangian. This is in accordance with electroweak precision measurements which allow only small deviations of the ρ parameter from unity. Such deviations from higher-order corrections, named $\Delta\rho$, originate from terms in the Lagrangian that break the custodial symmetry. For example, in the SM the Yukawa-interaction leads to a correction which is quadratic in the top mass [21–23]. In the THDM the custodial symmetry is in general broken by the Higgs potential, resulting in large corrections for large mass differences between charged and neutral scalars [85–88, 91, 131].

5.1 Custodial symmetry in the SM and the THDM

The Higgs potential in the SM has a global $SU(2)_L \times SU(2)_R$ symmetry. The non-vanishing vacuum expectation value of the Higgs field breaks this symmetry to a remaining $SU(2)_{L+R}$ symmetry, the custodial symmetry, which is responsible for the tree-level value of the ρ parameter [18–20]. Since the Higgs potential in the SM respects the custodial symmetry, the ρ parameter is protected from radiative corrections quadratic in the Higgs mass. In the gauge interaction the custodial symmetry is only approximate since it is broken by the hypercharge coupling g_1 . Moreover, the custodial symmetry is broken by the Yukawa interaction which leads to large corrections to the ρ parameter for large mass differences between quarks in the same doublet [21–23]. A detailed review can be found for example in [203].

5.1.1 Custodial symmetry in the SM

As already mentioned, the custodial symmetry is a global symmetry of the potential

$$V_{\text{SM}}(\Phi) = -\mu^2 \Phi^\dagger \Phi + \lambda (\Phi^\dagger \Phi)^2, \quad (5.1)$$

with the complex doublet

$$\Phi = \begin{pmatrix} \phi^+ \\ \phi^0 \end{pmatrix}. \quad (5.2)$$

To make the symmetry apparent, it is useful to introduce the complex matrix field

$$\mathcal{M} = (\tilde{\Phi}|\Phi) = \begin{pmatrix} \phi^{0*} & \phi^+ \\ -\phi^- & \phi^0 \end{pmatrix} \quad (5.3)$$

where

$$\tilde{\Phi} = i\sigma_2\Phi^* = \begin{pmatrix} 0 & 1 \\ -1 & 0 \end{pmatrix} \begin{pmatrix} \phi^- \\ \phi^{0*} \end{pmatrix}. \quad (5.4)$$

With this matrix field the potential can be expressed by

$$V_{\text{SM}}(\mathcal{M}) = -\mu^2 \frac{1}{2} \text{Tr} \mathcal{M}^\dagger \mathcal{M} + \lambda \left(\frac{1}{2} \text{Tr} \mathcal{M}^\dagger \mathcal{M} \right)^2. \quad (5.5)$$

In addition to the global version of the $SU(2)_L$ gauge symmetry, which transforms \mathcal{M} according to

$$\mathcal{M} \rightarrow L\mathcal{M} \quad (5.6)$$

the potential is also invariant for $SU(2)_R$ transformations of the form

$$\mathcal{M} \rightarrow \mathcal{M}R^\dagger. \quad (5.7)$$

While after electroweak symmetry breaking the vacuum expectation value

$$\langle \mathcal{M} \rangle = \frac{1}{2} \begin{pmatrix} v & 0 \\ 0 & v \end{pmatrix} \quad (5.8)$$

breaks both symmetries

$$L\langle \mathcal{M} \rangle \neq \langle \mathcal{M} \rangle; \quad \langle \mathcal{M} \rangle R^\dagger \neq \langle \mathcal{M} \rangle, \quad (5.9)$$

the potential is still invariant under the subgroup $SU(2)_{L+R}$ of simultaneous $SU(2)_L$ and $SU(2)_R$ transformations with $L = R$, since

$$L\langle \mathcal{M} \rangle L^\dagger = \langle \mathcal{M} \rangle. \quad (5.10)$$

This remaining $SU(2)_{L+R}$ is called the custodial symmetry.

However the custodial symmetry is not an exact symmetry of the SM. It is broken by the hypercharge coupling g_1 in the kinetic term of the Higgs Lagrangian which can be written with the matrix field \mathcal{M} as

$$\frac{1}{2} \text{Tr} (D_\mu \mathcal{M})^\dagger (D^\mu \mathcal{M}) \quad (5.11)$$

with the covariant derivative

$$D_\mu \mathcal{M} = \left(\partial_\mu \mathcal{M} + i \frac{g_2}{2} \vec{\sigma} \cdot \vec{W}_\mu \mathcal{M} - i \frac{g_1}{2} B_\mu \mathcal{M} \sigma_3 \right). \quad (5.12)$$

When neglecting g_1 the kinetic term is invariant under the custodial symmetry since \vec{W}_μ transforms as a triplet under the global $SU(2)_L$,

$$\vec{\sigma} \cdot \vec{W}_\mu \rightarrow L \vec{\sigma} \cdot \vec{W}_\mu L^\dagger, \quad (5.13)$$

which corresponds to a rotation of the triplet fields W_μ^a ($a = 1, 2, 3$). Since in addition the vacuum expectation value $\langle \mathcal{M} \rangle$ is invariant under the custodial symmetry, the masses of the gauge bosons fulfill the relation

$$\frac{M_W^2}{M_Z^2 c_W^2} = 1, \quad (5.14)$$

which is equivalent to the tree-level value of the ρ -parameter, as will be shown in Section 5.2.

The custodial symmetry in the SM is also broken by the Yukawa interaction. For simplicity we will consider only one quark family with a left handed doublet

$$Q_L = \begin{pmatrix} u_L \\ d_L \end{pmatrix} \quad (5.15)$$

and right handed singlets

$$u_R, d_R. \quad (5.16)$$

In this case the Yukawa interaction is given by

$$\mathcal{L}_Y = -y_u \bar{Q}_L \tilde{\Phi} u_R - y_d \bar{Q}_L \Phi d_R + \text{h.c.} \quad (5.17)$$

with the Yukawa couplings y_q . Inserting the vacuum expectation value leads to

$$\mathcal{L}_Y = -m_u \bar{u}_L u_R - m_d \bar{d}_L d_R + \text{h.c.}, \quad (5.18)$$

with the quark masses

$$m_q = y_q \frac{v}{\sqrt{2}}. \quad (5.19)$$

For

$$y_u = y_d \equiv y \quad (5.20)$$

we can write

$$\mathcal{L}_Y = -y \bar{Q}_L \mathcal{M} Q_R + \text{h.c.} \quad (5.21)$$

with

$$Q_R = \begin{pmatrix} u_R \\ d_R \end{pmatrix}. \quad (5.22)$$

The Yukawa interaction is then invariant under the $SU(2)_L \times SU(2)_R$ and the quark doublets transform as

$$Q_L \rightarrow L Q_L, \quad Q_R \rightarrow R Q_R. \quad (5.23)$$

Therefore the custodial symmetry is broken by mass differences of two quarks belonging to the same doublet. For example the mass difference between the top- and the bottom quark leads to an important correction to the ρ parameter, which is quadratic in the top mass.

5.1.2 Custodial symmetry in the THDM potential

A scalar potential with two doublets contains additional terms which can violate the custodial symmetry. A lot of work has been dedicated to investigations of how the custodial symmetry can be restored in the THDM [204–209], since there are several possibilities to implement the $SU(2)_L \times SU(2)_R$ transformations for two doublets. One way is to introduce matrix fields

$$\mathcal{M}_i = \left(\tilde{\Phi}_i | \Phi_i \right); \quad i = 1, 2, \quad (5.24)$$

similar to (5.3) with the two original doublets in (2.15). These matrices transform under the $SU(2)_L \times SU(2)_R$ as

$$\mathcal{M}_i \rightarrow L \mathcal{M}_i R^\dagger. \quad (5.25)$$

and the potential is then custodial invariant for $m_{H^\pm} = m_{A^0}$ [204, 205]. A different implementation of the custodial transformations was found in [205, 206] by introducing the matrix field

$$\mathcal{M}_{21} = \left(\tilde{\Phi}_2 | \Phi_1 \right) \quad (5.26)$$

which transforms as

$$\mathcal{M}_{21} \rightarrow L \mathcal{M}_{21} R^\dagger \quad (5.27)$$

under the $SU(2)_L \times SU(2)_R$. For an unbroken $SU(2)_{L+R}$ after electroweak symmetry breaking, the vacuum expectation values have to fulfill $v_1 = v_2$. An invariant potential under this custodial transformation requires $m_{H^\pm} = m_{H^0}$. However, as shown by [207–209] these different implementations of the $SU(2)_L \times SU(2)_R$ transformations are dependent on the selected basis of the two doublets and are related by a basis transformation of the form (2.17).

We will demonstrate how the custodial symmetry can be imposed in the alignment limit on the potential for the basis of Φ_{SM} and Φ_{NS} as defined in (2.94) and (2.95). This choice of basis corresponds to the so-called Higgs basis as defined for example in [128, 210] in which only one of the doublets has a non-vanishing vacuum expectation value in its neutral component. Note that the definition of the Higgs basis is only specified up to a rephasing of the second doublet. As explained in [208], the matrix fields

$$\mathcal{M}_{\text{SM}} = \left(\tilde{\Phi}_{\text{SM}} | \Phi_{\text{SM}} \right) \quad (5.28)$$

and

$$\mathcal{M}_{\text{NS}} = \left(\tilde{\Phi}_{\text{NS}} | \Phi_{\text{NS}} \right) \quad (5.29)$$

are the only two possible definitions that preserve the custodial $SU(2)_{L+R}$ after electroweak symmetry breaking. Following [206, 208] the transformations under the $SU(2)_L \times SU(2)_R$ are written as

$$\mathcal{M}_{\text{SM}} \rightarrow L \mathcal{M}_{\text{SM}} R^\dagger, \quad \mathcal{M}_{\text{NS}} \rightarrow L \mathcal{M}_{\text{NS}} R'^\dagger, \quad (5.30)$$

with $L \in SU(2)_L$ and $R, R' \in SU(2)_R$. Since both doublets transform in the same way under the weak $SU(2)_L$ gauge transformations, they have the same transformation matrix L in (5.30). The same requirement does not hold for transformations under $SU(2)_R$. As explained in [206, 208, 209], the matrices R and R' are only related by the fact that the doublets Φ_{SM} and Φ_{NS} have the same hypercharge and that the $U(1)_Y$ is a subgroup of the $SU(2)_R$. When writing $R = \exp(i\theta n^a T_R^a)$ in terms of an unit vector n^a and the generators $T_R^a = \sigma^a/2$ ($a = 1, 2, 3$), the hypercharge operator for the matrix fields is

$$Y = \text{diag}(-1, 1) = 2T_R^3. \quad (5.31)$$

In order to obtain the same hypercharge transformations for \mathcal{M}_{SM} and \mathcal{M}_{NS} the matrices R and R' are related by

$$R = X^{-1} R' X, \quad (5.32)$$

with

$$X \exp(i\theta Y) X^{-1} = \exp(i\theta Y). \quad (5.33)$$

This requires the matrix X to have the form

$$X = \begin{pmatrix} e^{-i\chi} & 0 \\ 0 & e^{i\chi} \end{pmatrix}, \quad 0 \leq \chi \leq 2\pi. \quad (5.34)$$

A scalar potential is invariant under the transformations in (5.30) if it contains only the invariant combinations

$$\text{Tr} \mathcal{M}_{\text{SM}}^\dagger \mathcal{M}_{\text{SM}} = 2\Phi_{\text{SM}}^\dagger \Phi_{\text{SM}}, \quad (5.35)$$

$$\text{Tr} \mathcal{M}_{\text{NS}}^\dagger \mathcal{M}_{\text{NS}} = 2\Phi_{\text{NS}}^\dagger \Phi_{\text{NS}}, \quad (5.36)$$

and

$$\text{Tr} \mathcal{M}_{\text{SM}}^\dagger \mathcal{M}_{\text{NS}} X = e^{-i\chi} \Phi_{\text{NS}}^\dagger \Phi_{\text{SM}} + e^{i\chi} \Phi_{\text{SM}}^\dagger \Phi_{\text{NS}}. \quad (5.37)$$

The parts V_{I} and V_{II} of the potential in (2.99) are clearly custodial invariant. The parts V_{III} and V_{IV} are in general not invariant under the transformations in (5.30). In order to restore the custodial symmetry the parameters have to be adjusted depending on the value of χ . For a CP -conserving potential with real parameters this is only possible for $\chi = 0$ and $\chi = \pi/2$.

For $\chi = 0$, we have $R = R'$ and therefore

$$\mathcal{M}_{\text{SM}} \rightarrow L \mathcal{M}_{\text{SM}} R^\dagger, \quad (5.38)$$

$$\mathcal{M}_{\text{NS}} \rightarrow L \mathcal{M}_{\text{NS}} R^\dagger. \quad (5.39)$$

This leads to the invariant quantity

$$\text{Tr} \mathcal{M}_{\text{SM}}^\dagger \mathcal{M}_{\text{NS}} X = \text{Tr} \mathcal{M}_{\text{SM}}^\dagger \mathcal{M}_{\text{NS}} = \Phi_{\text{NS}}^\dagger \Phi_{\text{SM}} + \Phi_{\text{SM}}^\dagger \Phi_{\text{NS}}. \quad (5.40)$$

The part V_{IV} from the potential in (2.99) is invariant under this custodial transformation since it can be written as follows:

$$V_{\text{IV}} = \left(\frac{1}{v^2 t_{2\beta}} \left(m_{H^0}^2 - \frac{m_{12}^2}{c_\beta s_\beta} \right) - \frac{\Lambda_7}{4c_\beta^2} + \frac{\Lambda_6}{4s_\beta^2} \right) \text{Tr} \mathcal{M}_{\text{NS}}^\dagger \mathcal{M}_{\text{NS}} \text{Tr} \mathcal{M}_{\text{SM}}^\dagger \mathcal{M}_{\text{NS}} \quad (5.41)$$

If we set $m_{A^0} = m_{H^\pm}$ we can also write V_{III} in terms of the invariant quantities,

$$V_{\text{III}} \xrightarrow{m_{A^0} = m_{H^\pm}} \frac{m_{H^0}^2 - m_{H^\pm}^2}{2v^2} \left(\text{Tr} \mathcal{M}_{\text{SM}}^\dagger \mathcal{M}_{\text{NS}} \right)^2 + \left(\frac{2m_{H^\pm}^2 + m_{h^0}^2}{v^2} - \frac{2m_{12}^2}{v^2 c_\beta s_\beta} \right) \cdot \frac{1}{4} \text{Tr} \mathcal{M}_{\text{SM}}^\dagger \mathcal{M}_{\text{SM}} \text{Tr} \mathcal{M}_{\text{NS}}^\dagger \mathcal{M}_{\text{NS}} \quad (5.42)$$

Consequently custodial invariance in the potential can be restored for $m_{A^0} = m_{H^\pm}$.

For $\chi = \frac{\pi}{2}$ we have

$$X = \begin{pmatrix} -i & 0 \\ 0 & i \end{pmatrix} \quad (5.43)$$

and

$$\text{Tr} \mathcal{M}_{\text{SM}}^\dagger \mathcal{M}_{\text{NS}} X = -i \Phi_{\text{NS}}^\dagger \Phi_{\text{SM}} + i \Phi_{\text{SM}}^\dagger \Phi_{\text{NS}}. \quad (5.44)$$

Invariance of V_{III} under this custodial transformation is obtained for $m_{H^0}^2 = m_{H^\pm}^2$:

$$V_{\text{III}} \xrightarrow{m_{H^0}=m_{H^\pm}} \frac{m_{A^0}^2 - m_{H^\pm}^2}{2v^2} \left(\text{Tr} \mathcal{M}_{\text{SM}}^\dagger \mathcal{M}_{\text{NS}} X \right)^2 + \left(\frac{2m_{H^\pm}^2 + m_{h^0}^2}{v^2} - \frac{2m_{12}^2}{v^2 c_\beta s_\beta} \right) \cdot \frac{1}{4} \text{Tr} \mathcal{M}_{\text{SM}}^\dagger \mathcal{M}_{\text{SM}} \text{Tr} \mathcal{M}_{\text{NS}}^\dagger \mathcal{M}_{\text{NS}}. \quad (5.45)$$

However, the part V_{IV} in the potential cannot be written in terms of the invariant quantity specified in (5.44). Consequently, it has to vanish in the case of a potential invariant under this custodial transformation. This can be achieved by setting

$$\frac{2m_{H^0}^2}{v^2} = \lambda_5 \quad (5.46)$$

or

$$t_\beta = 1. \quad (5.47)$$

5.1.3 Custodial symmetry in the Yukawa sector of the THDM

Here we investigate the custodial symmetry in the different types of Yukawa interactions in the THDM. For simplicity we restrict ourselves again to one quark family.

For the THDM of type-I or type-X the Yukawa interaction in the aligned doublets is given by

$$\mathcal{L}_Y = -y_d \bar{Q}_L \Phi_2 d_R - y_u \bar{Q}_L \tilde{\Phi}_2 u_R + \text{h.c.} \quad (5.48)$$

$$\begin{aligned} &= -s_\beta y_d \bar{Q}_L \Phi_{\text{SM}} d_R - s_\beta y_u \bar{Q}_L \tilde{\Phi}_{\text{SM}} u_R + \text{h.c.} \\ &\quad - c_\beta y_d \bar{Q}_L \Phi_{\text{NS}} d_R - c_\beta y_u \bar{Q}_L \tilde{\Phi}_{\text{NS}} u_R + \text{h.c.} \end{aligned} \quad (5.49)$$

Inserting the vacuum expectation value for Φ_{SM} leads to the quark masses

$$m_q = \frac{s_\beta y_q v}{\sqrt{2}}. \quad (5.50)$$

For

$$m_u = m_d \equiv m \quad (5.51)$$

we can write

$$\mathcal{L}_Y = -\sqrt{2} \frac{m}{v} \bar{Q}_L \mathcal{M}_{\text{SM}} Q_R - \sqrt{2} \frac{m}{v t_\beta} \bar{Q}_L \mathcal{M}_{\text{NS}} Q_R + \text{h.c.} \quad (5.52)$$

which is invariant under the custodial transformations (5.23) and (5.30) for $\chi = 0$.

For the THDM of type-II or type-Y the Yukawa couplings of the quarks to the aligned doublets are written as

$$\begin{aligned} \mathcal{L}_Y &= -y_d \bar{Q}_L \Phi_1 d_r - y_u \bar{Q}_L \tilde{\Phi}_2 u_R + \text{h.c.} \\ &= -c_\beta y_d \bar{Q}_L \Phi_{\text{SM}} d_R - s_\beta y_u \bar{Q}_L \tilde{\Phi}_{\text{SM}} u_R + \text{h.c.} \\ &\quad + s_\beta y_d \bar{Q}_L \Phi_{\text{NS}} d_R - c_\beta y_u \bar{Q}_L \tilde{\Phi}_{\text{NS}} u_R + \text{h.c.} \end{aligned} \quad (5.53)$$

The vacuum expectation value of Φ_{SM} leads to the quark masses

$$m_d = c_\beta \frac{y_d v}{\sqrt{2}}, \quad (5.54)$$

$$m_u = s_\beta \frac{y_u v}{\sqrt{2}}, \quad (5.55)$$

and the Yukawa interaction takes the form

$$\begin{aligned} \mathcal{L}_Y = & -\sqrt{2} \frac{m_d}{v} \bar{Q}_L \Phi_{\text{SM}} d_R - \sqrt{2} \frac{m_u}{v} \bar{Q}_L \tilde{\Phi}_{\text{SM}} u_R + \text{h.c.} \\ & + \sqrt{2} \frac{m_d t_\beta}{v} \bar{Q}_L \Phi_{\text{NS}} d_R - \sqrt{2} \frac{m_u}{v t_\beta} \bar{Q}_L \tilde{\Phi}_{\text{NS}} u_R + \text{h.c.} \end{aligned} \quad (5.56)$$

The requirement that the part with Φ_{SM} should be invariant under the custodial transformation leads again to

$$m_u = m_d = m. \quad (5.57)$$

If in addition

$$t_\beta = \frac{1}{t_\beta} = 1, \quad (5.58)$$

we can write the Yukawa interaction in the form

$$\mathcal{L}_Y = -\sqrt{2} \frac{m}{v} \bar{Q}_L \mathcal{M}_{\text{SM}} Q_R - i\sqrt{2} \frac{m}{v} \bar{Q}_L \mathcal{M}_{\text{NS}} X Q_R + \text{h.c.}, \quad (5.59)$$

with

$$X = \begin{pmatrix} -i & 0 \\ 0 & i \end{pmatrix}. \quad (5.60)$$

The Yukawa interaction in the THDM of type-II or type-Y is therefore invariant under the custodial transformations (5.23) and (5.30) for $\chi = \pi/2$ for equal quark masses and $t_\beta = 1$.

5.1.4 Custodial symmetry in the IHDM

The original doublets Φ_1 and Φ_2 are already corresponding to the Higgs basis due to the unbroken Z_2 symmetry, such that

$$\Phi_1 \equiv \Phi_{\text{SM}}, \quad \Phi_2 \equiv \Phi_{\text{NS}}, \quad (5.61)$$

in the IHDM. The matrix fields

$$\mathcal{M}_i = \left(\tilde{\Phi}_i | \Phi_i \right), \quad (i = 1, 2) \quad (5.62)$$

transform as

$$\mathcal{M}_1 \rightarrow L \mathcal{M}_1 R^\dagger, \quad \mathcal{M}_2 \rightarrow L \mathcal{M}_2 R^\dagger, \quad (5.63)$$

under the $SU(2)_L \times SU(2)_R$ and preserve the custodial $SU(2)_{L+R}$ after electroweak symmetry breaking. The discussion about the custodial breaking terms of the IHDM potential is then analogous to the discussion in the aligned THDM. Using the parameterization (2.115) of the potential in the IHDM, we see directly that the terms $V_{\text{I}}^{\text{IHDM}}$ and $V_{\text{II}}^{\text{IHDM}}$ respect the custodial symmetry, since they can be expressed by the invariant quantities

$$\text{Tr} \mathcal{M}_i^\dagger \mathcal{M}_i = 2\Phi_i^\dagger \Phi_i, \quad (i = 1, 2). \quad (5.64)$$

The term $V_{\text{III}}^{\text{IHDM}}$ is in general not custodial invariant. However a custodial symmetry can be restored for

$$m_{A^0} = m_{H^\pm} \quad (5.65)$$

or

$$m_{H^0} = m_{H^\pm}. \quad (5.66)$$

Differently from the potential in the aligned THDM, an additional custodial violating term, which would correspond to V_{IV} , is absent in the IHDM potential due to the exact Z_2 symmetry.

5.2 Corrections to the ρ parameter from quantum loops

The ρ parameter

$$\rho = \frac{G_{\text{NC}}}{G_{\text{CC}}} \quad (5.67)$$

was originally introduced [211] for four-fermion processes at low momentum. G_{NC} is the strength in the effective four-fermion interaction

$$\mathcal{L}_{\text{NC}}^{\text{eff}} = \frac{G_{\text{NC}}}{\sqrt{2}} g_{\mu\nu} J_{\text{NC}}^\mu J_{\text{NC}}^{\nu\dagger} \quad (5.68)$$

of the neutral current (NC)

$$J_{\text{NC}}^\mu = \bar{\psi}_f \gamma^\mu \left[\left(I_3^f - 2s_W^2 Q_f \right) - I_3^f \gamma_5 \right] \psi_f. \quad (5.69)$$

G_{NC} can be determined for example in neutrino-scattering experiments. G_{CC} is the strength of the effective four-fermion interaction

$$\mathcal{L}_{\text{CC}}^{\text{eff}} = \frac{G_{\text{CC}}}{\sqrt{2}} g_{\mu\nu} J_{\text{CC}}^\mu J_{\text{CC}}^{\nu\dagger} \quad (5.70)$$

of the charged current (CC)

$$J_{\text{CC}}^\mu = \bar{\psi}_{\nu_l} \gamma^\mu (1 - \gamma_5) \psi_l, \quad (5.71)$$

which is stated here for simplicity just for the interaction between leptons and neutrinos. The charged-current strength can be measured in the decay of the muon and is identical to the Fermi constant G_F . In the electroweak theory both classes of processes are mediated by the exchange of a heavy gauge boson, the Z boson for NC and the W^\pm boson for CC processes. In the effective theory for low momentum transfer we can approximate the propagators by $1/M_V^2$ ($V = W, Z$). Therefore the effective couplings at the tree level are given by

$$\frac{G_{\text{NC}}}{\sqrt{2}} = \frac{e^2}{8s_W^2 c_W^2 M_Z^2}, \quad (5.72)$$

$$\frac{G_{\text{CC}}}{\sqrt{2}} = \frac{e^2}{8s_W^2 M_W^2}, \quad (5.73)$$

which results in

$$\rho = \frac{M_W^2}{c_W^2 M_Z^2} = 1. \quad (5.74)$$

Including higher-order contributions in the calculation of the effective couplings G_{NC} and G_{CC} leads to a deviation from unity, written as [25, 27, 212]

$$\rho = \frac{1}{1 - \Delta\rho}, \quad (5.75)$$

with the loop expansion

$$\Delta\rho = \Delta\rho^{(1)} + \Delta\rho^{(2)} + \dots \quad (5.76)$$

Although conceptually defined at low-momentum scales, the quantity $\Delta\rho$ represents an important ingredient for electroweak precision observables as the leading universal correction, with a substantial impact e.g. on the effective electroweak mixing angle and the W mass.

The higher-order corrections to the charged and neutral current processes consist of the gauge-boson self-energies as well as corrections from vertex- and box-diagrams, all evaluated for vanishing external momentum $q^2 \approx 0$. The dominant part of $\Delta\rho$ originates from the self-energies, which lead in the SM for example in the one-loop correction quadratic in the top mass. The vertex- and box-contributions are small in comparison.

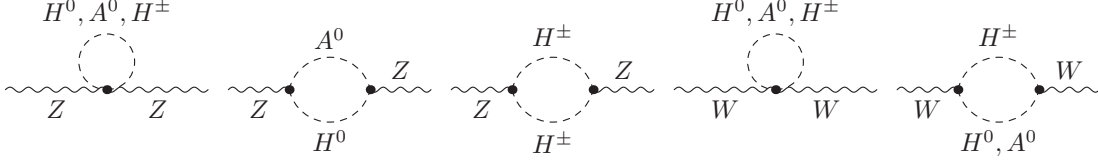


Figure 5.1: Non-standard contributions from the THDM scalars to the Z and W boson self-energies in the alignment limit at the one-loop level.

5.2.1 One-loop corrections in the SM and the THDM

The contributions to the effective coupling strengths from the self-energies is given at the one-loop order by

$$\frac{G_{\text{NC}}}{\sqrt{2}} = \frac{e_0^2}{8s_{W,0}^2 c_{W,0}^2 M_{Z,0}^2} \left[1 + \frac{\Sigma_Z^{(1)}(0)}{M_Z^2} \right] \quad (5.77)$$

and

$$\frac{G_{\text{CC}}}{\sqrt{2}} = \frac{e_0^2}{8s_{W,0}^2 M_{W,0}^2} \left[1 + \frac{\Sigma_W^{(1)}(0)}{M_W^2} \right]. \quad (5.78)$$

The expansions of the bare parameters cancel when calculating the ρ parameter. Therefore, the correction to the ρ parameter at the one-loop order is given by

$$\Delta\rho^{(1)} = \frac{\Sigma_Z^{(1)}(0)}{M_Z^2} - \frac{\Sigma_W^{(1)}(0)}{M_W^2}. \quad (5.79)$$

A large contribution to $\Delta\rho^{(1)}$ arises from the large mass splitting between the top and the bottom quark and is identical to the dominant part of the one-loop corrections to $\Delta\rho$ in the SM [21–23]. It reads

$$\Delta\rho_{\text{tb}}^{(1)} = \frac{3\alpha_{em}}{16\pi M_W^2 s_W^2} \left(m_t^2 + m_b^2 - 2 \frac{m_b^2 m_t^2}{m_t^2 - m_b^2} \log \left(\frac{m_t^2}{m_b^2} \right) \right). \quad (5.80)$$

When neglecting the mass of the bottom quark we obtain the one-loop result

$$\Delta\rho_t^{(1)} = \frac{3\alpha_{em}}{16\pi M_W^2 s_W^2} m_t^2, \quad (5.81)$$

which is proportional to m_t^2/v^2 due to the parameterization of v^2 in (2.74).

The extended scalar sector of the THDM gives additional scalar contributions to $\Delta\rho$ [85–88, 91, 131]. In the alignment limit the additional correction follows from the scalars H^0 , A^0 and H^\pm . The gauge-boson self-energies from the diagrams in Figure 5.1 give rise to the non-standard one-loop part

$$\begin{aligned} \Delta\rho_{\text{NS}}^{(1)} = \frac{\alpha_{em}}{16\pi s_W^2 M_W^2 D} & \left\{ 4m_{A^0}^2 B_0(0, m_{A^0}^2, m_{H^\pm}^2) + 4m_{H^0}^2 B_0(0, m_{H^0}^2, m_{H^\pm}^2) \right. \\ & - 4m_{A^0}^2 B_0(0, m_{A^0}^2, m_{H^0}^2) + (8 - 2D)A_0(m_{H^\pm}^2) \\ & \left. - 4A_0(m_{H^0}^2) \right\} \end{aligned} \quad (5.82)$$

which is finite for $D \rightarrow 4$, yielding

$$\begin{aligned} \Delta\rho_{\text{NS}}^{(1)} \xrightarrow{D \rightarrow 4} & \frac{\alpha_{em}}{16\pi s_W^2 M_W^2} \left\{ \frac{m_{A^0}^2 m_{H^0}^2}{m_{A^0}^2 - m_{H^0}^2} \log \left(\frac{m_{A^0}^2}{m_{H^0}^2} \right) - \frac{m_{A^0}^2 m_{H^\pm}^2}{m_{A^0}^2 - m_{H^\pm}^2} \log \left(\frac{m_{A^0}^2}{m_{H^\pm}^2} \right) \right. \\ & \left. - \frac{m_{H^0}^2 m_{H^\pm}^2}{m_{H^0}^2 - m_{H^\pm}^2} \log \left(\frac{m_{H^0}^2}{m_{H^\pm}^2} \right) + m_{H^\pm}^2 \right\}. \end{aligned} \quad (5.83)$$

This contribution contains only the Higgs-self-couplings, since it is proportional to m_S^2/v^2 (with $S = H^0, A^0, H^\pm$). It increases quadratically with the mass difference between the charged and the neutral Higgs states, and it vanishes for

$$m_{H^0} = m_{H^\pm} \quad (5.84)$$

or

$$m_{A^0} = m_{H^\pm}. \quad (5.85)$$

The reason is that this correction originates only from the couplings between the Goldstone bosons and the non-standard scalars H^0, A^0 and H^\pm which are determined by the part V_{III} of the potential. As explained in Section 5.1, the custodial symmetry in this part can be restored for equal charged and neutral Higgs masses.

In the SM no contributions to $\Delta\rho^{(1)}$ arise from the Higgs-self-coupling due to the custodial symmetry of the Higgs potential. In a similar way there is no scalar correction from the SM-like scalars h^0, G^0 and G^\pm in the THDM in the alignment limit described in Section 2.5, since the part V_{I} of the potential in (2.99) is custodial invariant. The contributions to the gauge-boson self-energies which are proportional to $m_{h^0}^2/v^2$ are given by

$$\frac{\Sigma_{V,\text{SM}}^{(1)}(0)}{M_V^2} = \frac{\alpha_{em}}{16\pi s_W^2 M_W^2} \frac{(D-4)}{D} A_0(m_{h^0}^2), \quad (5.86)$$

for both $V = W, Z$. They cancel in the difference for $\Delta\rho^{(1)}$ in (5.79). The remaining parts of the gauge-boson self-energies with the SM-like scalars as internal particles are proportional to the gauge couplings. Since their UV-divergences are not canceled in the difference in (5.79), a UV-finite result including also contributions from the gauge couplings requires a complete calculation of $\Delta\rho$.

In the THDM in the alignment limit the one-loop correction is therefore dominated by two parts

$$\Delta\rho^{(1)} = \Delta\rho_{\text{t}}^{(1)} + \Delta\rho_{\text{NS}}^{(1)} \quad (5.87)$$

originating from the top-Yukawa interaction and the scalar sector.

5.2.2 Approximations for the two-loop contributions

For an improved calculation of the ρ parameter in the THDM, we hence need the two-loop contributions from the top-Yukawa and the scalar-self-interaction, since these sectors give the dominant one-loop effects. Technically these two-loop corrections are obtained by applying the gauge-less limit (as done in [119] for the MSSM) and neglecting the light fermion masses, as explained in the following part.

In the gauge-less limit the electroweak gauge couplings $g_{1,2}$ are set to zero and thus the gauge-boson masses are also equal to zero,

$$M_W^2 = \frac{g_2^2 v^2}{4} \rightarrow 0, \quad M_Z^2 = \frac{(g_1^2 + g_2^2) v^2}{4} \rightarrow 0, \quad (5.88)$$

while their ratio in c_W and s_W stays constant. Moreover, the gauge-less limit sets the masses of the Goldstone bosons equal to zero,

$$m_{G^0} = m_{G^\pm} = 0. \quad (5.89)$$

The ratios

$$\frac{\Sigma_V(0)}{M_V^2} \quad (V = W, Z). \quad (5.90)$$

are non-zero in the gauge-less limit, since the gauge-couplings in self-energies of $\mathcal{O}(g_{1,2}^2)$ cancel with the ones contained in the gauge-boson masses. Consequently, only diagrams with internal scalars or fermions contribute to $\Delta\rho$. Also the ratios $\delta^{(1)} M_V^2/M_V^2$, which are contained in the counterterm of s_W^2 in (4.25) have remaining contributions. The resulting one-loop renormalization conditions in the gauge-less limit are given by

$$\frac{\delta^{(1)} M_W^2}{M_W^2} = \frac{\text{Re} \Sigma_W^{(1)}(0)}{M_W^2}, \quad \frac{\delta^{(1)} M_Z^2}{M_Z^2} = \frac{\text{Re} \Sigma_Z^{(1)}(0)}{M_Z^2}. \quad (5.91)$$

Due to a Ward identity valid in the gauge-less limit [26, 28] the ratios in (5.90) can be calculated also by the relations

$$\frac{\Sigma_Z(0)}{M_Z^2} = -\Sigma'_{G^0}(0), \quad \frac{\Sigma_W(0)}{M_W^2} = -\Sigma'_{G^\pm}(0), \quad (5.92)$$

where the Goldstone self-energies are decomposed according to

$$\Sigma_G(p^2) = \Sigma_G(0) + p^2 \Sigma'_G(p^2), \quad (G = G^0, G^\pm). \quad (5.93)$$

We use this Ward identity as a test for our result. Moreover, the origin of a specific contribution in $\Delta\rho$ is not always directly visible in the calculation based on the gauge-boson self-energies due to the cancellation of the gauge couplings in the ratio (5.90). In these cases, the involved couplings can be identified with the help of the Ward identity.

Note that in the alignment case the entire non-standard one-loop contribution to $\Delta\rho$ is exclusively given by the expression (5.83), corresponding to the gauge-less limit.

In addition to the gauge-less limit the Yukawa-couplings of the light fermions can also be neglected, since they are suppressed by the light masses. In the top-Yukawa approximation all the fermion masses with the exception of the top-quark mass are set to zero. Especially for the bottom quark, which appears in some of the diagrams for the $\mathcal{O}(\alpha_t^2)$ contributions, the mass is set to $m_b = 0$ in the top-Yukawa approximation. However, in contrast to the top-Yukawa coupling, which is universal in all of the four models, the Yukawa coupling of the bottom quark is model specific. In models of type-I and type-X, the bottom- and top-Yukawa interactions have the same structure, and the additional contributions to $\Delta\rho$ from the b quark are negligible due to the small value of m_b . In models of type-II or type-Y, the b -Yukawa coupling can be enhanced by t_β , and the top-Yukawa approximation is justified in these models only as long as we do not consider large values of t_β . Therefore, the two-loop correction to the ρ parameter from the Yukawa interaction is calculated with and without the contribution from the bottom quark. In this way we can test the values of t_β for which the top-Yukawa approximation is valid.

5.2.3 Higher-order corrections in the THDM

As mentioned above, it is sufficient to keep only the corrections from the gauge-boson self-energies in the calculation of the effective neutral and charged current interaction of the four fermion processes. The one- and two-loop contributions to the effective couplings from the gauge-boson self-energies are given by

$$\frac{G_{\text{NC}}}{\sqrt{2}} = \frac{e_0^2}{8s_{W,0}^2 c_{W,0}^2 M_{Z,0}^2} \left[1 + \frac{\Sigma_Z^{(1)}(0)}{M_Z^2} - \frac{\delta^{(1)} M_Z^2 \Sigma_Z^{(1)}(0)}{M_Z^2 M_Z^2} + \left(\frac{\Sigma_Z^{(1)}(0)}{M_Z^2} \right)^2 + \frac{\Sigma_Z^{(2)}(0)}{M_Z^2} \right] \quad (5.94)$$

and

$$\frac{G_{\text{CC}}}{\sqrt{2}} = \frac{e_0^2}{8s_{W,0}^2 M_{W,0}^2} \left[1 + \frac{\Sigma_W^{(1)}(0)}{M_W^2} - \frac{\delta^{(1)} M_W^2 \Sigma_W^{(1)}(0)}{M_W^2 M_W^2} + \left(\frac{\Sigma_W^{(1)}(0)}{M_W^2} \right)^2 + \frac{\Sigma_W^{(2)}(0)}{M_W^2} \right]. \quad (5.95)$$

With the renormalization condition (5.91) for the gauge-boson mass counterterms in the gauge-less limit the products of one-loop corrections in the brackets cancel. The calculation of ρ as defined by (5.67) then yields the deviation $\Delta\rho$ in (5.75) as follows,

$$\begin{aligned} \Delta\rho &= \left(\frac{\Sigma_Z^{(1)}(0)}{M_Z^2} - \frac{\Sigma_W^{(1)}(0)}{M_W^2} \right) \\ &\quad - \frac{\Sigma_Z^{(1)}(0)}{M_Z^2} \left(\frac{\Sigma_Z^{(1)}(0)}{M_Z^2} - \frac{\Sigma_W^{(1)}(0)}{M_W^2} \right) + \left(\frac{\Sigma_Z^{(2)}(0)}{M_Z^2} - \frac{\Sigma_W^{(2)}(0)}{M_W^2} \right) \\ &= \Delta\rho^{(1)} + \Delta\rho^{(2)}, \end{aligned} \quad (5.96)$$

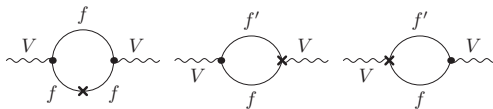


Figure 5.2: Generic diagrams for the gauge-boson self-energies containing quarks with counterterm insertions. $V = \{W, Z\}$; $f, f' = \{t, b\}$.

where the two-loop part is given by

$$\Delta\rho^{(2)} \equiv -\frac{\Sigma_Z^{(1)}(0)}{M_Z^2} \Delta\rho^{(1)} + \left(\frac{\Sigma_Z^{(2)}(0)}{M_Z^2} - \frac{\Sigma_W^{(2)}(0)}{M_W^2} \right). \quad (5.97)$$

$\Delta\rho^{(1)}$ summarizes the one-loop corrections as given by (5.79) and (5.87). The self-energy of the Z boson in the first term in (5.97) consists of all the corrections from the top quark and the scalars as internal particles. Note that it contains also the part from the SM-like scalars in (5.86), which cancel in $\Delta\rho^{(1)}$. The second part of (5.97) follows from the two-loop corrections to the gauge-boson self-energies. In addition to the part from the genuine two-loop diagrams (labelled as $\delta\rho^{(2\text{Loop})}$) it also includes one-loop diagrams with counterterm insertions for the subloop renormalization.

With the assumptions from Section 5.2.2 we have two sources for the two-loop contribution $\Delta\rho^{(2)}$: the top- and bottom-Yukawa interaction and the scalar self-interaction. Due to the alignment limit we can subdivide the Yukawa corrections into two parts. The first one is identical to the corresponding two-loop contribution in the SM and is discussed in Section 5.2.3.1. The second one originates from the coupling of the non-standard scalars H^0, A^0 and H^\pm to the top- and the bottom quark. It is described in more detail in Section 5.2.3.2. A similar separation can be made for the additional corrections to the ρ parameter from the scalar self-interaction. The part V_I of the potential (see (2.99a)), which describes only the interaction between h^0 and the Goldstone bosons G^0, G^\pm , is invariant under the custodial symmetry and the corresponding contributions to the vector-boson self-energies in $\Delta\rho$ cancel each other. The remaining part of the potential gives rise to two finite subsets in $\Delta\rho^{(2)}$. One follows from the interaction between the SM-like scalars h^0, G^0, G^\pm and the non-standard scalars H^0, A^0, H^\pm and is discussed in Section 5.2.3.4. The other one contains only the non-standard scalars H^0, A^0 and H^\pm as internal particles in the gauge-boson self-energies and is described in Section 5.2.3.3.

With this categorization we subdivide the contribution from the genuine two-loop diagrams (without subloop renormalization) to the vector-boson self-energies into different parts, according to their origin,

$$\delta\rho^{(2\text{Loop})} = \delta\rho_{\text{tb,SM}}^{(2\text{Loop})} + \delta\rho_{\text{tb,NS}}^{(2\text{Loop})} + \delta\rho_{\text{H,NS}}^{(2\text{Loop})} + \delta\rho_{\text{H,Mix}}^{(2\text{Loop})} \quad (5.98)$$

which are classified by the participating couplings:

- $\delta\rho_{\text{tb,SM}}^{(2\text{Loop})}$ originates from the coupling between the heavy quarks and the SM-like scalars h^0, G^0 and G^\pm (see Section 5.2.3.1);
- $\delta\rho_{\text{tb,NS}}^{(2\text{Loop})}$ is the part which follows from the Yukawa interaction of the non-standard scalars H^0, A^0 and H^\pm (see Section 5.2.3.2);
- $\delta\rho_{\text{H,NS}}^{(2\text{Loop})}$ contains the scalar self-coupling between the non-standard scalars (see Section 5.2.3.3);
- $\delta\rho_{\text{H,Mix}}^{(2\text{Loop})}$ follows from the interaction between the SM-like scalars and the non-standard scalars (see Section 5.2.3.4).

For one-loop subrenormalization we need the diagrams shown in Figure 5.2 for the self-energies with the top quarks and in Figure 5.3 for the scalar contribution. In the gauge-less limit only two types of renormalization constants contribute: the counterterm $\delta^{(1)}s_W^2$ from the counterterm insertions in the vertices, and the mass counterterms in the propagators of the

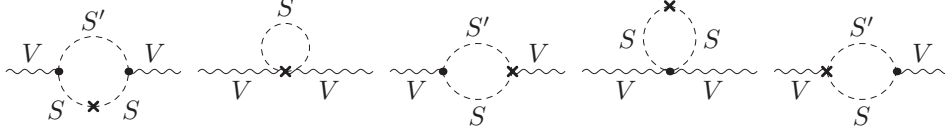


Figure 5.3: Generic diagrams for the gauge-boson self-energies $V = \{W, Z\}$ containing scalars with counterterm insertions. The contribution from the diagrams can be divided into two parts: one part with only the SM-like scalars ($S, S' = \{h^0, G^0, G^\pm\}$) and one part with only the non-standard scalars ($S, S' = \{H^0, A^0, H^\pm\}$).

internal particles. All field counterterms of the internal particles drop out in the calculation, and all other counterterms are zero in the gauge-less limit.

From the diagrams of Figure 5.2 we obtain the part of the subloop renormalization from the heavy quarks. The renormalization of the weak mixing angle is contained in the diagrams with vertex counterterm insertions (see Appendix A), which yield the term

$$\frac{s_W^2}{c_W^2} \frac{\delta^{(1)} s_W^2}{s_W^2} \frac{\Sigma_{Z, \text{tb}}^{(1)}(0)}{M_Z^2} - \frac{\delta^{(1)} s_W^2}{s_W^2} \Delta\rho_{\text{tb}}^{(1)}. \quad (5.99)$$

From the diagrams with counterterms in the propagators in Figure 5.2 we obtain the term

$$\begin{aligned} \delta\rho_{\text{tb}}^{(\text{CT})} &= \frac{3\alpha_{em}(D-2)}{16\pi D M_W^2 s_W^2 (m_b^2 - m_t^2)^2} \\ &\cdot \left\{ \frac{\delta m_b}{m_b} \left(A_0(m_b^2) [2(D-4)Dm_b^2 m_t^2 - (D^2 - 6D + 8)m_b^4 - (D-2)Dm_t^4] \right. \right. \\ &\quad \left. \left. + 8m_b^2 m_t^2 A_0(m_t^2) \right) \right. \\ &\quad \left. + \frac{\delta m_t}{m_t} \left(A_0(m_t^2) [2(D-4)Dm_b^2 m_t^2 - (D-2)Dm_b^4 - (D^2 - 6D + 8)m_t^4] \right. \right. \\ &\quad \left. \left. + 8m_b^2 m_t^2 A_0(m_b^2) \right) \right\} \end{aligned} \quad (5.100)$$

If the bottom-Yukawa coupling is neglected, the contribution simplifies to

$$\delta\rho_{\text{t}}^{(\text{CT})} = -\frac{3\alpha_{em}(D-4)(D-2)^2 A_0(m_t^2)}{16\pi D M_W^2 s_W^2} \frac{\delta m_t}{m_t}. \quad (5.101)$$

Due to the alignment limit we can split the result of the quark mass counterterms into a SM-like and a non-standard part. We use this for the separation

$$\delta\rho_{\text{tb}}^{(\text{CT})} = \delta\rho_{\text{tb, SM}}^{(\text{CT})} + \delta\rho_{\text{tb, NS}}^{(\text{CT})}, \quad (5.102)$$

where the two parts are defined as follows:

- the part $\delta\rho_{\text{tb, SM}}^{(\text{CT})}$ contains the correction to the quark-mass counterterms from the SM-like scalars h^0, G^0, G^\pm as shown in the self-energy diagrams in Figure 5.4;
- the second part $\delta\rho_{\text{tb, NS}}^{(\text{CT})}$ contains the part of the quark-mass counterterms which comes from the self-energy corrections from the non-standard scalars as depicted in Figure 5.5.

For the subloop renormalization diagrams in Figure 5.3 with the SM-like scalars h^0, G^0 and G^\pm we find that the mass counterterms drop out in the difference of the W and Z self-energy, due to custodial symmetry. From the vertex counterterms we obtain the contribution

$$\frac{s_W^2}{c_W^2} \frac{\delta^{(1)} s_W^2}{s_W^2} \frac{\Sigma_{Z, \text{SM}}^{(1)}(0)}{M_Z^2} \quad (5.103)$$

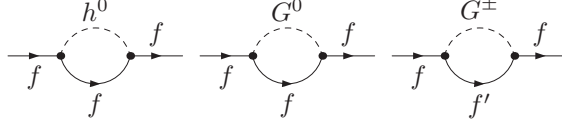


Figure 5.4: One-loop diagrams for the standard contribution to the quark mass counterterms. For δm_t : $f = t$ and $f' = b$. For δm_b : $f = b$ and $f' = t$.

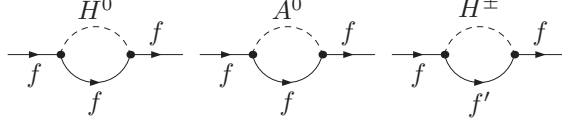


Figure 5.5: One-loop diagrams for the non-standard contribution to the quark mass counterterms. For δm_t : $f = t$ and $f' = b$. For δm_b : $f = b$ and $f' = t$.

with the one-loop self-energy from (5.86).

The diagrams in Figure 5.3 with the possible insertions of the non-standard scalars for S and S' give the last part of the subloop renormalization. With the Feynman rules of Appendix A the counterterms in the vertices yield the contribution

$$\frac{\Sigma_{Z,\text{NS}}^{(1)}(0)}{M_Z^2} \frac{s_W^2}{c_W^2} \frac{\delta^{(1)} s_W^2}{s_W^2} - \frac{\delta^{(1)} s_W^2}{s_W^2} \Delta\rho_{\text{NS}}^{(1)}, \quad (5.104)$$

where the Z self-energy in the first term contains just the contribution of the non-standard scalars.

The diagrams with the mass counterterms $\delta m_{H^0}^2$, $\delta m_{A^0}^2$ and $\delta m_{H^\pm}^2$ in Figure 5.3 yield the result, denoted by

$$\begin{aligned} \delta\rho_{\text{H}}^{(\text{CT})} &= \frac{\alpha_{em}}{16\pi D M_W^2 s_W^2} \times \\ &\times \left[2\delta m_{A^0}^2 \left(\frac{A_0(m_{A^0}^2) (Dm_{H^0}^2 - (D-2)m_{A^0}^2) - 2m_{H^0}^2 A_0(m_{H^0}^2)}{(m_{A^0}^2 - m_{H^0}^2)^2} \right. \right. \\ &\quad \left. \left. + \frac{A_0(m_{A^0}^2) ((D-2)m_{A^0}^2 - Dm_{H^\pm}^2) + 2m_{H^\pm}^2 A_0(m_{H^\pm}^2)}{(m_{A^0}^2 - m_{H^\pm}^2)^2} \right) \right. \\ &+ 2\delta m_{H^0}^2 \left(\frac{A_0(m_{H^0}^2) (Dm_{A^0}^2 - (D-2)m_{H^0}^2) - 2m_{A^0}^2 A_0(m_{A^0}^2)}{(m_{A^0}^2 - m_{H^0}^2)^2} \right. \\ &\quad \left. \left. + \frac{A_0(m_{H^0}^2) ((D-2)m_{H^0}^2 - Dm_{H^\pm}^2) + 2m_{H^\pm}^2 A_0(m_{H^\pm}^2)}{(m_{H^0}^2 - m_{H^\pm}^2)^2} \right) \right. \\ &+ \delta m_{H^\pm}^2 \left(\frac{(2A_0(m_{H^\pm}^2) ((D-2)m_{H^\pm}^2 - Dm_{A^0}^2) + 4A_0(m_{A^0}^2) m_{A^0}^2)}{(m_{A^0}^2 - m_{H^\pm}^2)^2} \right. \\ &\quad \left. \left. + \frac{(2A_0(m_{H^\pm}^2) ((D-2)m_{H^\pm}^2 - Dm_{H^0}^2) + 4m_{H^0}^2 A_0(m_{H^0}^2))}{(m_{H^0}^2 - m_{H^\pm}^2)^2} \right. \right. \\ &\quad \left. \left. - \frac{D(D-2)A_0(m_{H^\pm}^2)}{m_{H^\pm}^2} \right) \right]. \quad (5.105) \end{aligned}$$

We will classify three different parts

$$\delta\rho_{\text{H}}^{(\text{CT})} = \delta\rho_{\text{H,tb}}^{(\text{CT})} + \delta\rho_{\text{H,NS}}^{(\text{CT})} + \delta\rho_{\text{H,Mix}}^{(\text{CT})}, \quad (5.106)$$

which are defined by the insertions for the scalar mass counterterms as follows:

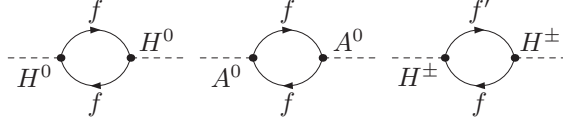


Figure 5.6: One-loop diagrams for the Yukawa contribution to the non-standard scalar mass counterterms. $f, f' = \{t, b\}$.

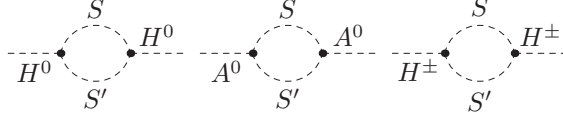


Figure 5.7: One-loop diagrams for the non-standard scalar mass counterterms from the interaction between the non-standard scalars. For the H^0 self-energy: $S = S' = H^0, A^0, H^\pm$. For the A^0 self-energy: $S = A^0$ and $S' = H^0$. For the H^\pm self-energy: $S = H^\pm$ and $S' = H^0$.

- $\delta\rho_{\text{H,tb}}^{(\text{CT})}$ contains the non-standard scalar mass counterterms originating from the Yukawa coupling of the non-standard scalars to the heavy quarks. The corresponding diagrams are shown in Figure 5.6.
- $\delta\rho_{\text{H,NS}}^{(\text{CT})}$ labels the part which contains only non-standard scalars in the calculation of $\delta m_{H^0}^2$, $\delta m_{A^0}^2$ and $\delta m_{H^\pm}^2$. The diagrams are displayed in Figure 5.7.
- $\delta\rho_{\text{H,Mix}}^{(\text{CT})}$ incorporates the contribution to the mass counterterms of H^0 , A^0 and H^\pm which originates from the couplings of the non-standard scalars to the SM-like scalars. The corresponding self-energy diagrams are presented in Figure 5.8.

When we combine the various parts from the subloop renormalization, their overall contribution to $\Delta\rho^{(2)}$ can be written as follows:

$$\Delta\rho^{(\text{CT})} = \frac{s_W^2}{c_W^2} \frac{\delta^{(1)} s_W^2}{s_W^2} \frac{\Sigma_Z^{(1)}(0)}{M_Z^2} - \frac{\delta^{(1)} s_W^2}{s_W^2} \left(\Delta\rho_{\text{tb}}^{(1)} + \Delta\rho_{\text{NS}}^{(1)} \right) + \delta\rho^{(\text{CT})}. \quad (5.107)$$

The first term incorporates all parts from (5.99), (5.103) and (5.104) involving a single Z -boson self-energy; the second term corresponds to the remaining terms from the renormalization of s_W in (5.99) and (5.104). The last term

$$\delta\rho^{(\text{CT})} = \delta\rho_{\text{tb}}^{(\text{CT})} + \delta\rho_{\text{H}}^{(\text{CT})} \quad (5.108)$$

collects the various parts resulting from the mass counterterm insertions in the internal lines.

The two-loop correction to the ρ parameter in (5.97) can be further simplified, since the counterterm of the weak mixing angle reduces to

$$\frac{\delta^{(1)} s_W^2}{s_W^2} = \frac{c_W^2}{s_W^2} \left(\frac{\Sigma_Z^{(1)}(0)}{M_Z^2} - \frac{\Sigma_W^{(1)}(0)}{M_W^2} \right) = \frac{c_W^2}{s_W^2} \Delta\rho^{(1)}. \quad (5.109)$$

in the gauge-less limit (see (5.91)). The first term in (5.107) cancels therefore the first term in (5.97) and we obtain

$$\Delta\rho^{(2)} = -\frac{c_W^2}{s_W^2} \left(\Delta\rho^{(1)} \right)^2 + \delta\rho^{(2)}. \quad (5.110)$$

In this notation, the genuine two-loop part

$$\delta\rho^{(2)} = \delta\rho^{(\text{CT})} + \delta\rho^{(2\text{Loop})} \quad (5.111)$$

contains $\delta\rho^{(\text{CT})}$ resulting exclusively from the insertions of the mass counterterms, and the contribution $\delta\rho^{(2\text{Loop})}$ from the pure two-loop diagrams for the Z, W self-energies (without subloop renormalization) in (5.97).

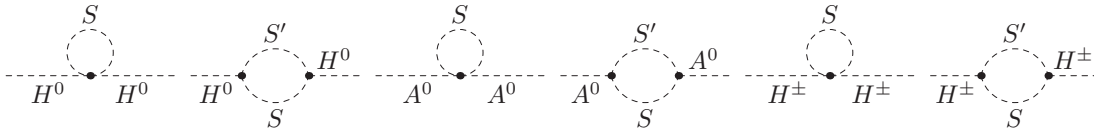


Figure 5.8: One-loop diagrams for the non-standard scalar mass counterterms from the interaction between the SM-like scalars $S = h^0, G^0, G^\pm$ and the non-standard scalars $S' = H^0, A^0, H^\pm$.

The appearance of the reducible term $(\Delta\rho^{(1)})^2$ in $\Delta\rho^{(2)}$ is a consequence of the parameterization of v^2 by

$$\frac{1}{v^2} = \frac{e^2}{4s_W^2 M_W^2} \quad (5.112)$$

together with the on-shell renormalization of s_W . A different parameterization in terms of the Fermi constant G_F can be introduced with the help of the relation

$$\sqrt{2}G_F = \frac{e^2}{4M_W^2 s_W^2} (1 + \Delta r), \quad (5.113)$$

where the quantity Δr describes the higher-order corrections (for more details see Chapter 6). In the gauge-less limit the one-loop contribution is given by

$$\Delta r = -\frac{\delta^{(1)} s_W^2}{s_W^2}. \quad (5.114)$$

Consequently, the reparameterization of the one-loop result $\Delta\rho^{(1)}$ in terms of G_F induces a two-loop shift originating from Δr , which effectively cancels the reducible term in $\Delta\rho^{(2)}$ in (5.110). Hence, in the G_F expansion, the two-loop contribution in $\Delta\rho$ is identified as the irreducible two-loop part $\delta\rho^{(2)}$ in (5.111). In this way, the same pattern for ρ is found as in the SM [212].

The structure of the irreducible quantity $\delta\rho^{(2)}$ in (5.111) with $\delta\rho^{(2\text{Loop})}$ defined in (5.98) allows us to divide it into four finite subsets of different origins,

$$\delta\rho^{(2)} = \delta\rho_{\text{tb,SM}}^{(2)} + \delta\rho_{\text{tb,NS}}^{(2)} + \delta\rho_{\text{H,NS}}^{(2)} + \delta\rho_{\text{H,Mix}}^{(2)}, \quad (5.115)$$

which we describe now in more detail.

5.2.3.1 Standard model corrections from the top-Yukawa coupling

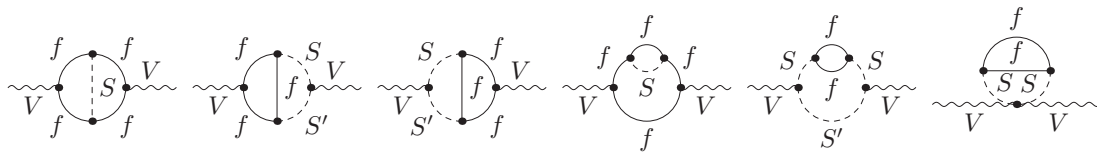


Figure 5.9: Generic two-loop diagrams for the top-Yukawa corrections to the vector boson self-energies with $V = \{W, Z\}$ and $f = \{t, b\}$. The standard contribution $\delta\rho_{\text{t,SM}}^{(2\text{Loop})}$ follows from $S, S' = \{h^0, G^0, G^\pm\}$. The non-standard contribution $\delta\rho_{\text{t,NS}}^{(2\text{Loop})}$ is obtained by all possible insertions of $S, S' = \{H^0, A^0, H^\pm\}$.

The first contribution under investigation are the two-loop corrections from the top- and bottom-Yukawa coupling. In the alignment limit these corrections can be separated into a SM-like and a non-standard part. The bottom-Yukawa coupling to the SM-like scalars can be neglected due to the light b-quark mass. From the coupling of the top quark to h^0, G^0 and G^\pm we obtain the finite correction

$$\delta\rho_{\text{t,SM}}^{(2)} = \delta\rho_{\text{t,SM}}^{(\text{CT})} + \delta\rho_{\text{t,SM}}^{(2\text{Loop})}. \quad (5.116)$$

The first part $\delta\rho_{t,\text{SM}}^{(2\text{Loop})}$ contains the pure two-loop contributions, which are depicted by the generic diagrams in Figure 5.9 for $S, S' = h^0, G^0, G^\pm$. Its divergences are cancelled by $\delta\rho_{t,\text{SM}}^{(\text{CT})}$, the part of (5.101) with the top-mass counterterm calculated from the diagrams in Figure 5.4. The contribution $\delta\rho_{t,\text{SM}}^{(2)}$ is identical to the already known SM contribution from the top-Yukawa interaction. First the result was calculated in the approximation $M_H = 0$ [25] and as an expansion for large values of M_H [24]. Later the full result for arbitrary Higgs masses was obtained [26–28]. We checked that our calculation leads to the same result.

5.2.3.2 Non-standard corrections from the top-Yukawa coupling

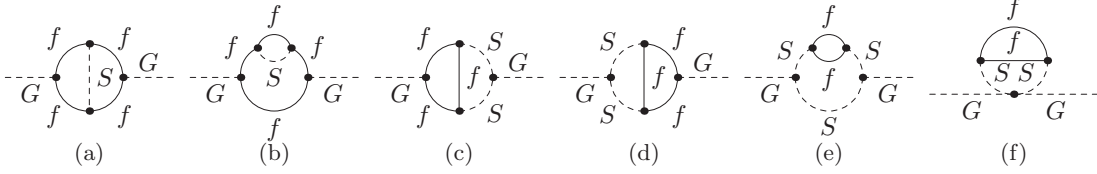


Figure 5.10: Generic two-loop diagrams for the top-Yukawa corrections to the Goldstone boson self-energies. $G = \{G^0, G^\pm\}$; $f = \{t, b\}$; $S = \{H^0, A^0, H^\pm\}$.

More interesting is the additional contribution due to the coupling of the non-standard scalars H^0, A^0 and H^\pm , to the heavy quarks. Since the bottom-Yukawa coupling can be enhanced in the THDM of type-II and type-Y, the top-Yukawa approximation might be insufficient for large values of t_β . In order to have a direct comparison the correction was calculated with and without the bottom-Yukawa contribution. The result including the b-Yukawa coupling is obtained by

$$\delta\rho_{t,b,\text{NS}}^{(2)} = \delta\rho_{t,b,\text{NS}}^{(\text{CT})} + \delta\rho_{H,t,b}^{(\text{CT})} + \delta\rho_{t,b,\text{NS}}^{(2\text{Loop})}. \quad (5.117)$$

The term $\delta\rho_{t,b,\text{NS}}^{(2\text{Loop})}$ is the pure two-loop part, originating from the generic diagrams shown in Figure 5.9 with $S, S' = \{H^0, A^0, H^\pm\}$. In this contribution the custodial symmetry is broken by the Yukawa-couplings and the couplings of the Goldstone bosons to the non-standard scalars. We checked analytically that the contribution vanishes if the custodial symmetry is restored. As discussed in Section 5.1, the requirements depend on the specific type of the Yukawa interaction. In the THDM of type-I (and equivalently type-X) we found that $\delta\rho_{t,b,\text{NS}}^{(2)}$ is zero for $m_b = m_t$ and $m_{A^0} = m_{H^\pm}$, since the Yukawa interaction and the Higgs potential are then invariant under the custodial transformations for $\chi = 0$. In the THDM of type-II, $\delta\rho_{t,b,\text{NS}}^{(2)}$ vanishes for $m_t = m_b$, $t_\beta = 1$ and $m_{H^0} = m_{H^\pm}$, since the Yukawa interaction and the part V_{III} of the scalar potential then fulfill the custodial symmetry for $\chi = \pi/2$.

If the mass of the bottom quark is neglected, the result in the top-Yukawa approximation is given by

$$\delta\rho_{t,\text{NS}}^{(2)} = \delta\rho_{t,\text{NS}}^{(\text{CT})} + \delta\rho_{H,t}^{(\text{CT})} + \delta\rho_{t,\text{NS}}^{(2\text{Loop})}, \quad (5.118)$$

resulting from (5.117) by taking $m_b \rightarrow 0$. The analytic expression can be found in Appendix C.2.1. The result does not only consist of terms of $\mathcal{O}(\alpha_t^2)$, which originate only from the top-Yukawa interaction, but also of contributions of $\mathcal{O}(\alpha_t \lambda_i)$ which contain the scalar self-couplings in addition to the top-Yukawa coupling. In the calculation by means of the gauge-boson self-energies the separation between the $\mathcal{O}(\alpha_t^2)$ and the $\mathcal{O}(\alpha_t \lambda_i)$ contributions is obscured. Using the Ward identity in (5.92) can help to disentangle the two different finite contributions of $\mathcal{O}(\alpha_t^2)$ and $\mathcal{O}(\alpha_t \lambda_i)$. The Goldstone boson self-energies corresponding to the diagrams (a) and (b) in Figure 5.10 lead to the $\mathcal{O}(\alpha_t^2)$ part. Its divergences are canceled by $\delta\rho_{t,\text{NS}}^{(\text{CT})}$ which originates from the subloop renormalization diagrams of Figure 5.2 with the top-mass counterterm calculated from the diagrams in Figure 5.5. The $\mathcal{O}(\alpha_t \lambda_i)$ corrections are obtained by the Goldstone boson self-energies from the diagrams (c)-(f) in Figure 5.10. The divergences are cancelled by $\delta\rho_{H,t}^{(\text{CT})}$ with the mass counterterms calculated from the diagrams in Figure 5.6. The two parts of the subloop renormalization can be found in Appendix C.2.1.

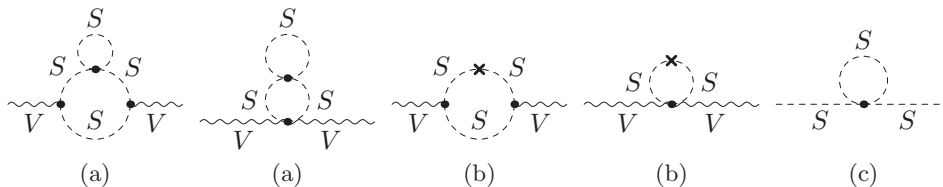


Figure 5.11: Corrections from the quartic couplings between four non-standard scalars. The diagrams of type (a) give the generic two-loop diagrams for the gauge-boson self-energies, which contain a coupling between four non-standard scalars. The diagrams of type (b) give the subloop renormalization diagrams which contain the mass counterterms of the non-standard scalars. These mass counterterms receive contributions from the scalar coupling between four non-standard scalars from the diagrams of type (c). $V = \{W, Z\}$; $S = \{H^0, A^0, H^\pm\}$.

5.2.3.3 Scalar corrections from the interaction of the non-standard scalars

The interaction between the non-standard scalars gives another finite subset. When inspecting this contribution we found that all the corrections from a coupling between four non-standard scalars are cancelled. The generic two-loop diagrams which contain such a coupling are given by the diagrams of type (a) in Figure 5.11. They can be written as a product of two scalar one-loop integrals. If the mass counterterms of the non-standard scalars are calculated from the diagrams (c) in Figure 5.11 and inserted in the subloop renormalization (depicted by the diagrams (b) in Figure 5.11) one obtains the same product of scalar one-loop integrals, but with an opposite sign. Consequently the two terms cancel each other.

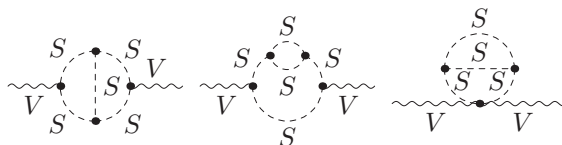


Figure 5.12: Generic two-loop diagrams for the vector-boson self-energies from the interaction between the non-standard scalars. $V = \{W, Z\}$; $S = \{H^0, A^0, H^\pm\}$.

The remaining contribution

$$\delta\rho_{\text{H,NS}}^{(2)} = \delta\rho_{\text{H,NS}}^{(\text{CT})} + \delta\rho_{\text{H,NS}}^{(2\text{Loop})} \quad (5.119)$$

results from all the diagrams which include a triple scalar coupling between H^0 , A^0 and H^\pm . $\delta\rho_{\text{H,NS}}^{(2\text{Loop})}$ is the result for the vector-boson self-energies of the generic two-loop diagrams in Figure 5.12. For the subloop renormalization we need the corrections from the triple non-standard scalar coupling to the scalar self-energies, as shown in Figure 5.7. Inserting the corresponding mass counterterms into (5.105) leads to the result of $\delta\rho_{\text{H,NS}}^{(\text{CT})}$. The expressions for both terms are shown in Appendix C.2.2.

As discussed in Section 2.5, the triple non-standard coupling in the alignment limit follows from the part V_{IV} of the potential in (2.99). For calculation in the THDM without the hard Z_2 -violating terms in the potential, the correction $\delta\rho_{\text{H,NS}}^{(2)}$ depends on the parameters λ_5 , t_β and the masses of the non-standard scalars. The result in the most general CP -conserving THDM in the alignment limit would contain an additional dependence on the parameters Λ_6 and Λ_7 .

5.2.3.4 Scalar corrections from the interaction of the non-standard scalars with the SM scalars

As already mentioned another finite subset of two-loop corrections to the ρ parameter comes from the interaction between the scalars h^0 , G^0 , G^\pm with the non-standard scalars H^0 , A^0 , H^\pm . This interaction originates exclusively from the part V_{III} of the potential (see (2.99c)) which is custodial-symmetry breaking. We denote the resulting contribution by

$$\delta\rho_{\text{H,Mix}}^{(2)} = \delta\rho_{\text{H,Mix}}^{(\text{CT})} + \delta\rho_{\text{H,Mix}}^{(2\text{Loop})}, \quad (5.120)$$

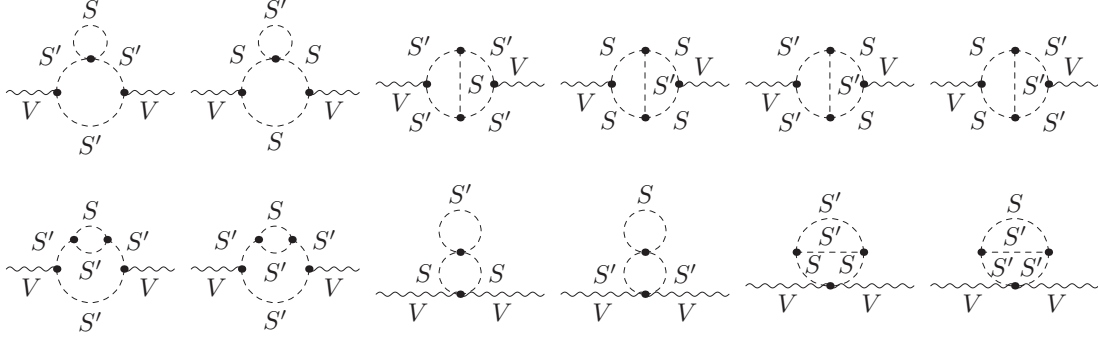


Figure 5.13: Generic two-loop diagrams from the interaction between the SM-like scalars $S = h^0, G^0, G^\pm$ and the non-standard scalars $S' = H^0, A^0, H^\pm$. $V = \{W, Z\}$

where $\delta\rho_{\text{H,Mix}}^{(2\text{Loop})}$ is the part from the two-loop diagrams shown in Figure 5.13. The divergences are canceled by $\delta\rho_{\text{H,Mix}}^{(\text{CT})}$ from (5.106). The analytic result can be found in Appendix C.2.3.

Since the correction $\delta\rho_{\text{H,Mix}}^{(2)}$ originates solely from the part V_{III} of the potential (see (2.99c)), it is independent of the parameters Λ_6 and Λ_7 . However the coupling of h^0 to the non-standard scalars contains an additional dependence on m_{12}^2 (or equivalently λ_5), which is absent in the one-loop correction $\Delta\rho_{\text{NS}}^{(1)}$.

5.2.4 Corrections to the ρ parameter in the IHDM

Since the IHDM and the THDM in the alignment limit are very similar, the results from the previous section can be used to discuss the corrections to $\Delta\rho$ in the IHDM. Using the potential of the IHDM in the form of (2.115), the following considerations can be made:

- There is no non-standard correction to $\Delta\rho$ from the top-Yukawa interaction, since the interaction of the fermions with the non-standard scalars is forbidden by the Z_2 symmetry.
- The part $V_{\text{I}}^{\text{IHDM}}$ has the same structure as the scalar potential of the SM and will not lead to contributions to the ρ parameter since it is invariant under the custodial symmetry (see Section 5.1).
- In the IHDM all the quartic couplings between four non-standard scalars are proportional to Λ_2 , which is selected as a free parameter in Section 2.6. However, as discussed in Section 5.2.3.3, all the two-loop corrections from couplings between four non-standard scalars vanish in the calculation of $\Delta\rho$. The two-loop contribution to the ρ parameter is therefore not dependent on Λ_2 .
- As mentioned in Section 5.2.3.3, the correction $\delta\rho_{\text{H,NS}}^{(2)}$ contains the interaction between three of the non-standard scalars H^0, A^0 and H^\pm , which follows from the part V_{IV} of the potential in (2.99). Couplings between three non-standard scalars are forbidden in the IHDM because of the exact Z_2 symmetry. As a consequence, corrections to the ρ parameter which would correspond to $\delta\rho_{\text{H,NS}}^{(2)}$ are absent in the IHDM.
- The only part of the IHDM potential which violates the custodial symmetry is $V_{\text{III}}^{\text{IHDM}}$. It describes the interaction of the SM-like scalars h^0, G^0 and G^\pm with the non-standard scalars H^0, A^0 and H^\pm . The resulting non-standard one-loop correction $\Delta\rho_{\text{NS}}^{(1)}$ depends only on the masses of the non-standard scalars and therefore takes the same form in the IHDM and the aligned THDM. The two-loop correction is denoted by $\delta\rho_{\text{IHDM}}^{(2)}$: It is the only non-standard, two-loop contribution in the IHDM, if the gauge-less limit is applied. It is similar to the correction $\delta\rho_{\text{H,Mix}}^{(2)}$ in the aligned THDM: it originates from the two-loop diagrams shown in Figure 5.13 and the scalar mass counterterms for the subloop renormalization are calculated from the diagrams in Figure 5.8. In contrast to the one-loop correction, $\delta\rho_{\text{IHDM}}^{(2)}$ has an additional dependence on the IHDM parameter Λ_{345} from the couplings between h^0 and the non-standard scalars.

5.3 Numerical analysis

In this part we investigate the numerical impact of the two-loop corrections on the ρ parameter. We study the dependence on the various parameters of the aligned THDM and compare the non-standard two-loop contributions with the one-loop result which is part of existing calculations of electroweak precision observables so far. In this way the parameter regions emerge where the one-loop calculations are insufficient and bounds on parameters derived from experimental precision data will be significantly changed when the two-loop terms are taken into account. The values for the SM input parameters are [213]

$$M_W = 80.385 \text{ GeV}, \quad (5.121)$$

$$M_Z = 91.1876 \text{ GeV}, \quad (5.122)$$

$$m_t = 173.21 \text{ GeV}. \quad (5.123)$$

Since we want to investigate also the corrections from the bottom-Yukawa coupling, we also need the pole mass of the bottom quark. It can be obtained from the $\overline{\text{MS}}$ mass, which is given in [213] as

$$\overline{m}_b(\overline{m}_b) = 4.18 \text{ GeV}. \quad (5.124)$$

The relation to the pole mass reads [213]

$$\begin{aligned} m_b &= \overline{m}_b(\overline{m}_b) [1 + 0.10 + 0.05 + 0.03] \\ &= 4.93 \text{ GeV}. \end{aligned} \quad (5.125)$$

For the mass of the SM-like Higgs state h^0 we use the value $m_{h^0} = 125 \text{ GeV}$.

The corrections to the ρ parameter are calculated in the THDM without Z_2 -violating terms of mass dimension 4. Consequently, we have $\Lambda_6 = \Lambda_7 = 0$. As free parameters we take the scalar masses, t_β and the parameter λ_5 , defined by (2.50).

The effect of non-standard corrections to electroweak observables is often parameterized in terms of the parameter set S, T, U , originally defined in [214, 215]. Following the conventions of [213], the quantity T is related to the correction $\Delta\rho$ via

$$\Delta\rho = \hat{\alpha}(M_Z) T \quad (5.126)$$

with the running electromagnetic fine structure constant [213]

$$\hat{\alpha}(M_Z)^{-1} = 127.950 \pm 0.017. \quad (5.127)$$

The current value of T [213], determined from experimental data,

$$T = 0.08 \pm 0.12, \quad (5.128)$$

can be translated into bounds for $\Delta\rho$ according to

$$-0.000313 \leq \Delta\rho \leq 0.00156, \quad (5.129)$$

which can be used for a quick estimate of the effect of the higher-order contributions to $\Delta\rho$ in view of current experimental constraints.

5.3.1 Results for the top-Yukawa contribution

We start with the analysis of the contribution $\delta\rho_{t,\text{NS}}^{(2)}$ which originates from the coupling between the top quark and the non-standard scalars. As a first test of our result we examine the behaviour in the so-called decoupling limit [67], in which the masses of the non-standard scalars are much larger than m_h^0 . In this limit the scalar sector of the THDM can be described by an effective theory which is identical to the SM Higgs sector. Consequently we expect $\delta\rho_{t,\text{NS}}^{(2)}$ to vanish for large, equal non-standard Higgs masses. The decoupling scenario is investigated on the left side of Figure 5.14, where $\delta\rho_{t,\text{NS}}^{(2)}$ is shown for degenerate masses of the non-standard scalars. The solid lines represent results for different values of t_β . Since the top-Yukawa coupling breaks the custodial symmetry this contribution is still non-zero, even if the custodial symmetry in the Higgs potential is restored by equal masses of the charged and neutral Higgs states. As

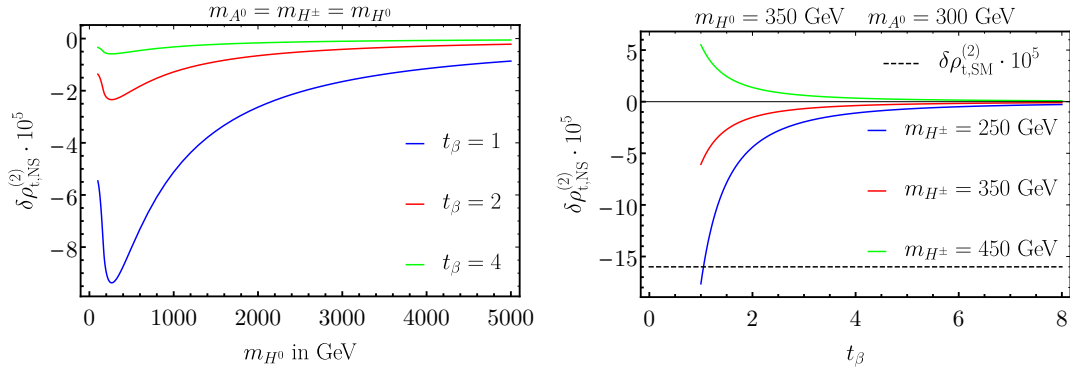


Figure 5.14: Analysis of $\delta\rho_{t,\text{NS}}^{(2)}$. The left side presents a variation of the degenerate masses m_{H^0} , m_{A^0} and m_{H^\pm} up to large values. The solid lines correspond to different values of t_β . On the right side $\delta\rho_{t,\text{NS}}^{(2)}$ is plotted as a function of t_β for different values of m_{H^\pm} . The masses of H^0 and A^0 are fixed at $m_{H^0} = 350$ GeV and $m_{A^0} = 300$ GeV. The value of the two-loop top-Yukawa correction in the SM, $\delta\rho_{t,\text{SM}}^{(2)} = -1.60 \cdot 10^{-4}$, is shown by the black dashed line for comparison.

expected it approaches zero when the masses increase. Moreover, we can see that larger values of t_β suppress the correction. The reason is that the coupling of the top quark to the scalars H^0 , A^0 and H^\pm scales with t_β^{-1} in the alignment limit (see Section 2.5).

The influence of t_β is visualized on the right side of Figure 5.14 with $\delta\rho_{t,\text{NS}}^{(2)}$ for the mass configurations as described by the legend, showing the decrease of the contribution with t_β . In addition different mass splittings between charged and neutral scalars yield noticeable deviations in the result and can even lead to different signs. In general, the top-Yukawa contribution is of the order of the SM value $\delta\rho_{t,\text{SM}}^{(2)}$ or smaller.

5.3.2 Quality of the top-Yukawa approximation

In order to test the validity of the top-Yukawa approximation, we compare the result with and without the bottom-Yukawa corrections in Figure 5.15. In the THDM of type-I and type-X the additional corrections from the bottom-Yukawa coupling are negligibly small, as expected from their suppression by the b -quark mass (see Section 5.2.2). Therefore we only present results in the type-II or type-Y models, in which the contribution from the bottom-Yukawa coupling can be enhanced for large values of t_β . On the left-hand side both results are plotted in dependence of t_β . The solid lines represent $\delta\rho_{t,\text{NS}}^{(2)}$ and the dashed lines represent $\delta\rho_{t,\text{tb,NS}}^{(2)}$. The difference between the two results is plotted directly in the right graph. The different colours correspond to results for different charged Higgs masses, as it is indicated by the legend on the bottom. We see that the bottom-Yukawa contributions lead to visible differences for $t_\beta \geq 10$. Additional two-loop contributions from finite m_b that reach the level of $\delta\rho_{t,\text{SM}}^{(2)}$, require $t_\beta \simeq 40 - 50$. For such large values of t_β , however, one has to prevent the non-standard scalar self-couplings from becoming non-perturbative by restricting the parameter λ_5 to be very close to $\lambda_5 v^2 = 2m_{H^0}^2$ [151, 216]. Moreover, the constraints from flavour physics give further significant restrictions for large values of t_β (see for example [81, 82]). Consequently the top-Yukawa approximation is justified for the allowed values of t_β and we will use $\delta\rho_{t,\text{NS}}^{(2)}$ in the calculation of the electroweak precision observables in Chapter 6 and Chapter 7.

5.3.3 Results for the non-standard scalar contribution

We now discuss the numerical results of the contribution $\delta\rho_{\text{H,NS}}^{(2)}$ which originates from the coupling between three non-standard scalars as described in Section 5.2.3.3. The influence of a mass splitting between charged and neutral scalars is presented in Figure 5.16. The two panels show results for $m_{H^0} = 350$ GeV, $m_{A^0} = 400$ GeV and $\lambda_5 = \pm 1$. The variation of m_{H^\pm} yields similar mass differences for the specified parameter settings. The different lines correspond to

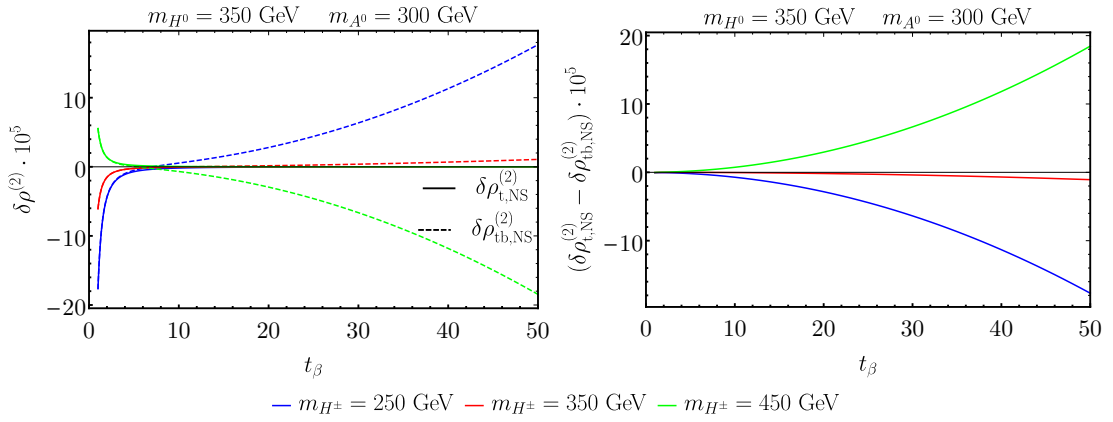


Figure 5.15: Comparison between $\delta\rho_{t,\text{NS}}^{(2)}$ and $\delta\rho_{tb,\text{NS}}^{(2)}$ in the THDM of type-II and type-Y. On the left side both results are plotted in dependence of t_β . The solid lines represent $\delta\rho_{t,\text{NS}}^{(2)}$. The dashed lines represent $\delta\rho_{tb,\text{NS}}^{(2)}$. The difference is shown directly on the right hand side. The different colours correspond to different charged Higgs masses as stated by the legend on the bottom. The masses of the neutral scalars are given on top of the figures.

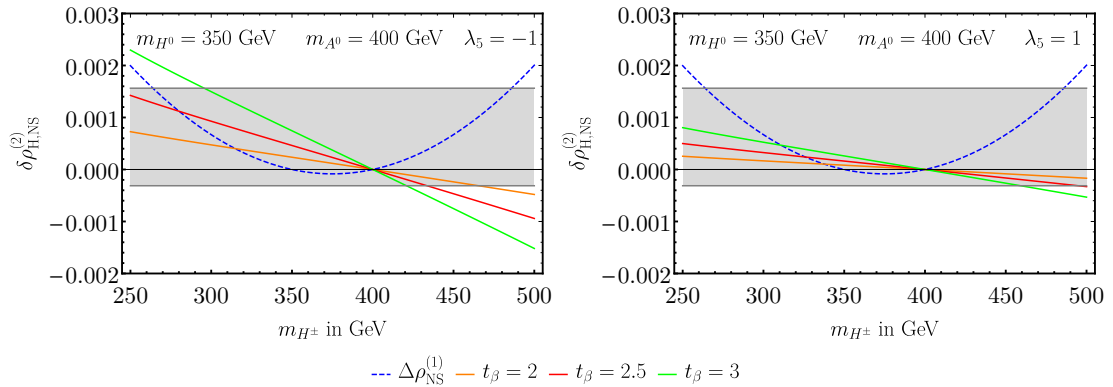


Figure 5.16: Effect of mass differences between neutral and charged scalars on $\delta\rho_{H,\text{NS}}^{(2)}$ for $\lambda_5 = \pm 1$. The neutral masses are fixed at $m_{H^0} = 350$ GeV and $m_{A^0} = 400$ GeV. The mass of H^\pm is varied from 250 GeV to 500 GeV. The solid lines represent different values of t_β as explained in the legend. The blue dashed line shows the non-standard one-loop correction $\Delta\rho_{\text{NS}}^{(1)}$ for comparison. The grey area depicts the bounds from the experimental limits of the T parameter.

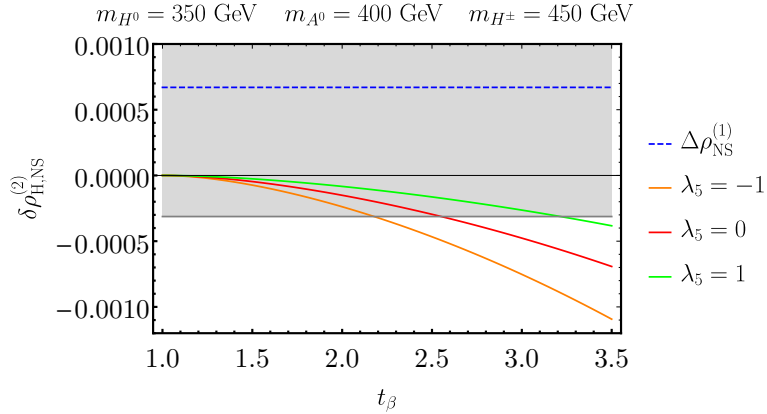


Figure 5.17: Influence of a variation of t_β on $\delta\rho_{\text{H,NS}}^{(2)}$ for the specified mass configurations. The solid lines present different values of λ_5 . The blue dashed line gives the value of the non-standard one-loop correction $\Delta\rho_{\text{NS}}^{(1)}$ for the specified masses. The grey area depicts the bounds from the experimental limits of the T parameter.

different values of t_β as defined in the legend. For comparison the blue dashed line displays the result for the one-loop non-standard correction $\Delta\rho_{\text{NS}}^{(1)}$. The grey area indicates the bounds from the T parameter in (5.128).

Rather moderate values for the scalar masses are selected, since very heavy scalars are excluded due to unitarity constraints. Moreover a small difference between m_{A^0} and m_{H^\pm} is chosen, in order to illustrate the effect of the custodial transformations as described in Section 5.1. The one-loop contribution $\Delta\rho_{\text{NS}}^{(1)}$ is zero for $m_{H^0} = m_{H^\pm}$ and $m_{A^0} = m_{H^\pm}$ since it originates only from the part V_{III} of the potential which is custodial symmetric for these two mass settings. As explained in Section 5.1.2 the part V_{IV} is invariant under the custodial transformation for $\chi = 0$. Consequently $\delta\rho_{\text{H,NS}}^{(2)} = 0$ for $m_{A^0} = m_{H^\pm}$ since all the involved couplings are custodial invariant for this mass degeneracy. However, for $m_{H^0} = m_{H^\pm}$ we have $\delta\rho_{\text{H,NS}}^{(2)} \neq 0$ since in that case V_{III} is invariant only under custodial transformations for $\chi = \frac{\pi}{2}$, but then V_{IV} is not invariant and the triple couplings between three non-standard scalars hence break the custodial symmetry (see Section 5.1.2). Degenerate masses of A^0 and H^0 will lead to similar result, but with one common zero at $m_{H^\pm} = m_{H^0} = m_{A^0}$ for both $\Delta\rho_{\text{NS}}^{(1)}$ and $\delta\rho_{\text{H,NS}}^{(2)}$.

We see that the contribution $\delta\rho_{\text{H,NS}}^{(2)}$ can give corrections to the ρ parameter which are comparable in size or even larger than the one-loop correction. This enhancement follows from the new couplings between three non-standard scalars which enter for the first time in the two-loop contribution. Adding the two-loop corrections to the one-loop result can lead to noticeable modifications of the parameter region allowed by the constraints on T .

The triple non-standard scalar couplings arise from the term V_{IV} of the potential in (2.99), when the vacuum expectation value is inserted for the doublet Φ_{SM} . Since they enter quadratically in all the diagrams in Figure 5.12, the contribution $\delta\rho_{\text{H,NS}}^{(2)}$ is proportional to (see (2.99d))

$$\frac{1}{4} \left(\frac{1}{t_\beta} - t_\beta \right)^2 \left(\frac{2m_{H^0}^2}{v^2} - \lambda_5 \right)^2. \quad (5.130)$$

The prefactor explains the strong influence of t_β on the results in Figure 5.16. The enhancement of the coupling can be weakened for positive values of λ_5 (see the right side of Figure 5.16) or increased for negative values of λ_5 (see the left side of Figure 5.16).

The dependence of $\delta\rho_{\text{H,NS}}^{(2)}$ on t_β is visualized directly in Figure 5.17 for different values of λ_5 , displaying the increase with t_β and the modification by the choice of λ_5 according to (5.130).

Due to the alignment limit the result for $\delta\rho_{\text{H,NS}}^{(2)}$ will be similar in the most-general, CP -conserving THDM with additional Z_2 -violating terms. Since the coupling between four non-standard scalars drops out in the calculation, the only difference will be the parameterization of the coupling between three non-standard scalars (see the discussion in Section 2.5). If Z_2 -violating terms of mass-dimension four are allowed in the potential, this triple non-standard

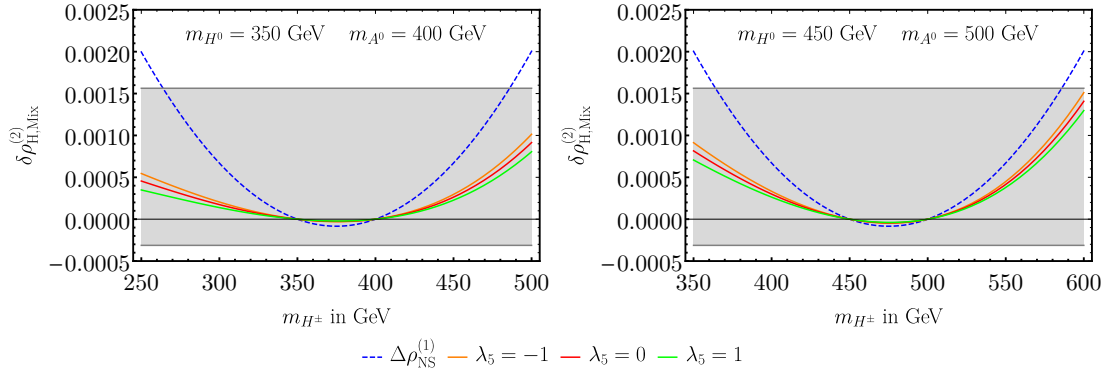


Figure 5.18: Influence of mass splitting between charged and neutral scalars on $\delta\rho_{\text{H,Mix}}^{(2)}$. The two plots show different values of m_{H^0} and m_{A^0} , and the variation of m_{H^\pm} leads to comparable mass differences for the different mass configurations. The results are independent of t_β . The different lines represent different values of λ_5 . The blue dashed line shows the result of the non-standard one-loop correction $\Delta\rho_{\text{NS}}^{(1)}$ for comparison. The grey area depicts the bounds from the experimental limits of the T parameter.

coupling is proportional to

$$C[S_{NS}, S_{NS}, S_{NS}] \propto \frac{2}{vt_{2\beta}} \left(m_{H^0}^2 - \frac{m_{12}^2}{c_\beta s_\beta} \right) + \frac{1}{2} v \left(\frac{\Lambda_6}{s_\beta^2} - \frac{\Lambda_7}{c_\beta^2} \right). \quad (5.131)$$

Since this coupling enters twice in each diagram of $\delta\rho_{\text{H,NS}}^{(2)}$, the result in the most-general, CP -conserving THDM will be directly proportional to the square of (5.131). Besides the different parameterization the properties of $\delta\rho_{\text{H,NS}}^{(2)}$ are unchanged: due to the custodial breaking terms in the potential it will vanish for $m_{A^0} = m_{H^\pm}$ but in general not for $m_{H^0} = m_{H^\pm}$.

5.3.4 Results for the mixed scalar contribution

In this part we discuss the contribution $\delta\rho_{\text{H,Mix}}^{(2)}$ from the interaction of the SM-like scalars h^0 , G^0 , G^\pm with the non-standard scalars H^0 , A^0 , H^\pm . Similar to the one-loop correction $\Delta\rho_{\text{NS}}^{(1)}$ it originates only from the part V_{III} of the potential in (2.99). Consequently it is independent of t_β (see (2.99c)).

In Figure 5.18 we analyse the influence of a mass splitting between the charged and neutral scalars. We show two scenarios for different values of m_{H^0} and m_{A^0} , while the mass of m_{H^\pm} is varied in such a way that the mass splittings are comparable. The three solid lines present the results for different values of λ_5 . The blue dashed line gives the one-loop contribution $\Delta\rho_{\text{NS}}^{(1)}$ for comparison.

The results of Figure 5.18 can again be explained with the help of the custodial symmetry. As discussed in Section 5.1 there are the two possible ways,

$$m_{H^0} = m_{H^\pm} \quad (5.132)$$

or

$$m_{A^0} = m_{H^\pm}, \quad (5.133)$$

to restore a custodial symmetry in V_{III} . For these two mass configurations $\Delta\rho_{\text{NS}}^{(1)}$ and $\delta\rho_{\text{H,Mix}}^{(2)}$ vanish, since they do not contain any additional custodial-symmetry breaking couplings.

While the one-loop contribution originates only from the coupling of the non-standard scalars to the Goldstone bosons, new couplings between h^0 and the non-standard scalars enter the two-loop diagrams in Figure 5.13. These are proportional to the combination

$$2m_S^2 + m_{h^0}^2 - \lambda_5 v^2 \quad (5.134)$$

where S can be either of H^0 , A^0 or H^\pm , depending on which scalar couples to h^0 (see the Feynman rules in Appendix A). The effect of these new couplings is clearly visible in the

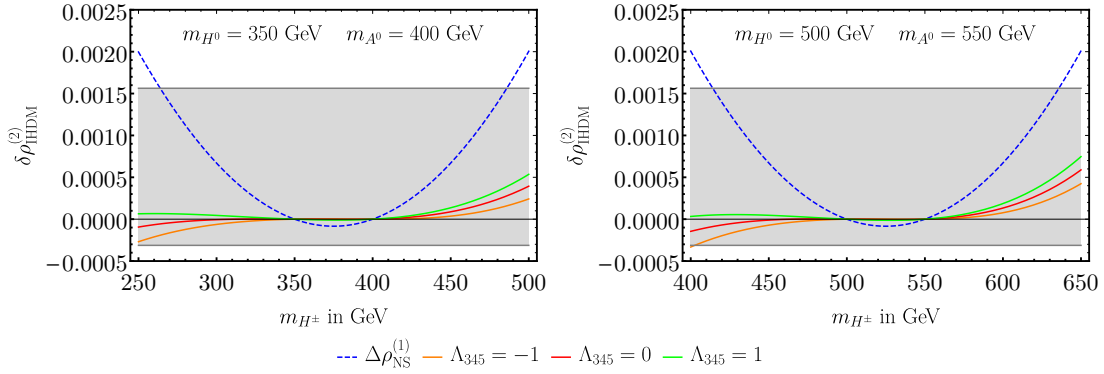


Figure 5.19: Results for the two-loop corrections to the ρ parameter in the IHDM. The two graphs show $\delta\rho_{\text{IHDM}}^{(2)}$ in dependence of the charged Higgs mass. The selected masses of the remaining non-standard scalars are stated at the top of the corresponding graph. The different solid lines correspond to different values of Λ_{345} as indicated by the legend at the bottom. The blue dashed line shows the result of the non-standard one-loop correction $\Delta\rho_{\text{NS}}^{(1)}$. The gray area depicts the bounds from the experimental limits of the T parameter.

numerical results. By comparing the left- and the right-hand side of Figure 5.18 we see that larger masses of the non-standard scalars yield larger values of $\delta\rho_{\text{H,Mix}}^{(2)}$. In addition the couplings can be enhanced or suppressed by negative or positive values of λ_5 , which explains the variation between the different solid lines representing different values of λ_5 .

Since the correction $\delta\rho_{\text{H,Mix}}^{(2)}$ is independent of t_β it will be the dominant scalar two-loop correction to the ρ parameter for $t_\beta \approx 1$, where $\delta\rho_{\text{H,NS}}^{(2)}$ is small. However, for $m_{H^0} = m_{H^\pm}$ both the one-loop correction $\Delta\rho_{\text{NS}}^{(1)}$ and $\delta\rho_{\text{H,Mix}}^{(2)}$ vanish independently of t_β , and $\delta\rho_{\text{H,NS}}^{(2)}$ is the only remaining scalar correction to the ρ parameter (for $t_\beta \neq 1$).

5.3.5 Results in the IHDM

The non-standard two-loop correction to the ρ parameter in the IHDM is investigated in Figure 5.19. In order to show the dependence on the mass splitting between charged and neutral Higgs states, the charged Higgs mass is varied around different values of m_{H^0} and m_{A^0} in the two graphs. The blue dashed line shows the one-loop correction $\Delta\rho_{\text{NS}}^{(1)}$, which is identical in the IHDM and the aligned THDM. The visible characteristics of $\delta\rho_{\text{IHDM}}^{(2)}$ are similar to the ones of $\delta\rho_{\text{H,Mix}}^{(2)}$ in the aligned THDM. The contribution vanishes for equal masses of charged and neutral Higgs states, due to the restoration of a custodial symmetry. Also the influence of the coupling of h^0 to the non-standard Higgs states is apparent: the contribution increases for larger non-standard Higgs masses and for larger values of Λ_{345} . The coupling of h^0 to the charged Higgs states is especially striking if m_{H^\pm} is smaller than m_{H^0} . The sign of this coupling changes with the size of Λ_{345} (see the Feynman rules in Appendix A). For smaller values of Λ_{345} , the coupling can lead to a negative contribution of $\delta\rho_{\text{IHDM}}^{(2)}$, as displayed for $m_{H^\pm} < m_{H^0}$ by the orange and red lines in Figure 5.19.

Chapter 6

The M_W – M_Z interdependence

The decay of the muon leads to a relation between the gauge boson masses (M_W , M_Z), the fine structure constant α_{em} and the Fermi constant G_F , which provides an important precision test of electroweak theories. The calculation of the μ -lifetime τ_μ in the effective four-point Fermi interaction leads to the result

$$\frac{1}{\tau_\mu} = \frac{G_F^2 m_\mu^5}{192\pi^3} F\left(\frac{m_e^2}{m_\mu^2}\right) \left(1 + \frac{3}{5} \frac{m_\mu^2}{M_W^2}\right) (1 + \Delta q), \quad (6.1)$$

with $F(x) = 1 - 8x - 12x^2 \ln x + 8x^3 - x^4$. By convention the QED corrections Δq are included in the calculation in the Fermi model. Results for Δq have been obtained at the one-loop [217–219] and at the two-loop level [220–222]. Equation (6.1) is used as the defining equation for G_F in terms of the experimental μ -lifetime.

In the electroweak theory the muon decays via the exchange of the W boson. Neglecting the transferred momentum due to the light external fermion gives the relation

$$M_W^2 \left(1 - \frac{M_W^2}{M_Z^2}\right) = \frac{\pi\alpha_{em}}{\sqrt{2}G_F} (1 + \Delta r). \quad (6.2)$$

The higher-order corrections to the muon decay are incorporated in the quantity Δr . Note that the finite QED corrections are absent, since these are already included in the definition of G_F in (6.1). The (numerically insignificant) term $3m_\mu^2/(5M_W^2)$, which arises from tree-level W propagator effects, is also included conventionally in (6.1) although it is not part of the Fermi model prediction.

Since

$$\Delta r = \Delta r(M_W, M_Z, m_t, \dots) \quad (6.3)$$

depends on all the parameters of the virtual particles in the loop corrections, it is a model-dependent quantity. Equation (6.2) provides a prediction of M_W in terms of M_Z , α_{em} , G_F and the result of Δr . The comparison with the measured value of M_W allows precise tests of the SM and its extensions. After a short overview of the corrections in the SM, we will discuss the non-standard corrections from the THDM in the alignment limit. Numerical results are presented in Chapter 8.

6.1 Corrections in the SM

Calculating the muon decay amplitude in the SM for vanishing transferred momentum ($q^2 \approx 0$) and comparing the result with the same quantity in the effective four-point Fermi interaction leads at the one-loop order to the relation

$$\frac{G_F}{\sqrt{2}} = \frac{e_0^2}{8s_{W,0}^2 M_{W,0}^2} \left[1 + \frac{\Sigma_W^{(1)}(0)}{M_W^2} + \delta_{\text{vertex+box}}\right]. \quad (6.4)$$

The last term incorporates the vertex and box corrections, without the QED corrections that are already included in (6.1). The bare parameters are defined in Chapter 4. Expanding the

bare parameters in (6.4) and keeping only terms of one loop order leads to (see for example [172, 223])

$$\Delta r^{(1)} = 2\delta^{(1)} Z_e + \frac{\Sigma_W^{(1)}(0) - \delta^{(1)} M_W^2}{M_W^2} - \frac{\delta^{(1)} s_W^2}{s_W^2} + \delta_{\text{vertex+box}} \quad (6.5)$$

The explicit expressions for the one-loop counterterms and self-energies in the SM can be found for example in [172]. The one-loop vertex- and box-corrections in the SM are given by (see for example [173])

$$\delta_{\text{vertex+box}} = -\frac{2}{s_W c_W} \frac{\Sigma_{\gamma Z}^{(1)}(0)}{M_Z^2} + \frac{\alpha}{4\pi s_W^2} \left(6 + \frac{7 - 4s_W^2}{2s_W^2} \log c_W^2 \right). \quad (6.6)$$

The dominant one-loop contribution to Δr in the SM can be identified as

$$\Delta r_{\text{SM}}^{(1)} = \Delta\alpha - \frac{c_W^2}{s_W^2} \Delta\rho_t^{(1)} + \Delta r_{\text{rem}}^{(1)}(M_H). \quad (6.7)$$

The first term contains the contribution of the light fermion loops to the photon vacuum polarization, which is defined in (4.21) and (4.22). The finite part

$$\Delta\alpha = -\text{Re} \Pi_\gamma^{(1)}(M_Z^2) + \Pi_\gamma^{(1)}(0) \quad (6.8)$$

contains logarithmic terms of the form $\log M_Z/m_f$ ($f \neq t$) and represent a QED-induced shift in the electromagnetic fine structure constant. With the renormalization of the electric charge in (4.20), the contribution $\Delta\alpha$ in the quantity Δr originates from the one-loop counterterm

$$\delta^{(1)} Z_e = \frac{1}{2} \Pi_\gamma^{(1)}(0) + \dots \simeq \frac{1}{2} \Delta\alpha + \dots \quad (6.9)$$

The second term in (6.7) contains the correction to the ρ parameter given in (5.81), which is quadratic in the mass of the top quark. This correction enters the quantity Δr due to the renormalization of s_W^2 (see (4.25)) as part of the one-loop counterterm,

$$\frac{\delta^{(1)} s_W^2}{s_W^2} \simeq \frac{c_W^2}{s_W^2} \Delta\rho^{(1)} + \dots \quad (6.10)$$

The remainder part $\Delta r_{\text{rem}}^{(1)}$ contains all the other terms, especially the dependence on the Higgs boson mass in the SM and a term logarithmic in the top mass.

Beyond the one-loop order, the corrections to Δr contain reducible contributions which consist of products of finite one-loop quantities, as well as irreducible higher-order contributions that cannot be written in terms of one-loop quantities. For the reducible contributions, resummations of the leading one-loop contributions $\Delta\alpha$ and $\Delta\rho^{(1)}$ were derived in [212, 224, 225], which incorporate the two-loop terms of the form $(\Delta\rho^{(1)})^2$ and $(\Delta\alpha\Delta\rho^{(1)})$ as well as $(\Delta\alpha)^n$ to all orders. In the following part we will briefly sketch the appearance of these reducible terms at the two-loop order.

As discussed before, the dominant corrections $\Delta\alpha$ and $\Delta\rho$ are contained in the renormalization of the electric charge and the weak mixing angle (see (6.9) and (6.10)). The reducible contributions can be traced back to products of the one-loop counterterms of the form

$$\left(\delta^{(1)} Z_e \right)^2, \quad \delta^{(1)} s_W^2 \delta^{(1)} Z_e, \quad \left(\delta^{(1)} s_W^2 \right)^2. \quad (6.11)$$

Such terms follow directly from the expansion of the bare parameters in (6.4), which at the two-loop order gives

$$\begin{aligned} \Delta r = & 2\delta^{(1)} Z_e - \frac{\delta^{(1)} s_W^2}{s_W^2} - 2\delta^{(1)} Z_e \frac{\delta^{(1)} s_W^2}{s_W^2} + \left(\delta^{(1)} Z_e \right)^2 + \left(\frac{\delta^{(1)} s_W^2}{s_W^2} \right)^2 \\ & + 2\delta^{(2)} Z_e - \frac{\delta^{(2)} s_W^2}{s_W^2} + \dots \end{aligned} \quad (6.12)$$

Additional terms with the products given in (6.11) are contained in the two-loop counterterms $\delta^{(2)}s_W^2$ and $\delta^{(2)}Z_e$:

- The two-loop counterterm of s_W^2 is given in (4.37). With the decomposition of the gauge-boson self-energies in (4.28) and (4.29), the following products of one-loop counterterms can be identified

$$\frac{\delta^{(2)}s_W^2}{s_W^2} = 2\delta^{(1)}Z_e \frac{\delta^{(1)}s_W^2}{s_W^2} + \frac{c_W}{s_W} \frac{\delta^{(1)}s_W^2}{s_W^2} \delta^{(1)}Z_{\gamma Z} - \frac{1}{4} \frac{c_W^2}{s_W^2} \left(\delta^{(1)}Z_{\gamma Z} \right)^2 - \left(\frac{\delta^{(1)}s_W^2}{s_W^2} \right)^2 + \dots \quad (6.13)$$

We are only interested in the terms given in (6.11), since these give the contributions from $\Delta\alpha$ and $\Delta\rho^{(1)}$. Keeping only these terms in (6.13) and inserting (6.9) and (6.10) for the one-loop counterterms leads to

$$\frac{\delta^{(2)}s_W^2}{s_W^2} \simeq \Delta\alpha \frac{c_W^2}{s_W^2} \Delta\rho^{(1)} - \frac{c_W^4}{s_W^4} \left(\Delta\rho^{(1)} \right)^2 + \dots \quad (6.14)$$

- The two-loop counterterm of the electric charge is given in (4.38). From this counterterm we are only interested in the terms, which are quadratic in the one-loop photon vacuum polarization,

$$\left(\Pi_\gamma^{(1)}(0) \right)^2, \quad (6.15)$$

since these lead to the terms quadratic in $\Delta\alpha$. The two-loop field counterterm of the photon, $\delta^{(2)}Z_{\gamma\gamma}$, does not contain the one-loop photon vacuum polarization as can be seen from the decomposition of the two-loop photon self-energy in (4.30). If we insert

$$\delta^{(1)}Z_e = \frac{1}{2} \Pi_\gamma^{(1)}(0) + \dots, \quad (6.16)$$

$$\delta^{(1)}Z_{\gamma\gamma} = -\Pi_\gamma^{(1)}(0), \quad (6.17)$$

into the first term of (4.30), we see that the one-loop photon vacuum polarization cancels in the subloop renormalization of the photon self-energy and consequently also in the two-loop field counterterm of the photon, due to the renormalization condition in (4.39). Therefore, the only terms in (4.38), which are quadratic in the one-loop photon vacuum polarization follow from the squared one-loop counterterms

$$\left(\delta^{(1)}Z_e \right)^2 \quad (6.18)$$

and

$$\left(\delta^{(1)}Z_{\gamma\gamma} \right)^2, \quad (6.19)$$

which together with (6.16) and (6.17) leads to

$$\delta^{(2)}Z_e = \frac{3}{8} \left(\Pi_\gamma^{(1)}(0) \right)^2 + \dots \simeq \frac{3}{8} (\Delta\alpha)^2 + \dots, \quad (6.20)$$

as the correction from the one-loop photon vacuum polarization in the two-loop counterterm of the electric charge.

Inserting the dominant terms from (6.9), (6.10), (6.14) and (6.20) into (6.12) leads then to

$$\Delta r = \Delta\alpha + \Delta\alpha^2 - \frac{c_W^2}{s_W^2} \Delta\rho^{(1)} \left(1 + 2\Delta\alpha - 2\frac{c_W^2}{s_W^2} \Delta\rho^{(1)} \right) + \dots \quad (6.21)$$

The appearance of these reducible products at the two-loop order is affected by the parameterization of

$$\Delta\rho_t^{(1)} = \frac{3e^2 m_t^2}{64\pi^2 M_W^2 s_W^2} = \frac{3m_t^2}{16\pi^2 v^2} \quad (6.22)$$

in terms of

$$\frac{1}{v^2} = \frac{e^2}{4s_W^2 M_W^2}. \quad (6.23)$$

If v^2 is expressed in term of the Fermi-constant G_F , the corrections from $\Delta r^{(1)}$ in

$$\frac{G_F}{\sqrt{2}} = \frac{e^2}{8s_W^2 M_W^2} \left(1 + \Delta r^{(1)} + \dots \right) \quad (6.24)$$

lead to the parameterization

$$\frac{1}{v^2} = \sqrt{2} G_F \left(1 - \Delta r^{(1)} + \dots \right), \quad (6.25)$$

which introduces an additional two-loop shift in $\Delta\rho^{(1)}$. If only the one-loop corrections from (6.21) are kept for $\Delta r^{(1)}$ in (6.25), the reparameterization of $\Delta\rho^{(1)}$ in terms of G_F leads to

$$\Delta\rho_t^{(1)} \rightarrow \Delta\bar{\rho}_t^{(1)} - \Delta\alpha\Delta\bar{\rho}_t^{(1)} + \frac{c_W^2}{s_W^2} \left(\Delta\bar{\rho}_t^{(1)} \right)^2, \quad (6.26)$$

where

$$\Delta\bar{\rho}_t^{(1)} = \frac{3G_F}{8\sqrt{2}\pi^2} m_t^2, \quad (6.27)$$

denotes the one-loop corrections to the ρ -parameter expressed in terms of G_F . Consequently the dominant terms in Δr expressed in the G_F -expansion

$$\Delta r = \Delta\alpha + \Delta\alpha^2 - \frac{c_W^2}{s_W^2} \Delta\bar{\rho}^{(1)} \left(1 + \Delta\alpha - \frac{c_W^2}{s_W^2} \Delta\bar{\rho}^{(1)} \right) + \dots \quad (6.28)$$

show the same pattern as in the expanded form

$$\frac{1}{1 - \Delta\alpha} \cdot \frac{1}{1 + \frac{c_W^2}{s_W^2} \Delta\bar{\rho}^{(1)}} \simeq 1 + \Delta\alpha + \Delta\alpha^2 - \frac{c_W^2}{s_W^2} \Delta\bar{\rho}^{(1)} \left(1 + \Delta\alpha - \frac{c_W^2}{s_W^2} \Delta\bar{\rho}^{(1)} \right) + \dots \quad (6.29)$$

given in [212].

QCD corrections to Δr are calculated at $\mathcal{O}(\alpha\alpha_s)$ [29–31, 96–98, 226], $\mathcal{O}(\alpha\alpha_s^2)$ [32, 33, 113, 114] and $\mathcal{O}(\alpha\alpha_s^3 m_t^2)$ [36–38]. The electroweak corrections in the SM are known at the complete two-loop level and contain the fermionic [99–101] and the purely bosonic contributions [102–105]. The leading three-loop corrections to the ρ parameter are obtained at $\mathcal{O}(G_F^3 m_t^3)$ and $\mathcal{O}(G_F^2 m_t^2 \alpha_s)$ [34, 35]. Three-loop corrections in the limit of a large Higgs mass are calculated in [115, 227]. In addition the pure fermion-loop corrections [228, 229] up to four-loop order are known.

In [106] a simple parameterization is given,

$$M_W = M_W^0 - c_1 dH - c_2 dH^2 + c_3 dH^4 + c_4 (dh - 1) - c_5 d\alpha + c_6 dt - c_7 dt^2 - c_8 dH dt + c_9 dh dt - c_{10} d\alpha_S + c_{11} dZ, \quad (6.30)$$

which reproduces the SM prediction for M_W with the following loop contributions

$$\Delta r = \Delta r^{(\alpha)} + \Delta r^{(\alpha\alpha_s)} + \Delta r^{(\alpha\alpha_s^2)} + \Delta r^{(\alpha\alpha_s^3 m_t)} + \Delta r_{\text{ferm}}^{(\alpha^2)} + \Delta r_{\text{bos}}^{(\alpha^2)} + \Delta r^{(G_F^2 \alpha_s m_t^4)} + \Delta r^{(G_F^3 m_t^6)}, \quad (6.31)$$

where $\Delta r^{(\alpha)}$ is the one-loop result of (6.7), $\Delta r^{(\alpha\alpha_s)}$, $\Delta r^{(\alpha\alpha_s^2)}$ and $\Delta r^{(\alpha\alpha_s^3 m_t)}$ are the two-loop, three-loop and approximate four-loop QCD corrections, and $\Delta r_{\text{ferm}}^{(\alpha^2)}$ and $\Delta r_{\text{bos}}^{(\alpha^2)}$ are the fermionic and the bosonic electroweak two-loop corrections, respectively. The contributions $\Delta r^{(G_F^2 \alpha_s m_t^4)}$ and $\Delta r^{(G_F^3 m_t^6)}$ are the leading three-loop contributions to the ρ -parameter. The required input parameters for

$$\begin{aligned} dH &= \log \left(\frac{M_H}{100 \text{ GeV}} \right), & dh &= \left(\frac{M_H}{100 \text{ GeV}} \right)^2, & dt &= \left(\frac{m_t}{174,3 \text{ GeV}} \right)^2 - 1, \\ dZ &= \frac{M_Z}{91.1875 \text{ GeV}} - 1, & d\alpha &= \frac{\Delta\alpha}{0.05907} - 1, & d\alpha_s &= \frac{\alpha_s (M_Z)^2}{0.119} - 1, \end{aligned} \quad (6.32)$$

are the masses of the top quark, the Z boson and the SM Higgs boson, the strong coupling constant α_S (M_Z^2) and the quantity $\Delta\alpha$. The coefficients in (6.30) are¹

$$\begin{aligned}
 M_W^0 &= 80.3799 \text{ GeV}, & c_1 &= 0.05263 \text{ GeV}, & c_2 &= 0.010239 \text{ GeV}, \\
 c_3 &= 0.000954 \text{ GeV}, & c_4 &= -0.000054 \text{ GeV}, & c_5 &= 1.077 \text{ GeV}, \\
 c_6 &= 0.5252 \text{ GeV}, & c_7 &= 0.0700 \text{ GeV}, & c_8 &= 0.004102 \text{ GeV}, \\
 c_9 &= 0.000111 \text{ GeV}, & c_{10} &= 0.0774 \text{ GeV}, & c_{11} &= 115.0 \text{ GeV}.
 \end{aligned}
 \tag{6.33}$$

6.2 Non-standard corrections in the THDM

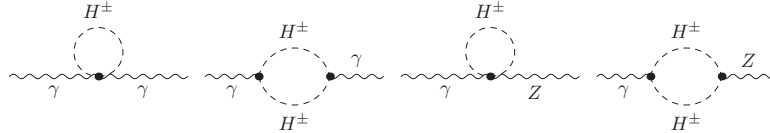


Figure 6.1: Non-standard contributions to the photon self-energy and $\gamma - Z$ mixing from the charged scalars in the alignment limit

In the THDM, the extended scalar sector leads to additional non-standard corrections, which have to be combined with the known SM contributions. The THDM prediction for Δr in the alignment limit can be written as

$$\Delta r = \Delta r_{\text{SM}} + \Delta r_{\text{NS}},
 \tag{6.34}$$

where Δr_{SM} contains all the known SM corrections and Δr_{NS} contains the additional non-standard contributions. The corrections which originate only from the SM-like scalars h^0 , G^0 and G^\pm are identical to the scalar contributions in the SM which are already included in the SM result Δr_{SM} . The non-standard contribution originates therefore only from the non-standard scalars H^0 , A^0 and H^\pm . The vertex- and box-corrections from the non-standard scalars can be neglected due to the small Yukawa couplings to the external fermions. Consequently the non-standard part Δr_{NS} can be obtained from the contributions to the gauge-boson self-energies with the scalars H^0 , A^0 and H^\pm as internal particles. We write the resulting non-standard contribution as the sum

$$\Delta r_{\text{NS}} = \Delta r_{\text{NS}}^{(1)} + \Delta r_{\text{NS}}^{(2)},
 \tag{6.35}$$

with the non-standard one-loop contribution $\Delta r_{\text{NS}}^{(1)}$ and the leading two-loop contribution $\Delta r_{\text{NS}}^{(2)}$. For the contribution $\Delta r_{\text{NS}}^{(1)}$ the result from [94] in the alignment limit is used. The non-standard one-loop result is supplemented in this thesis with the contribution $\Delta r_{\text{NS}}^{(2)}$, which incorporates the non-standard two-loop corrections to the ρ parameter as discussed below.

The non-standard one-loop contribution has the same form as (6.5), except that the non-standard vertex- and box-corrections can be neglected due to the light masses of the external fermions. The contribution $\Delta r_{\text{NS}}^{(1)}$ can be calculated therefore in terms of the non-standard one-loop contributions to the gauge-boson self-energies from the diagrams shown in Figure 5.1 and Figure 6.1. The resulting one-loop contribution to Δr is given by

$$\Delta r_{\text{NS}}^{(1)} = \delta^{(1)} Z_e^{\text{NS}} + \frac{\Sigma_{W,\text{NS}}^{(1)}(0) - \delta^{(1)} M_{W,\text{NS}}^2}{M_W^2} - \frac{\delta^{(1)} s_{W,\text{NS}}^2}{s_W^2},
 \tag{6.36}$$

where the subindex at the counterterms indicates that only the non-standard self-energies are used for their calculation. The expressions for the one-loop non-standard self-energies can be found in Appendix C.1. We denote the result of M_W with just the one-loop non-standard contribution by $M_W^{(1)}$. The one-loop contribution $\Delta r_{\text{NS}}^{(1)}$ has a high sensitivity on large mass differences between neutral and charged Higgs states. This dominant effect can be traced back

¹Note that the coefficients changed in comparison to the ones used in [94], since the parameterization in [106] was updated to include also the corrections of $\mathcal{O}(\alpha\alpha_s^2 m_t^2)$.

to the non-standard correction to the ρ parameter, since the violation of the custodial symmetry for $m_{H^0} \neq m_{H^\pm}$ or $m_{A^0} \neq m_{H^\pm}$ leads to large contributions from $\Delta\rho_{\text{NS}}^{(1)}$.

The non-standard two-loop contribution $\Delta r_{\text{NS}}^{(2)}$ in (6.35) contains the non-standard corrections from the top-Yukawa coupling and the self-interaction of the non-standard scalars. These contributions are of special interest, since these sectors give already dominant corrections at the one-loop order in terms of $\Delta\rho_t^{(1)}$ and $\Delta\rho_{\text{NS}}^{(1)}$. Analogous to the corrections in the SM, the non-standard two-loop contribution can be written in terms of a reducible part $\Delta r_{\text{NS,red}}^{(2)}$ and an irreducible part $\Delta r_{\text{NS,irr}}^{(2)}$, such that

$$\Delta r_{\text{NS}}^{(2)} = \Delta r_{\text{NS,red}}^{(2)} + \Delta r_{\text{NS,irr}}^{(2)}. \quad (6.37)$$

The reducible non-standard contribution, $\Delta r_{\text{NS,red}}^{(2)}$, arises from the non-standard one-loop correction to the ρ parameter, which introduces additional factorized terms in (6.21). In the THDM in the alignment limit $\Delta\rho^{(1)}$ contains the two terms

$$\Delta\rho^{(1)} = \Delta\rho_t^{(1)} + \Delta\rho_{\text{NS}}^{(1)}. \quad (6.38)$$

The reducible two-loop contribution is obtained by inserting (6.38) for $\Delta\rho^{(1)}$ in (6.21). However, the reducible terms which contain only $\Delta\alpha$ and $\Delta\rho_t^{(1)}$ are already included in the SM result. Therefore we need only the non-standard term

$$\Delta r_{\text{NS,red}}^{(2)} = -2 \frac{c_W^2}{s_W^2} \Delta\alpha \Delta\rho_{\text{NS}}^{(1)} + 4 \frac{c_W^4}{s_W^4} \Delta\rho_{\text{NS}}^{(1)} \Delta\rho_t^{(1)} + 2 \frac{c_W^4}{s_W^4} \left(\Delta\rho_{\text{NS}}^{(1)} \right)^2, \quad (6.39)$$

which originates from the presence of $\Delta\rho_{\text{NS}}^{(1)}$ in (6.38).

The irreducible part $\Delta r_{\text{NS,irr}}^{(2)}$ in (6.37) follows from $\delta\rho^{(2)}$, the irreducible two-loop contribution to the ρ parameter given in (5.111). This irreducible correction enters via the two-loop counterterm of s_W^2 , as we will discuss in the following part by writing the renormalization condition (4.37) in the gauge-less limit.

In the gauge-less limit the ratios $\delta^{(1)} M_V^2 / M_V^2$ in the first term of (4.37) are given by the relations (5.91) (see the discussion in Section 5.2.2). Analogous relations hold for the ratios $\delta^{(2)} M_V^2 / M_V^2$ in the second term of (4.37). The two-loop mass counterterms for the gauge-bosons are given in (4.26) and (4.27). In addition to the two-loop self-energies, these renormalization conditions contain also terms with the gauge-boson field counterterms and the imaginary parts of the one-loop self-energies. In the gauge-less limit the gauge-boson field counterterms and the imaginary parts are zero. The two-loop renormalization conditions for the ratios $\delta^{(2)} M_V^2 / M_V^2$ in the gauge-less limit are therefore given by

$$\frac{\delta^{(2)} M_W^2}{M_W^2} = \frac{\text{Re} \Sigma_W^{(2)}(0)}{M_W^2}, \quad \frac{\delta^{(2)} M_Z^2}{M_Z^2} = \frac{\text{Re} \Sigma_Z^{(2)}(0)}{M_Z^2}, \quad (6.40)$$

where the gauge-couplings of $\mathcal{O}(g_{1,2}^2)$ in the self-energies are again canceled by the ones contained in the gauge-boson masses. With the relations (5.91) and (6.40) the two-loop renormalization condition in (4.37) in the gauge-less yields

$$\begin{aligned} \frac{\delta^{(2)} s_W^2}{s_W^2} &= \frac{c_W^2}{s_W^2} \left(-\frac{\Sigma_Z^{(1)}(0)}{M_Z^2} \Delta\rho^{(1)} + \left(\frac{\Sigma_Z^{(2)}(0)}{M_Z^2} - \frac{\Sigma_W^{(2)}(0)}{M_W^2} \right) \right) \\ &= \frac{c_W^2}{s_W^2} \Delta\rho^{(2)}, \end{aligned} \quad (6.41)$$

where $\Delta\rho^{(2)}$ is the two-loop correction to the ρ parameter as obtained in (5.97). In (5.110) the two-loop contribution $\Delta\rho^{(2)}$ is divided into a term quadratic in the one-loop contribution $\Delta\rho^{(1)}$ and the irreducible part $\delta\rho^{(2)}$ from (5.111). The term quadratic in $\Delta\rho^{(1)}$ is already included in $\Delta r_{\text{NS,red}}^{(2)}$. The irreducible two-loop part

$$\Delta r_{\text{irr}}^{(2)} = -\frac{c_W^2}{s_W^2} \delta\rho^{(2)} \quad (6.42)$$

contains therefore only the non-standard parts of $\delta\rho^{(2)}$. According to the separation in (5.115), we define the non-standard parts²

$$\Delta r_{t,\text{NS}}^{(2)} = -\frac{c_W^2}{s_W^2} \delta\rho_{t,\text{NS}}^{(2)}, \quad (6.43)$$

$$\Delta r_{\text{H,NS}}^{(2)} = -\frac{c_W^2}{s_W^2} \delta\rho_{\text{H,NS}}^{(2)}, \quad (6.44)$$

$$\Delta r_{\text{H,Mix}}^{(2)} = -\frac{c_W^2}{s_W^2} \delta\rho_{\text{H,Mix}}^{(2)}, \quad (6.45)$$

such that

$$\Delta r_{\text{NS,irr}}^{(2)} = \Delta r_{t,\text{NS}}^{(2)} + \Delta r_{\text{H,NS}}^{(2)} + \Delta r_{\text{H,Mix}}^{(2)}. \quad (6.46)$$

6.3 Non-standard corrections in the IHDM

The non-standard one-loop contributions to the gauge-boson self-energies in the IHDM are identical to the ones in the general THDM in the alignment limit. Consequently the non-standard one-loop correction $\Delta r_{\text{NS}}^{(1)}$ and the reducible two-loop correction $\Delta r_{\text{NS,red}}^{(2)}$ are equal in both models. Differences arise in the irreducible two-loop corrections to Δr . In the IHDM in the gauge-less limit, we have just one non-standard irreducible two-loop correction to the ρ parameter, labelled as $\delta\rho_{\text{IHDM}}^{(2)}$ in Chapter 5. The corresponding contribution to Δr is given by

$$\Delta r_{\text{IHDM}}^{(2)} = -\frac{c_W^2}{s_W^2} \delta\rho_{\text{IHDM}}^{(2)}. \quad (6.47)$$

This correction introduces an additional dependence on the IHDM parameter Λ_{345} , which is absent in the contributions $\Delta r_{\text{NS}}^{(1)}$ and $\Delta r_{\text{NS,red}}^{(2)}$. As discussed in Chapter 5, the quartic coupling between four non-standard scalars cancels in the two-loop result of $\Delta\rho$ which is therefore not sensitive on Λ_2 . Consequently our prediction of M_W in the IHDM will also be independent of Λ_2 .

6.4 Incorporation of non-standard corrections

For a prediction of M_W in the THDM, which is as accurate as possible, we have to combine the higher-order contributions from the SM with all the available non-standard corrections. The resulting quantity Δr depends on all the free parameters in the THDM. The prediction of M_W fulfills the relation (6.2) for a specific set of parameters. Formally it is obtained by solving (6.2) for M_W . However, since Δr itself depends on M_W , the prediction of M_W is calculated in practice by evaluating

$$M_W^2 = M_Z^2 \left[\frac{1}{2} + \sqrt{\frac{1}{4} - \frac{\pi\alpha_{em}}{\sqrt{2}G_F M_Z^2} (1 + \Delta r)} \right] \quad (6.48)$$

iteratively. Since the full SM result is a lengthy expression which involves furthermore numerical integrations, we proceed as follows: we use the explicit one-loop result in the SM

$$\Delta r_{\text{SM}}^{(1)}(M_W, \dots) \quad (6.49)$$

for the iteration and approximate the higher-order corrections by the constant term

$$\delta r_{\text{SM}}^{\text{h.o.}} = \Delta r_{\text{SM}}^{\text{h.o.}} - \Delta r_{\text{SM}}^{(1)}(M_{W,\text{SM}}). \quad (6.50)$$

The contribution $\Delta r_{\text{SM}}^{\text{h.o.}}$ corresponds to the result of Δr in the SM with the corrections from (6.31). It is obtained from $M_{W,\text{SM}}$, the mass of the W boson in the SM calculated from the parameterization in (6.30). Inverting (6.2) for Δr , we obtain

$$\Delta r_{\text{SM}}^{\text{h.o.}} = \frac{\sqrt{2}G_F M_{W,\text{SM}}^2}{\pi\alpha_{em}} \left(1 - \frac{M_{W,\text{SM}}^2}{M_Z^2} \right) - 1. \quad (6.51)$$

²We neglect the corrections from the bottom Yukawa-coupling, since the contribution is small except for a THDM of type-II or type-Y for very large values of t_β (see the discussion in Chapter 5).

From this result we subtract the one-loop contribution in the SM with $M_W = M_{W,\text{SM}}$ and obtain the contribution $\delta r_{\text{SM}}^{\text{h.o.}}$, which stays constant during the iteration.

Adding all the available non-standard corrections we obtain as the complete result for Δr

$$\Delta r(M_W, \dots) = \Delta r_{\text{SM}}^{(1)}(M_W) + \delta r_{\text{SM}}^{\text{h.o.}} + \Delta r_{\text{NS}}^{(1)}(M_W) + \Delta r_{\text{NS,red}}^{(2)}(M_W) + \Delta r_{\text{NS,irr}}^{(2)}(M_W) \quad (6.52)$$

with (6.46) for the general THDM in the alignment limit.

In an analogous way, we obtain

$$\Delta r(M_W, \dots) = \Delta r_{\text{SM}}^{(1)}(M_W) + \delta r_{\text{SM}}^{\text{h.o.}} + \Delta r_{\text{NS}}^{(1)}(M_W) + \Delta r_{\text{NS,red}}^{(2)}(M_W) + \Delta r_{\text{IHDM}}^{(2)}(M_W) \quad (6.53)$$

in the IHDM.

Chapter 7

Precision observables at the Z pole

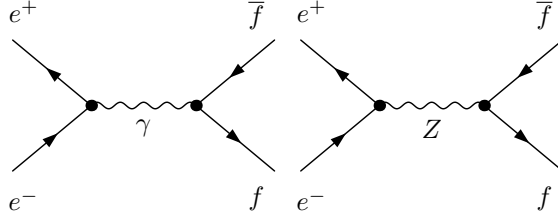
The production of a fermion-antifermion pair in electron-positron collisions has been studied comprehensively by the experiments at LEP and SLC [230]. The energy-dependent cross-sections and the polarization and angular asymmetries have been measured with high accuracy. From these "realistic" observables a set of pseudo-observables [231] is obtained by applying deconvolution processes under specific assumptions with the help of sophisticated programs like ZFITTER [232, 233] and TOPAZO [234]. The set of pseudo-observables is chosen in order to describe the features of the Z resonance in a largely model-independent manner (for more details see the discussion in the introduction of [230]). Examples for such pseudo-observables are the total width of the Z boson or the effective leptonic mixing angle.

The tree-level amplitude, depicted by the diagrams in Figure 7.1, consists of the QED contributions due to the photon-exchange and the electroweak contributions due to the Z -exchange. When higher-order corrections are included, the separation is only partially preserved. At the one-loop level the corrections can be classified in terms of QED and electroweak corrections in a gauge-invariant way and additional QCD corrections for quarks in the final state. The QED corrections are given by the loop-diagrams with a virtual photon (which couples to the external fermions) and the bremsstrahlung diagrams with real photon emission from the external legs and are therefore dependent on the experimental cuts applied to the emitted final-state photon. Although numerically very important, the QED corrections are not sensitive on the specific structure of the electroweak theory. A large part in the difference between realistic observables and pseudo-observables originates from the deconvolution of model-independent QED corrections. The electroweak corrections, which are given by the residual electroweak loop diagrams, depend on the remaining parameters of the electroweak theory and are also sensitive on contributions from new physics.

The only QCD corrections at the one-loop level occur as diagrams with real or virtual gluons for quark pair production processes ($e^+e^- \rightarrow q\bar{q}$). At higher-orders also mixed QCD-electroweak corrections appear, for example as gluonic corrections to quark loops in gauge-boson self-energies. A review of the QCD corrections can be found in [235].

At the Z resonance the total cross section for $e^+e^- \rightarrow f\bar{f}$ is dominated by the Z -exchange due to the enhancement by the resonant propagator. In the Z pole approximation the non-resonant loop-contributions are therefore neglected. For example the relative contribution of weak box diagrams is less than 10^{-4} and is therefore negligible. The matrix-element can then again be separated into a dressed photon- and a dressed Z -exchange contribution. The higher-order electroweak corrections are incorporated in terms of effective couplings of the fermions to the Z boson. For more details see for example [231].

In [94] the calculation of the non-standard one-loop correction to precision observables at the Z resonance was discussed. In this chapter we describe how the two-loop corrections to the ρ parameter can be incorporated in the effective couplings and how they enter the calculation of the Z width and the effective leptonic mixing angle as two representative examples for precision observables. Numerical results are given in Chapter 8.


 Figure 7.1: Feynman diagrams for the process $e^+e^- \rightarrow f\bar{f}$ at the tree-level.

7.1 The width of the Z boson

The total width Γ_Z of the Z boson is obtained from the sum of all partial widths $\Gamma_f \equiv \Gamma(Z \rightarrow f\bar{f})$ [112, 231],

$$\Gamma_Z = \sum_{f \neq t} \Gamma_f = 3\Gamma_\nu + \Gamma_e + \Gamma_\mu + \Gamma_\tau + \Gamma_{\text{had}}, \quad (7.1)$$

with the hadronic width given by the decay into quark pairs

$$\Gamma_{\text{had}} = \Gamma_u + \Gamma_d + \Gamma_c + \Gamma_s + \Gamma_b. \quad (7.2)$$

The partial widths are all described in terms of effective coupling $g_{V,A}^f$ by

$$\Gamma_f = \Gamma_0 N_c^f \left[\left(g_V^f \right)^2 R_V^f + \left(g_A^f \right)^2 R_A^f \right] \quad (7.3)$$

or alternatively in terms of form factors ρ_f and κ_f by

$$\Gamma_f = \Gamma_0 N_c^f \rho_f \left[\left(I_3^f - 2Q_f s_W^2 \kappa_f \right)^2 R_V^f + \left(I_3^f \right)^2 R_A^f \right]. \quad (7.4)$$

N_c^f is a colour factor, such that $N_c^f = 1$ for leptons and $N_c^f = 3$ for quarks. The normalization factor Γ_0 is written as

$$\Gamma_0 = \frac{G_F M_Z^3}{6\sqrt{2}\pi}. \quad (7.5)$$

The final-state QED and QCD corrections are incorporated into factorized radiation factors $R_{V,A}^f$. The electroweak corrections are included either in the effective couplings $g_{V,A}^f$ or in the form factors ρ_f and κ_f . They contain the electroweak vertex-corrections, the contribution from $\gamma - Z$ mixing and the wave function renormalization of the external legs, all evaluated at the center-of-mass energy $s = M_Z^2$.

The effective couplings are written in the loop expansion as follows,

$$g_V^f = v_f + \Delta^{(1)} g_V^f + \Delta^{(2)} g_V^f + \dots, \quad (7.6)$$

$$g_A^f = a_f + \Delta^{(1)} g_A^f + \Delta^{(2)} g_A^f + \dots, \quad (7.7)$$

where

$$a_f = I_3^f, \quad (7.8)$$

$$v_f = I_3^f - 2s_W^2 Q_f, \quad (7.9)$$

denote the tree-level vector and axial-vector couplings of the Z boson to the fermion species f . I_3^f is the third isospin component and Q_f the electric charge of f . The form factors ρ_f and κ_f are related to the effective couplings $g_{V,A}^f$ via

$$\rho_f = \left(\frac{g_A^f}{a_f} \right)^2, \quad (7.10)$$

$$\kappa_f = \frac{1}{4s_W^2 |Q_f|} \left(1 - \frac{g_V^f}{g_A^f} \right). \quad (7.11)$$

Using the expansion of the effective couplings in (7.6) and (7.7), the expansion of (7.10) and (7.11) gives

$$\rho_f = 1 + \Delta^{(1)}\rho_f + \Delta^{(2)}\rho_f + \dots, \quad (7.12)$$

$$\kappa_f = 1 + \Delta^{(1)}\kappa_f + \Delta^{(2)}\kappa_f + \dots, \quad (7.13)$$

with

$$\Delta^{(1)}\rho_f = 2\frac{\Delta^{(1)}g_A^f}{a_f}, \quad (7.14)$$

$$\Delta^{(2)}\rho_f = \left(\frac{\Delta^{(1)}g_A^f}{a_f}\right)^2 + 2\frac{\Delta^{(2)}g_A^f}{a_f}, \quad (7.15)$$

and

$$\Delta^{(1)}\kappa_f = -\frac{v_f}{a_f} \frac{1}{4s_W^2 |Q_f|} \left(\frac{\Delta^{(1)}g_V^f}{v_f} - \frac{\Delta^{(1)}g_A^f}{a_f} \right), \quad (7.16)$$

$$\Delta^{(2)}\kappa_f = -\frac{\Delta^{(1)}g_A^f}{a_f} \Delta^{(1)}\kappa_f - \frac{v_f}{a_f} \frac{1}{4s_W^2 |Q_f|} \left(\frac{\Delta^{(2)}g_V^f}{v_f} - \frac{\Delta^{(2)}g_A^f}{a_f} \right). \quad (7.17)$$

7.1.1 QED and QCD corrections in radiation factors

The radiation factors $R_{V,A}^f$ in (7.3) and (7.4) include the final state QED and QCD interactions and finite mass corrections. For consistency with the most recent calculation of the partial widths in the SM the results given in the appendix of [112] are used.¹

For neutrinos the radiation factors are equal to one, such that

$$\Gamma_\nu = \frac{G_F M_Z^3}{3\sqrt{2}\pi} (g^\nu)^2, \quad (7.18)$$

with

$$g^\nu = g_V^\nu = g_A^\nu. \quad (7.19)$$

For the charged leptons, the radiation factors depend on the electromagnetic coupling constant $\alpha(M_Z^2)$, and on the lepton mass [231]. Additional $\mathcal{O}(\alpha^2)$ contributions from diagrams with closed fermion loops [236] are also included, resulting in

$$R_V^l = 1 + \frac{3Q_l^2}{4} \frac{\alpha(M_Z^2)}{\pi} + Q_l^2 (2C_2^t(M_Z^2/m_t^2) + C_{\gamma 2}) \left(\frac{\alpha(M_Z^2)}{\pi} \right)^2 - 6 \frac{m_l^4}{M_Z^4}, \quad (7.20)$$

$$R_A^l = 1 + \frac{3Q_l^2}{4} \frac{\alpha(M_Z^2)}{\pi} + Q_l^2 (2C_2^t(M_Z^2/m_t^2) + C_{\gamma 2}) \left(\frac{\alpha(M_Z^2)}{\pi} \right)^2 - 6 \frac{m_l^2}{M_Z^2} + 6 \frac{m_l^4}{M_Z^4}. \quad (7.21)$$

¹For the calculation of the Z widths in [94] the radiation factors were evaluated with the help of ZFITTER. In order to allow a self-contained calculation, the radiation factors are now also implemented in the Fortran code for the evaluation of precision observables in the THDM developed in this thesis.

For the decays into quarks additional QCD corrections have to be included in the radiation factors. They contain corrections up to $\mathcal{O}(\alpha_s^4)$ for massless final-state quarks and $\mathcal{O}(\alpha_s^2)$ for terms including the masses of the external quarks [235, 237, 238]. Neglecting terms of $\mathcal{O}(m_f^6)$, $\mathcal{O}(m_f^4\alpha_s)$, $\mathcal{O}(m_f^2\alpha_s^2)$ and $\mathcal{O}(m_f^2\alpha)$, the radiation factors for the quarks read

$$\begin{aligned}
 R_V^q = & 1 + \frac{3Q_q^2 \alpha(M_Z^2)}{4\pi} + \frac{\alpha_s(M_Z^2)}{\pi} - \frac{Q_q^2 \alpha(M_Z^2) \alpha_s(M_Z^2)}{4\pi^2} \\
 & + (C_2^t(M_Z^2/m_t^2) + C_{02}) \left(\frac{\alpha_s(M_Z^2)}{\pi} \right)^2 + Q_q^2 (2C_2^t(M_Z^2/m_t^2) + C_{\gamma 2}) \left(\frac{\alpha(M_Z^2)}{\pi} \right)^2 \\
 & + C_{03} \left(\frac{\alpha_s(M_Z^2)}{\pi} \right)^3 + C_{04} \left(\frac{\alpha_s(M_Z^2)}{\pi} \right)^4 + \frac{12\bar{m}_q^2(M_Z^2) \alpha_s(M_Z^2)}{M_Z^2 \pi} - \frac{6\bar{m}_q^4(M_Z^2)}{M_Z^4}, \quad (7.22)
 \end{aligned}$$

$$\begin{aligned}
 R_A^q = & 1 + \frac{3Q_q^2 \alpha(M_Z^2)}{4\pi} + \frac{\alpha_s(M_Z^2)}{\pi} - \frac{Q_q^2 \alpha(M_Z^2) \alpha_s(M_Z^2)}{4\pi^2} \\
 & + Q_q^2 (2C_2^t(M_Z^2/m_t^2) + C_{\gamma 2}) \left(\frac{\alpha(M_Z^2)}{\pi} \right)^2 \\
 & + (C_2^t(M_Z^2/m_t^2) + C_{02} - 2I_3^q \mathcal{I}_2(M_Z^2/m_t^2)) \left(\frac{\alpha_s(M_Z^2)}{\pi} \right)^2 \\
 & + (C_{03} - 2I_3^q \mathcal{I}_3(M_Z^2/m_t^2)) \left(\frac{\alpha_s(M_Z^2)}{\pi} \right)^3 \\
 & + (C_{04} - 2I_3^q \mathcal{I}_4(M_Z^2/m_t^2)) \left(\frac{\alpha_s(M_Z^2)}{\pi} \right)^4 \\
 & - 22 \frac{\alpha_s(M_Z^2) \bar{m}_q^2(M_Z^2)}{\pi M_Z^2} + \frac{6\bar{m}_q^4(M_Z^2)}{M_Z^4} - \frac{6\bar{m}_q^2(M_Z^2)}{M_Z^2}. \quad (7.23)
 \end{aligned}$$

The masses of the u , d and s quarks are neglected in the radiation factors. For the c and the b quark the running masses in the $\overline{\text{MS}}$ scheme at the scale M_Z^2 are used, which can be obtained with the Mathematica program `RunDec` [239].

The following abbreviations are introduced for the above formulas:

$$C_{\gamma 2} = -\frac{55}{6} + \frac{20}{3}\zeta_3, \quad (7.24)$$

$$C_{02} = \frac{365}{24} - 11\zeta_3 + n_q \left(\frac{2}{3}\zeta_3 - \frac{11}{12} \right), \quad (7.25)$$

$$C_{03} = -6.63694 - 1.20013n_q - 0.005178n_q^2, \quad (7.26)$$

$$C_{04} = -156.61 + 0.0215n_q^3 - 0.7974n_q^2 + 18.77n_q, \quad (7.27)$$

$$C_2^t(x) = x \left(\frac{44}{675} - \frac{2\log(x)}{135} \right), \quad (7.28)$$

$$\mathcal{I}_2(x) = -\frac{37}{12}\log(x) + \frac{7}{81}x + \frac{79}{6000}x^2 + \mathcal{O}(x^3), \quad (7.29)$$

$$\mathcal{I}_3(x) = -15.9877 + \frac{67}{18}\log(x) + \frac{23}{12}\log^2(x) + \mathcal{O}(x), \quad (7.30)$$

$$\mathcal{I}_4(x) = 49.0309 - 17.6637\log(x) + 14.6597\log^2(x) + 3.6736\log^3(x) + \mathcal{O}(x), \quad (7.31)$$

where $n_q = 5$ is the number of active quarks and

$$\zeta_3 = 1.2020569 \quad (7.32)$$

is the Riemann Zeta function

$$\zeta_s = \sum_{k=1}^{\infty} k^{-s} \quad (7.33)$$

evaluated at $s = 3$.



Figure 7.2: Higher-order corrections to the $Z \rightarrow f\bar{f}$ decay. The left diagram represents the sum of all electroweak loop diagrams for the vertex corrections. The right diagram corresponds to the vertex counterterm.

7.1.2 Electroweak corrections in effective couplings

The electroweak corrections to the partial widths are incorporated into the effective couplings $g_{V,A}^f$ in (7.3) or alternatively into the form factors ρ_f and κ_f in (7.4). In the THDM the electroweak corrections consist of a SM-like part and a non-standard part from the extended scalar sector. In the alignment limit the corrections which originate only from the scalars h^0 , G^0 and G^\pm are identical to the scalar corrections in the SM and are therefore already included in the SM-like part. The non-standard contribution originate from the scalars H^0 , A^0 and H^\pm . For the one-loop corrections to the effective couplings $g_{V,A}^f$ the results from [94] are used. In this thesis also the non-standard two-loop corrections to the ρ parameter are incorporated in the partial Z widths, for which it is more convenient to use the parameterization (7.4) with the form factors ρ_f and κ_f .

The effective couplings at the one-loop order are identical to the results obtained in [94], where more details can be found. The expressions are just repeated here for completeness. The one-loop corrections for $Z \rightarrow f\bar{f}$ are symbolized by Figure 7.2. The resulting contributions to the effective couplings are

$$\begin{aligned} \Delta^{(1)} g_V^f = v_f \left\{ -\frac{1}{2} \Delta r^{(1)} + \frac{1}{2} \delta^{(1)} Z_{ZZ} + \delta^{(1)} Z_e + \frac{1}{2} \frac{s_W^2 - c_W^2}{s_W^2} \frac{\delta^{(1)} s_W^2}{s_W^2} \right\} \\ + 2s_W c_W Q_f \left\{ \frac{1}{2} \delta^{(1)} Z_{\gamma Z} - \frac{c_W}{s_W} \frac{\delta^{(1)} s_W^2}{s_W^2} \right\} + F_V^f(M_Z^2), \end{aligned} \quad (7.34)$$

$$\begin{aligned} \Delta^{(1)} g_A^f = a_f \left\{ -\frac{1}{2} \Delta r^{(1)} + \frac{1}{2} \delta^{(1)} Z_{ZZ} + \delta^{(1)} Z_e + \frac{1}{2} \frac{s_W^2 - c_W^2}{s_W^2} \frac{\delta^{(1)} s_W^2}{s_W^2} \right\} \\ + F_A^f(M_Z^2). \end{aligned} \quad (7.35)$$

The renormalization conditions for the various counterterms in (7.34) and (7.35) can be found in Chapter 4. Due to our renormalization scheme, the corrections in the external legs appear as a part of the vertex-counterterms in Figure 7.2. The quantity $\Delta r^{(1)}$ originates from the normalization of the partial widths in terms of G_F . The form factors $F_{V,A}^f$ in (7.34) and (7.35) are build by the non-photon vertex corrections and the non-QED parts of the counterterms $\delta Z_f^{L,R}$, which contain the fermion field renormalization with the renormalization conditions given in (4.53) and (4.54).

A short discussion about the normalization of the partial widths is appropriate. With the tree-level couplings v_f and a_f the tree-level matrix element for $Z \rightarrow f\bar{f}$ is written as

$$\mathcal{M}_{Zf\bar{f}}^{\text{Born}} = \frac{e}{2s_W c_W} \epsilon^\mu(p) \bar{u}(q) [v_f \gamma_\mu - a_f \gamma_\mu \gamma_5] v(q') \quad (7.36)$$

where $q' = p - q$ and $\bar{u}(q)$, $v(q')$ and $\epsilon^\mu(p)$ are the wave-functions of the fermion f , the antifermion \bar{f} , and the Z boson. In the on-shell scheme from Section 4.2 the vector- and axial-vector couplings are defined without the overall prefactor

$$\frac{e}{2s_W c_W}. \quad (7.37)$$

Neglecting the higher-order corrections as well as finite-mass terms from the external fermions yields the tree-level widths

$$\hat{\Gamma}_f = \hat{\Gamma}_0 N_c^f [v_f^2 + a_f^2] \quad (7.38)$$

with the normalization factor²

$$\hat{\Gamma}_0 = \frac{\alpha_{em} M_Z}{12 s_W^2 c_W^2}. \quad (7.39)$$

This normalization depends on the W boson mass due to the definition of the weak mixing angle in the on-shell scheme. Since M_W is calculated in terms of the relation (6.2) it contains an implicit dependence also on the THDM parameters. Therefore a distinct separation between standard and non-standard corrections to the partial widths is obscured. A normalization factor in terms of G_F , which is independent of THDM corrections, is achieved by using the relation

$$\frac{e^2}{4 s_W^2 c_W^2} (1 + \Delta r) = G_F M_Z^2 \sqrt{2} \quad (7.40)$$

and incorporating Δr in the effective couplings. In this way the normalization leads to (7.5) and the corrections in the effective couplings can be separated into a standard and a non-standard part. The partial widths in both parameterizations were implemented in the Fortran code developed in this thesis. A direct comparison of the results of the total widths showed deviations less than 0.3 MeV. This small deviation is negligible in comparison to the experimental uncertainties and reassures us that the normalization in terms of the Fermi constant is sensible.

The normalization of the partial widths in terms of G_F allows a clear separation of the effective couplings into a SM-like part and a non-standard part, since the quantity Δr can be written as

$$\Delta r = \Delta r_{\text{SM}} + \Delta r_{\text{NS}}. \quad (7.41)$$

For the effective couplings at the one-loop order in (7.34) and (7.35) this separation yields

$$g_V^f = v_f + \Delta^{(1)} g_{V,\text{SM}}^f + \Delta^{(1)} g_{V,\text{NS}}^f, \quad (7.42)$$

$$g_A^f = a_f + \Delta^{(1)} g_{A,\text{SM}}^f + \Delta^{(1)} g_{A,\text{NS}}^f. \quad (7.43)$$

The SM parts are given by

$$\begin{aligned} \Delta^{(1)} g_{V,\text{SM}}^f = v_f & \left\{ -\frac{1}{2} \Delta r_{\text{SM}}^{(1)} + \frac{1}{2} \delta^{(1)} Z_{ZZ}^{\text{SM}} + \delta^{(1)} Z_e^{\text{SM}} + \frac{1}{2} \frac{s_W^2 - c_W^2}{s_W^2} \frac{\delta s_{W,\text{SM}}^2}{s_W^2} \right\} \\ & + 2 s_W c_W Q_f \left\{ \frac{1}{2} \delta^{(1)} Z_{\gamma Z}^{\text{SM}} - \frac{c_W}{s_W} \frac{\delta s_{W,\text{SM}}^2}{s_W^2} \right\} + F_{V,\text{SM}}^f (M_Z^2), \end{aligned} \quad (7.44)$$

$$\begin{aligned} \Delta^{(1)} g_{A,\text{SM}}^f = a_f & \left\{ -\frac{1}{2} \Delta r_{\text{SM}}^{(1)} + \frac{1}{2} \delta^{(1)} Z_{ZZ}^{\text{SM}} + \delta^{(1)} Z_e^{\text{SM}} + \frac{1}{2} \frac{s_W^2 - c_W^2}{s_W^2} \frac{\delta s_{W,\text{SM}}^2}{s_W^2} \right\} \\ & + F_{A,\text{SM}}^f (M_Z^2), \end{aligned} \quad (7.45)$$

where the index denotes that only the corrections from the SM particles are kept in the calculation of the counterterms and the form factors. The scalar contributions to the vertex form factors $F_{V,A}^f$ can be neglected for $f \neq b$, because of the small Yukawa couplings. For the decay into two bottom quarks, the scalar contributions with a virtual top quark have to be taken into account due to the large top mass.

²In order to distinguish the different normalization factors, we denote the parameterization via α_{em} with a caret.

The non-standard parts in (7.42) and (7.43) are

$$\begin{aligned} \Delta^{(1)} g_{V,\text{NS}}^f = v_f & \left\{ -\frac{1}{2} \Delta r_{\text{NS}}^{(1)} + \frac{1}{2} \delta^{(1)} Z_{ZZ}^{\text{NS}} + \delta^{(1)} Z_e^{\text{NS}} + \frac{1}{2} \frac{s_W^2 - c_W^2}{s_W^2} \frac{\delta s_{W,\text{NS}}^2}{s_W^2} \right\} \\ & + 2s_W c_W Q_f \left\{ \frac{1}{2} \delta^{(1)} Z_{\gamma Z}^{\text{NS}} - \frac{c_W}{s_W} \frac{\delta s_{W,\text{NS}}^2}{s_W^2} \right\} + F_{V,\text{NS}}^f (M_Z^2), \end{aligned} \quad (7.46)$$

$$\begin{aligned} \Delta^{(1)} g_{A,\text{NS}}^f = a_f & \left\{ -\frac{1}{2} \Delta r_{\text{NS}}^{(1)} + \frac{1}{2} \delta^{(1)} Z_{ZZ}^{\text{NS}} + \delta^{(1)} Z_e^{\text{NS}} + \frac{1}{2} \frac{s_W^2 - c_W^2}{s_W^2} \frac{\delta s_{W,\text{NS}}^2}{s_W^2} \right\} \\ & + F_{A,\text{NS}}^f (M_Z^2). \end{aligned} \quad (7.47)$$

The non-standard form factors $F_{V,\text{NS}}^f (M_Z^2)$ and $F_{A,\text{NS}}^f (M_Z^2)$ in (7.46) and (7.47) can be neglected due to the small Yukawa couplings, except for the couplings of $Z \rightarrow b\bar{b}$, where the large top mass enters via loops including the charged Higgs bosons. Moreover the bottom-Yukawa couplings can be enhanced by large values of $\tan \beta$ in the THDM of type-II and type-Y. In the IHDM, the non-standard scalars do not couple to the fermions and the effective couplings are given by (7.46) and (7.47) without the non-standard form factors $F_{V,\text{NS}}^f (M_Z^2)$ and $F_{A,\text{NS}}^f (M_Z^2)$.

In the alternative parameterization of the partial widths in (7.4), the electroweak corrections are incorporated in the form factors ρ_f and κ_f . The form factors can be divided in an universal part (independent of the fermion species) and a non-universal part (depending on the fermion species). At the one-loop order, the universal part arises from the gauge-boson self energies in terms of the gauge-boson counterterms in (7.34) and (7.35). The non-universal part arises from the vertex-corrections and the fermion field renormalization contained in the vertex form factors $F_{V,A}^f$.

The leading one-loop contribution to the universal parts are the corrections to the ρ parameter contained in the counterterm of the weak mixing angle. The light-fermion contributions via $\Delta\alpha$ is absent in the effective couplings at the one-loop order. The corresponding corrections which are contained in the electric-charge counterterm and $\Delta r^{(1)}$ cancel each other in (7.34) and (7.35). The dominant one-loop parts of ρ_f and κ_f are thus given by

$$\Delta^{(1)} \rho_f = \Delta\rho^{(1)} + \dots \quad (7.48)$$

$$\Delta^{(1)} \kappa_f = \frac{c_W^2}{s_W^2} \Delta\rho^{(1)} + \dots \quad (7.49)$$

For a more accurate prediction of the partial Z widths in the THDM we want to improve the calculation by including also the non-standard two-loop corrections to the ρ parameter, as well as additional reducible two-loop contributions arising from the non-standard one-loop correction $\Delta\rho_{\text{NS}}^{(1)}$. These contributions are incorporated very conveniently in terms of the form factors ρ_f and κ_f , as we will describe in the following part. The resulting non-standard contributions to the partial widths are presented in Section 7.1.3.

For the additional reducible and irreducible two-loop corrections, we are interested in the contributions to the form factors from $\Delta\alpha$ and $\Delta\rho$ at the two-loop order. As discussed in Chapter 6 the corrections from $\Delta\alpha$ and $\Delta\rho$ can be traced back to the counterterms of the electric charge and weak mixing angles with the help of the relations (6.9), (6.10), (6.14) and (6.20). Only these counterterms are therefore needed in the two-loop counterterm vertex for $Zf\bar{f}$ (the corresponding Feynman rule can be found in Appendix A). Additional corrections from $\Delta\alpha$ and $\Delta\rho$ are contained in the two-loop contributions to Δr from (6.21) and (6.42), which enter the form factors ρ_f and κ_f due to the normalization of the partial widths in terms of G_F . The combination of the contributions from Δr with the ones from the vertex counterterms leads to the following two-loop parts

$$\Delta^{(2)} \rho_f = \Delta\alpha \Delta\rho^{(1)} + \left(1 - \frac{c_W^2}{s_W^2}\right) \left(\Delta\rho^{(1)}\right)^2 + \delta\rho^{(2)} + \dots, \quad (7.50)$$

$$\Delta^{(2)} \kappa_f = \Delta\alpha \frac{c_W^2}{s_W^2} \Delta\rho^{(1)} - \frac{c_W^4}{s_W^4} \left(\Delta\rho^{(1)}\right)^2 + \frac{c_W^2}{s_W^2} \delta\rho^{(2)} + \dots \quad (7.51)$$

Γ_f [MeV]	Γ_ν	$\Gamma_{e,\mu}$	Γ_τ	Γ_u	$\Gamma_{d,s}$	Γ_c	Γ_b	Γ_Z
X_0	167.157	83.966	83.776	299.936	382.770	299.860	375.724	2494.254
c_1	-0.055	-0.047	-0.047	-0.34	-0.34	-0.34	-0.30	-2.0
c_2	1.26	0.807	0.806	4.07	3.83	4.07	-2.28	19.7
c_3	-0.19	-0.095	-0.095	14.27	10.20	14.27	10.53	58.60
c_4	-0.02	-0.01	-0.01	1.8	-2.4	1.8	-2.4	-4.0
c_5	0.36	0.25	0.25	1.8	0.67	1.8	1.2	8.0
c_6	-0.1	-1.1	-1.1	-11.1	-10.1	-11.1	-10.0	-55.9
c_7	503	285	285	1253	1469	1253	1458	9267

Table 7.1: Coefficients for the parameterisation formula (7.59) of the partial widths in the SM.

for the form factors in (7.12) and (7.13).

The appearance of the light fermion contribution $\Delta\alpha$ in the two-loop terms is a consequence of the parameterization of v^2 via (6.23). Using the reparameterization of $\Delta\rho^{(1)}$ in terms of the Fermi-constant leads to the two-loop shift from (6.26). This two-loop shift cancels the reducible contributions with $\Delta\alpha$, and the form factors in the G_F -expansion are given by

$$\Delta^{(1)}\bar{\rho}_f = \Delta\bar{\rho}^{(1)} + \dots, \quad (7.52)$$

$$\Delta^{(2)}\bar{\rho}_f = \left(\Delta\bar{\rho}^{(1)}\right)^2 + \delta\bar{\rho}^{(2)} + \dots, \quad (7.53)$$

and

$$\Delta^{(1)}\bar{\kappa}_f = \frac{c_W^2}{s_W^2} \Delta\bar{\rho}^{(1)} + \dots, \quad (7.54)$$

$$\Delta^{(2)}\bar{\kappa}_f = \frac{c_W^2}{s_W^2} \delta\bar{\rho}^{(2)} + \dots, \quad (7.55)$$

where $\Delta\bar{\rho}^{(1)}$ and $\delta\bar{\rho}^{(2)}$ give the corrections to the ρ parameter in the parameterization in terms of G_F (see (6.26) and (6.27)). These leading reducible contributions can also be obtained from the expansions

$$\bar{\rho}_f = \frac{1}{1 - \Delta\bar{\rho}^{(1)} - \delta\bar{\rho}^{(2)}} + \dots = 1 + \Delta\bar{\rho}^{(1)} + \left(\Delta\bar{\rho}^{(1)}\right)^2 + \delta\bar{\rho}^{(2)} + \dots, \quad (7.56)$$

$$\bar{\kappa}_f = 1 + \frac{c_W^2}{s_W^2} \Delta\bar{\rho}^{(1)} + \frac{c_W^2}{s_W^2} \delta\bar{\rho}^{(2)} + \dots, \quad (7.57)$$

as derived in [212, 240]

7.1.3 Partial Z widths

Since the initial- and final-state QED+QCD corrections are contained in the radiation factors $R_{V,A}^f$, the non-standard electroweak corrections to the partial widths can be incorporated with the help of the loop-expansion of the effective couplings given in (7.6) and (7.7). With the separation of the one-loop couplings into a standard and a non-standard part in (7.42) and (7.43), the one-loop SM result is denoted by

$$\Gamma_{f,\text{SM}}^{(1)} = N_c^f \Gamma_0 \left[\left(v_f^2 + 2v_f \Delta^{(1)} g_{V,\text{SM}}^f \right) R_V^f + \left(a_f^2 + 2a_f \Delta^{(1)} g_{A,\text{SM}}^f \right) R_A^f \right]. \quad (7.58)$$

For the electroweak corrections to the partial widths in the SM the complete one-loop contribution together with the two-loop corrections which contain one or two closed fermion loops [112] are known. For the most accurate prediction of the partial widths, they are combined

with the $\mathcal{O}(\alpha\alpha_s)$ corrections of the gauge boson self-energies [29–31, 98, 226], the higher-order corrections from the top quark at $\mathcal{O}(\alpha_t\alpha_s^2)$ [32, 33, 113], $\mathcal{O}(\alpha_t^2\alpha_s^2)$, $\mathcal{O}(\alpha_t^3)$ [34, 35] and $\mathcal{O}(\alpha_t\alpha_s^3)$ [36–38]. The final-state QED- and QCD corrections are incorporated through the radiation functions $R_{V,A}$ given in (7.20), (7.21), (7.22) and (7.23). Moreover, an additional vertex-correction of $\mathcal{O}(\alpha\alpha_s)$ [241–246] is included, which cannot be factorized into electroweak correction and final-state QED/QCD corrections. Since numerical integrations are necessary in the calculation of the two-loop integrals, a simple parameterization formula

$$\Gamma_f^{\text{SM}} = X_0 + c_1 L_H + c_2 \Delta_t + c_3 \Delta_{\alpha_s} + c_4 \Delta_{\alpha_s}^2 + c_5 \Delta_{\alpha_s} \Delta_t + c_6 \Delta_\alpha + c_7 \Delta_Z \quad (7.59)$$

with

$$\begin{aligned} L_H &= \log \frac{M_H}{125.7 \text{ GeV}}, \quad \Delta_t = \left(\frac{m_t^2}{173.2 \text{ GeV}} \right), \quad \Delta_{\alpha_s} = \frac{\alpha_s (M_Z^2)}{0.1184} - 1, \\ \Delta_\alpha &= \frac{\Delta\alpha}{0.059} - 1, \quad \Delta_Z = \frac{M_Z}{91.1876 \text{ GeV}} - 1, \end{aligned} \quad (7.60)$$

is provided in [112], which reproduces the result to a very good accuracy. The coefficients for the different partial widths and the total Z width are given in Table 7.1. They correspond to the partial widths in the SM calculated with the SM-result of the W boson mass, $M_{W,\text{SM}}$. In order to capture the M_W -dependence of the corrections of the partial widths, we use the explicit one-loop result in the SM given in (7.58) and approximate the higher-order corrections by

$$\Delta\Gamma_{f,\text{SM}}^{(\text{h.o.})} = \Gamma_f^{\text{SM}} - \Gamma_{f,\text{SM}}^{(1)}(M_{W,\text{SM}}). \quad (7.61)$$

This constant approximation is added to the SM one-loop result evaluated for the prediction of M_W in the THDM, yielding

$$\Gamma_{f,\text{SM}} = \Gamma_{f,\text{SM}}^{(1)}(M_W) + \Delta\Gamma_{f,\text{SM}}^{(\text{h.o.})}. \quad (7.62)$$

The additional non-standard corrections are added on top of the SM result, which leads to

$$\Gamma_f = \Gamma_{f,\text{SM}} + \Delta\Gamma_{f,\text{NS}}. \quad (7.63)$$

for the partial widths in the THDM. The non-standard part

$$\Delta\Gamma_{f,\text{NS}} = \Delta^{(1)}\Gamma_{\text{NS}}^f + \Delta^{(2)}\Gamma_{\text{NS}}^f \quad (7.64)$$

includes the complete non-standard one-loop part $\Delta^{(1)}\Gamma_{\text{NS}}^f$, as well as the leading two-loop contributions in $\Delta^{(2)}\Gamma_{\text{NS}}^f$.

The one-loop non-standard terms of the effective couplings in (7.46) and (7.47) give

$$\Delta^{(1)}\Gamma_{\text{NS}}^f = N_c^f \Gamma_0 \left[2v_f \Delta^{(1)} g_{V,\text{NS}}^f R_V^f + 2a_f \Delta^{(1)} g_{A,\text{NS}}^f R_A^f \right] \quad (7.65)$$

as the one-loop non-standard corrections to the partial widths. We denote the result of the total Z width with just the one-loop non-standard corrections by

$$\Gamma_Z^{(1)} = \sum_{f \neq t} \left(\Gamma_{f,\text{SM}} + \Delta^{(1)}\Gamma_{\text{NS}}^f \right). \quad (7.66)$$

The one-loop non-standard corrections are complemented with the leading two-loop corrections to the ρ parameter together with reducible products of the dominant one-loop contributions $\Delta\alpha$ and $\Delta\rho^{(1)}$. For these contributions it is more convenient to use the parameterization in terms of the form factors ρ_f and κ_f . Using the loop-expansions in (7.12) and (7.13) and keeping only the terms up to the two-loop order results

$$\begin{aligned} \Delta^{(2)}\Gamma^f &= \Gamma_f^{(0)} \Delta^{(2)}\rho_f - 4\Gamma_0 N_c^f s_W^2 Q_f v_f R_V^f \Delta^{(2)}\kappa_f \\ &\quad + 4\Gamma_0 N_c^f s_W^2 Q_f R_V^f \Delta^{(1)}\kappa_f \left(Q_f s_W^2 \Delta^{(1)}\kappa_f - v_f \Delta^{(1)}\rho_f \right), \end{aligned} \quad (7.67)$$

where we introduced

$$\Gamma_f^{(0)} = N_c^f \Gamma_0 \left[v_f^2 R_V^f + a_f^2 R_A^f \right]. \quad (7.68)$$

The two-loop corrections $\Delta^{(2)}\rho_f$ and $\Delta^{(2)}\kappa_f$ in (7.50) and (7.51) contain factorized terms with $\Delta\alpha$ and $\Delta\rho^{(1)}$ as well as terms with the irreducible two-loop correction to the ρ parameter, $\delta\rho^{(2)}$. Consequently, we can write the non-standard part of the two-loop contribution in (7.67) as

$$\Delta^{(2)}\Gamma_{\text{NS}}^f = \Delta^{(2)}\Gamma_{\text{NS,red}}^f + \Delta^{(2)}\Gamma_{\text{NS,irr}}^f, \quad (7.69)$$

where the reducible part $\Delta^{(2)}\Gamma_{\text{NS,red}}^f$ contains only the factorized terms with $\Delta\alpha$ and $\Delta\rho^{(1)}$ and the irreducible part $\Delta^{(2)}\Gamma_{\text{NS,irr}}^f$ contains the irreducible two-loop contribution $\delta\rho^{(2)}$.

The reducible part $\Delta^{(2)}\Gamma_{\text{NS,red}}^f$ follows from (7.67) by taking for $\Delta^{(2)}\rho_f$ and $\Delta^{(2)}\kappa_f$ only the factorized terms with $\Delta\alpha$ and $\Delta\rho^{(1)}$ from (7.50) and (7.51). For the non-standard part of the reducible contribution, the quantity $\Delta\rho^{(1)}$ has to be divided in the top-Yukawa correction $\Delta\rho_t^{(1)}$ and the non-standard correction $\Delta\rho_{\text{NS}}^{(1)}$ (see (5.87)). The terms without $\Delta\rho_{\text{NS}}^{(1)}$ are already incorporated in the SM result of the partial widths. Therefore, the non-standard part contains only

$$\begin{aligned} \Delta^{(2)}\Gamma_{\text{NS,red}}^f = & \Gamma_f^{(0)} \left[\Delta\alpha \Delta\rho_{\text{NS}}^{(1)} + \left(1 - \frac{c_W^2}{s_W^2} \right) \left(2\Delta\rho_t^{(1)} \Delta\rho_{\text{NS}}^{(1)} + \left(\Delta\rho_{\text{NS}}^{(1)} \right)^2 \right) \right] \\ & - 4\Gamma_0 N_c^f s_W^2 Q_f v_f R_V^f \left[\Delta\alpha \frac{c_W^2}{s_W^2} \Delta\rho_{\text{NS}}^{(1)} - \frac{c_W^4}{s_W^4} \left(2\Delta\rho_t^{(1)} \Delta\rho_{\text{NS}}^{(1)} + \left(\Delta\rho_{\text{NS}}^{(1)} \right)^2 \right) \right] \\ & + 4\Gamma_0 N_c^f c_W^2 Q_f R_V^f (c_W^2 Q_f - v_f) \left[2\Delta\rho_t^{(1)} \Delta\rho_{\text{NS}}^{(1)} + \left(\Delta\rho_{\text{NS}}^{(1)} \right)^2 \right]. \end{aligned} \quad (7.70)$$

The irreducible part $\Delta^{(2)}\Gamma_{\text{NS,irr}}^f$ from (7.67) follows from the irreducible terms of $\Delta^{(2)}\rho_f$ and $\Delta^{(2)}\kappa_f$ in (7.50) and (7.51), which are given by

$$\Delta^{(2)}\rho_{f,\text{irr}} = \delta\rho^{(2)}, \quad (7.71)$$

$$\Delta^{(2)}\kappa_{f,\text{irr}} = \frac{c_W^2}{s_W^2} \delta\rho^{(2)}. \quad (7.72)$$

With the separation in (5.115) the following non-standard contributions to the partial widths are specified in the aligned THDM:

- the non-standard two-loop top-Yukawa corrections

$$\Delta^{(2)}\Gamma_{t,\text{NS}}^f = \Gamma_f^{(0)} \delta\rho_{t,\text{NS}}^{(2)} - 4\Gamma_0 N_c^f Q_f v_f R_V^f c_W^2 \delta\rho_{t,\text{NS}}^{(2)}, \quad (7.73)$$

- the pure non-standard scalar two-loop corrections

$$\Delta^{(2)}\Gamma_{\text{H,NS}}^f = \Gamma_f^{(0)} \delta\rho_{\text{H,NS}}^{(2)} - 4\Gamma_0 N_c^f Q_f v_f R_V^f c_W^2 \delta\rho_{\text{H,NS}}^{(2)}, \quad (7.74)$$

- the mixed non-standard scalar corrections

$$\Delta^{(2)}\Gamma_{\text{H,Mix}}^f = \Gamma_f^{(0)} \delta\rho_{\text{H,Mix}}^{(2)} - 4\Gamma_0 N_c^f Q_f v_f R_V^f c_W^2 \delta\rho_{\text{H,Mix}}^{(2)}. \quad (7.75)$$

The total irreducible two-loop part $\Delta^{(2)}\Gamma_{\text{NS,irr}}^f$ is given by the sum

$$\Delta^{(2)}\Gamma_{\text{NS,irr}}^f = \Delta^{(2)}\Gamma_{t,\text{NS}}^f + \Delta^{(2)}\Gamma_{\text{H,NS}}^f + \Delta^{(2)}\Gamma_{\text{H,Mix}}^f. \quad (7.76)$$

The reducible part in the IHDM is identical to $\Delta^{(2)}\Gamma_{\text{NS,red}}^f$ from the THDM in the alignment limit. Differences arise in the irreducible part, since there exists only one irreducible two-loop contribution $\delta\rho_{\text{IHDM}}^{(2)}$ to the ρ parameter in the IHDM. The corresponding correction to the partial widths is given by

$$\Delta^{(2)}\Gamma_{\text{IHDM}}^f = \Gamma_f^{(0)} \delta\rho_{\text{IHDM}}^{(2)} - 4\Gamma_0 N_c^f Q_f v_f R_V^f c_W^2 \delta\rho_{\text{IHDM}}^{(2)}, \quad (7.77)$$

and is corresponding to $\Delta^{(2)}\Gamma_{\text{H,Mix}}^f$ (see the discussion in Section 5.2.4).

In total the result for the partial widths is

$$\Gamma^f = \Gamma_{f,\text{SM}} + \Delta^{(1)}\Gamma_{\text{NS}}^f + \Delta^{(2)}\Gamma_{\text{NS}}^f \quad (7.78)$$

with

$$\Delta^{(2)}\Gamma_{\text{NS}}^f = \Delta^{(2)}\Gamma_{\text{NS,red}}^f + \Delta^{(2)}\Gamma_{\text{t,NS}}^f + \Delta^{(2)}\Gamma_{\text{H,NS}}^f + \Delta^{(2)}\Gamma_{\text{H,Mix}}^f \quad (7.79)$$

in the aligned THDM, and

$$\Delta^{(2)}\Gamma_{\text{NS}} = \Delta^{(2)}\Gamma_{\text{NS,red}}^f + \Delta^{(2)}\Gamma_{\text{IHDM}}^f \quad (7.80)$$

in the IHDM.

The decay of the Z boson into the b and the \bar{b} quark receives additional non-standard corrections from the two-loop vertex diagrams with the non-standard scalars and the top quark as internal particles. These diagrams lead to corrections of $\mathcal{O}(\alpha_t^2)$ or of $\mathcal{O}(\alpha_t\lambda_i)$, which are of the same order as the two-loop corrections to the ρ parameter from the top-Yukawa coupling, $\delta\rho_{\text{t,NS}}^{(2)}$. The calculation of these vertex corrections is however beyond the scope of this work and they are therefore not included in the prediction of the total Z width.

7.2 The effective leptonic weak mixing angle

The effective mixing angles are commonly used to parameterize the ratio of the effective couplings via

$$\sin^2\theta_{\text{eff}}^f = s_f^2 \equiv \frac{1}{4|Q_f|} \left(1 - \frac{g_V^f}{g_A^f} \right) = s_W^2 \kappa^f. \quad (7.81)$$

Assuming lepton universality and separating off lepton mass effects, a common leptonic mixing angle,

$$s_l^2 = \sin^2\theta_{\text{eff}}^l \equiv s_W^2 \kappa = s_W^2 (1 + \Delta\kappa), \quad (7.82)$$

is defined, which has been measured with a high accuracy and is therefore well suited for testing the Standard Model and its extensions. Experimentally it is determined by the forward-backward asymmetry A_{FB} in e^+e^- annihilations, obtained by the difference between the integrated cross-sections over the forward and backward hemispheres, or the left-right asymmetry A_{LR} between the cross-sections for left- and right-handed electron helicities. At the tree-level the effective couplings are given by the tree-level coupling v_l and a_l and the effective leptonic mixing angle is identical to the on-shell mixing angle s_W^2 from (4.23),

$$s_l^2 = s_W^2 = \frac{1}{4} \left(1 - \frac{v_l}{a_l} \right). \quad (7.83)$$

The higher-order corrections are conventionally absorbed in the quantity $\Delta\kappa$. It depends on all the particles which enter in the virtual corrections. An additional model-dependence is contained in the on-shell weak-mixing angle s_W^2 , since it is calculated from the prediction of M_W in terms of the Fermi-constant G_F .

The loop corrections to $g_{V,A}^l$ lead to deviations from $\kappa = 1$. The one-loop expansion (7.16) results in

$$s_l^2 = s_W^2 \left(1 + \frac{v_l}{v_l - a_l} \left(\frac{\Delta^{(1)}g_V^l}{v_l} - \frac{\Delta^{(1)}g_A^l}{a_l} \right) \right). \quad (7.84)$$

The expressions from (7.34) and (7.35) give the one-loop contribution

$$\Delta\kappa^{(1)} = -\frac{1}{2} \frac{s_W}{c_W} \delta^{(1)} Z_{AZ} + \frac{\delta^{(1)} s_W^2}{s_W^2} + \frac{v_l}{v_l - a_l} \left(\frac{F_V^l(M_Z^2)}{v_l} - \frac{F_A^l(M_Z^2)}{a_l} \right). \quad (7.85)$$

The one-loop SM correction to the effective couplings in (7.44) and (7.45) lead to

$$\Delta\kappa_{\text{SM}}^{(1)} = -\frac{1}{2} \frac{s_W}{c_W} \delta^{(1)} Z_{AZ}^{\text{SM}} + \frac{\delta^{(1)} s_{W,\text{SM}}^2}{s_W^2} + \frac{v_l}{v_l - a_l} \left(\frac{F_{V,\text{SM}}^l}{v_l} - \frac{F_{A,\text{SM}}^l}{a_l} \right), \quad (7.86)$$

as the one-loop contribution to $\Delta\kappa$ in the SM. For the leptonic form factors we use $l = e$.

The one-loop result of s_l^2 in the SM was calculated in [247–250]. QCD corrections are known at the two-loop order [29–31, 96–98, 226], as well as the leading three-loop [32, 33, 113] and four-loop corrections [36–38] from the top quark. The two-loop electroweak contributions in the SM are calculated in [107–110]. The leading three-loop corrections to the ρ parameter at $\mathcal{O}(G_F^3 m_t^3)$ and $\mathcal{O}(G_F^2 \alpha_s^2 m_t^2)$ are calculated for a massless Higgs in [35] and with Higgs mass dependence in [34]. Three-loop electroweak corrections of $\mathcal{O}(G_F^3 M_H^4)$ for a large Higgs mass were obtained in [115, 227].

In [110] a simple parameterization is given, which incorporates the complete electroweak one- and two-loop corrections together with the QCD corrections of $\mathcal{O}(\alpha\alpha_s)$ [29–31, 96–98, 226] and $\mathcal{O}(\alpha\alpha_s^2)$ [32, 33, 113] and the leading electroweak three-loop corrections of $\mathcal{O}(G_F^3 m_t^3)$ and $\mathcal{O}(G_F^2 \alpha_s^2 m_t^2)$ [34, 35]:

$$s_{l,\text{SM}}^2 = s_0 + d_1 L_H + d_2 L_H^2 + d_3 L_H^4 + d_4 (\Delta_H^2 - 1) + d_5 \Delta_\alpha + d_6 \Delta_t + d_7 \Delta_t^2 + d_8 \Delta_t (\Delta_H - 1) + d_9 \Delta_{\alpha_s} + d_{10} \Delta_Z, \quad (7.87)$$

with

$$L_H = \log\left(\frac{M_H}{100 \text{ GeV}}\right), \quad \Delta_H = \frac{M_H}{100 \text{ GeV}}, \quad \Delta_\alpha = \frac{\Delta\alpha}{0.05907} - 1, \quad (7.88)$$

$$\Delta_t = \left(\frac{m_t^2}{178.0 \text{ GeV}}\right)^2 - 1, \quad \Delta_{\alpha_s} = \frac{\alpha_s(M_Z)}{0.117} - 1, \quad \Delta_Z = \frac{M_Z}{91.1876 \text{ GeV}} - 1.$$

The coefficients are specified by

$$s_0 = 0.2312527, \quad d_1 = 4.729 \cdot 10^{-4}, \quad d_2 = 2.07 \cdot 10^{-5}, \quad d_3 = 3.85 \cdot 10^{-6},$$

$$d_4 = -1.85 \cdot 10^{-6}, \quad d_5 = 2.07 \cdot 10^{-2}, \quad d_6 = -2.851 \cdot 10^{-3}, \quad d_7 = 1.82 \cdot 10^{-4}, \quad (7.89)$$

$$d_8 = -9.74 \cdot 10^{-6}, \quad d_9 = 3.98 \cdot 10^{-4}, \quad d_{10} = -0.655.$$

Not included are the higher-order corrections of $\mathcal{O}(G_F^3 M_H^4)$ [115, 227] and $\mathcal{O}(G_F m_t^2 \alpha_s^3)$ [36–38].

The effective leptonic mixing angle in the THDM receives additional non-standard contributions in two ways. The on-shell weak mixing angle s_W^2 in (7.82) depends on the THDM parameters since it is calculated from the prediction of M_W in the THDM, which is described in Chapter 6. In addition there exist also explicit non-standard contributions to the quantity $\Delta\kappa$. Due to the alignment limit we can write $\Delta\kappa$ as

$$\Delta\kappa = \Delta\kappa_{\text{SM}} + \Delta\kappa_{\text{NS}}, \quad (7.90)$$

with a SM-like part $\Delta\kappa_{\text{SM}}$ and a non-standard part $\Delta\kappa_{\text{NS}}$.

The standard part $\Delta\kappa_{\text{SM}}$ depends also on the W boson mass. For the one-loop correction of $\Delta\kappa$ in the SM we use the explicit result from (7.86), which depends on the given input of M_W . Furthermore, we approximate the higher-order contribution to $\Delta\kappa$ in the SM by the constant term

$$\delta\kappa_{\text{SM}}^{(\text{h.o.})} = \Delta\kappa_{\text{SM}}^{(\text{h.o.})} - \Delta\kappa_{\text{SM}}^{(1)}(M_{W,\text{SM}}). \quad (7.91)$$

The part $\Delta\kappa_{\text{SM}}^{(\text{h.o.})}$ is extracted from $s_{l,\text{SM}}^2$ in (7.87), which corresponds to the prediction of the effective leptonic mixing in the SM for $M_W = M_{W,\text{SM}}$. By solving (7.82) for $\Delta\kappa$ we obtain

$$\Delta\kappa_{\text{SM}}^{(\text{h.o.})} = \frac{s_{l,\text{SM}}^2}{1 - \frac{M_{W,\text{SM}}^2}{M_Z^2}} - 1. \quad (7.92)$$

In total the SM part of $\Delta\kappa$ is obtained as

$$\Delta\kappa_{\text{SM}} = \Delta\kappa_{\text{SM}}^{(1)}(M_W) + \delta\kappa_{\text{SM}}^{(\text{h.o.})}. \quad (7.93)$$

The non-standard part

$$\Delta\kappa_{\text{NS}} = \Delta\kappa_{\text{NS}}^{(1)} + \Delta\kappa_{\text{NS}}^{(2)} \quad (7.94)$$

contains the non-standard one-loop contribution $\Delta\kappa_{\text{NS}}^{(1)}$ and the leading two-loop contribution $\Delta\kappa_{\text{NS}}^{(2)}$. The vertex corrections and the corrections to the lepton self-energies from the non-standard scalars are suppressed due to the small Yukawa couplings of the leptons. Consequently, we neglect the non-standard contributions to the form-factors $F_{V,A}^{(l)}$. The one-loop non-standard correction to $\Delta\kappa$ is then given by

$$\Delta\kappa_{\text{NS}}^{(1)} = -\frac{1}{2} \frac{s_W}{c_W} \delta^{(1)} Z_{\gamma Z}^{\text{NS}} + \frac{\delta^{(1)} s_{W,\text{NS}}^2}{s_W^2}. \quad (7.95)$$

The index on the counterterm indicates that only the non-standard part of the self-energies are used in the renormalization conditions in (4.19) and (4.25). We denote the result of the effective leptonic mixing angle including just the one-loop non-standard corrections by

$$\sin^2 \theta_{\text{eff}}^{(1)} = \left(1 - \left(\frac{M_W^{(1)}}{M_Z} \right)^2 \right) \left(1 + \Delta\kappa_{\text{SM}} + \Delta\kappa_{\text{NS}}^{(1)} \right), \quad (7.96)$$

where $M_W^{(1)}$ is the result for the W boson mass, which includes just the one-loop part of the non-standard contribution Δr_{NS} (see the discussion in Chapter 6).

The non-standard two-loop part $\Delta\kappa_{\text{NS}}^{(2)}$ incorporates the leading two-loop corrections to the ρ parameter from the top-Yukawa coupling and the scalar self-interaction. With the two-loop contribution to κ from (7.51) the non-standard two-loop part $\Delta\kappa_{\text{NS}}^{(2)}$ can be written as

$$\Delta\kappa_{\text{NS}}^{(2)} = \Delta\kappa_{\text{NS,red}}^{(2)} + \Delta\kappa_{\text{NS,irr}}^{(2)}, \quad (7.97)$$

where the reducible part $\Delta\kappa_{\text{NS,red}}^{(2)}$ contains the factorized terms with $\Delta\alpha$ and $\Delta\rho^{(1)}$ and the irreducible part $\Delta\kappa_{\text{NS,irr}}^{(2)}$ contains the terms with $\delta\rho^{(2)}$.

For the reducible non-standard part $\Delta\kappa_{\text{NS,red}}^{(2)}$ we insert the one-loop contribution

$$\Delta\rho^{(1)} = \Delta\rho_t^{(1)} + \Delta\rho_{\text{NS}}^{(1)} \quad (7.98)$$

into the factorized terms with $\Delta\alpha$ and $\Delta\rho^{(1)}$ in (7.51). Since the terms without $\Delta\rho_{\text{NS}}^{(1)}$ are already incorporated in $\Delta\kappa_{\text{SM}}$, the non-standard reducible part is given by

$$\Delta\kappa_{\text{NS,red}}^{(2)} = \Delta\alpha \frac{c_W^2}{s_W^2} \Delta\rho_{\text{NS}}^{(1)} - \frac{c_W^4}{s_W^4} \left(2\Delta\rho_t^{(1)} \Delta\rho_{\text{NS}}^{(1)} + \left(\Delta\rho_{\text{NS}}^{(1)} \right)^2 \right). \quad (7.99)$$

The irreducible part $\Delta\kappa_{\text{NS,irr}}^{(2)}$ incorporates the terms from (7.51) which contain $\delta\rho^{(2)}$. In (5.115) the non-standard part of $\delta\rho^{(2)}$ is divided in the different finite contributions, which lead to the following irreducible two-loop corrections to κ :

- the contribution from the non-standard top-Yukawa correction

$$\Delta\kappa_{t,\text{NS}}^{(2)} = \frac{c_W^2}{s_W^2} \delta\rho_{t,\text{NS}}^{(2)}, \quad (7.100)$$

- the contribution from the pure non-standard scalar corrections

$$\Delta\kappa_{\text{H,NS}}^{(2)} = \frac{c_W^2}{s_W^2} \delta\rho_{\text{H,NS}}^{(2)}, \quad (7.101)$$

- the contribution from the mixed scalar corrections

$$\Delta\kappa_{\text{H,Mix}}^{(2)} = \frac{c_W^2}{s_W^2} \delta\rho_{\text{H,Mix}}^{(2)}. \quad (7.102)$$

The total irreducible non-standard part is then given by

$$\Delta\kappa_{\text{NS,irr}}^{(2)} = \Delta\kappa_{\text{t,NS}}^{(2)} + \Delta\kappa_{\text{H,NS}}^{(2)} + \Delta\kappa_{\text{H,Mix}}^{(2)}. \quad (7.103)$$

The reducible part $\Delta\kappa_{\text{NS,red}}^{(2)}$ is identical in the IHDM and the THDM in the alignment limit. Differences arise however in the irreducible part, since there exists just one irreducible non-standard two-loop correction to the ρ parameter in the IHDM, which is denoted by $\delta\rho_{\text{IHDM}}^{(2)}$ in Section 5.2.4. The corresponding contribution to $\Delta\kappa$ is

$$\Delta\kappa_{\text{IHDM}}^{(2)} = \frac{c_W^2}{s_W^2} \delta\rho_{\text{IHDM}}^{(2)}. \quad (7.104)$$

With these non-standard corrections, the prediction of the effective leptonic mixing angle is given by

$$s_l^2 = \left(1 - \frac{M_W^2}{M_Z^2}\right) \left(1 + \Delta\kappa_{\text{SM}}^{(1)} + \delta\kappa_{\text{SM}}^{(\text{h.o.})} + \Delta\kappa_{\text{NS}}^{(1)} + \Delta\kappa_{\text{NS}}^{(2)}\right) \quad (7.105)$$

with

$$\Delta\kappa_{\text{NS}}^{(2)} = \Delta\kappa_{\text{NS,red}}^{(2)} + \Delta\kappa_{\text{t,NS}}^{(2)} + \Delta\kappa_{\text{H,NS}}^{(2)} + \Delta\kappa_{\text{H,Mix}}^{(2)} \quad (7.106)$$

in the aligned THDM and

$$\Delta\kappa_{\text{NS}}^{(2)} = \Delta\kappa_{\text{NS,red}}^{(2)} + \Delta\kappa_{\text{IHDM}}^{(2)} \quad (7.107)$$

in the IHDM. As mentioned before, the prefactor in (7.105) contains also the non-standard corrections in M_W . In order to have a consistent calculation, the non-standard corrections in the calculation of M_W are always corresponding to those in $\Delta\kappa$. For example, since $\sin^2\theta_{\text{eff}}^{(1)}$ in (7.96) includes only the non-standard one-loop contribution $\Delta\kappa_{\text{NS}}^{(1)}$, the calculation of $M_W^{(1)}$ includes also only the one-loop contribution $\Delta r_{\text{NS}}^{(1)}$ as the non-standard correction. If furthermore the reducible contribution $\Delta\kappa_{\text{NS,red}}^{(2)}$ is added to the calculation of $\Delta\kappa$, also the reducible contribution $\Delta r_{\text{NS,red}}^{(2)}$ is contained in the calculation of M_W , and so forth.

Chapter 8

Numerical Results

In this chapter we present numerical results for the prediction of the W boson mass, M_W , the effective leptonic mixing angle, $\sin^2 \theta_{\text{eff}}^l \equiv s_l^2$, and the total width of the Z boson, Γ_Z in the various step of the approximations. The predictions are compared with the experimental results

$$M_W = 80.385 \pm 0.015 \text{ GeV}, \quad (8.1)$$

$$s_l^2 = 0.23153 \pm 0.00016, \quad (8.2)$$

$$\Gamma_Z = 2.4952 \pm 0.0023 \text{ GeV}. \quad (8.3)$$

The value for M_W is taken from [213]; for the other two observables the experimental values are given in [230].

We present specific parameter configurations which highlight the impact of the different two-loop corrections. After this general discussion we investigate specific scenarios which are motivated by different phenomenological aspects of the THDM. Of particular interest are the results in the IHDM, for which we investigate also scenarios preferred by astrophysical constraints.

The comparison of the theoretical predictions with the experimental results yields restrictions on the free parameters. Additionally shown are the theoretical constraints from tree-level unitarity and vacuum stability, as given in Section 2.7. Since these constraints are obtained only at the tree-level, they should be regarded as an estimate for parameters that are of interest in physical scenarios. A more thorough analysis should include the theoretical constraints at next-to-leading order.

8.1 Input parameters

For the analysis of the precision observables the following input for the SM parameters [213] are used

$$M_Z = 91.1876 \text{ GeV}, \quad (8.4)$$

$$m_t = 173.21 \text{ GeV}, \quad (8.5)$$

$$\alpha_s(M_Z^2) = 0.1181, \quad (8.6)$$

$$G_\mu = 1.1663787 \cdot 10^{-5} \text{ GeV}^{-2}, \quad (8.7)$$

$$\alpha_{em}^{-1} = 137.035999139. \quad (8.8)$$

For the mass of SM-like Higgs boson we use the value

$$m_{h^0} = 125 \text{ GeV}. \quad (8.9)$$

In addition we also need the input for the shift $\Delta\alpha$ in the electromagnetic fine structure constant, given in (6.8). It can be split into a leptonic and a hadronic part

$$\Delta\alpha = \Delta\alpha_{\text{lept}} + \Delta\alpha_{\text{had}}. \quad (8.10)$$

The leptonic contribution can be calculated directly with the measured lepton masses. Taking into account the corrections up to the three-loop order [251] leads to

$$\Delta\alpha_{\text{lept}} = 0.031497. \quad (8.11)$$

Since perturbative QCD is not applicable in the low-energy range, the hadronic part has to be extracted from experimental data with the help of dispersion relations. For our analysis we use

$$\Delta\alpha_{\text{had}} = 0.027572 \pm 0.000359 \quad (8.12)$$

from [252], which is also used in [106] for the prediction of M_W in the SM. In total we have

$$\Delta\alpha = 0.05907, \quad (8.13)$$

which is the default value for $\Delta\alpha$ in the parameterizations in (6.30) and (7.87).

With these input parameters the SM prediction for M_W , s_l^2 and Γ_Z from (6.30), (7.59) and (7.87) yield

$$M_{W,\text{SM}} = 80.360 \pm 0.004 \text{ GeV}, \quad (8.14)$$

$$s_{l,\text{SM}}^2 = 0.231514 \pm 0.000047, \quad (8.15)$$

$$\Gamma_{Z,\text{SM}} = 2.49405 \pm 0.0005 \text{ GeV}, \quad (8.16)$$

with the intrinsic theoretical uncertainties from currently unknown higher-order corrections, which are estimated in [106, 110, 112].¹ While the prediction of the effective leptonic mixing angle and the total Z width are in good agreement with the measurements, there is a slight tension between the prediction of M_W and its experimental value.

For the radiation factors $R_{V,A}^f$ of the partial widths in (7.3) and (7.4) we also need the running masses of the charm and the bottom quark at the scale M_Z^2 . The result from the program RunDec [239] gives

$$\bar{m}_c(M_Z^2) = 0.435 \text{ GeV}, \quad (8.17)$$

$$\bar{m}_b(M_Z^2) = 2.859 \text{ GeV}. \quad (8.18)$$

The total Z width also depends on the bottom-Yukawa coupling, due to the decay $Z \rightarrow b\bar{b}$. The coupling of the non-standard scalars to the bottom quark, which are contained in the non-standard one-loop corrections to the $Zb\bar{b}$ -vertex, differ in the various types of the THDM. The following results for the total Z width are obtained for a THDM of type-II (which has the same structure for the bottom-Yukawa coupling as the THDM of type-Y).

The predictions of M_W and s_l^2 do not depend on the type of THDM, since the bottom-Yukawa coupling is neglected in the two-loop contribution $\delta\rho_{t,\text{NS}}^{(2)}$ and the remaining non-standard corrections are independent of the Yukawa couplings.

We present results for a THDM without a hard violation of the Z_2 symmetry, such that $\Lambda_6 = \Lambda_7 = 0$. As discussed in Chapter 5 this version of the THDM covers already the main characteristics of the two-loop corrections. The free parameters entering the predictions of M_W , s_l^2 and Γ_Z are therefore the masses of the non-standard scalars, t_β and the parameter λ_5 , which is used to replace m_{12}^2 with the help of (2.50).

In the IHDM the one-loop non-standard corrections of M_W , s_l^2 and Γ_Z depend only on the masses of the non-standard scalars. The non-standard two-loop correction $\delta\rho_{\text{IHDM}}^{(2)}$ introduces an additional dependence on the parameter Λ_{345} defined in (2.114), which controls the coupling of the dark matter candidate to the SM-like Higgs.

8.2 Influence of reducible two-loop corrections

The two-loop contributions to the precision observables are classified in Chapter 6 and Chapter 7 into reducible and irreducible contributions. The reducible parts contain only the factorized

¹Additional parametric uncertainties in the theoretical predictions arise from the experimental errors of the input parameters. These parametric uncertainties can be obtained from variations of the input parameters in the parameterizations in (6.30), (7.59) and (7.87).

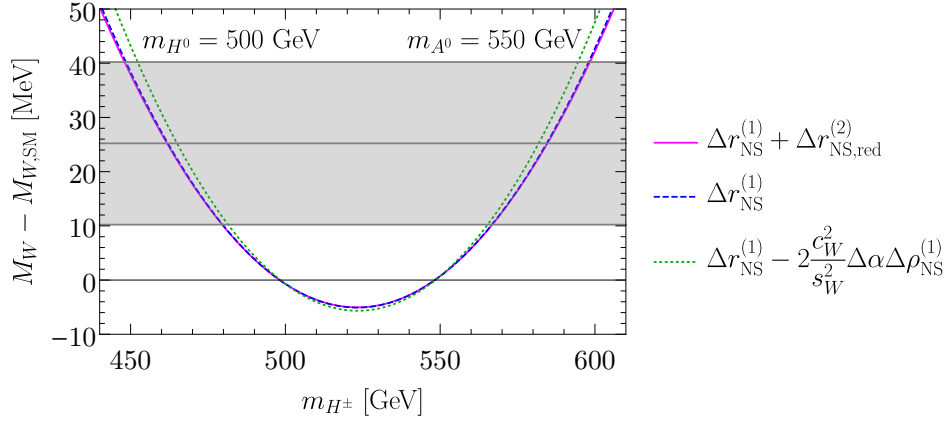


Figure 8.1: Influence of the reducible two-loop corrections on M_W . The difference to the SM result is shown for a variation of the charged Higgs mass with $m_{H^0} = 500$ GeV and $m_{A^0} = 550$ GeV. The blue dashed line corresponds to the result, which includes just the one-loop non-standard correction $\Delta r_{NS}^{(1)}$. The green dotted line includes in addition the reducible product between $\Delta\alpha$ and $\Delta\rho_{NS}^{(1)}$. The solid magenta line presents the result which contains the complete non-standard reducible correction $\Delta r_{NS,red}^{(2)}$. The grey shaded region displays the measurement with its 1σ uncertainties.

terms with the one-loop quantities $\Delta\alpha$ and $\Delta\rho^{(1)}$. In the following we investigate the influence of the non-standard reducible contributions to M_W , s_l^2 and Γ_Z , which arise due to the non-standard one-loop correction to the ρ parameter, $\Delta\rho_{NS}^{(1)}$. These contributions are identical in the different types of the THDM and also in the IHDM. Since $\Delta\rho_{NS}^{(1)}$ has a great sensitivity on the mass difference between the charged and neutral scalars, the results are presented for a variation of m_{H^\pm} for fixed values of m_{H^0} and m_{A^0} . As discussed in Chapter 5, the contribution $\Delta\rho_{NS}^{(1)}$ is equal to zero for $m_{H^\pm} = m_{H^0}$ and $m_{H^\pm} = m_{A^0}$ due to a restoration of the custodial symmetry. A small mass difference between H^0 and A^0 is therefore selected, in order to highlight the effect of the custodial symmetry. Since very heavy masses of the non-standard scalars are forbidden by unitarity constraints, the values $m_{H^0} = 500$ GeV and $m_{A^0} = 550$ GeV are chosen, which are in accordance with the theoretical constraints. Degenerate masses of H^0 and A^0 would lead to just one zero of $\Delta\rho_{NS}^{(1)}$ at $m_{H^\pm} = m_{H^0} = m_{A^0}$.

The influence of the reducible two-loop contribution on the prediction of M_W is shown in Figure 8.1. The results are not depending on the parameters λ_5 and t_β . The different lines show the difference to the SM prediction for different non-standard corrections. The result with the one-loop non-standard correction $\Delta r_{NS}^{(1)}$ is presented by the blue dashed line. The effects of the different reducible terms in (6.39) are displayed separately. The green dotted line corresponds to the result, which includes the product between $\Delta\alpha$ and $\Delta\rho_{NS}^{(1)}$ in addition to the one-loop non-standard correction. The solid magenta line corresponds to the result with the complete reducible two-loop correction $\Delta r_{NS,red}^{(2)}$. The grey shaded area presents the measurement of M_W with the 1σ uncertainties.

All the three lines show the quadratic dependence on the mass splitting between charged and neutral Higgs states and the corrections are small for $m_{H^0} \simeq m_{H^\pm}$ or $m_{A^0} \simeq m_{H^\pm}$. The reducible contributions lead only to very small deviations from the blue dashed line. The contribution from the product of $\Delta\alpha$ and $\Delta\rho_{NS}^{(1)}$ increases with the mass difference between charged and neutral Higgs bosons. However, adding the residual reducible terms leads to a cancellation (see (6.39)), such that the solid magenta line is almost identical to the blue dashed line.

Similar cancellations take place also in the quantities $\Delta\kappa_{NS,red}^{(2)}$ and $\Delta^{(2)}\Gamma_{NS,red}^f$ (see (7.70) and (7.99)). The reducible contribution to the effective leptonic mixing or the total Z width therefore yield also only small corrections as can be seen in Figure 8.2. The left panel shows the results for s_l^2 and the right panel shows the results for Γ_Z . Again the difference to the SM prediction is presented for a variation of m_{H^\pm} around $m_{H^0} = 500$ GeV and $m_{A^0} = 550$ GeV. The prediction of Γ_Z depends also on t_β due to the non-standard one-loop corrections to the

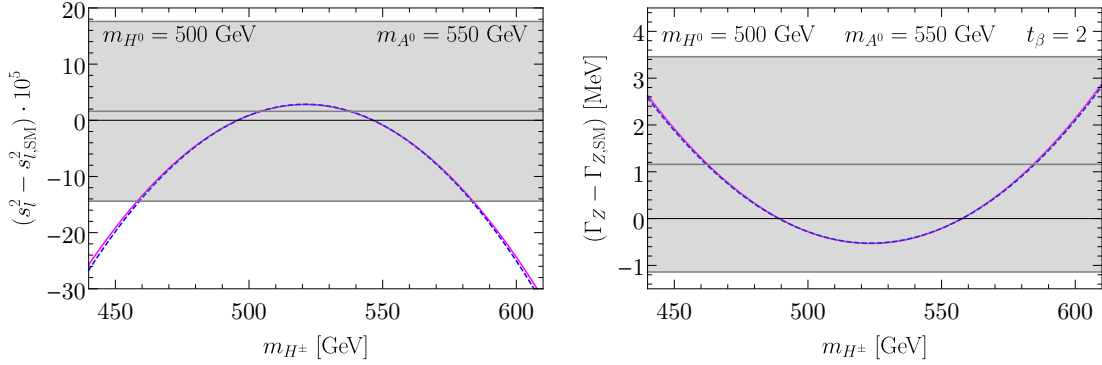


Figure 8.2: Influence of the reducible two-loop corrections on s_l^2 (left panel) and Γ_Z (right panel). The difference to the SM prediction in dependence of the charged Higgs mass is shown for the calculation including just the one-loop non-standard corrections (blue dashed lines) as well as the calculation with the additional reducible two-loop corrections (solid magenta lines). The grey shaded region displays the measurements with their 1σ uncertainties.

decay $Z \rightarrow b\bar{b}$. The results in the right panel of Figure 8.2 correspond to $t_\beta = 2$. The blue dashed lines present the prediction with the one-loop non-standard corrections. The solid magenta lines give the prediction including also the reducible two-loop corrections. The grey shaded area correspond to the measurements with their 1σ uncertainties. For both observables only small differences due to the reducible contributions are visible.

In total the investigation of the reducible corrections showed that their effect on the predictions of M_W , s_l^2 and Γ_Z is negligible, due to the cancellation between the different terms.

8.3 Results in the aligned THDM

Since the non-standard one-loop contribution $\Delta\rho_{NS}^{(1)}$ is very sensitive on the difference between the masses of the charged and neutral scalars, we investigate the effect of a variation of m_{H^\pm} for constant masses of the neutral Higgs states. In order to highlight the influence of the custodial symmetry, we select again the values $m_{H^0} = 500$ GeV and $m_{A^0} = 550$ GeV for the masses of the neutral scalars. Results for different values of t_β and λ_5 are presented in Figure 8.3. The upper row shows the prediction of M_W , the middle row shows the prediction for the effective leptonic mixing angle and the lower row shows the prediction for the total Z width. In the upper panels of the different graphs we display the deviation from the SM result for the calculation which includes either just the one-loop non-standard corrections (blue dashed line) or all the available non-standard corrections (purple solid line). The grey shaded areas display the experimental results with their 1σ uncertainties. The lower panels show the results with the individual two-loop contributions. To highlight the effect of the two-loop corrections, we subtract the result which includes just the one-loop and the reducible non-standard parts. The different lines in Figure 8.3 correspond to the calculation with different irreducible two-loop corrections. The result of the red line includes just the corrections from the non-standard top-Yukawa contribution, $\delta\rho_{t,NS}^{(2)}$, which is described in Section 5.2.3.2. The orange line includes just the non-standard correction $\delta\rho_{H,NS}^{(2)}$, which originates only from the interaction between the non-standard scalars and is described in Section 5.2.3.3. The green line includes just $\delta\rho_{H,Mix}^{(2)}$, which originates from the interaction of the non-standard scalars with the SM-like scalars and is described in Section 5.2.3.4. Note that the W boson mass used in the prediction of s_l^2 and Γ_Z is also calculated with the corresponding two-loop contribution.

The one-loop non-standard quantities $\Delta r_{NS}^{(1)}$ and $\Delta\kappa_{NS}^{(1)}$ are only dependent on the scalar masses and not on t_β and λ_5 . The one-loop corrections to the Z width has a dependence on t_β from the non-standard one-loop vertex corrections to $Z \rightarrow b\bar{b}$. The blue dashed lines show clearly that the dominant one-loop correction to the precision observables is $\Delta\rho_{NS}^{(1)}$. The resulting corrections to the SM predictions are small for $m_{H^\pm} \simeq m_{H^0}$ or $m_{H^\pm} \simeq m_{A^0}$ and grow quadratically with the mass difference between charged and neutral scalars. Since the

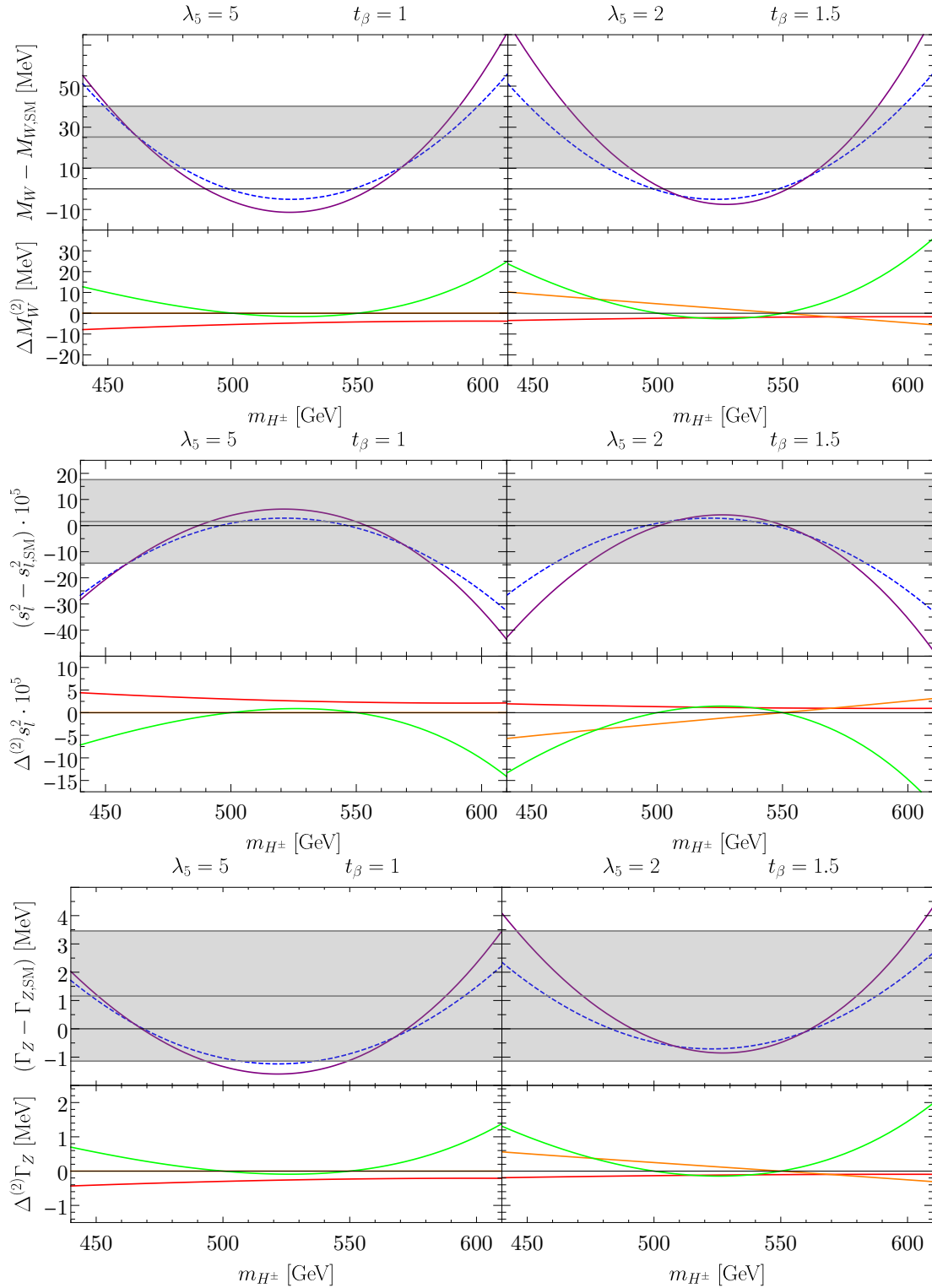


Figure 8.3: Results of M_W (upper row), s_l^2 (middle row) and Γ_Z (lower row) for a variation of m_{H^\pm} . The masses of the neutrals scalars are $m_{H^0} = 500$ GeV and $m_{A^0} = 550$ GeV. The upper panels show the difference to the SM result for the calculation with the one-loop non-standard correction (blue dashed line) and the calculation including all the available non-standard correction (purple line). The measured values with the 1σ uncertainties are indicated by the grey area. The lower panels display the effect from the different corrections of $\delta\rho_{t,\text{NS}}^{(2)}$ (red line), $\delta\rho_{H,\text{NS}}$ (orange line) or $\delta\rho_{H,\text{Mix}}^{(2)}$ (green line). In order to reveal the effect of the additional two-loop corrections the results which contain only the one-loop and two-loop reducible non-standard corrections are subtracted.

SM prediction of M_W lies slightly below the experimental 1σ limits, a moderate mass splitting between charged and neutral scalars can improve the agreement of the theoretical prediction with the measurement. For the effective leptonic mixing angle, on the other hand, increasing the mass splitting between neutral and charged Higgs states distorts the good agreement between theory and experiment. The 1σ limits of the Z width are violated only for very large mass differences in the order of 70–80 GeV. Such large mass splittings lead already to strong conflicts between the theoretical predictions and the measurements of M_W and s_l^2 . The restrictions of the mass difference between the charged and neutral scalars which is obtained from Γ_Z are therefore not competitive with the restrictions from M_W and s_l^2 .

For $t_\beta = 1$ the contribution from $\delta\rho_{H,NS}^{(2)}$ is zero. The top-Yukawa contribution $\delta\rho_{t,NS}^{(2)}$ can have a noticeable influence, especially for equal charged and neutral masses, for which both $\Delta\rho_{NS}^{(1)}$ and $\delta\rho_{H,Mix}^{(2)}$ are zero. For M_W the top-Yukawa correction can result in a shift of 5–10 MeV. Increasing t_β suppresses the top-Yukawa contribution and the non-standard contributions $\delta\rho_{H,NS}^{(2)}$ is enhanced by the quadratic dependence in t_β (see the discussion in Section 5.3). The sign of $\delta\rho_{H,NS}^{(2)}$ depends on the mass hierarchy between H^\pm and A^0 . For $m_{H^\pm} = m_{H^0}$ both the corrections from $\Delta\rho_{NS}^{(1)}$ and $\delta\rho_{H,Mix}^{(2)}$ are equal to zero, and $\delta\rho_{H,NS}^{(2)}$ gives the largest non-standard effect. The contribution $\delta\rho_{H,Mix}^{(2)}$ is not affected by the choice of t_β . Similar to the correction from $\Delta\rho_{NS}^{(1)}$ it is zero for $m_{H^\pm} = m_{H^0}$ or $m_{H^\pm} = m_{A^0}$ and grows quadratically with the mass difference between charged and neutral scalars. Larger positive values of λ_5 suppress the couplings between h^0 and the non-standard scalars and reduce the size of the correction $\delta\rho_{H,Mix}^{(2)}$.

In Figure 8.4 and Figure 8.5 we display regions in the parameter space of the THDM, which lead to an agreement between the theoretical prediction and the measurement of M_W (in the upper rows), the effective leptonic mixing angle (in the middle rows) and the total Z width (in the lower rows). Results including all the available two-loop corrections are shown for a variation of t_β and λ_5 (Figure 8.4) or m_{H^\pm} and t_β (Figure 8.5). The masses of the neutral scalars are again set to $m_{H^0} = 500$ GeV and $m_{A^0} = 550$ GeV. The values of the remaining parameters are specified above the different plots. The coloured regions illustrate the parameter configurations, which lead to a prediction in accordance with the 1σ uncertainty level of the measurements. Different shades are used to indicate the variation of the result, as specified by the legends on the right. Moreover the red-shaded areas display the excluded parameters from the constraints from vacuum stability and tree-level unitarity. In Figure 8.5 we illustrate the mass configurations for which the predictions including just the one-loop non-standard corrections are within the 1σ uncertainty level of the measurement by the grey shaded regions.

Figure 8.4 illustrates the influence of t_β and λ_5 on the precision observables in more detail. Since the one-loop contributions $\Delta r_{NS}^{(1)}$ and $\Delta\kappa_{NS}^{(1)}$ are only affected by the scalar masses, the predictions for $M_W^{(1)}$ and $\sin^2\theta_{\text{eff}}^{(1)}$ stay constant for the variation of t_β and λ_5 and their value are given in the right corner at the bottom of the different panels. As discussed before the prediction of $\Gamma_Z^{(1)}$ contains a dependence on t_β , and the value given in the bottom corner of the lower row corresponds to $t_\beta = 1$. In both scenarios $M_W^{(1)}$ and $\Gamma_Z^{(1)}$ are within the experimental 1σ limits, whereas $\sin^2\theta_{\text{eff}}^{(1)}$ lies on the lower edge of the 1σ limits (on the left side) or below the 1σ limits (on the right side). The contribution $\delta\rho_{H,NS}^{(2)}$ has the highest sensitivity on t_β and λ_5 . The corrections from this contribution are small for the regions around $t_\beta \simeq 1$ or $\lambda_5 v^2 \simeq 2m_{H^0}^2$, in which the coupling between three non-standard scalars is small (see (5.130)). Going away from this regions enhances the size of $\delta\rho_{H,NS}^{(2)}$. The two different values of m_{H^\pm} lead to different signs of $\delta\rho_{H,NS}^{(2)}$. On the left side the theoretical predictions of M_W and Γ_Z overshoot the 1σ bounds of the measurements. On the right side they fall below the 1σ limits due to the different sign of $\delta\rho_{H,NS}^{(2)}$. The result of s_l^2 on the right side runs through the 1σ limit due to the positive correction from $\delta\rho_{H,NS}^{(2)}$. For $t_\beta = 1$ the other two non-standard two-loop contribution can become important. In the right panel in the top of Figure 8.4 the enhancement of $\Delta r_{H,Mix}^{(2)}$ with λ_5 forbids the region around $t_\beta = 1$ for $\lambda_5 < 0$. In the left panel at the top, the negative top-Yukawa contribution $\Delta r_{t,NS}^{(2)}$ is large enough to compensate the enhancement of $\Delta r_{H,Mix}^{(2)}$,

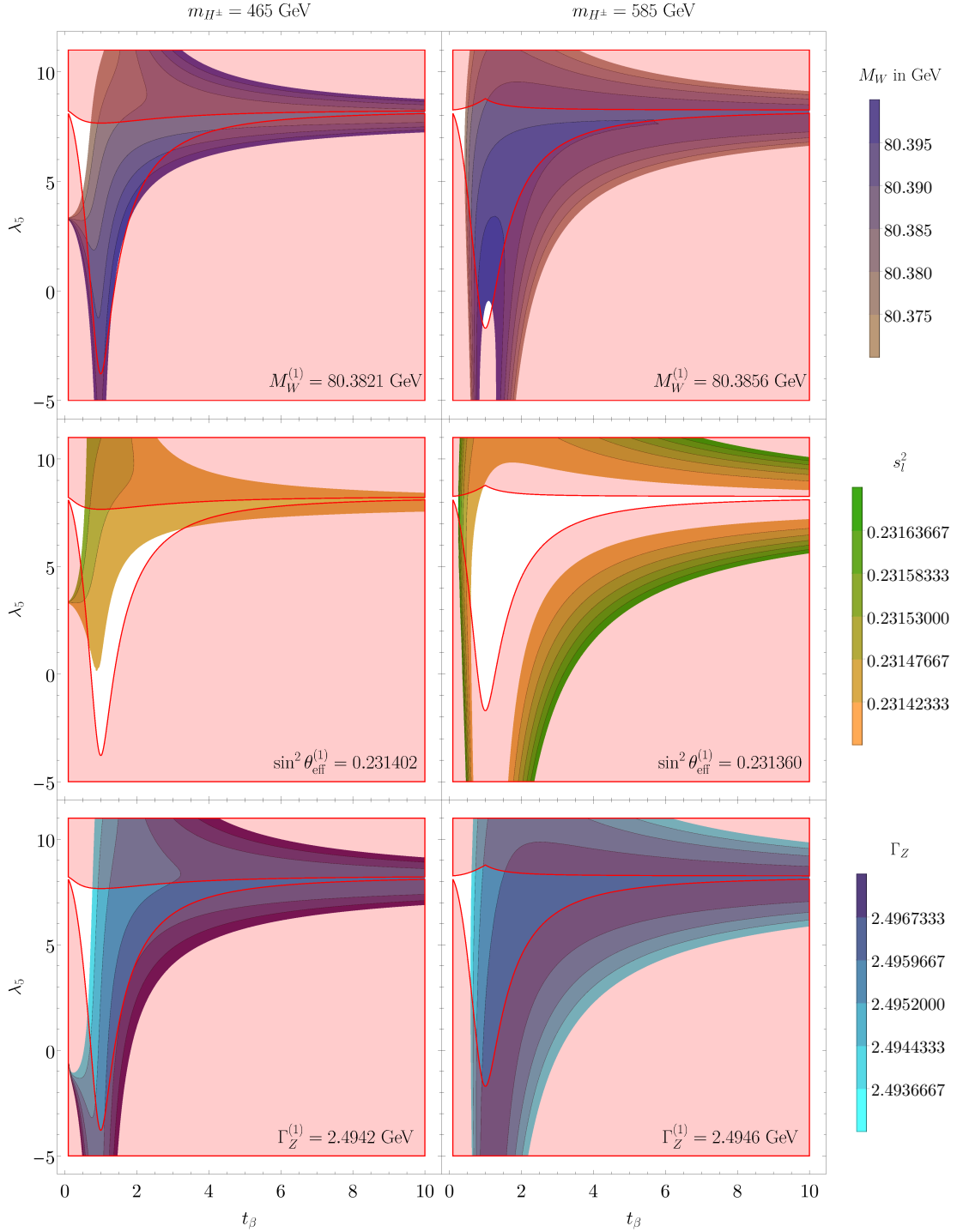


Figure 8.4: Influence of t_β and λ_5 on the theoretical prediction of M_W (upper row), s_l^2 (middle row) and Γ_Z (lower row). The coloured areas indicate parameter configurations for which the calculation with all the available non-standard corrections are within the measured 1σ limits (see the legends on the right). The value of the mass of H^\pm are given above the corresponding figures. The masses of the neutral scalars are set to $m_{H^0} = 500$ GeV and $m_{A^0} = 550$ GeV. The corresponding results of the calculation with just the non-standard one-loop correction is given in the right corner at the bottom. The red-shaded areas give the parameter regions which are excluded by vacuum stability and tree-level unitarity.

allowing also negative values of λ_5 for $t_\beta = 1$. The theoretical constraints from vacuum stability and tree-level unitarity are displayed by the red-shaded areas in Figure 8.4. The upper bound on λ_5 is coming mainly from the requirement of the stable vacuum. The lower bound on λ_5 is coming only from the unitarity of the tree-level scattering matrix. In the alignment limit this constraint on the quartic scalar couplings can be fulfilled either for $t_\beta \simeq 1$ or $\lambda_5 v^2 \simeq 2m_{H^0}^2$ (see for example the discussion in [216]). The theoretical constraints are already very restrictive and exclude a large part of the regions in which the two-loop contribution give large corrections. However with more precise measurements of the observables at the LHC and future colliders, the two-loop contributions can lead to bounds on the parameter space, which are competitive with the theoretical constraints.

Figure 8.5 repeats the analysis for a variation of m_{H^\pm} and t_β . The neutral masses are set again to $m_{H^0} = 500$ GeV and $m_{A^0} = 550$ GeV. Results are shown for $\lambda_5 = 1$ on the left side and for $\lambda_5 = 6$ on the right side. As before, the coloured areas display the regions in which the prediction with all the available non-standard corrections agrees with the experimental 1σ limit. For comparison, the grey-shaded areas illustrate the corresponding regions for $M_W^{(1)}$, $\sin^2 \theta_{\text{eff}}^{(1)}$ and $\Gamma_Z^{(1)}$. Around $t_\beta = 1$ the contribution $\delta\rho_{\text{H,NS}}^{(2)}$ is close to zero and the main deviations from the grey areas arise from $\delta\rho_{\text{H,Mix}}^{(2)}$, which gives additional corrections in the mass-splitting between charged and neutral scalars. Increasing t_β enhances $\delta\rho_{\text{H,NS}}^{(2)}$, which leads to additional deviations from the grey areas. These deviations are especially influential for $m_{H^0} = m_{H^\pm}$, where $\Delta\rho_{\text{NS}}^{(1)}$ and $\delta\rho_{\text{H,Mix}}^{(2)}$ are zero. For t_β smaller than one, the corrections from the top-Yukawa coupling become relevant. In the total Z width this coupling influences already the non-standard one-loop corrections to the decay into the b quarks. However, such small values of t_β are restricted strongly by flavour observables like the leptonic decays of B^0 mesons or the mass difference in $B^0 - \bar{B}^0$ mixing (see for example [82]).

The scenarios in the previous section are representative examples for the modification of the theoretical prediction by the two-loop corrections. Selecting other values for the scalar masses will not change the influence of t_β . For heavier scalars the results in the t_β - λ_5 -plane look similar to Figure 8.4 but for larger values of λ_5 . The regions of the grey areas in the m_{H^\pm} - t_β -plane are affected by the values of m_{H^0} and m_{A^0} , since these correspond to the zeros of $\Delta\rho_{\text{NS}}^{(1)}$ in a m_{H^\pm} variation. Especially striking are the corrections from $\delta\rho_{\text{H,NS}}^{(2)}$ in the region $m_{H^0} \simeq m_{H^\pm}$, which can be additionally increased with a larger mass difference between H^0 and A^0 . The scenario with equal masses of H^0 and H^\pm is often selected in phenomenological studies of the THDM, since $\Delta\rho_{\text{NS}}^{(1)}$ is equal to zero and large corrections to electroweak precision observables are absent at the one-loop order. We will look at a few examples which demonstrate that the two-loop contributions can become essential in such scenarios. We start with a scenario in which A^0 is light. Such a scenario can provide an explanation for the discrepancy between the SM prediction and the measurement of the anomalous magnetic moment of the muon. Afterwards we will look at two benchmark scenarios which have been worked out by the LHC Higgs Cross Section Working Group [253].

8.3.1 Results for a light pseudoscalar

A light pseudoscalar with $m_{A^0} < 125$ GeV is still not ruled out by the collider experiments. A detailed analysis of theoretical and experimental constraints on the THDM parameter space with a light pseudoscalar can be found in [77]. In the following we present the additional restrictions arising from the two-loop corrections to M_W , s_l^2 and Γ_Z . The mass of the charged scalar has to be close to one of the masses of the neutral scalars, in order to avoid large one-loop corrections to the precision observables. Since a light charged scalar is excluded by direct searches at LEP and LHC [70, 83], m_{H^\pm} has to be close to m_{H^0} and both masses are heavier than m_{A^0} . However, the mass splitting between A^0 and the other scalars cannot be arbitrary large, due to the theoretical constraints in Section 2.7. In Figure 8.6 we present results with $m_{A^0} = 60$ GeV for a variation of the charged Higgs mass around $m_{H^0} = 250$ GeV, a value which is still compatible with the restrictions from vacuum stability and tree-level unitarity. For $m_{A^0} < m_{h^0}/2$, the coupling of h^0 to two pseudoscalars has to be small to suppress the decay channel $h^0 \rightarrow A^0 A^0$ [77]. In the alignment limit this requires $\lambda_5 v^2 \simeq 2m_{A^0}^2 + m_{h^0}^2$ (see

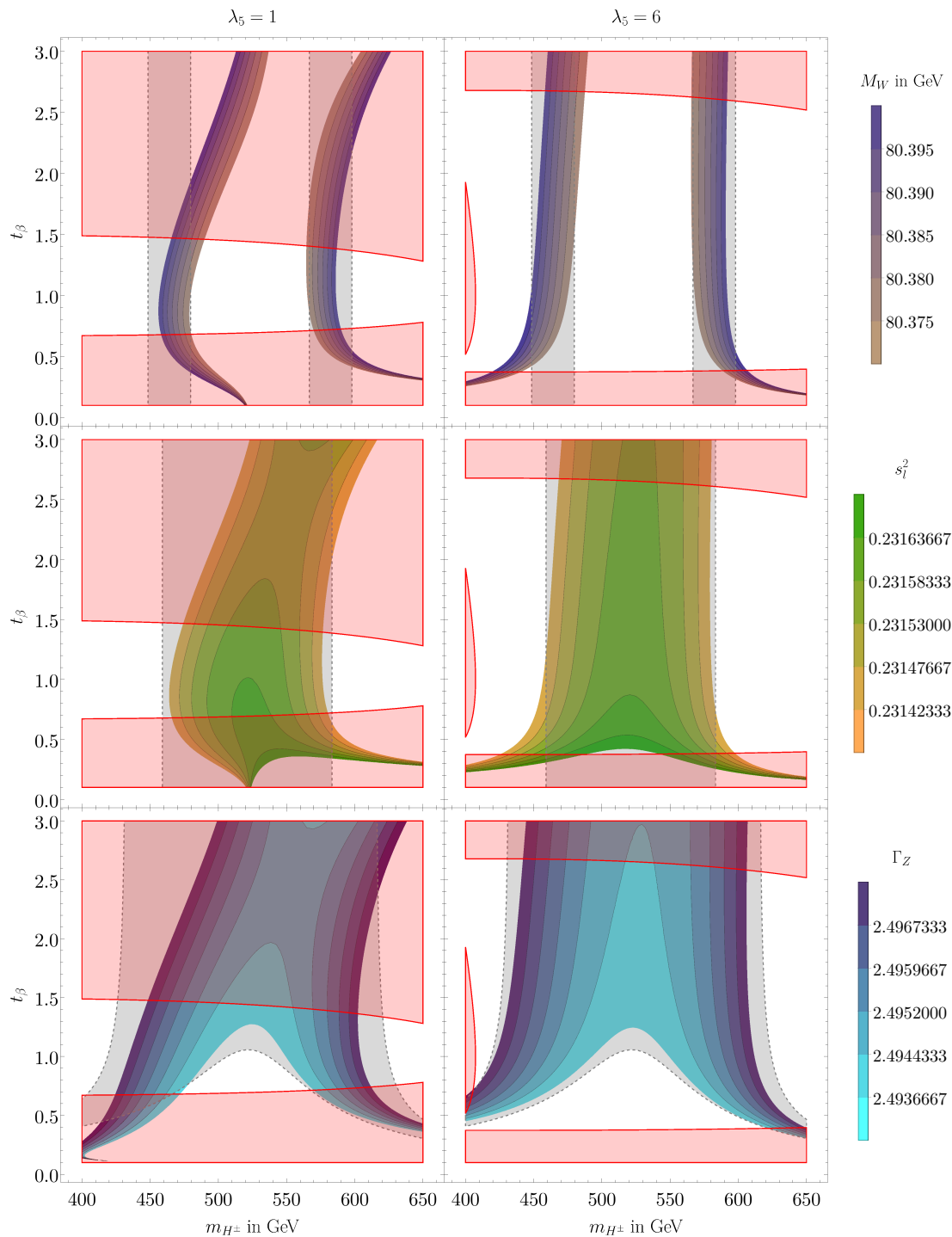


Figure 8.5: Influence of m_{H^\pm} and t_β on the theoretical prediction of M_W (upper row), s_l^2 (middle row) and Γ_Z (lower row). The coloured areas indicate parameter configurations for which the calculation with all the non-standard corrections reproduces the measured values (see the legend on the right). For the masses of the neutral scalars the values $m_{H^0} = 500$ GeV and $m_{A^0} = 550$ GeV are chosen. The value of the parameter λ_5 is given above the corresponding figures. The red-shaded areas give the parameter regions which are excluded by vacuum stability and tree-level unitarity. The grey areas display the mass configurations for which the calculation with just the one-loop non-standard contributions lies within the 1σ limits of the measured value.

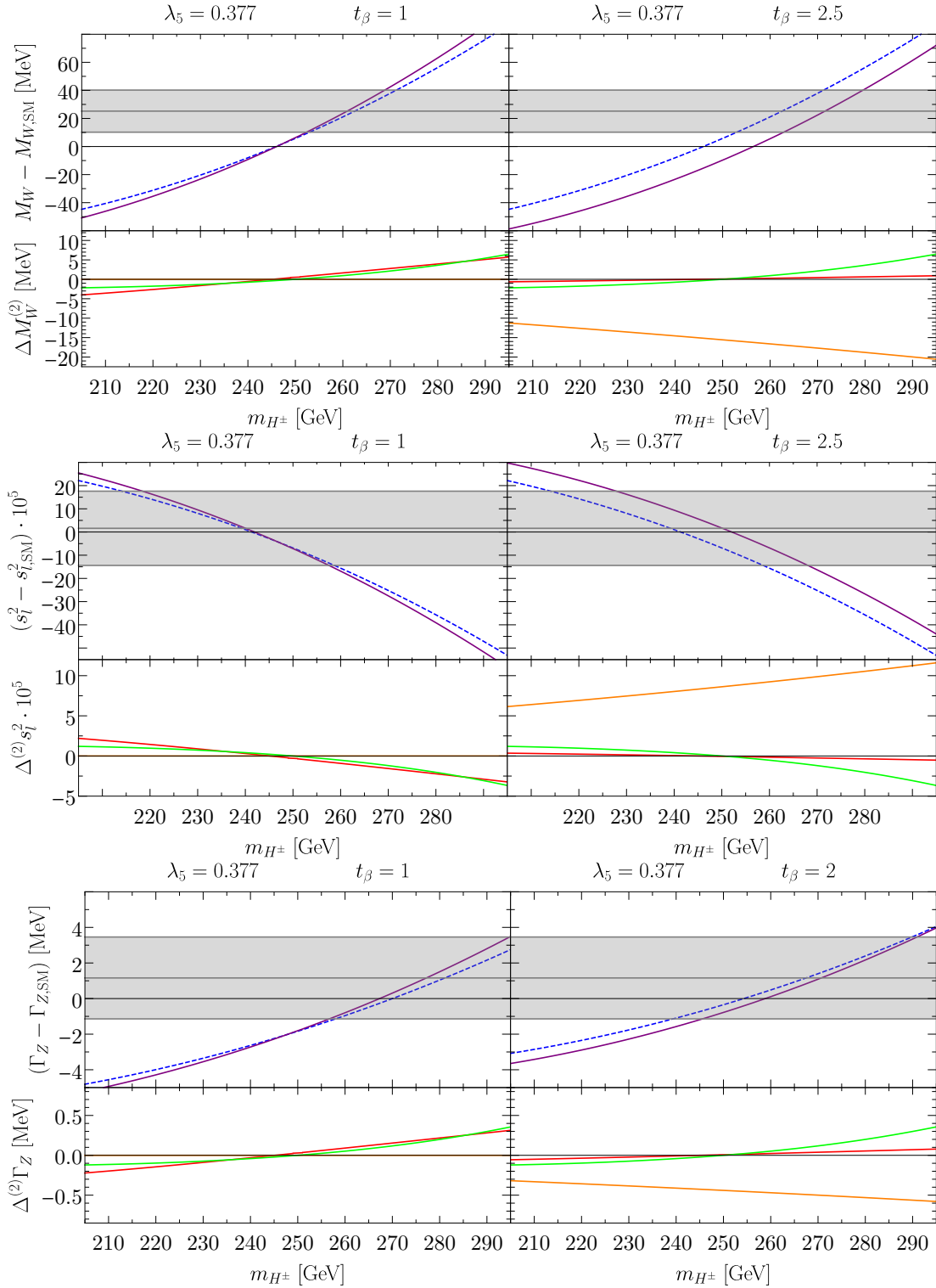


Figure 8.6: Results of M_W (upper row), s_l^2 (middle row) and Γ_Z (lower row) for a light A^0 . The masses of the neutral scalars are set to $m_{H^0} = 250$ GeV and $m_{A^0} = 60$ GeV. The upper panels show the difference to the SM result for the calculation with the one-loop non-standard correction (blue dashed line) and the calculation including all the available non-standard corrections (purple line). The measured values with the 1σ uncertainties are indicated by the grey area. The lower panels display the effect from the different corrections of $\delta\rho_{t,NS}^{(2)}$ (red line), $\delta\rho_{H,NS}^{(2)}$ (orange line) or $\delta\rho_{H,Mix}^{(2)}$ (green line). In order to reveal the effect of the additional two-loop corrections the results which contain only the one-loop and two-loop reducible non-standard corrections are subtracted.

(5.134)), resulting in

$$\lambda_5 = 0.377 \quad (8.19)$$

for $m_{A^0} = 60$ GeV. The structure of Figure 8.6 is similar to Figure 8.3. The upper panels show the difference to the SM predictions arising from the one-loop non-standard corrections (blue dashed line) or all the available non-standard corrections (purple solid line). The lower panels show the influence on $\delta\rho_{t,\text{NS}}^{(2)}$ (red line), $\delta\rho_{H,\text{NS}}^{(2)}$ (orange line) or $\delta\rho_{H,\text{Mix}}^{(2)}$ (green line). The results including just the non-standard one-loop and two-loop reducible contributions are subtracted again, in order to highlight the effect of the different irreducible corrections. On the left side t_β is equal to one and $\delta\rho_{H,\text{NS}}^{(2)}$ is zero. The remaining two-loop corrections are small for $m_{H^\pm} \simeq m_{H^0}$. The contribution $\delta\rho_{H,\text{Mix}}^{(2)}$ follows the direction of $\Delta\rho_{\text{NS}}^{(1)}$ and amplifies the dependence on the mass difference between H^0 and H^\pm . On the right side $t_\beta = 2.5$ and the corrections from $\delta\rho_{H,\text{NS}}^{(2)}$ give a notable effect, especially for $m_{H^\pm} \simeq m_{H^0}$, where the other two-loop corrections are small. For $m_{H^\pm} > m_{H^0}$, $\delta\rho_{H,\text{Mix}}^{(2)}$ starts to compensate the influence of $\delta\rho_{H,\text{NS}}^{(2)}$, since both contributions enter with an opposite sign.

Results for a light pseudoscalar with $m_{A^0} = 60$ GeV in the t_β - λ_5 -plane are presented in the left side of Figure 8.7. As before the coloured regions indicate the parameter configurations for which the predictions including all the available non-standard corrections are in good agreement with the experimental 1σ limits (as indicated by the legends on the right). For the selected values $m_{H^0} = 250$ GeV and $m_{H^\pm} = 260$ GeV of the remaining scalar masses, the results for $M_W^{(1)}$ and $\Gamma_Z^{(1)}$ are within the experimental 1σ limits, whereas the prediction of $\sin^2\theta_{\text{eff}}^{(1)}$ is slightly below the 1σ limits (see the values in the right corner at the bottom of the panels). As in Figure 8.4 the contribution $\delta\rho_{H,\text{NS}}^{(2)}$ leads to large corrections for regions away from $t_\beta \simeq 1$ and $\lambda_5 v^2 \simeq 2m_{H^0}^2$. This corrections are enhanced additionally by the larger mass difference between H^0 and A^0 .

In the right side of Figure 8.7, the analysis is repeated in the m_{H^\pm} - t_β -plane. The masses of the neutral scalars are again equal to $m_{A^0} = 60$ GeV and $m_{H^0} = 250$ GeV. The regions in which $M_W^{(1)}$, $\sin^2\theta_{\text{eff}}^{(1)}$ and $\Gamma_Z^{(1)}$ are in good agreement with their experimental 1σ limits are again indicated by the grey areas. The value of λ_5 is set again to 0.377, in order to suppress the coupling of h^0 to two pseudoscalars. For $t_\beta = 1$ only slight deviations from the grey areas by the contributions $\delta\rho_{t,\text{NS}}^{(2)}$ and $\delta\rho_{H,\text{Mix}}^{(2)}$ are visible. For larger values of t_β the enhanced influence of $\delta\rho_{H,\text{NS}}^{(2)}$ leads to large deviations.

Scenarios with a light A^0 are especially appealing with respect to the measured value of the muon anomalous magnetic moment a_μ , since Barr-Zee type two-loop diagrams can provide an explanation for the 3σ difference between the SM prediction and the measurement [254]. An improved agreement between theory and experiment consistent with several theoretical and experimental constraints require a type-X model with very large values of t_β (see [95, 255] and references therein). Usually $m_{H^\pm} = m_{H^0}$ is assumed, to fulfill the constraints from electroweak precision observables. In this scenario the contributions from $\Delta\rho_{\text{NS}}^{(1)}$ and $\delta\rho_{H,\text{Mix}}^{(2)}$ vanish. Furthermore, the top-Yukawa contribution $\delta\rho_{t,\text{NS}}^{(2)}$ is strongly suppressed for such large values of t_β . However in order to avoid large corrections from the non-standard scalar contribution $\delta\rho_{H,\text{NS}}^{(2)}$ the parameter λ_5 needs to be adjusted very close to $\lambda_5 = 2m_{H^0}^2/v^2$.

8.3.2 Results in the CP -overlap scenario

A selection of different benchmark scenarios of the THDM is given by the LHC Higgs Cross Section Working Group in [253]. Usually these require equal masses of charged and neutral Higgs states in order to fulfill the electroweak precision constraints imposed in terms of one-loop corrections to the S , T and U parameters [214, 215]. For $m_{A^0} = m_{H^\pm}$ both scalar two-loop corrections to the ρ parameter are zero. Therefore, we concentrate on scenarios with $m_{H^0} = m_{H^\pm}$ in which additional additional corrections from $\delta\rho_{H,\text{NS}}^{(2)}$ arise.

The CP -overlap scenario, labelled as the benchmark scenario $BP1_C$ in [253], is characterized by mass-degenerate Higgs-states h^0 and A^0 with $m_{h^0} = m_{A^0} = 125$ GeV [256]. The scenario is used to parameterize a CP -odd admixture to the signal rates of the 125 GeV resonance. A significant contribution of the pseudoscalar is visible for a production of the two scalars via

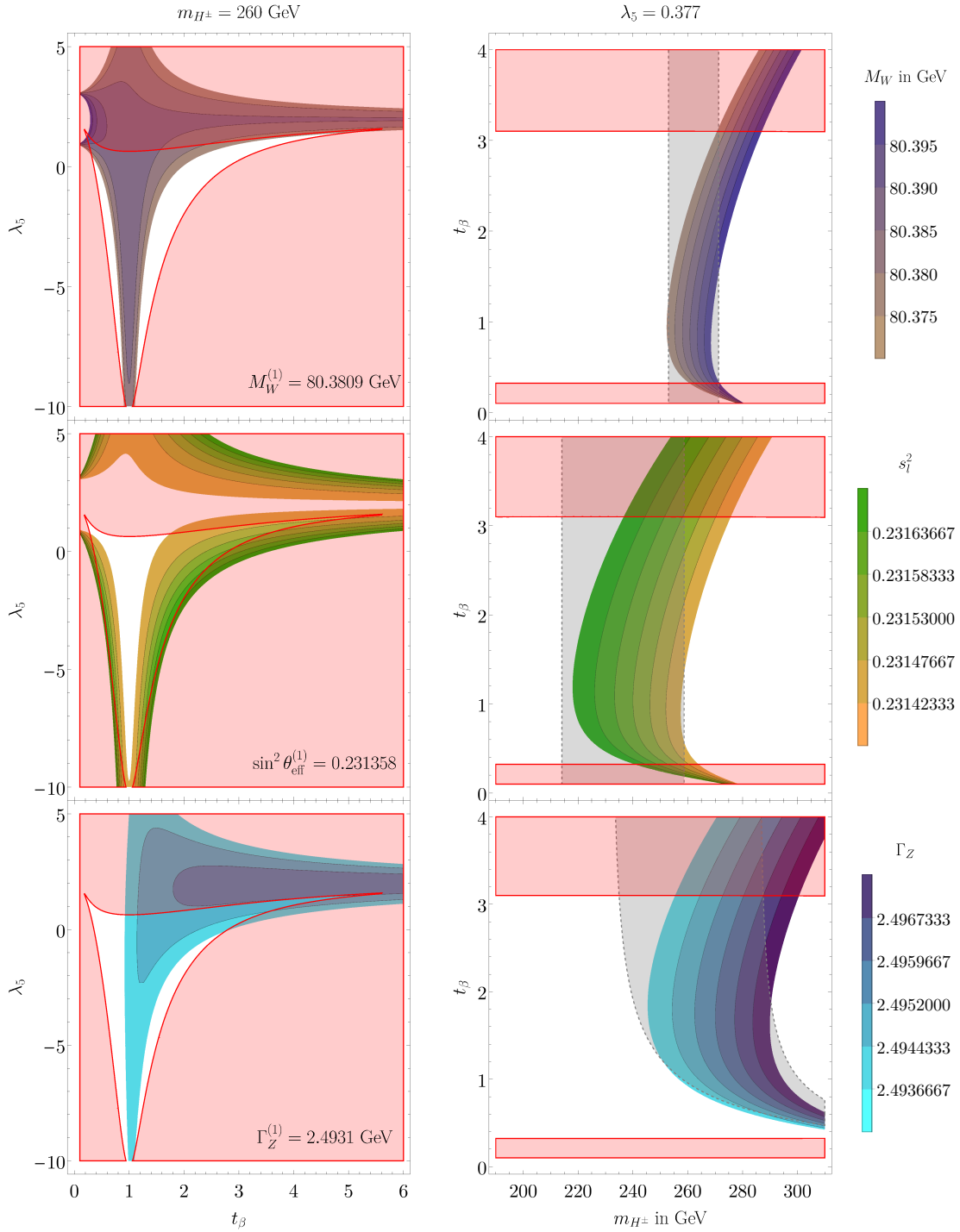


Figure 8.7: Prediction of M_W , s_l^2 and Γ_Z for a light A^0 in the t_β - λ_5 -plane (left side) and the m_{H^\pm} - t_β -plane (right side). For the masses of the neutral scalars the values $m_{H^0} = 250$ GeV and $m_{A^0} = 60$ GeV are selected. The values of the other parameters are specified above the corresponding plots. The coloured areas indicate parameter configurations for which the calculation with all the non-standard corrections agrees with the measured values (see the legends on the right). The red-shaded areas give the parameter regions which are excluded by vacuum stability and tree-level unitarity. The grey areas in the right panels display the mass configurations for which the predictions including just the one-loop non-standard contribution are within the 1σ limits of the measured values.

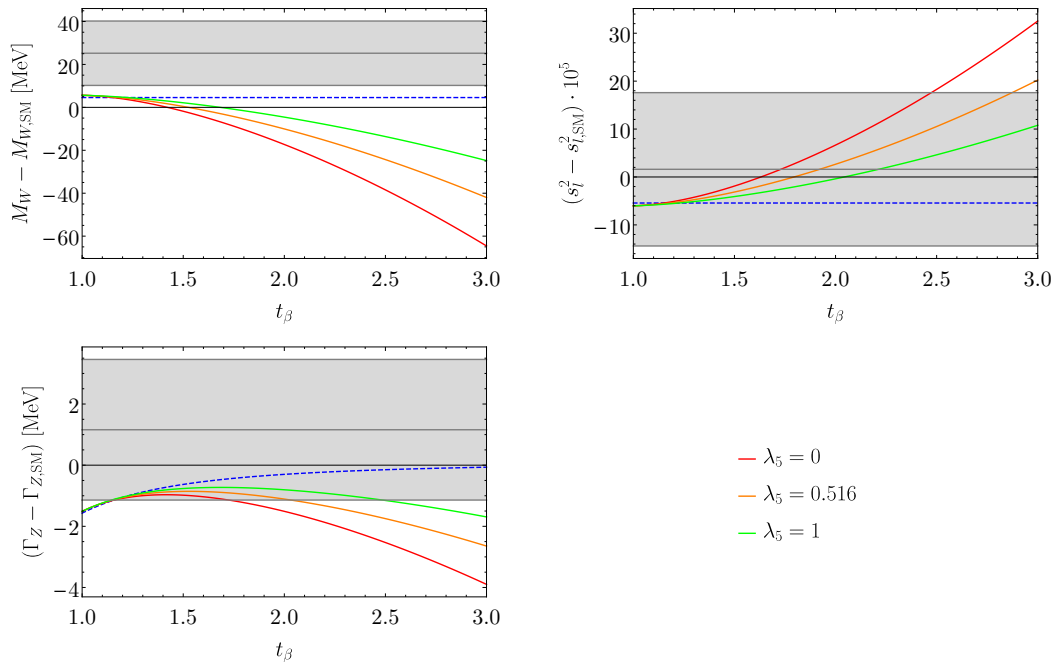


Figure 8.8: Prediction of M_W , s_l^2 and Γ_Z for a variation of t_β in the CP -overlap benchmark scenario with $m_{A^0} = m_{h^0} = 125$ GeV. The other scalar masses are fixed at 300 GeV. The different lines show the difference to the SM result. The blue dashed lines show the predictions including just the one-loop non-standard corrections. The predictions including also the available two-loop corrections are presented by the solid lines. The different colours correspond to different values of λ_5 , as indicated by the legend. The measured values with the 1σ uncertainties are displayed by the grey areas.

$gg \rightarrow h^0/A^0$ or $b\bar{b} \rightarrow h^0/A^0$, followed by the decay into τ^\pm . The predicted rate depends on t_β and differs in the various version of the THDM. In the THDM of type-I, the $b\bar{b}$ -production can be neglected since there is no enhancement of the bottom-Yukawa coupling with t_β . For gluon fusion, the production of h^0 is dominant except for small values of t_β , which enhance the coupling of the top quark to A^0 . Since the CP -odd contribution decreases with t_β , the scenario in the type-I THDM can be used to parameterize an arbitrary small CP -odd contribution to the 125 GeV signal. In the THDM of type-II, the CP -odd contribution becomes much more important due to the enhancement of the bottom-Yukawa coupling with t_β , such that the total cross section does not approach the SM value for any t_β . The magnitudes of the CP -even and CP -odd contributions are similar in the investigated range of $1 < t_\beta < 10$ and the scenario is well-suited to test the CP -properties of the 125 GeV Higgs boson in the $\tau^+\tau^-$ channel. For an elaborate discussion of the benchmark scenario see [256].

In order to obtain an SM-like h^0 , the alignment limit is chosen in the CP -overlap scenario. The masses of H^0 and H^\pm are set to be equal, but their explicit values have no influence on the decay of the overlapping states h^0 and A^0 . The remaining free parameter λ_5 has also only a minor impact on the signal rate in the $\tau\tau$ channel. In the analysis of [256] the values

$$m_{H^0} = m_{H^\pm} = 300 \text{ GeV} \quad (8.20)$$

and

$$\lambda_5 = \frac{2m_{A^0}^2}{v^2} \simeq 0.516 \quad (8.21)$$

are selected.

The electroweak precision observables M_W , s_l^2 and Γ_Z in the CP -overlap scenario are presented in Figure 8.8. The differences of the predictions to the SM results are shown for a variation of t_β . The blue dashed lines show the predictions including just the one-loop non-standard corrections. The different solid lines present the prediction including also the two-loop corrections for three values of λ_5 . The value in the middle corresponds to the one used in the analysis of [256]. We present also values below and above, since the contribution from $\delta\rho_{\text{H,NS}}^{(2)}$ is very

sensitive on λ_5 . The masses of H^0 and H^\pm are set to 300 GeV, but different masses will lead to similar results. As discussed before the results for M_W and s_l^2 are not dependent on the different versions of the THDM. For Γ_Z the model-dependence of the one-loop corrections to the decay of the Z into b quarks is negligible for such small values of t_β . The results of Figure 8.8 are therefore applicable in both versions of the CP -overlap scenario. The strong dependence of $\delta\rho_{\text{H,NS}}^{(2)}$ on t_β is clearly visible in Figure 8.8. Increasing t_β enhances the deviations from the blue-dashed lines. For the effective leptonic mixing angle, the good accordance between measurement and prediction is preserved for a wide range of t_β and the 1σ limits are violated only for large values of t_β . The situation is different for the mass of the W boson and the total Z width. The negative corrections to these two observables distort the agreement between theory and experiment already for smaller values of t_β . Especially for M_W this leads to an increasing tension between theory and experiment. A precise fine-tuning of $\lambda_5 v^2 \simeq 2m_{H^0}^2$ is required, in order to keep the two-loop corrections in this scenario small in the complete range of $1 < t_\beta < 10$ used in the CP -overlap scenario.

8.3.3 Results in the exotic decay scenario

Another set of benchmark scenarios is motivated by decays of a heavy Higgs state into light Higgses [257]. These 'exotic' decay modes require a sizable mass splitting among the different non-standard Higgs states. Once these decay modes are kinematically allowed, they will dominate over the 'conventional' decay channels of the heavy Higgs into fermions or gauge bosons. Since the current exclusion limits from direct searches rely mostly on the conventional decays, the exotic decay modes can significantly relax these limits. Furthermore the exotic decay modes provide also new discovery channels, which lead to complementary exclusion limits. First searches with the LHC data at 8 TeV were already conducted by CMS [258].

A large number of benchmark scenarios (labelled as $BP2$ in [253]) for the exotic Higgs decays are specified in [257]. In order to fulfill the one-loop constraints from the electroweak precision measurements the masses of the charged scalar and one of the neutral scalars are set equal, resulting in the two possible benchmark planes m_{A^0} vs. $m_{H^0} = m_{H^\pm}$ and m_{H^0} vs. $m_{A^0} = m_{H^\pm}$. For the remaining parameters, two scenarios are motivated by the theoretical constraints from unitarity and vacuum stability:

- Case 1: $\lambda_5 v^2 = 2m_{H^0}^2$ with $t_\beta = 1.5, 7, 30$;
- Case 2: $\lambda_5 = 0$ with $t_\beta = 1.5$.

We will focus on the scenarios with $m_{H^0} = m_{H^\pm}$, in which the two-loop contribution $\delta\rho_{\text{H,NS}}^{(2)}$ can give additional corrections to precision observables. The possible exotic decays are depending on the mass hierarchy between the non-standard scalars. For $m_{A^0} > m_{H^0} = m_{H^\pm}$ the decays $A^0 \rightarrow H^\pm W^\mp$ and $A^0 \rightarrow H^0 Z$ are allowed. For $m_{A^0} < m_{H^0} = m_{H^\pm}$ the decays $H^0 \rightarrow A^0 Z$, $H^0 \rightarrow A^0 A^0$ and $H^\pm \rightarrow A^0 W^\pm$ are open. The products of the cross sections and decay branching ratios in the benchmark planes can be found in [257]. In Figure 8.9 we present the precision observables M_W , s_l^2 and Γ_Z for a variation of m_{A^0} with $m_{H^0} = m_{H^\pm} = 350$ GeV as a representative example for these benchmark scenarios. Similar to the previous figures, the upper panels show the difference to the SM result with the one-loop and two-loop non-standard corrections. The lower panels highlight the effect of the different two-loop contributions. Results are shown for $\lambda_5 = 0$ (left side) and $\lambda_5 = 2m_{H^0}^2/v^2$ (right side). The parameter t_β is always set to $t_\beta = 1.5$. The larger values of t_β in Case 1 can be omitted, since the only surviving two-loop contribution $\delta\rho_{\text{t,NS}}^{(2)}$ scales as t_β^{-2} .

For equal masses of H^0 and H^\pm , the two-loop contribution $\delta\rho_{\text{H,Mix}}^{(2)}$ is zero. On the left side of Figure 8.9, $\delta\rho_{\text{H,NS}}^{(2)}$ is the dominant two-loop contribution. Its sign depends on the hierarchy between m_{A^0} and $m_{H^0} = m_{H^\pm}$. The dependence of $\delta\rho_{\text{H,NS}}^{(2)}$ on m_{A^0} is roughly opposite to the one of the one-loop non-standard corrections in this example. For s_l^2 and Γ_Z the resulting modifications are much smaller than the current experimental uncertainties. For M_W the correction from $\delta\rho_{\text{H,NS}}^{(2)}$ can become important for $m_{A^0} < m_{H^0}$, since the negative shift moves the prediction further away from the current measurement. This effect will be enhanced for larger masses of H^0 , since the coupling between three non-standard scalars is directly proportional to $m_{H^0}^2$ for $\lambda_5 = 0$. The region $m_{A^0} < m_{H^0} = m_{H^\pm}$ is constrained additionally from the

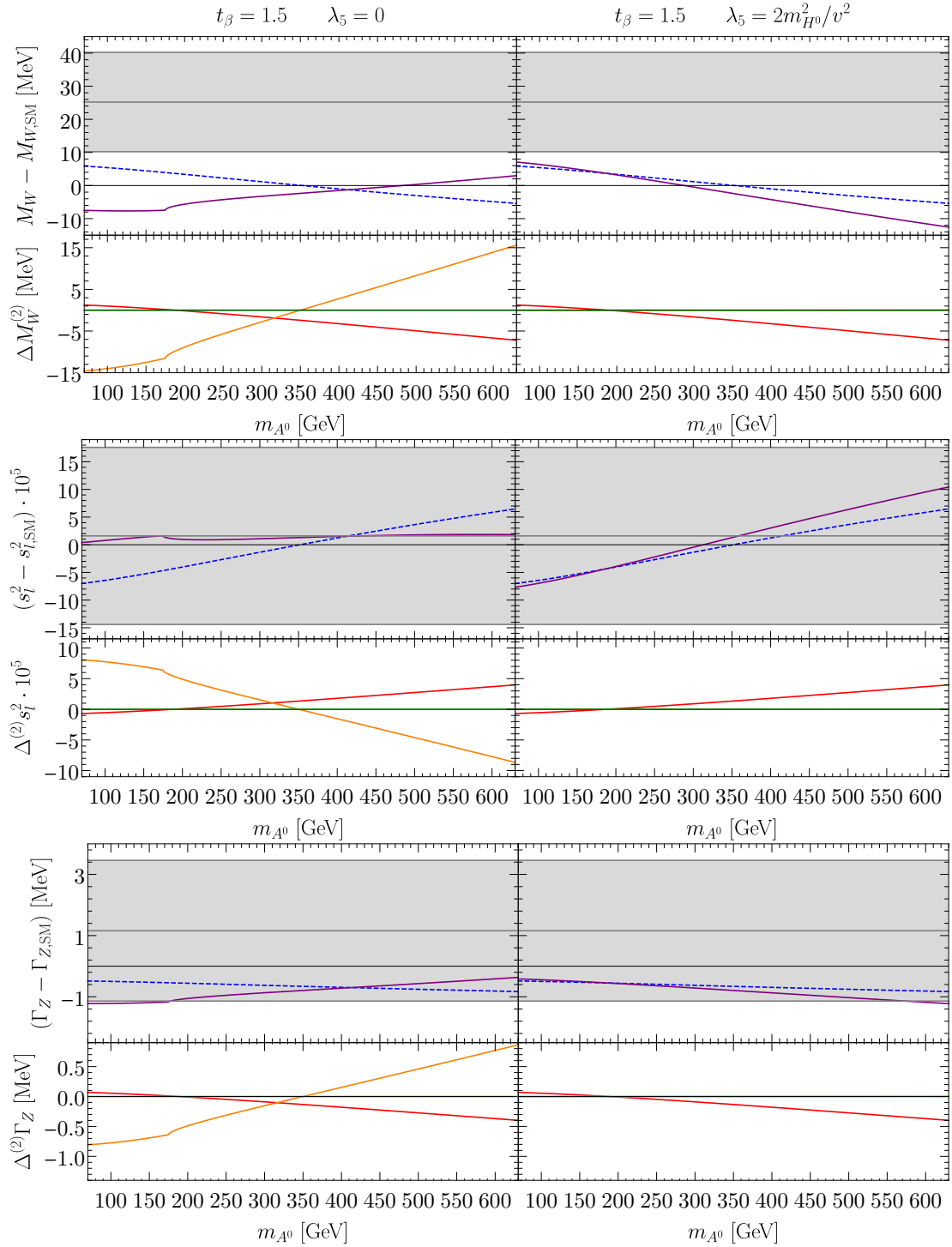


Figure 8.9: Results of M_W , s_t^2 and Γ_Z for a variation of m_{A^0} with $m_{H^0} = m_{H^\pm} = 350$ GeV and $t_\beta = 1.5$. The two sides show results for different values of λ_5 , which are given at the top of the figure. The upper panels show the difference to the SM result. Results are shown for the calculation with the one-loop non-standard correction (blue dashed line) and the calculation including all the available non-standard correction (purple line). The measured values with their 1σ uncertainties are displayed by the grey area. The lower panels display the effect from the different corrections of $\delta\rho_{t,\text{NS}}^{(2)}$ (red line), $\delta\rho_{H,\text{NS}}^{(2)}$ (orange line) or $\delta\rho_{H,\text{Mix}}^{(2)}$ (green line). In order to reveal the effect of the additional two-loop corrections the results which contain only the one-loop and two-loop reducible non-standard corrections are subtracted.

direct search of the decay $H^0 \rightarrow A^0 Z$ by CMS [258]. For $m_{H^0} = 350$ GeV only a narrow window around $m_{A^0} \simeq 100$ GeV survives, in which the corrections to M_W are substantial. If $m_{A^0} > m_{H^0} = m_{H^\pm}$, the correction from $\delta\rho_{\text{H,NS}}^{(2)}$ is positive and moves the prediction of M_W nearer to the experimental limits. However for large values of m_{A^0} the top-Yukawa contribution $\delta\rho_{\text{t,NS}}^{(2)}$ starts to become important, leading to a partial cancellation of the different two-loop contributions. This cancellation is absent on the right side of Figure 8.9, where the choice of λ_5 sets the contribution $\delta\rho_{\text{H,NS}}^{(2)}$ equal to zero. The only surviving contribution $\delta\rho_{\text{t,NS}}^{(2)}$ leads to a negative shift in the prediction of M_W . This shift will be further enhanced for smaller values of t_β , which increase the top-Yukawa contribution. In this context it is interesting to note that a THDM with $t_\beta \simeq 1$ and a heavy A^0 with $m_{H^0} \simeq m_{H^\pm} < m_{A^0}$ is favoured by the requirement of a strong electroweak phase transition in the early universe [57].

8.4 Results in the IHDM

The predictions of the precision observables in the IHDM are dominantly influenced by the mass difference between the neutral and charged Higgs states. If only the one-loop corrections $\Delta r_{\text{NS}}^{(1)}$ and $\Delta\kappa_{\text{NS}}^{(1)}$ are considered, the results for M_W and s_t^2 are equivalent to the results in the aligned THDM, which are shown in the previous section. In the prediction of the total Z width the non-standard one-loop vertex corrections to $Z \rightarrow b\bar{b}$ are absent in the IHDM. The corrections from the reducible products from $\Delta\rho_{\text{NS}}^{(1)}$ and $\Delta\alpha$ are also identical in the IHDM and in the THDM in the alignment limit. Differences arise by the irreducible corrections in the gauge-less limit, which consists of just $\delta\rho_{\text{IHDM}}^{(2)}$ in the IHDM. These corrections introduce an additional dependence on the parameter Λ_{345} , which is absent in the one-loop corrections.

Figure 8.10 shows the difference to the SM predictions for a variation of the charged Higgs mass for different values of Λ_{345} as indicated by the legend on the bottom. The results with just the non-standard one-loop corrections are displayed by the blue dashed line for comparison. The values selected for m_{H^0} and m_{A^0} are specified above the corresponding plots. In order to emphasize the dependence of the result on the mass splitting, we allow also H^\pm to be the lightest scalar in the variation of m_{H^\pm} , although in this scenario the IHDM provides no dark matter candidate. As in the previous section, the one-loop results are very sensitive on the mass difference between charged and neutral scalars. The additional two-loop corrections follow the behaviour of the one-loop result and enhance the dependence on the mass difference. The two-loop corrections can be further increased by larger values of Λ_{345} , due to the larger couplings of the non-standard scalars to h^0 .

In Figure 8.11 we investigate values in the m_{H^\pm} - Λ_{345} -plane which lead to an agreement between the theoretical prediction and the experimental 1σ limits. The corresponding regions are presented again by the coloured areas, as indicated by the legend on the right. The grey areas show the corresponding regions for $M_W^{(1)}$, $\sin\theta_{\text{eff}}^{(1)}$ and $\Gamma_Z^{(1)}$. The red-shaded areas display the theoretical constraints on the parameter space. In addition to the constraints from tree-level unitarity and vacuum stability, the constraint of the inert vacuum, as given in (2.131), is also included. Note that, in difference to the two-loop corrections to the ρ parameter, the theoretical constraints are also affected by the choice of Λ_2 . The selected value $\Lambda_2 = 1$ results in rather loose bounds. The two columns in Figure 8.11 correspond to different values of m_{H^0} and m_{A^0} , which are given above the corresponding panels. The larger mass difference between H^0 and A^0 on the right side splits up the parameter configurations preferred by s_t^2 and Γ_Z into the two distinct regions around $m_{H^\pm} \simeq m_{H^0}$ and $m_{H^\pm} \simeq m_{A^0}$, where the non-standard corrections are small. In a similar manner, the two regions preferred by M_W are narrowed for a larger separation of m_{A^0} and m_{H^0} . By comparing the coloured and the grey regions, the additional sensitivity on the mass splitting between charged and neutral scalars from the two-loop corrections is visible, which narrows the allowed regions especially for larger values of Λ_{345} .

After this more general presentation of the two-loop corrections to precision observables in the IHDM, we want to investigate these contributions in scenarios in which the IHDM agrees well with dark matter constraints. Apart from direct and indirect searches, dark matter models are mainly restricted by the measurement of the dark matter relic density

$$\Omega_{\text{DM}} h^2 = 0.1184 \pm 0.0012 \quad (8.22)$$

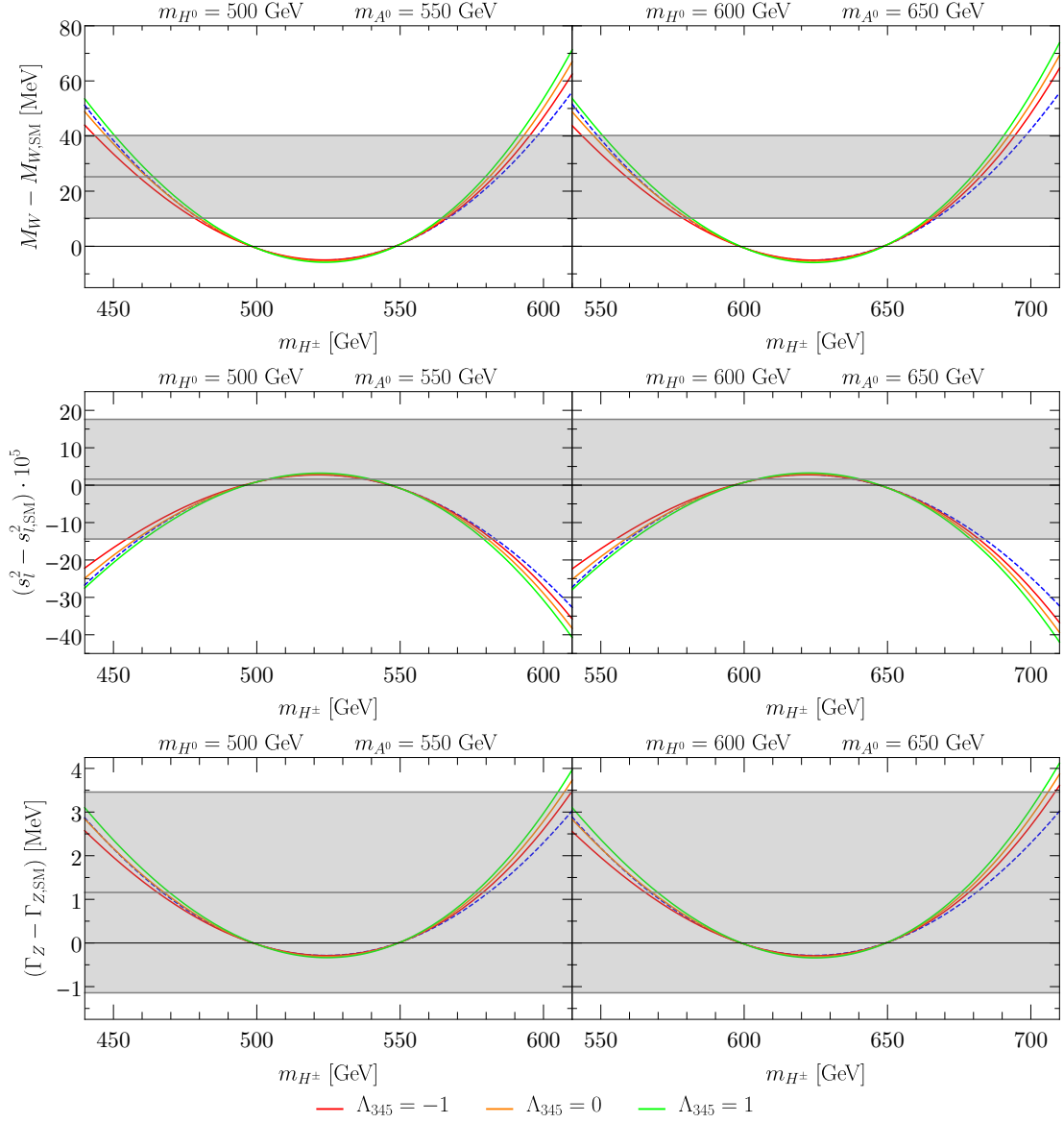


Figure 8.10: Prediction of M_W , s_l^2 and Γ_Z in the IHDM in dependence of the charged Higgs mass. The values of m_{H^0} and m_{A^0} are given above the different panels. The different solid lines represent different values of Λ_{345} , as indicated in the legend at the bottom. The blue dashed line gives the result including just the non-standard one-loop corrections for comparison. The experimental values with the 1σ uncertainties are displayed by the grey area.

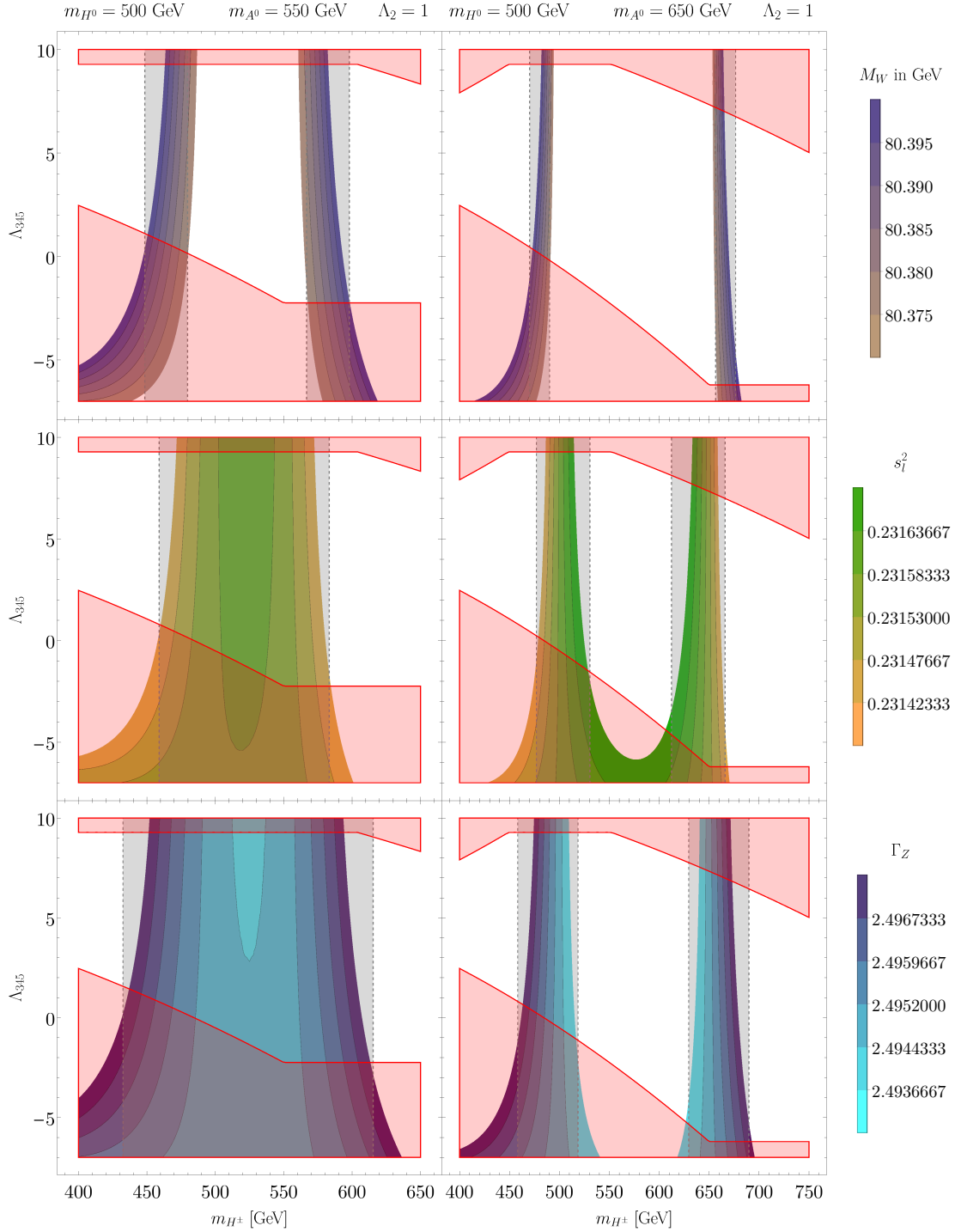


Figure 8.11: Results in the IHDM in the m_{H^\pm} - Λ_{345} -plane. The different colour-shades indicate the size of the prediction, as explained by the legend on the right. The red areas give the parameter configurations, which are excluded by the theoretical constraints in Section 2.7. The grey areas display the values of m_{H^\pm} , for which $M_W^{(1)}$, $\sin^2 \theta_{\text{eff}}^{(1)}$ and $\Gamma_Z^{(1)}$ are within the 1σ limits of the measurement.

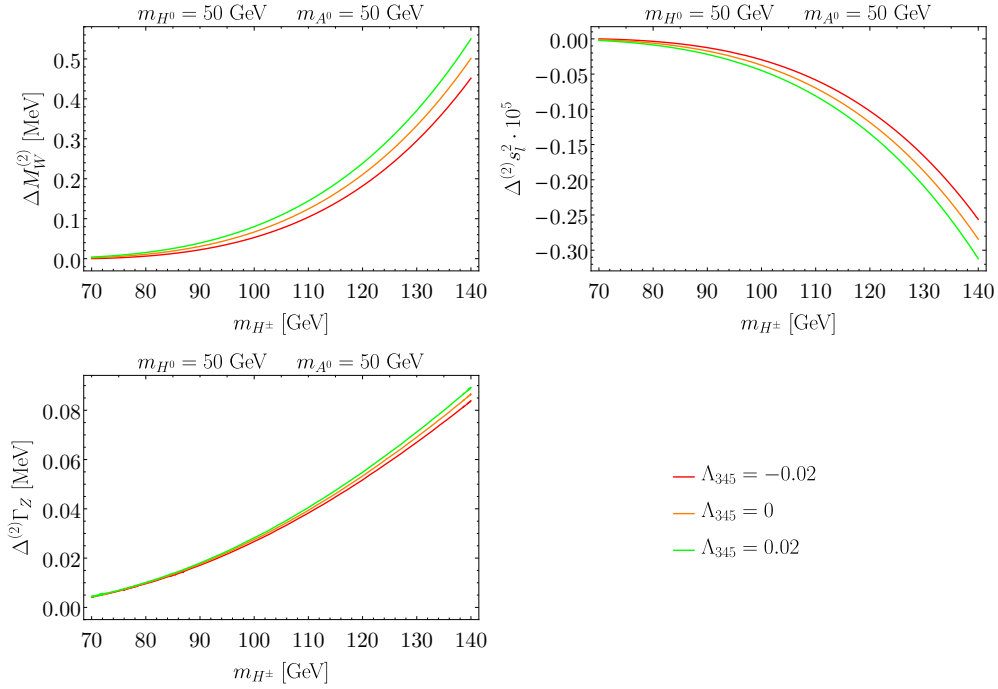


Figure 8.12: Two-loop corrections to precision observables in the IHDM for a light dark matter candidate. A variation of the charged Higgs mass is presented for mass degenerate neutral scalars with $m_{H^0} = m_{A^0} = 50$ GeV. The different solid lines correspond to different values of Λ_{345} as indicated by the legend. The results of the precision observables which include only the non-standard one-loop contributions and the non-standard two-loop reducible contributions are subtracted to highlight the difference arising from the irreducible two-loop correction $\delta\rho_{\text{IHDM}}^{(2)}$.

from Planck [259, 260]. Following the discussion in [66], we focus on two mass regions

$$45 \text{ GeV} \lesssim m_{H^0} \lesssim 62.5 \text{ GeV} \quad (8.23)$$

and

$$62.5 \text{ GeV} \lesssim m_{H^0} \lesssim 80 \text{ GeV}, \quad (8.24)$$

in which the stable scalar H^0 can contribute substantially to the relic density, without leading to dark matter overabundance. The region below $m_{H^0} = 45$ GeV is excluded by an interplay of the relic density measurement with LEP and LHC limits. For a mass of the dark matter candidate which is larger than M_W , the decay channel $H^0 H^0 \rightarrow W^+ W^-$ is open and the relic density drops below the lower bound of the Planck limit. This is of course no hard exclusion limit, since different sources of dark matter could also contribute to the relic density. Nevertheless we will concentrate on the parameter regions in which the IHDM provides an essential part of the relic density. Another possible region in this respect are large dark matter masses with $m_{H^0} \gtrsim 490$ GeV, which however requires a large mass degeneracy between the inert scalars, to avoid the suppression of the relic density by the annihilation into longitudinal vector bosons. Therefore no large corrections to the ρ parameters can be expected in this scenario. For a more detailed analysis of the different limits on the IHDM see [66] and references therein.

As an example for the first scenario, results of the precision observables in the IHDM are presented in Figure 8.12 for $m_{H^0} = m_{A^0} = 50$ GeV. Since $m_{H^0} < \frac{m_{h^0}}{2}$, annihilation of the DM candidate into the scalar h^0 is impossible. The only possibility to suppress the relic density below the upper experimental limit is the coannihilation process $H^0 + A^0 \rightarrow Z$, which requires almost mass degenerate scalars H^0 and A^0 . The results are presented for a variation of the charged Higgs mass, starting at the lower bound $m_{H^\pm} = 70$ GeV, which was obtained in [261] by a reinterpretation of LEP limits. The size of Λ_{345} is constrained in this scenario by the LHC limits on the invisible Higgs decay, since the decay $h^0 \rightarrow H^0 H^0$ is kinematically open. The analysis in [66], which takes into account the ATLAS search for an invisible Higgs decay [262], leads to approximately $|\Lambda_{345}| \lesssim 0.02$. For such small values

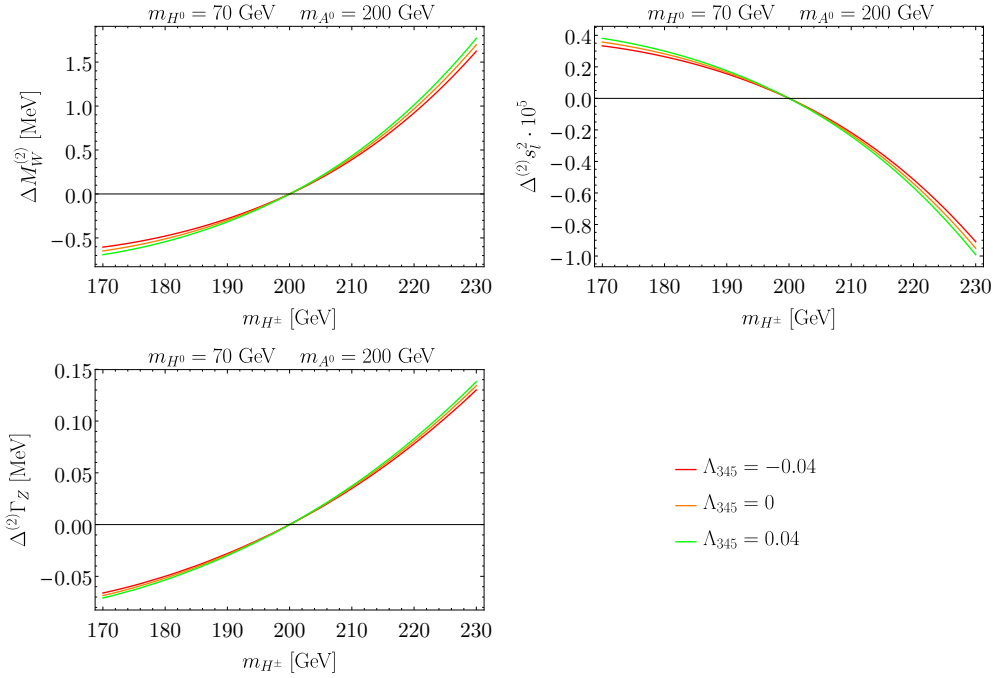


Figure 8.13: Precision observables in the IHDM for $m_{H^0} = 70$ GeV and $m_{A^0} = 200$ GeV. Results are presented for a variation of the charged Higgs mass. The different solid lines correspond to different values of Λ_{345} as indicated by the legend. The results of the precision observables which include only the non-standard one-loop contributions and the non-standard two-loop reducible contributions are subtracted to highlight the difference arising from the irreducible two-loop correction $\delta\rho_{\text{IHDM}}^{(2)}$.

the effect of the two-loop corrections are tiny, as can be seen in Figure 8.12. The solid lines present the non-standard corrections to M_W , s_l^2 and Γ_Z which arise only from the irreducible two-loop contribution $\delta\rho_{\text{IHDM}}^{(2)}$. The different colours correspond to different values of Λ_{345} , as indicated by the legend. The resulting corrections to the precision observables are negligible in comparison to the experimental uncertainties.

For the scenario with $62.5 \text{ GeV} \lesssim m_{H^0} \lesssim 80 \text{ GeV}$, results with $m_{H^0} = 70$ GeV are presented in Figure 8.13. In contrast to the previous scenario, the annihilation of the dark matter candidate into h^0 is sufficient to suppress the relic density and the masses of A^0 and H^0 do not need to be degenerate. The examples in Figure 8.13 correspond to $m_{A^0} = 200$ GeV and the charged Higgs mass is varied around this value. As discussed before, the results vanish for $m_{H^\pm} = m_{A^0}$. The increase with the mass-splitting between H^\pm and A^0 is enhanced if the scalar A^0 is much heavier than H^0 . Since the decay $h^0 \rightarrow H^0 H^0$ is kinematically forbidden, the LHC limits allow a broader range for Λ_{345} . Additional restrictions arise however from direct dark matter searches. As discussed in [66], limits from LUX [263] lead to approximately $|\Lambda_{345}| \lesssim 0.04$. The different solid lines correspond to different values within this range, as indicated by the legend. As before, only the non-standard corrections to M_W , s_l^2 and Γ_Z which arise from the irreducible contribution $\delta\rho_{\text{IHDM}}^{(2)}$ are presented. The remaining corrections are a little bit larger than in the previous scenario but still not comparable to the experimental uncertainties. In total the analysis showed that for very small values of Λ_{345} , which are preferred by astrophysical constraints, the scalar two-loop corrections can be neglected in the calculation of precision observables.

Chapter 9

Conclusions

The indirect restriction of free parameters via the comparison of precisely measured observables with accurate theoretical predictions played an important role in the validation of the electroweak Standard Model (SM). At higher-orders, also those parameters that are not present at the tree-level enter through the quantum corrections. After the discovery of a scalar particle at the LHC all the input parameters of the SM are fixed, such that these precision observables offer now an excellent possibility to constrain also new physic scenarios. The main subject of this thesis is the improvement of theoretical prediction in extensions of the SM by a second Higgs doublet, known as Two-Higgs-Doublet Models (THDM). Most of the previous calculations of the non-standard contributions in these models are done at the one-loop order only. The dominant correction is related to the one-loop non-standard contribution to the ρ parameter, which is very sensitive on the mass difference between charged and neutral scalars. Consequently, large differences between the masses of charged and neutral scalars yield substantial corrections to the electroweak precision observables. In order to achieve a more accurate prediction, the leading two-loop corrections to the ρ parameter in the THDM and their influence on electroweak precision observables are presented in this work.

To be more specific, the top-Yukawa corrections and the corrections from the scalar self-interaction are calculated in the CP -conserving THDM. Since the Higgs-signal measurements by the ATLAS and CMS experiments are in good agreement with the predictions in the SM, the alignment limit is applied in which the lighter of the CP -even scalars is identified with the scalar resonance observed at the LHC with couplings identical to ones of the Higgs boson in the SM. The leading contributions are obtained in the top-Yukawa approximation, in which all the fermions except the top-quark are considered massless, and in the gauge-less limit, in which the gauge couplings are neglected by setting the masses of the gauge bosons to zero, but keeping their ratio in the electroweak mixing angle constant. In the special case of the Inert-Higgs-Doublet Model (IHDM) the non-standard top-Yukawa corrections are absent and the only non-standard two-loop corrections to the ρ parameter in the gauge-less limit are following from the scalar self-interaction.

The results for the two-loop corrections to the ρ parameter are incorporated in Fortran routines, which allow a fast numerical evaluation of the model predictions. As a by-product of the calculation, most of the vertex counterterms are now incorporated in the THDM modelfile of `FeynArts`. The details of the renormalization procedure can be found in this work.

The non-standard contribution to the ρ parameter from the coupling of the non-standard scalars to the heavy quarks has been calculated with and without the contribution from the bottom-Yukawa coupling. An explicit comparison has shown that the corrections from the bottom-Yukawa coupling are only important in a THDM of type-II or type-Y for very large values of t_β . Such large values of t_β are however strongly restricted by unitarity constraints and flavour observables. If the mass of the bottom quark is set to zero this contribution is universal for the different versions of the THDM (type-I, type-II, type-X and type-Y). The remaining top-Yukawa correction scales as t_β^{-2} , and can be enhanced by large mass differences between the non-standard scalars.

The scalar self-interaction gives rise to two distinct finite contributions to $\Delta\rho$ at the two-loop level. One contains only the non-standard scalars as virtual particles and is labelled as $\delta\rho_{\text{H,NS}}^{(2)}$. The second contribution contains in addition also the SM-like scalar, as well as the Goldstone

bosons. It is labelled as $\delta\rho_{\text{H,Mix}}^{(2)}$.

The characteristics of the contribution $\delta\rho_{\text{H,Mix}}^{(2)}$ are very similar to those of the non-standard one-loop correction to $\Delta\rho$. It grows with the mass difference between charged and neutral scalars and is zero for $m_{H^0} = m_{H^\pm}$ or $m_{A^0} = m_{H^\pm}$. For these mass settings a custodial symmetry is restored in the Higgs potential, which protects the ρ parameter from large corrections. Furthermore this contribution contains an additional dependence on the parameter λ_5 . This free parameter of the Higgs potential is absent in the one-loop corrections and enters in the couplings between the SM-like Higgs boson to the non-standard scalars. It can give an additional enhancement in the two-loop correction $\delta\rho_{\text{H,Mix}}^{(2)}$.

The pure non-standard scalar contribution $\delta\rho_{\text{H,NS}}^{(2)}$ introduces a lot of distinct new features, which distinguish it from the one-loop correction. It contains the coupling between three non-standard scalars, which is very sensitive on the parameters t_β and λ_5 and vanishes for $t_\beta = 1$ or $\lambda_5 v^2 = 2m_{H^0}^2$. This coupling can enhance the contribution substantially. Furthermore it breaks the custodial symmetry which is responsible for the vanishing one-loop contribution at $m_{H^0} = m_{H^\pm}$ such that the additional two-loop contribution $\delta\rho_{\text{H,NS}}^{(2)}$ can become very important for this mass setting. For $m_{A^0} = m_{H^\pm}$ also the two-loop contribution $\delta\rho_{\text{H,NS}}^{(2)}$ vanishes, since all the participating couplings respect the corresponding custodial symmetry.

In the IHDM the non-standard scalars do not couple to the fermions and therefore no additional non-standard top-Yukawa corrections are present. The only non-standard two-loop correction in the IHDM originates from the scalar self-interaction and resembles the contribution $\delta\rho_{\text{H,Mix}}^{(2)}$ in the aligned THDM: it grows with the mass difference between charged and neutral scalars and is zero for $m_{H^0} = m_{H^\pm}$ or $m_{A^0} = m_{H^\pm}$. It can be additionally enhanced by Λ_{345} , a combination of the parameters in the Higgs potential which controls the coupling of the SM-like Higgs to the dark matter candidate in the IHDM.

The loop corrections to the ρ parameter are important entries for the calculation of electroweak precision observables. The second part of this thesis describes the incorporation of the two-loop contributions into prominent examples for such observables namely the mass of the W boson, the effective leptonic mixing angle and the total width of the Z boson. These non-standard corrections are combined with the complete one-loop corrections and the known higher-order contributions from the SM. The results are encoded in Fortran routines.

For the THDM in the alignment limit the investigation of representative parameter settings has shown that the various two-loop contributions can lead to significant deviations from the one-loop predictions. The sensitivity on the mass splitting between charged and neutral scalars, which is already present in the one-loop correction, is amplified further by the contribution $\delta\rho_{\text{H,Mix}}^{(2)}$. Moreover, the scalar two-loop corrections introduce additional dependencies on the parameters λ_5 and t_β , which are absent at the one-loop order. This can be used to obtain improved constraints on the Higgs potential of the THDM. Especially interesting is the case $m_{H^0} = m_{H^\pm}$. This mass configuration is often assumed in phenomenological studies in order to fulfill the constraints from electroweak precision observables at the one-loop order. However, the non-standard scalar two-loop corrections can give a non-vanishing contribution to the precision observables also for $m_{H^0} = m_{H^\pm}$. Various examples of such benchmark scenarios have demonstrated that the two-loop correction can result in an increased tension between the prediction and the measurement.

In the IHDM the main feature from the additional two-loop correction to the precision observables is an increased sensitivity on the mass difference between charged and neutral scalars. Furthermore a new dependence on the parameter Λ_{345} is introduced in the prediction of the precision observables. However this parameter is already strongly constrained by direct dark matter searches and collider limits. Analysing the precision observables in two mass ranges motivated from astrophysical constraints has shown that the two-loop corrections are negligible for small values of $|\Lambda_{345}|$, which are required by the constraints from direct dark matter searches and LHC limits.

If future measurements of the precision observables reduce the experimental uncertainties further the constraints on the parameters become more restrictive. For the mass of the W boson, a more accurate experimental determination can be expected in foreseeable future at the LHC. A first measurement with the 7 TeV data by ATLAS [264] is similar in precision to the measurements performed at Tevatron. A significant improvement in the measurement of the effective leptonic mixing angle and the total Z width could be obtained by a future linear

e^+e^- collider running at the Z pole [265–267].

A higher accuracy at the experimental side requires also more precise theoretical predictions. For the CP -conserving THDM in the alignment limit, the two-loop corrections to the ρ parameter provide the first contributions beyond the one-loop order. A further improvement of the prediction is of course desirable. A relaxation of the alignment limit will probably lead to no significant modifications, since the Higgs-signal measurements allow only small deviations. More interesting are additional corrections from the gauge-couplings. A complete two-loop calculation of the non-standard corrections to electroweak precision observables requires additional numerical integration and is a much more challenging and time-consuming task. However with the recent improvements in the computation of higher-order corrections also these calculations are in principle feasible.

The calculation of electroweak precision observables provides an important test for the validity of the THDM. Its interplay with theoretical constraints, flavour observables and direct searches, can severely limit this model, especially if the LHC would find evidence for additional scalars in the future.

Appendix A

Feynman Rules of the THDM

This appendix gives the Feynman rules of the THDM in the 't Hooft-Feynman gauge. For the propagator counterterms and the vertices of the scalars with the gauge bosons or fermions the counterterms at the one-loop order are included. The vertices of the scalar self-interaction are given for the THDM with a soft Z_2 violation in the alignment limit as well as for the IHDM. In the vertices all the momenta are considered as incoming.

Propagator counterterms of the gauge bosons

$$\begin{array}{c} p \\ \text{~~~~~} \\ V_{1,\mu} \text{~~~~~} \times \text{~~~~~} p \\ \text{~~~~~} \\ V_{2,\nu} \end{array} = -ig_{\mu\nu} [C_1 p^2 - C_2]$$

$V_1 V_2$	C_1	C_2
$W^\pm W^\pm$	δZ_W	$M_W^2 \delta Z_W + \delta M_W^2$
ZZ	δZ_{ZZ}	$M_Z^2 \delta Z_{ZZ} + \delta M_Z^2$
AZ	$\frac{1}{2} \delta Z_{\gamma Z} + \frac{1}{2} \delta Z_{ZA}$	$M_Z^2 \frac{1}{2} \delta Z_{Z\gamma}$
AA	$\delta Z_{\gamma\gamma}$	0

Propagator counterterms of the scalars:

$$\begin{array}{c} p \\ \text{-----} \\ S_1 \text{-----} \times \text{-----} p \\ \text{-----} \\ S_2 \end{array} = i [C_1 p^2 - C_2]$$

$S_1 S_2$	C_1	C_2
$h^0 h^0$	δZ_{h^0}	$\delta m_{h^0}^2 + m_{h^0}^2 \delta Z_{h^0}$
$H^0 H^0$	δZ_{H^0}	$\delta m_{H^0}^2 + m_{H^0}^2 \delta Z_{H^0}$
$A^0 A^0$	δZ_{A^0}	$\delta m_{A^0}^2 + m_{A^0}^2 \delta Z_{A^0}$
$H^\pm H^\pm$	δZ_{H^\pm}	$\delta m_{H^\pm}^2 + m_{H^\pm}^2 \delta Z_{H^\pm}$
$G^0 G^0$	δZ_{G^0}	$\delta m_{G^0}^2$
$G^\pm G^\pm$	δZ_{G^\pm}	$\delta m_{G^\pm}^2$
$h^0 H^0$	$\delta Z_{h^0 H^0}$	$\delta m_{h^0 H^0}^2 + \frac{1}{2} (m_{h^0}^2 + m_{H^0}^2) \delta Z_{h^0 H^0}$
$A^0 G^0$	$\delta Z_{A^0 G^0}$	$\delta m_{A^0 G^0}^2 + \frac{1}{2} m_{A^0}^2 \delta Z_{A^0 G^0}$
$H^\pm G^\pm$	$\delta Z_{G^\pm H^\pm}$	$\delta m_{G^\pm H^\pm}^2 + \frac{1}{2} m_{H^\pm}^2 \delta Z_{G^\pm H^\pm}$

Propagator counterterms of the fermions



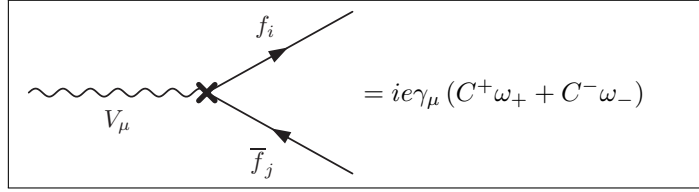
$$f \xrightarrow{p} \text{X} \xrightarrow{p} f = i [\not{p}\omega_- C_L + \not{p}\omega_+ C_R - C_S]$$

$$C_L = \delta Z_f^L$$

$$C_R = \delta Z_f^R$$

$$C_S = \left(\delta m_f + \frac{1}{2} (\delta Z_f^L + \delta Z_f^R) \right)$$

Feynman rules for the interaction between gauge bosons and fermions



$$= ie\gamma_\mu (C^+ \omega_+ + C^- \omega_-)$$

$$\gamma f \bar{f} : \begin{cases} C^- = -Q_f \left(1 + \delta Z_e + \frac{1}{2} \delta Z_{\gamma\gamma} + \delta Z_f^L \right) + g_f^- \frac{\delta Z_{Z\gamma}}{2} \\ C^+ = -Q_f \left(1 + \delta Z_e + \frac{1}{2} \delta Z_{\gamma\gamma} + \delta Z_f^R \right) + g_f^+ \frac{\delta Z_{Z\gamma}}{2} \end{cases}$$

$$Z f \bar{f} : \begin{cases} C^- = g_f^- \left(1 + \delta Z_e + \frac{\delta g_f^-}{g_f^-} + \frac{1}{2} \delta Z_{ZZ} + \delta Z_f^L \right) - \frac{1}{2} Q_f \delta Z_{\gamma Z} \\ C^+ = g_f^- \left(1 + \delta Z_e + \frac{\delta g_f^+}{g_f^+} + \frac{1}{2} \delta Z_{ZZ} + \delta Z_f^R \right) - \frac{1}{2} Q_f \delta Z_{\gamma Z} \end{cases}$$

$$W^+ d \bar{u} : \begin{cases} C^- = -\frac{1}{\sqrt{2}s_W} \left(1 + \delta Z_e + \frac{1}{2} \delta Z_W - 2 \frac{\delta s_W^2}{s_W^2} + \frac{1}{2} \delta Z_u^L + \frac{1}{2} \delta Z_d^L \right) \\ C^+ = 0 \end{cases}$$

$$W^- u \bar{d} : \begin{cases} C^- = -\frac{1}{\sqrt{2}s_W} \left(1 + \delta Z_e + \frac{1}{2} \delta Z_W - 2 \frac{\delta s_W^2}{s_W^2} + \frac{1}{2} \delta Z_u^L + \frac{1}{2} \delta Z_d^L \right) \\ C^+ = 0 \end{cases}$$

$$W^+ \nu \bar{l} : \begin{cases} C^- = -\frac{1}{\sqrt{2}s_W} \left(1 + \delta Z_e + \frac{1}{2} \delta Z_W - 2 \frac{\delta s_W^2}{s_W^2} + \frac{1}{2} \delta Z_\nu^L + \frac{1}{2} \delta Z_l^L \right) \\ C^+ = 0 \end{cases}$$

$$W^- \nu \bar{l} : \begin{cases} C^- = -\frac{1}{\sqrt{2}s_W} \left(1 + \delta Z_e + \frac{1}{2} \delta Z_W - 2 \frac{\delta s_W^2}{s_W^2} + \frac{1}{2} \delta Z_\nu^L + \frac{1}{2} \delta Z_l^L \right) \\ C^+ = 0 \end{cases}$$

In the coupling of the fermions to the Z boson the abbreviations

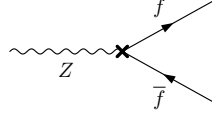
$$g_f^+ = \frac{s_W}{c_W} Q_f, \quad \delta g_f^+ = g_f^+ \frac{2}{c_W^2} \frac{\delta s_W^2}{s_W^2}, \quad (\text{A.1})$$

and

$$g_f^- = -\frac{(I_3^f - s_W^2 Q_f)}{s_W c_W}, \quad \delta g_f^- = -\frac{I_3^f}{s_W c_W} \frac{s_W^2 - c_W^2}{c_W^2} \frac{\delta s_W^2}{s_W^2} + \delta g_f^+. \quad (\text{A.2})$$

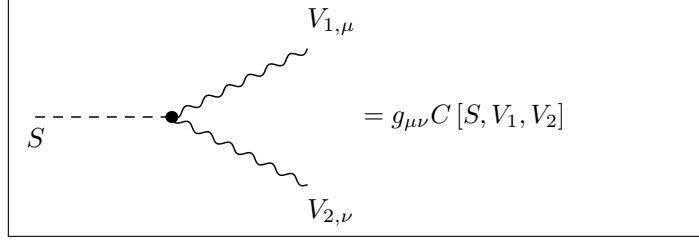
are introduced. I_3^f is the third isospin component and Q_f the electric charge of the fermion f . The effect of CKM mixing is neglected and the CKM matrix is approximated by the identity matrix in the vertices between the fermions and the W boson.

The counterterm for the $Zf\bar{f}$ vertex is needed at the two-loop order for the calculation of the Z observables. Here we indicate explicitly the one-loop and two-loop parts of the counterterms.



$$\begin{aligned}
&= \frac{-ie\gamma_\mu}{2c_W s_W} \left\{ (v_f - a_f \gamma_5) \left(\delta^{(1)} Z_e \frac{(s_W^2 - c_W^2)}{2c_W^2} \frac{\delta^{(1)} s_W^2}{s_W^2} \right. \right. \\
&\quad + \frac{(3c_W^4 - 2c_W^2 s_W^2 + 3s_W^4)}{8c_W^4} \left(\frac{\delta^{(1)} s_W^2}{s_W^2} \right)^2 \\
&\quad + \left. \frac{(s_W^2 - c_W^2)}{2c_W^2} \frac{\delta^{(2)} s_W^2}{s_W^2} + \delta^{(2)} Z_e \right) \\
&\quad - 2Q_f s_W^2 \left(\delta^{(1)} Z_e \frac{\delta^{(1)} s_W^2}{s_W^2} - \frac{(c_W^2 - s_W^2)}{2c_W^2} \left(\frac{\delta^{(1)} s_W^2}{s_W^2} \right)^2 \right. \\
&\quad \left. \left. + \frac{\delta^{(2)} s_W^2}{s_W^2} \right) + \dots \right\}
\end{aligned} \tag{A.3}$$

Omitted terms indicated by the ellipsis are not required for the leading two-loop contributions considered in this thesis.

Feynman rules for the scalar-vector-vector couplings


$$C [h^0, Z, Z] = -\frac{ieM_W s_{\alpha-\beta}}{c_W^2 s_W} \left(1 + \delta Z_e + \frac{\delta M_W^2}{2M_W^2} + \delta s_W^2 \left(\frac{1}{c_W^2} - \frac{1}{2s_W^2} \right) - \frac{c_\beta^2}{t_{\alpha-\beta}} \delta t_\beta \right. \\ \left. - \frac{\delta Z_{h^0 H^0}}{2t_{\alpha-\beta}} + \frac{\delta Z_{h^0}}{2} + \delta Z_{ZZ} \right)$$

$$C [H^0, Z, Z] = \frac{ieM_W c_{\alpha-\beta}}{c_W^2 s_W} \left(1 + \delta Z_e + \frac{\delta M_W^2}{2M_W^2} + \delta s_W^2 \left(\frac{1}{c_W^2} - \frac{1}{2s_W^2} \right) + \delta t_\beta c_\beta^2 t_{\alpha-\beta} \right. \\ \left. - \frac{1}{2} t_{\alpha-\beta} \delta Z_{h^0 H^0} + \frac{\delta Z_{H^0}}{2} + \delta Z_{ZZ} \right)$$

$$C [h^0, W^-, W^+] = -\frac{ieM_W s_{\alpha-\beta}}{s_W} \left(1 + \delta Z_e + \frac{\delta M_W^2}{2M_W^2} - \frac{\delta s_W^2}{2s_W^2} - \frac{\delta t_\beta c_\beta^2}{t_{\alpha-\beta}} - \frac{\delta Z_{h^0 H^0}}{2t_{\alpha-\beta}} + \frac{\delta Z_{h^0}}{2} + \delta Z_W \right)$$

$$C [H^0, W^-, W^+] = \frac{ieM_W c_{\alpha-\beta}}{s_W} \left(1 + \delta Z_e + \frac{\delta M_W^2}{2M_W^2} - \frac{\delta s_W^2}{2s_W^2} + \delta t_\beta c_\beta^2 t_{\alpha-\beta} \right. \\ \left. - \frac{1}{2} t_{\alpha-\beta} \delta Z_{h^0 H^0} + \frac{\delta Z_{H^0}}{2} + \delta Z_W \right)$$

$$C [G^\pm, \gamma, W^\mp] = ieM_W \left(1 + \delta Z_e + \frac{\delta M_W^2}{2M_W^2} - \frac{s_W}{2c_W} \delta Z_{Z\gamma} + \frac{\delta Z_{\gamma\gamma}}{2} + \frac{\delta Z_{G^\pm}}{2} + \frac{\delta Z_W}{2} \right)$$

$$C [G^\pm, Z, W^\mp] = -\frac{ieM_W s_W}{c_W} \left(1 + \delta Z_e + \frac{\delta M_W^2}{2M_W^2} + \frac{\delta s_W^2}{2c_W^2 s_W^2} - \frac{c_W}{2s_W} \delta Z_{\gamma Z} + \frac{\delta Z_{G^\pm}}{2} + \frac{\delta Z_W}{2} + \frac{\delta Z_{ZZ}}{2} \right)$$

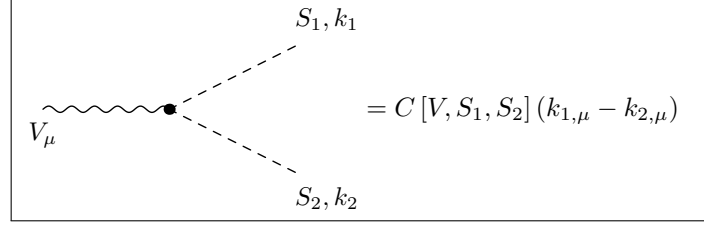
$$C [H^\pm, \gamma, W^\mp] = ieM_W \left(\delta t_\beta c_\beta^2 + \frac{1}{2} \delta Z_{G^\pm H^\pm} \right)$$

$$C [H^\pm, Z, W^\mp] = -i \frac{eM_W s_W}{2c_W} (\delta Z_{G^\pm H^\pm} + 2\delta t_\beta c_\beta^2)$$

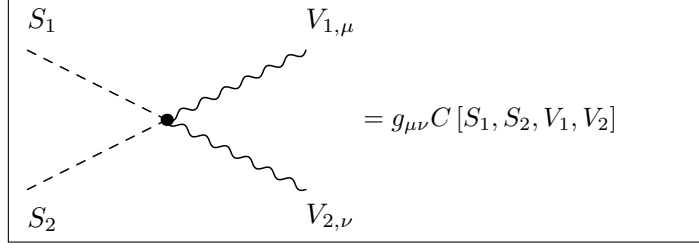
$$C [h^0, \gamma, Z] = -\frac{ieM_W s_{\alpha-\beta}}{2c_W^2 s_W} \delta Z_{Z\gamma}$$

$$C [H^0, \gamma, Z] = \frac{ieM_W c_{\alpha-\beta}}{2c_W^2 s_W} \delta Z_{Z\gamma}$$

Feynman rules for the vector-scalar-scalar couplings



$$\begin{aligned}
C[Z, h^0, A^0] &= \frac{ec_{\alpha-\beta}}{2c_W s_W} \left(1 + \delta Z_e + \frac{\delta s_W^2 (s_W^2 - c_W^2)}{2c_W^2 s_W^2} + \frac{\delta Z_{A^0}}{2} + \frac{1}{2} t_{\alpha-\beta} (\delta Z_{h^0 H^0} - \delta Z_{A^0 G^0}) + \frac{\delta Z_{h^0}}{2} + \frac{\delta Z_{ZZ}}{2} \right) \\
C[Z, h^0, G^0] &= -\frac{es_{\alpha-\beta}}{2c_W s_W} \left(1 + \delta Z_e + \frac{\delta s_W^2 (s_W^2 - c_W^2)}{2c_W^2 s_W^2} - \frac{\delta Z_{A^0 G^0}}{2t_{\alpha-\beta}} + \frac{\delta Z_{G^0}}{2} - \frac{\delta Z_{h^0 H^0}}{2t_{\alpha-\beta}} + \frac{\delta Z_{h^0}}{2} + \frac{\delta Z_{ZZ}}{2} \right) \\
C[Z, H^0, A^0] &= \frac{es_{\alpha-\beta}}{2c_W s_W} \left(1 + \delta Z_e + \frac{\delta s_W^2 (s_W^2 - c_W^2)}{2c_W^2 s_W^2} + \frac{\delta Z_{A^0 G^0}}{2t_{\alpha-\beta}} + \frac{\delta Z_{A^0}}{2} + \frac{\delta Z_{h^0 H^0}}{2t_{\alpha-\beta}} + \frac{\delta Z_{H^0}}{2} + \frac{\delta Z_{ZZ}}{2} \right) \\
C[Z, H^0, G^0] &= \frac{ec_{\alpha-\beta}}{2c_W s_W} \left(1 + \delta Z_e + \frac{\delta s_W^2 (s_W^2 - c_W^2)}{2c_W^2 s_W^2} + \frac{1}{2} t_{\alpha-\beta} \delta Z_{A^0 G^0} + \frac{\delta Z_{G^0}}{2} \right. \\
&\quad \left. - \frac{1}{2} t_{\alpha-\beta} \delta Z_{h^0 H^0} + \frac{\delta Z_{H^0}}{2} + \frac{\delta Z_{ZZ}}{2} \right) \\
C[W^\mp, G^\pm, h^0] &= \pm \frac{ies_{\alpha-\beta}}{2s_W} \left(1 + \delta Z_e - \frac{\delta s_W^2}{2s_W^2} - \frac{\delta Z_{G^\pm H^\pm}}{2t_{\alpha-\beta}} + \frac{\delta Z_{G^\pm}}{2} - \frac{\delta Z_{h^0 H^0}}{2t_{\alpha-\beta}} + \frac{\delta Z_{h^0}}{2} + \frac{\delta Z_W}{2} \right) \\
C[W^\mp, G^\pm, H^0] &= \mp \frac{iec_{\alpha-\beta}}{2s_W} \left(1 + \delta Z_e - \frac{\delta s_W^2}{2s_W^2} + \frac{1}{2} t_{\alpha-\beta} \delta Z_{G^\pm H^\pm} + \frac{\delta Z_{G^\pm}}{2} - \frac{1}{2} t_{\alpha-\beta} \delta Z_{h^0 H^0} + \frac{\delta Z_{H^0}}{2} + \frac{\delta Z_W}{2} \right) \\
C[W^\mp, G^\pm, A^0] &= -\frac{e}{4s_W} \delta Z_{A^0 G^0} - \frac{e}{4s_W} \delta Z_{G^\pm H^\pm} \\
C[W^\mp, G^\pm, G^0] &= -\frac{e}{2s_W} \left(1 + \delta Z_e - \frac{\delta s_W^2}{2s_W^2} + \frac{\delta Z_{G^0}}{2} + \frac{\delta Z_{G^\pm}}{2} + \frac{\delta Z_W}{2} \right) \\
C[W^\mp, H^\pm, h^0] &= \mp \frac{iec_{\alpha-\beta}}{2s_W} \left(1 + \delta Z_e - \frac{\delta s_W^2}{2s_W^2} - \frac{1}{2} t_{\alpha-\beta} \delta Z_{G^\pm H^\pm} + \frac{1}{2} t_{\alpha-\beta} \delta Z_{h^0 H^0} + \frac{\delta Z_{h^0}}{2} + \frac{\delta Z_{H^\pm}}{2} + \frac{\delta Z_W}{2} \right) \\
C[W^\mp, H^\pm, H^0] &= \mp \frac{ies_{\alpha-\beta}}{2s_W} \left(1 + \delta Z_e - \frac{\delta s_W^2}{2s_W^2} + \frac{\delta Z_{G^\pm H^\pm}}{2t_{\alpha-\beta}} + \frac{\delta Z_{h^0 H^0}}{2t_{\alpha-\beta}} + \frac{\delta Z_{H^0}}{2} + \frac{\delta Z_{H^\pm}}{2} + \frac{\delta Z_W}{2} \right) \\
C[W^\mp, H^\pm, A^0] &= -\frac{e}{2s_W} \left(1 + \delta Z_e - \frac{\delta s_W^2}{2s_W^2} + \frac{\delta Z_{A^0}}{2} + \frac{\delta Z_{H^\pm}}{2} + \frac{\delta Z_W}{2} \right) \\
C[W^\mp, H^\pm, G^0] &= -\frac{e}{4s_W} \delta Z_{A^0 G^0} - \frac{e}{4s_W} \delta Z_{G^\pm H^\pm} \\
C[\gamma, G^+, G^-] &= -ie \left(1 + \delta Z_e + \frac{(c_W^2 - s_W^2)}{4c_W s_W} \delta Z_{Z\gamma} + \frac{\delta Z_{\gamma\gamma}}{2} + \delta Z_{G^\pm} \right) \\
C[\gamma, H^+, H^-] &= -ie \left(1 + \delta Z_e + \frac{(c_W^2 - s_W^2)}{4c_W s_W} \delta Z_{Z\gamma} + \frac{\delta Z_{\gamma\gamma}}{2} + \delta Z_{H^\pm} \right) \\
C[\gamma, G^\pm, H^\mp] &= \mp ie \delta Z_{G^\pm H^\pm} \\
C[Z, G^+, G^-] &= -\frac{ie(c_W^2 - s_W^2)}{2c_W s_W} \left(1 + \delta Z_e - \frac{\delta s_W^2}{2c_W^2 s_W^2 (c_W^2 - s_W^2)} + \frac{c_W s_W}{c_W^2 - s_W^2} \delta Z_{\gamma Z} + \delta Z_{G^\pm} + \frac{\delta Z_{ZZ}}{2} \right) \\
C[Z, H^+, H^-] &= -\frac{ie(c_W^2 - s_W^2)}{2c_W s_W} \left(1 + \delta Z_e - \frac{\delta s_W^2}{2c_W^2 s_W^2 (c_W^2 - s_W^2)} + \frac{c_W s_W}{c_W^2 - s_W^2} \delta Z_{\gamma Z} + \delta Z_{H^\pm} + \frac{\delta Z_{ZZ}}{2} \right) \\
C[Z, G^\pm, H^\mp] &= \mp \frac{ie(c_W^2 - s_W^2)}{2c_W s_W} \delta Z_{G^\pm H^\pm} \\
C[\gamma, h^0, A^0] &= \frac{ec_{\alpha-\beta}}{4c_W s_W} \delta Z_{Z\gamma} \\
C[\gamma, h^0, G^0] &= -\frac{es_{\alpha-\beta}}{4c_W s_W} \delta Z_{Z\gamma} \\
C[\gamma, H^0, A^0] &= \frac{es_{\alpha-\beta}}{4c_W s_W} \delta Z_{Z\gamma} \\
C[\gamma, H^0, G^0] &= \frac{ec_{\alpha-\beta}}{4c_W s_W} \delta Z_{Z\gamma}
\end{aligned}$$

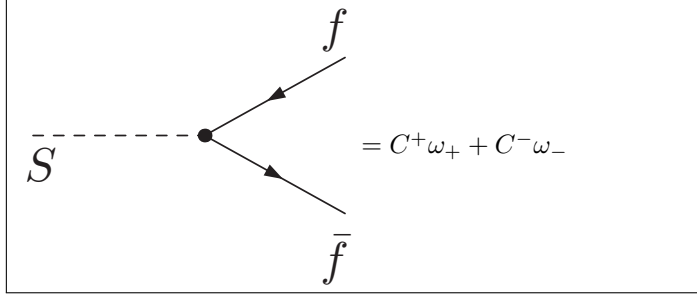
Feynman rules for the scalar-scalar-vector-vector couplings


$$\begin{aligned}
C [h^0, h^0, Z, Z] &= \frac{ie^2}{2c_W^2 s_W^2} \left(1 + 2\delta Z_e + \frac{\delta s_W^2 (s_W^2 - c_W^2)}{c_W^2 s_W^2} + \delta Z_{h^0} + \delta Z_{ZZ} \right) \\
C [h^0, h^0, W^-, W^+] &= \frac{ie^2}{2s_W^2} \left(1 + 2\delta Z_e + \delta Z_{h^0} - \frac{\delta s_W^2}{s_W^2} + \delta Z_W \right) \\
C [H^0, H^0, Z, Z] &= \frac{ie^2}{2c_W^2 s_W^2} \left(1 + 2\delta Z_e + \frac{\delta s_W^2 (s_W^2 - c_W^2)}{c_W^2 s_W^2} + \delta Z_{H^0} + \delta Z_{ZZ} \right) \\
C [H^0, H^0, W^-, W^+] &= \frac{ie^2}{2s_W^2} \left(1 + 2\delta Z_e - \frac{\delta s_W^2}{s_W^2} + \delta Z_{H^0} + \delta Z_W \right) \\
C [A^0, A^0, Z, Z] &= \frac{ie^2}{2c_W^2 s_W^2} \left(1 + 2\delta Z_e + \frac{\delta s_W^2 (s_W^2 - c_W^2)}{c_W^2 s_W^2} + \delta Z_{A^0} + \delta Z_{ZZ} \right) \\
C [A^0, A^0, W^-, W^+] &= \frac{ie^2}{2s_W^2} \left(1 + 2\delta Z_e + \delta Z_{A^0} - \frac{\delta s_W^2}{s_W^2} + \delta Z_W \right) \\
C [G^0, G^0, Z, Z] &= \frac{ie^2}{2c_W^2 s_W^2} \left(1 + 2\delta Z_e + \frac{\delta s_W^2 (s_W^2 - c_W^2)}{c_W^2 s_W^2} + \delta Z_{G^0} + \delta Z_{ZZ} \right) \\
C [G^0, G^0, W^-, W^+] &= \frac{ie^2}{2s_W^2} \left(1 + 2\delta Z_e - \frac{\delta s_W^2}{s_W^2} + \delta Z_{G^0} + \delta Z_W \right) \\
C [G^-, G^+, Z, Z] &= \frac{ie^2 (c_W^2 - s_W^2)^2}{2c_W^2 s_W^2} \left(1 + 2\delta Z_e - \frac{\delta s_W^2}{c_W^2 s_W^2 (c_W^2 - s_W^2)} + \delta Z_{G^\pm} + \delta Z_{ZZ} + \frac{2c_W s_W}{c_W^2 - s_W^2} \delta Z_{\gamma Z} \right) \\
C [G^-, G^+, W^-, W^+] &= \frac{ie^2}{2s_W^2} \left(1 + 2\delta Z_e - \frac{\delta s_W^2}{s_W^2} + \delta Z_{G^\pm} + \delta Z_W \right) \\
C [H^-, H^+, Z, Z] &= \frac{ie^2 (c_W^2 - s_W^2)^2}{2c_W^2 s_W^2} \left(1 + 2\delta Z_e - \frac{\delta s_W^2}{c_W^2 s_W^2 (c_W^2 - s_W^2)} + \frac{2c_W s_W}{c_W^2 - s_W^2} \delta Z_{\gamma Z} + \delta Z_{H^\pm} + \delta Z_{ZZ} \right) \\
C [H^-, H^+, W^-, W^+] &= \frac{ie^2}{2s_W^2} \left(1 + 2\delta Z_e - \frac{\delta s_W^2}{s_W^2} + \delta Z_{H^\pm} + \delta Z_W \right) \\
C [G^-, G^+, \gamma, \gamma] &= 2ie^2 \left(1 + 2\delta Z_e + \frac{(c_W^2 - s_W^2)}{2c_W s_W} \delta Z_{Z\gamma} + \delta Z_{\gamma\gamma} + \delta Z_{G^\pm} \right) \\
C [G^-, G^+, \gamma, Z] &= \frac{ie^2 (c_W^2 - s_W^2)}{c_W s_W} \left(1 + 2\delta Z_e - \frac{\delta s_W^2}{2c_W^2 s_W^2 (c_W^2 - s_W^2)} + \frac{c_W s_W}{c_W^2 - s_W^2} \delta Z_{\gamma Z} \right. \\
&\quad \left. + \frac{(c_W^2 - s_W^2)}{4c_W s_W} \delta Z_{Z\gamma} + \frac{\delta Z_{\gamma\gamma}}{2} + \delta Z_{G^\pm} + \frac{\delta Z_{ZZ}}{2} \right) \\
C [H^-, H^+, \gamma, \gamma] &= 2ie^2 \left(1 + 2\delta Z_e + \frac{\delta Z_{Z\gamma} (c_W^2 - s_W^2)}{2c_W s_W} + \delta Z_{\gamma\gamma} + \delta Z_{H^\pm} \right) \\
C [H^-, H^+, \gamma, Z] &= \frac{ie^2 (c_W^2 - s_W^2)}{c_W s_W} \left(1 + 2\delta Z_e - \frac{\delta s_W^2}{2c_W^2 s_W^2 (c_W^2 - s_W^2)} + \frac{c_W s_W}{c_W^2 - s_W^2} \delta Z_{\gamma Z} \right. \\
&\quad \left. + \frac{(c_W^2 - s_W^2)}{4c_W s_W} \delta Z_{Z\gamma} + \frac{\delta Z_{\gamma\gamma}}{2} + \delta Z_{H^\pm} + \frac{\delta Z_{ZZ}}{2} \right) \\
C [G^\pm, h^0, \gamma, W^\mp] &= -\frac{ie^2 s_{\alpha-\beta}}{2s_W} \left(1 + 2\delta Z_e - \frac{\delta s_W^2}{2s_W^2} - \frac{s_W}{2c_W} \delta Z_{Z\gamma} + \frac{\delta Z_{\gamma\gamma}}{2} - \frac{\delta Z_{G^\pm H^\pm}}{2t_{\alpha-\beta}} + \frac{\delta Z_{G^\pm}}{2} \right. \\
&\quad \left. - \frac{\delta Z_{h^0 H^0}}{2t_{\alpha-\beta}} + \frac{\delta Z_{h^0}}{2} + \frac{\delta Z_W}{2} \right) \\
C [G^\pm, h^0, Z, W^\mp] &= \frac{ie^2 s_{\alpha-\beta}}{2c_W} \left(1 + 2\delta Z_e + \frac{\delta s_W^2}{2c_W^2} - \frac{c_W}{2s_W} \delta Z_{\gamma Z} - \frac{\delta Z_{G^\pm H^\pm}}{2t_{\alpha-\beta}} + \frac{\delta Z_{G^\pm}}{2} \right)
\end{aligned}$$

$$\begin{aligned}
& -\frac{\delta Z_{h^0 H^0}}{2t_{\alpha-\beta}} + \frac{\delta Z_{h^0}}{2} + \frac{\delta Z_W}{2} + \frac{\delta Z_{ZZ}}{2} \Big) \\
C[H^\mp, h^0, \gamma, W^\pm] &= \frac{ie^2 c_{\alpha-\beta}}{2s_W} \left(1 + 2\delta Z_e - \frac{\delta s_W^2}{2s_W^2} - \frac{s_W}{2c_W} \delta Z_{Z\gamma} + \frac{\delta Z_{\gamma\gamma}}{2} - \frac{1}{2} t_{\alpha-\beta} \delta Z_{G^\pm H^\pm} \right. \\
& \quad \left. + \frac{1}{2} t_{\alpha-\beta} \delta Z_{h^0 H^0} + \frac{\delta Z_{h^0}}{2} + \frac{\delta Z_{H^\pm}}{2} + \frac{\delta Z_W}{2} \right) \\
C[H^\pm, h^0, Z, W^\mp] &= -\frac{ie^2 c_{\alpha-\beta}}{2c_W} \left(1 + 2\delta Z_e + \frac{\delta s_W^2}{2c_W^2} - \frac{c_W}{2s_W} \delta Z_{\gamma Z} - \frac{1}{2} t_{\alpha-\beta} \delta Z_{G^\pm H^\pm} + \frac{1}{2} t_{\alpha-\beta} \delta Z_{h^0 H^0} \right. \\
& \quad \left. + \frac{\delta Z_{h^0}}{2} + \frac{\delta Z_{H^\pm}}{2} + \frac{\delta Z_W}{2} + \frac{\delta Z_{ZZ}}{2} \right) \\
C[G^\pm, H^0, \gamma, W^\mp] &= \frac{ie^2 c_{\alpha-\beta}}{2s_W} \left(1 + 2\delta Z_e - \frac{\delta s_W^2}{2s_W^2} - \frac{s_W}{2c_W} \delta Z_{Z\gamma} + \frac{\delta Z_{\gamma\gamma}}{2} + \frac{1}{2} t_{\alpha-\beta} \delta Z_{G^\pm H^\pm} + \frac{\delta Z_{G^\pm}}{2} \right. \\
& \quad \left. - \frac{1}{2} t_{\alpha-\beta} \delta Z_{h^0 H^0} + \frac{\delta Z_{H^0}}{2} + \frac{\delta Z_W}{2} \right) \\
C[G^\pm, H^0, Z, W^\mp] &= -\frac{ie^2 c_{\alpha-\beta}}{2c_W} \left(1 + 2\delta Z_e + \frac{\delta s_W^2}{2c_W^2} - \frac{c_W}{2s_W} \delta Z_{\gamma Z} + \frac{1}{2} t_{\alpha-\beta} \delta Z_{G^\pm H^\pm} + \frac{\delta Z_{G^\pm}}{2} \right. \\
& \quad \left. - \frac{1}{2} t_{\alpha-\beta} \delta Z_{h^0 H^0} + \frac{\delta Z_{H^0}}{2} + \frac{\delta Z_W}{2} + \frac{\delta Z_{ZZ}}{2} \right) \\
C[H^\pm, H^0, \gamma, W^\mp] &= \frac{ie^2 s_{\alpha-\beta}}{2s_W} \left(1 + 2\delta Z_e - \frac{\delta s_W^2}{2s_W^2} - \frac{s_W}{2c_W} \delta Z_{Z\gamma} + \frac{\delta Z_{\gamma\gamma}}{2} + \frac{\delta Z_{G^\pm H^\pm}}{2t_{\alpha-\beta}} + \frac{\delta Z_{h^0 H^0}}{2t_{\alpha-\beta}} \right. \\
& \quad \left. + \frac{\delta Z_{H^0}}{2} + \frac{\delta Z_{H^\pm}}{2} + \frac{\delta Z_W}{2} \right) \\
C[H^\pm, H^0, Z, W^\mp] &= -\frac{ie^2 s_{\alpha-\beta}}{2c_W} \left(1 + 2\delta Z_e + \frac{\delta s_W^2}{2c_W^2} - \frac{c_W}{2s_W} \delta Z_{\gamma Z} + \frac{\delta Z_{G^\pm H^\pm}}{2t_{\alpha-\beta}} + \frac{\delta Z_{h^0 H^0}}{2t_{\alpha-\beta}} \right. \\
& \quad \left. + \frac{\delta Z_{H^0}}{2} + \frac{\delta Z_{H^\pm}}{2} + \frac{\delta Z_W}{2} + \frac{\delta Z_{ZZ}}{2} \right) \\
C[G^\mp, A^0, \gamma, W^\pm] &= \mp \left(\frac{e^2}{4s_W} \delta Z_{A^0 G^0} + \frac{e^2}{4s_W} \delta Z_{G^\pm H^\pm} \right) \\
C[G^\mp, A^0, Z, W^\pm] &= \pm \left(\frac{e^2 \delta Z_{A^0 G^0}}{4c_W} + \frac{e^2 \delta Z_{G^\pm H^\pm}}{4c_W} \right) \\
C[H^\pm, A^0, \gamma, W^\mp] &= \pm \frac{e^2}{2s_W} \left(1 + 2\delta Z_e - \frac{\delta s_W^2}{2s_W^2} + \frac{\delta Z_{A^0}}{2} - \frac{s_W}{2c_W} \delta Z_{Z\gamma} + \frac{\delta Z_{\gamma\gamma}}{2} + \frac{\delta Z_{H^\pm}}{2} + \frac{\delta Z_W}{2} \right) \\
C[H^\pm, A^0, Z, W^\mp] &= \mp \frac{e^2}{2c_W} \left(1 + 2\delta Z_e + \frac{\delta s_W^2}{2c_W^2} + \frac{\delta Z_{A^0}}{2} - \frac{c_W}{2s_W} \delta Z_{\gamma Z} + \frac{\delta Z_{H^\pm}}{2} + \frac{\delta Z_W}{2} + \frac{\delta Z_{ZZ}}{2} \right) \\
C[G^\pm, G^0, \gamma, W^\mp] &= \pm \frac{e^2}{2s_W} \left(1 + 2\delta Z_e - \frac{\delta s_W^2}{2s_W^2} - \frac{s_W}{2c_W} \delta Z_{Z\gamma} + \frac{\delta Z_{\gamma\gamma}}{2} + \frac{\delta Z_{G^0}}{2} + \frac{\delta Z_{G^\pm}}{2} + \frac{\delta Z_W}{2} \right) \\
C[G^\pm, G^0, Z, W^\mp] &= \mp \frac{e^2}{2c_W} \left(1 + 2\delta Z_e + \frac{\delta s_W^2}{2c_W^2} - \frac{c_W}{2s_W} \delta Z_{\gamma Z} + \frac{\delta Z_{G^0}}{2} + \frac{\delta Z_{G^\pm}}{2} + \frac{\delta Z_W}{2} + \frac{\delta Z_{ZZ}}{2} \right) \\
C[H^\pm, G^0, \gamma, W^\mp] &= \left(\frac{e^2}{4s_W} \delta Z_{A^0 G^0} + \frac{e^2}{4s_W} \delta Z_{G^\pm H^\pm} \right) \\
C[H^\pm, G^0, Z, W^\mp] &= \mp \left(\frac{e^2 \delta Z_{A^0 G^0}}{4c_W} + \frac{e^2 \delta Z_{G^\pm H^\pm}}{4c_W} \right) \\
C[H^0, h^0, Z, Z] &= \frac{ie^2}{2c_W^2 s_W^2} \delta Z_{h^0 H^0} \\
C[H^0, h^0, W^-, W^+] &= \frac{ie^2}{2s_W^2} \delta Z_{h^0 H^0} \\
C[G^0, A^0, Z, Z] &= \frac{ie^2}{2c_W^2 s_W^2} \delta Z_{A^0 G^0} \\
C[G^0, A^0, W^-, W^+] &= \frac{ie^2}{2s_W^2} \delta Z_{A^0 G^0}
\end{aligned}$$

$$\begin{aligned}
C[h^0, h^0, \gamma, Z] &= \frac{ie^2}{4c_W^2 s_W^2} \delta Z_{Z\gamma} \\
C[H^0, H^0, \gamma, Z] &= \frac{ie^2}{4c_W^2 s_W^2} \delta Z_{Z\gamma} \\
C[A^0, A^0, \gamma, Z] &= \frac{ie^2}{4c_W^2 s_W^2} \delta Z_{Z\gamma} \\
C[G^0, G^0, \gamma, Z] &= \frac{ie^2}{4c_W^2 s_W^2} \delta Z_{Z\gamma} \\
C[H^\pm, G^\mp, \gamma, \gamma] &= 2ie^2 \delta Z_{G^\pm H^\pm} \\
C[H^\pm, G^\mp, \gamma, Z] &= \frac{ie^2 (c_W^2 - s_W^2)}{c_W s_W} \delta Z_{G^\pm H^\pm} \\
C[H^\pm, G^\mp, Z, Z] &= \frac{ie^2 (c_W^2 - s_W^2)^2}{2c_W^2 s_W^2} \delta Z_{G^\pm H^\pm} \\
C[H^+, G^-, W^-, W^+] &= \frac{ie^2 \delta Z_{G^\pm H^\pm}}{2s_W^2} \\
C[H^-, G^+, W^-, W^+] &= \frac{ie^2 \delta Z_{G^\pm H^\pm}}{2s_W^2}
\end{aligned}$$

Feynman rules for the Yukawa interaction in the THDM



$$\begin{aligned}
h^0 \bar{l} : & \begin{cases} C^+ = -\frac{iem_l \xi_h^l}{2M_W s_W} \left(1 + \delta Z_e - \frac{\delta M_W^2}{2M_W^2} - \frac{\delta s_W^2}{2s_W^2} + \frac{\delta m_l}{m_l} + \frac{\delta Z_{h^0}}{2} + \frac{\delta Z_{h^0 H^0} \xi_H^l}{2\xi_h^l} + \frac{\delta \xi_h^l}{\xi_h^l} + \frac{\delta Z_L^L}{2} + \frac{\delta Z_L^R}{2} \right) \\ C^- = -\frac{iem_l \xi_h^l}{2M_W s_W} \left(1 + \delta Z_e - \frac{\delta M_W^2}{2M_W^2} - \frac{\delta s_W^2}{2s_W^2} + \frac{\delta m_l}{m_l} + \frac{\delta Z_{h^0}}{2} + \frac{\delta Z_{h^0 H^0} \xi_H^l}{2\xi_h^l} + \frac{\delta \xi_h^l}{\xi_h^l} + \frac{\delta Z_L^L}{2} + \frac{\delta Z_L^R}{2} \right) \end{cases} \\
H^0 \bar{l} : & \begin{cases} C^+ = -\frac{iem_l \xi_H^l}{2M_W s_W} \left(1 + \delta Z_e - \frac{\delta M_W^2}{2M_W^2} - \frac{\delta s_W^2}{2s_W^2} + \frac{\delta m_l}{m_l} + \frac{\delta Z_{H^0}}{2} + \frac{\delta Z_{h^0 H^0} \xi_H^l}{2\xi_H^l} + \frac{\delta \xi_H^l}{\xi_H^l} + \frac{\delta Z_L^L}{2} + \frac{\delta Z_L^R}{2} \right) \\ C^- = -\frac{iem_l \xi_H^l}{2M_W s_W} \left(1 + \delta Z_e - \frac{\delta M_W^2}{2M_W^2} - \frac{\delta s_W^2}{2s_W^2} + \frac{\delta m_l}{m_l} + \frac{\delta Z_{H^0}}{2} + \frac{\delta Z_{h^0 H^0} \xi_H^l}{2\xi_H^l} + \frac{\delta \xi_H^l}{\xi_H^l} + \frac{\delta Z_L^L}{2} + \frac{\delta Z_L^R}{2} \right) \end{cases} \\
A^0 \bar{l} : & \begin{cases} C^+ = -\frac{em_l \xi_A^l}{2M_W s_W} \left(1 + \delta Z_e - \frac{\delta M_W^2}{2M_W^2} - \frac{\delta s_W^2}{2s_W^2} + \frac{\delta m_l}{m_l} + \frac{\delta Z_{A^0}}{2} - \frac{\delta Z_{A^0 G^0}}{2\xi_A^l} + \frac{\delta \xi_A^l}{\xi_A^l} + \frac{\delta Z_L^L}{2} + \frac{\delta Z_L^R}{2} \right) \\ C^- = \frac{em_l \xi_A^l}{2M_W s_W} \left(1 + \delta Z_e - \frac{\delta M_W^2}{2M_W^2} - \frac{\delta s_W^2}{2s_W^2} + \frac{\delta m_l}{m_l} + \frac{\delta Z_{A^0}}{2} - \frac{\delta Z_{A^0 G^0}}{2\xi_A^l} + \frac{\delta \xi_A^l}{\xi_A^l} + \frac{\delta Z_L^L}{2} + \frac{\delta Z_L^R}{2} \right) \end{cases} \\
G^0 \bar{l} : & \begin{cases} C^+ = \frac{em_l}{2M_W s_W} \left(1 + \delta Z_e - \frac{\delta M_W^2}{2M_W^2} - \frac{\delta s_W^2}{2s_W^2} + \frac{\delta m_l}{m_l} + \frac{\delta Z_{G^0}}{2} + \frac{\delta Z_L^L}{2} + \frac{\delta Z_L^R}{2} \right) \\ C^- = -\frac{em_l}{2M_W s_W} \left(1 + \delta Z_e - \frac{\delta M_W^2}{2M_W^2} - \frac{\delta s_W^2}{2s_W^2} + \frac{\delta m_l}{m_l} + \frac{\delta Z_{G^0}}{2} + \frac{\delta Z_L^L}{2} + \frac{\delta Z_L^R}{2} \right) \end{cases} \\
G^+ \bar{\nu} : & \begin{cases} C^+ = -\frac{iem_l}{\sqrt{2}M_W s_W} \left(1 + \delta Z_e - \frac{\delta M_W^2}{2M_W^2} - \frac{\delta s_W^2}{2s_W^2} + \frac{\delta m_l}{m_l} + \frac{\delta Z_{G^\pm}}{2} + \frac{\delta Z_L^R}{2} + \frac{\delta Z_L^L}{2} \right) \\ C^- = 0 \end{cases} \\
G^- \bar{\nu} : & \begin{cases} C^+ = 0 \\ C^- = -\frac{iem_l}{\sqrt{2}M_W s_W} \left(1 + \delta Z_e - \frac{\delta M_W^2}{2M_W^2} - \frac{\delta s_W^2}{2s_W^2} + \frac{\delta m_l}{m_l} + \frac{\delta Z_{G^\pm}}{2} + \frac{\delta Z_L^R}{2} + \frac{\delta Z_L^L}{2} \right) \end{cases} \\
H^+ \bar{\nu} : & \begin{cases} C^+ = \frac{iem_l \xi_A^l}{\sqrt{2}M_W s_W} \left(1 + \delta Z_e - \frac{\delta M_W^2}{2M_W^2} - \frac{\delta s_W^2}{2s_W^2} + \frac{\delta m_l}{m_l} + \frac{\delta Z_{H^\pm}}{2} - \frac{\delta Z_{G^\pm H^\pm}}{2\xi_A^l} + \frac{\delta \xi_A^l}{\xi_A^l} + \frac{\delta Z_L^L}{2} + \frac{\delta Z_L^R}{2} \right) \\ C^- = 0 \end{cases} \\
H^- \bar{\nu} : & \begin{cases} C^+ = 0 \\ C^- = \frac{iem_l \xi_A^l}{\sqrt{2}M_W s_W} \left(1 + \delta Z_e - \frac{\delta M_W^2}{2M_W^2} - \frac{\delta s_W^2}{2s_W^2} + \frac{\delta m_l}{m_l} + \frac{\delta Z_{H^\pm}}{2} - \frac{\delta Z_{G^\pm H^\pm}}{2\xi_A^l} + \frac{\delta \xi_A^l}{\xi_A^l} + \frac{\delta Z_L^L}{2} + \frac{\delta Z_L^R}{2} \right) \end{cases}
\end{aligned}$$

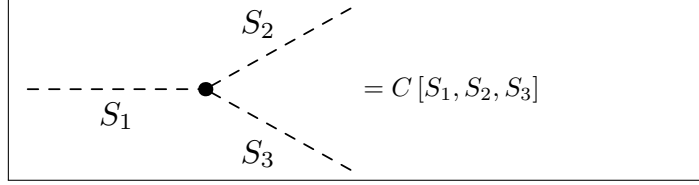
$$\begin{aligned}
h^0 \bar{u}u : & \begin{cases} C^+ = -\frac{iem_u \xi_h^u}{2M_W s_W} \left(1 + \delta Z_e - \frac{\delta M_W^2}{2M_W^2} - \frac{\delta s_W^2}{2s_W^2} + \frac{\delta m_u}{m_u} + \frac{\delta Z_{h0}}{2} + \frac{\delta Z_{h^0 H^0} \xi_H^u}{2\xi_h^u} + \frac{\delta \xi_h^u}{\xi_h^u} + \frac{\delta Z_u^L}{2} + \frac{\delta Z_u^R}{2} \right) \\ C^- = -\frac{iem_u \xi_h^u}{2M_W s_W} \left(1 + \delta Z_e - \frac{\delta M_W^2}{2M_W^2} - \frac{\delta s_W^2}{2s_W^2} + \frac{\delta m_u}{m_u} + \frac{\delta Z_{h0}}{2} + \frac{\delta Z_{h^0 H^0} \xi_H^u}{2\xi_h^u} + \frac{\delta \xi_h^u}{\xi_h^u} + \frac{\delta Z_u^L}{2} + \frac{\delta Z_u^R}{2} \right) \end{cases} \\
H^0 \bar{u}u : & \begin{cases} C^+ = -\frac{iem_u \xi_H^u}{2M_W s_W} \left(1 + \delta Z_e - \frac{\delta M_W^2}{2M_W^2} - \frac{\delta s_W^2}{2s_W^2} + \frac{\delta m_u}{m_u} + \frac{\delta Z_{H^0}}{2} + \frac{\delta Z_{h^0 H^0} \xi_H^u}{2\xi_H^u} + \frac{\delta \xi_H^u}{\xi_H^u} + \frac{\delta Z_u^L}{2} + \frac{\delta Z_u^R}{2} \right) \\ C^- = -\frac{iem_u \xi_H^u}{2M_W s_W} \left(1 + \delta Z_e - \frac{\delta M_W^2}{2M_W^2} - \frac{\delta s_W^2}{2s_W^2} + \frac{\delta m_u}{m_u} + \frac{\delta Z_{H^0}}{2} + \frac{\delta Z_{h^0 H^0} \xi_H^u}{2\xi_H^u} + \frac{\delta \xi_H^u}{\xi_H^u} + \frac{\delta Z_u^L}{2} + \frac{\delta Z_u^R}{2} \right) \end{cases} \\
A^0 \bar{u}u : & \begin{cases} C^+ = -\frac{em_u \xi_A^u}{2M_W s_W} \left(1 + \delta Z_e - \frac{\delta M_W^2}{2M_W^2} - \frac{\delta s_W^2}{2s_W^2} + \frac{\delta m_u}{m_u} + \frac{\delta Z_{A^0}}{2} + \frac{\delta Z_{A^0 G^0}}{2\xi_A^u} + \frac{\delta \xi_A^u}{\xi_A^u} + \frac{\delta Z_u^L}{2} + \frac{\delta Z_u^R}{2} \right) \\ C^- = \frac{em_u \xi_A^u}{2M_W s_W} \left(1 + \delta Z_e - \frac{\delta M_W^2}{2M_W^2} - \frac{\delta s_W^2}{2s_W^2} + \frac{\delta m_u}{m_u} + \frac{\delta Z_{A^0}}{2} + \frac{\delta Z_{A^0 G^0}}{2\xi_A^u} + \frac{\delta \xi_A^u}{\xi_A^u} + \frac{\delta Z_u^L}{2} + \frac{\delta Z_u^R}{2} \right) \end{cases} \\
G^0 \bar{u}u : & \begin{cases} C^+ = -\frac{em_u}{2M_W s_W} \left(1 + \delta Z_e - \frac{\delta M_W^2}{2M_W^2} - \frac{\delta s_W^2}{2s_W^2} + \frac{\delta m_u}{m_u} + \frac{\delta Z_{G^0}}{2} + \frac{\delta Z_u^L}{2} + \frac{\delta Z_u^R}{2} \right) \\ C^- = \frac{em_u}{2M_W s_W} \left(1 + \delta Z_e - \frac{\delta M_W^2}{2M_W^2} - \frac{\delta s_W^2}{2s_W^2} + \frac{\delta m_u}{m_u} + \frac{\delta Z_{G^0}}{2} + \frac{\delta Z_u^L}{2} + \frac{\delta Z_u^R}{2} \right) \end{cases} \\
h^0 \bar{d}d : & \begin{cases} C^+ = -\frac{iem_d \xi_h^d}{2M_W s_W} \left(1 + \delta Z_e - \frac{\delta M_W^2}{2M_W^2} - \frac{\delta s_W^2}{2s_W^2} + \frac{\delta m_d}{m_d} + \frac{\delta Z_{h0}}{2} + \frac{\xi_H^d \delta Z_{h^0 H^0}}{2\xi_h^d} + \frac{\delta \xi_h^d}{\xi_h^d} + \frac{\delta Z_d^L}{2} + \frac{\delta Z_d^R}{2} \right) \\ C^- = -\frac{iem_d \xi_h^d}{2M_W s_W} \left(1 + \delta Z_e - \frac{\delta M_W^2}{2M_W^2} - \frac{\delta s_W^2}{2s_W^2} + \frac{\delta m_d}{m_d} + \frac{\delta Z_{h0}}{2} + \frac{\xi_H^d \delta Z_{h^0 H^0}}{2\xi_h^d} + \frac{\delta \xi_h^d}{\xi_h^d} + \frac{\delta Z_d^L}{2} + \frac{\delta Z_d^R}{2} \right) \end{cases} \\
H^0 \bar{d}d : & \begin{cases} C^+ = -\frac{iem_d \xi_H^d}{2M_W s_W} \left(1 + \delta Z_e - \frac{\delta M_W^2}{2M_W^2} - \frac{\delta s_W^2}{2s_W^2} + \frac{\delta m_d}{m_d} + \frac{\delta Z_{H^0}}{2} + \frac{\xi_H^d \delta Z_{h^0 H^0}}{2\xi_H^d} + \frac{\delta \xi_H^d}{\xi_H^d} + \frac{\delta Z_d^L}{2} + \frac{\delta Z_d^R}{2} \right) \\ C^- = -\frac{iem_d \xi_H^d}{2M_W s_W} \left(1 + \delta Z_e - \frac{\delta M_W^2}{2M_W^2} - \frac{\delta s_W^2}{2s_W^2} + \frac{\delta m_d}{m_d} + \frac{\delta Z_{H^0}}{2} + \frac{\xi_H^d \delta Z_{h^0 H^0}}{2\xi_H^d} + \frac{\delta \xi_H^d}{\xi_H^d} + \frac{\delta Z_d^L}{2} + \frac{\delta Z_d^R}{2} \right) \end{cases} \\
A^0 \bar{d}d : & \begin{cases} C^+ = -\frac{em_d \xi_A^d}{2M_W s_W} \left(1 + \delta Z_e - \frac{\delta M_W^2}{2M_W^2} - \frac{\delta s_W^2}{2s_W^2} + \frac{\delta m_d}{m_d} + \frac{\delta Z_{A^0}}{2} - \frac{\delta Z_{A^0 G^0}}{2\xi_A^d} + \frac{\delta \xi_A^d}{\xi_A^d} + \frac{\delta Z_d^L}{2} + \frac{\delta Z_d^R}{2} \right) \\ C^- = \frac{em_d \xi_A^d}{2M_W s_W} \left(1 + \delta Z_e - \frac{\delta M_W^2}{2M_W^2} - \frac{\delta s_W^2}{2s_W^2} + \frac{\delta m_d}{m_d} + \frac{\delta Z_{A^0}}{2} - \frac{\delta Z_{A^0 G^0}}{2\xi_A^d} + \frac{\delta \xi_A^d}{\xi_A^d} + \frac{\delta Z_d^L}{2} + \frac{\delta Z_d^R}{2} \right) \end{cases} \\
G^0 \bar{d}d : & \begin{cases} C^+ = \frac{em_d}{2M_W s_W} \left(1 + \delta Z_e - \frac{\delta M_W^2}{2M_W^2} - \frac{\delta s_W^2}{2s_W^2} + \frac{\delta m_d}{m_d} + \frac{\delta Z_{G^0}}{2} + \frac{\delta Z_d^L}{2} + \frac{\delta Z_d^R}{2} \right) \\ C^- = -\frac{em_d}{2M_W s_W} \left(1 + \delta Z_e - \frac{\delta M_W^2}{2M_W^2} - \frac{\delta s_W^2}{2s_W^2} + \frac{\delta m_d}{m_d} + \frac{\delta Z_{G^0}}{2} + \frac{\delta Z_d^L}{2} + \frac{\delta Z_d^R}{2} \right) \end{cases} \\
G^+ \bar{u}d : & \begin{cases} C^+ = -\frac{iem_d}{\sqrt{2}M_W s_W} \left(1 + \delta Z_e - \frac{\delta M_W^2}{2M_W^2} - \frac{\delta s_W^2}{2s_W^2} + \frac{\delta m_d}{m_d} + \frac{\delta Z_{G^\pm}}{2} + \frac{\delta Z_d^R}{2} + \frac{\delta Z_u^L}{2} \right) \\ C^- = \frac{iem_u}{\sqrt{2}M_W s_W} \left(1 + \delta Z_e - \frac{\delta M_W^2}{2M_W^2} - \frac{\delta s_W^2}{2s_W^2} + \frac{\delta m_u}{m_u} + \frac{\delta Z_{G^\pm}}{2} + \frac{\delta Z_d^L}{2} + \frac{\delta Z_u^R}{2} \right) \end{cases} \\
G^- \bar{d}u : & \begin{cases} C^+ = \frac{iem_u}{\sqrt{2}M_W s_W} \left(1 + \delta Z_e - \frac{\delta M_W^2}{2M_W^2} - \frac{\delta s_W^2}{2s_W^2} + \frac{\delta m_u}{m_u} + \frac{\delta Z_{G^\pm}}{2} + \frac{\delta Z_d^L}{2} + \frac{\delta Z_u^R}{2} \right) \\ C^- = -\frac{iem_d}{\sqrt{2}M_W s_W} \left(1 + \delta Z_e - \frac{\delta M_W^2}{2M_W^2} - \frac{\delta s_W^2}{2s_W^2} + \frac{\delta m_d}{m_d} + \frac{\delta Z_{G^\pm}}{2} + \frac{\delta Z_d^R}{2} + \frac{\delta Z_u^L}{2} \right) \end{cases} \\
H^+ \bar{u}d : & \begin{cases} C^+ = \frac{iem_d \xi_A^d}{\sqrt{2}M_W s_W} \left(1 + \delta Z_e - \frac{\delta M_W^2}{2M_W^2} - \frac{\delta s_W^2}{2s_W^2} + \frac{\delta m_d}{m_d} + \frac{\delta Z_{H^\pm}}{2} - \frac{\delta Z_{G^\pm H^\pm}}{2\xi_A^d} + \frac{\delta \xi_A^d}{\xi_A^d} + \frac{\delta Z_d^R}{2} + \frac{\delta Z_u^L}{2} \right) \\ C^- = \frac{iem_u \xi_A^u}{\sqrt{2}M_W s_W} \left(1 + \delta Z_e - \frac{\delta M_W^2}{2M_W^2} - \frac{\delta s_W^2}{2s_W^2} + \frac{\delta m_u}{m_u} + \frac{\delta Z_{H^\pm}}{2} + \frac{\delta Z_{G^\pm H^\pm}}{2\xi_A^u} + \frac{\delta \xi_A^u}{\xi_A^u} + \frac{\delta Z_d^L}{2} + \frac{\delta Z_u^R}{2} \right) \end{cases} \\
H^- \bar{d}u : & \begin{cases} C^+ = \frac{iem_u \xi_A^u}{\sqrt{2}M_W s_W} \left(1 + \delta Z_e - \frac{\delta M_W^2}{2M_W^2} - \frac{\delta s_W^2}{2s_W^2} + \frac{\delta m_u}{m_u} + \frac{\delta Z_{H^\pm}}{2} + \frac{\delta Z_{G^\pm H^\pm}}{2\xi_A^u} + \frac{\delta \xi_A^u}{\xi_A^u} + \frac{\delta Z_d^L}{2} + \frac{\delta Z_u^R}{2} \right) \\ C^- = \frac{iem_d \xi_A^d}{\sqrt{2}M_W s_W} \left(1 + \delta Z_e - \frac{\delta M_W^2}{2M_W^2} - \frac{\delta s_W^2}{2s_W^2} + \frac{\delta m_d}{m_d} + \frac{\delta Z_{H^\pm}}{2} - \frac{\delta Z_{G^\pm H^\pm}}{2\xi_A^d} + \frac{\delta \xi_A^d}{\xi_A^d} + \frac{\delta Z_d^R}{2} + \frac{\delta Z_u^L}{2} \right) \end{cases}
\end{aligned}$$

The effect of CKM mixing is neglected and the CKM matrix is approximated by the identity matrix in the vertices between the fermions and the charged scalars. The proportionality factors ξ_S^f are dependent on the specific versions of the THDM. The actual values can be found in Table 2.4. The corresponding counterterms are listed in Table A.1.

	type-I	type-II	type-X	type-Y
$\frac{\delta\xi_h^u}{\xi_h^u}$	$-C_\beta^2 \frac{\delta t_\beta}{t_\beta}$	$-C_\beta^2 \frac{\delta t_\beta}{t_\beta}$	$-C_\beta^2 \frac{\delta t_\beta}{t_\beta}$	$-C_\beta^2 \frac{\delta t_\beta}{t_\beta}$
$\frac{\delta\xi_h^d}{\xi_h^d}$	$-C_\beta^2 \frac{\delta t_\beta}{t_\beta}$	$S_\beta^2 \frac{\delta t_\beta}{t_\beta}$	$-C_\beta^2 \frac{\delta t_\beta}{t_\beta}$	$S_\beta^2 \frac{\delta t_\beta}{t_\beta}$
$\frac{\delta\xi_h^l}{\xi_h^l}$	$-C_\beta^2 \frac{\delta t_\beta}{t_\beta}$	$S_\beta^2 \frac{\delta t_\beta}{t_\beta}$	$S_\beta^2 \frac{\delta t_\beta}{t_\beta}$	$-C_\beta^2 \frac{\delta t_\beta}{t_\beta}$
$\frac{\delta\xi_H^u}{\xi_H^u}$	$-C_\beta^2 \frac{\delta t_\beta}{t_\beta}$	$-C_\beta^2 \frac{\delta t_\beta}{t_\beta}$	$-C_\beta^2 \frac{\delta t_\beta}{t_\beta}$	$-C_\beta^2 \frac{\delta t_\beta}{t_\beta}$
$\frac{\delta\xi_H^d}{\xi_H^d}$	$-C_\beta^2 \frac{\delta t_\beta}{t_\beta}$	$S_\beta^2 \frac{\delta t_\beta}{t_\beta}$	$-C_\beta^2 \frac{\delta t_\beta}{t_\beta}$	$S_\beta^2 \frac{\delta t_\beta}{t_\beta}$
$\frac{\delta\xi_H^l}{\xi_H^l}$	$-C_\beta^2 \frac{\delta t_\beta}{t_\beta}$	$S_\beta^2 \frac{\delta t_\beta}{t_\beta}$	$S_\beta^2 \frac{\delta t_\beta}{t_\beta}$	$-C_\beta^2 \frac{\delta t_\beta}{t_\beta}$
$\frac{\delta\xi_A^u}{\xi_A^u}$	$-C_\beta^2 \frac{\delta t_\beta}{t_\beta}$	$-C_\beta^2 \frac{\delta t_\beta}{t_\beta}$	$-C_\beta^2 \frac{\delta t_\beta}{t_\beta}$	$-C_\beta^2 \frac{\delta t_\beta}{t_\beta}$
$\frac{\delta\xi_A^d}{\xi_A^d}$	$-C_\beta^2 \frac{\delta t_\beta}{t_\beta}$	$S_\beta^2 \frac{\delta t_\beta}{t_\beta}$	$-C_\beta^2 \frac{\delta t_\beta}{t_\beta}$	$S_\beta^2 \frac{\delta t_\beta}{t_\beta}$
$\frac{\delta\xi_A^l}{\xi_A^l}$	$-C_\beta^2 \frac{\delta t_\beta}{t_\beta}$	$S_\beta^2 \frac{\delta t_\beta}{t_\beta}$	$S_\beta^2 \frac{\delta t_\beta}{t_\beta}$	$-C_\beta^2 \frac{\delta t_\beta}{t_\beta}$

Table A.1: Counterterms from the proportionality factors ξ_S^f in the different versions of the THDM

Feynman rules for the triple scalar couplings in the aligned THDM



$$C[h^0, h^0, h^0] = -\frac{3im_{h^0}^2}{v}$$

$$C[h^0, H^0, H^0] = -\frac{i(m_{h^0}^2 + 2m_{H^0}^2 - \lambda_5 v^2)}{v}$$

$$C[H^0, H^0, H^0] = -\frac{3i(\lambda_5 v^2 - 2m_{H^0}^2)}{vt_{2\beta}}$$

$$C[h^0, A^0, A^0] = -\frac{i(2m_{A^0}^2 + m_{h^0}^2 - \lambda_5 v^2)}{v}$$

$$C[H^0, A^0, A^0] = -\frac{i(\lambda_5 v^2 - 2m_{H^0}^2)}{vt_{2\beta}}$$

$$C[H^0, A^0, G^0] = -\frac{i(m_{A^0}^2 - m_{H^0}^2)}{v}$$

$$C[h^0, G^0, G^0] = -\frac{im_{h^0}^2}{v}$$

$$C[h^0, G^+, G^-] = -\frac{im_{h^0}^2}{v}$$

$$C[H^0, G^-, H^+] = \frac{i(m_{H^0}^2 - m_{H^\pm}^2)}{v}$$

$$C[A^0, G^-, H^+] = \frac{m_{H^\pm}^2 - m_{A^0}^2}{v}$$

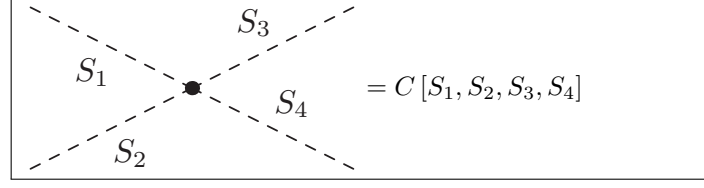
$$C[H^0, G^+, H^-] = \frac{i(m_{H^0}^2 - m_{H^\pm}^2)}{v}$$

$$C[A^0, G^+, H^-] = \frac{m_{A^0}^2 - m_{H^\pm}^2}{v}$$

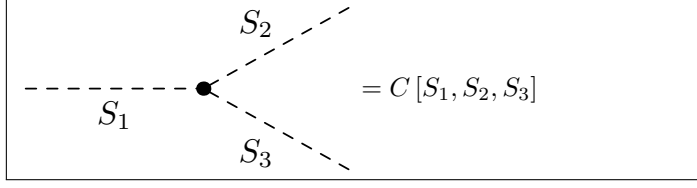
$$C[h^0, H^+, H^-] = -\frac{i(2m_{H^\pm}^2 + m_{h^0}^2 - \lambda_5 v^2)}{v}$$

$$C[H^0, H^+, H^-] = -\frac{i(\lambda_5 v^2 - 2m_{H^0}^2)}{vt_{2\beta}}$$

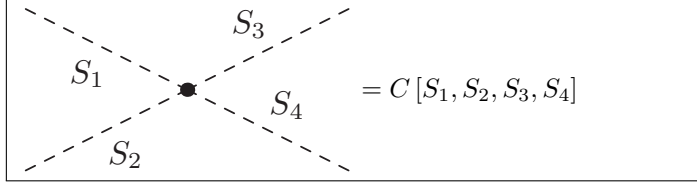
Feynman rules for the quartic scalar couplings in the aligned THDM



$$\begin{aligned}
 C[h^0, h^0, h^0, h^0] &= -\frac{3im_{h^0}^2}{v^2} \\
 C[h^0, h^0, H^0, H^0] &= -\frac{i(m_{h^0}^2 + 2m_{H^0}^2 - \lambda_5 v^2)}{v^2} \\
 C[h^0, H^0, H^0, H^0] &= -\frac{3i(\lambda_5 v^2 - 2m_{H^0}^2)}{v^2 t_{2\beta}} \\
 C[h^0, h^0, A^0, A^0] &= -\frac{i(2m_{A^0}^2 + m_{h^0}^2 - \lambda_5 v^2)}{v^2} \\
 C[h^0, h^0, H^+, H^-] &= -\frac{i(2m_{H^\pm}^2 + m_{h^0}^2 - \lambda_5 v^2)}{v^2} \\
 C[H^0, H^0, G^0, G^0] &= -\frac{i(2m_{A^0}^2 + m_{h^0}^2 - \lambda_5 v^2)}{v^2} \\
 C[H^0, H^0, G^+, G^-] &= -\frac{i(2m_{H^\pm}^2 + m_{h^0}^2 - \lambda_5 v^2)}{v^2} \\
 C[H^0, H^0, H^+, H^-] &= -\frac{i(m_{h^0}^2 t_{2\beta}^2 + 4m_{H^0}^2 - 2\lambda_5 v^2)}{v^2 t_{2\beta}^2} \\
 C[A^0, A^0, A^0, A^0] &= -\frac{3i(m_{h^0}^2 t_{2\beta}^2 + 4m_{H^0}^2 - 2\lambda_5 v^2)}{v^2 t_{2\beta}^2} \\
 C[H^+, H^+, H^-, H^-] &= -\frac{2i(m_{h^0}^2 t_{2\beta}^2 + 4m_{H^0}^2 - 2\lambda_5 v^2)}{v^2 t_{2\beta}^2} \\
 C[H^0, H^0, H^0, H^0] &= -\frac{3i(m_{h^0}^2 t_{2\beta}^2 + 4m_{H^0}^2 - 2\lambda_5 v^2)}{v^2 t_{2\beta}^2} \\
 C[A^0, A^0, H^+, H^-] &= -\frac{i(m_{h^0}^2 t_{2\beta}^2 + 4m_{H^0}^2 - 2\lambda_5 v^2)}{v^2 t_{2\beta}^2} \\
 C[H^0, H^0, A^0, A^0] &= -\frac{i(m_{h^0}^2 t_{2\beta}^2 + 4m_{H^0}^2 - 2\lambda_5 v^2)}{v^2 t_{2\beta}^2} \\
 C[A^0, A^0, G^0, G^0] &= -\frac{i(m_{h^0}^2 + 2m_{H^0}^2 - \lambda_5 v^2)}{v^2} \\
 C[A^0, A^0, G^+, G^-] &= -\frac{i(2m_{H^\pm}^2 + m_{h^0}^2 - \lambda_5 v^2)}{v^2} \\
 C[G^0, G^0, H^+, H^-] &= -\frac{i(2m_{H^\pm}^2 + m_{h^0}^2 - \lambda_5 v^2)}{v^2} \\
 C[G^+, G^-, H^+, H^-] &= -\frac{i(m_{A^0}^2 + m_{h^0}^2 + m_{H^0}^2 - \lambda_5 v^2)}{v^2} \\
 C[G^\mp, H^\pm, H^+, H^-] &= \frac{2i(\lambda_5 v^2 - 2m_{H^0}^2)}{v^2 t_{2\beta}} \\
 C[h^0, h^0, G^0, G^0] &= -\frac{im_{h^0}^2}{v^2} \\
 C[h^0, H^0, H^+, H^-] &= -\frac{i(\lambda_5 v^2 - 2m_{H^0}^2)}{v^2 t_{2\beta}} \\
 C[H^0, H^0, A^0, G^0] &= \frac{i(\lambda_5 v^2 - 2m_{H^0}^2)}{v^2 t_{2\beta}} \\
 C[h^0, h^0, G^+, G^-] &= -\frac{im_{h^0}^2}{v^2} \\
 C[h^0, H^0, A^0, A^0] &= -\frac{i(\lambda_5 v^2 - 2m_{H^0}^2)}{v^2 t_{2\beta}} \\
 C[h^0, H^0, A^0, G^0] &= -\frac{i(m_{A^0}^2 - m_{H^0}^2)}{v^2} \\
 C[h^0, H^0, G^\mp, H^\pm] &= \pm \frac{i(m_{H^0}^2 - m_{H^\pm}^2)}{v^2} \\
 C[H^0, G^0, G^\mp, H^\pm] &= \pm \frac{m_{H^\pm}^2 - m_{A^0}^2}{v^2} \\
 C[A^0, A^0, A^0, G^0] &= \frac{3i(\lambda_5 v^2 - 2m_{H^0}^2)}{v^2 t_{2\beta}} \\
 C[A^0, A^0, G^\mp, H^\pm] &= \frac{i(\lambda_5 v^2 - 2m_{H^0}^2)}{v^2 t_{2\beta}} \\
 C[A^0, G^0, G^\mp, H^\pm] &= -\frac{i(m_{H^0}^2 - m_{H^\pm}^2)}{v^2} \\
 C[A^0, G^0, H^+, H^-] &= \frac{i(\lambda_5 v^2 - 2m_{H^0}^2)}{v^2 t_{2\beta}} \\
 C[G^+, G^+, G^-, G^-] &= -\frac{2im_{h^0}^2}{v^2} \\
 C[G^\pm, G^\pm, H^\mp, H^\mp] &= \frac{2i(m_{A^0}^2 - m_{H^0}^2)}{v^2} \\
 C[G^0, G^0, G^0, G^0] &= -\frac{3im_{h^0}^2}{v^2} \\
 C[G^0, G^0, G^+, G^-] &= -\frac{im_{h^0}^2}{v^2} \\
 C[H^0, H^0, G^\mp, H^\pm] &= \frac{i(\lambda_5 v^2 - 2m_{H^0}^2)}{v^2 t_{2\beta}} \\
 C[h^0, A^0, G^\mp, H^\pm] &= \pm \frac{m_{H^\pm}^2 - m_{A^0}^2}{v^2}
 \end{aligned}$$

Feynman rules for the triple scalar couplings in the IHDM


$$\begin{aligned}
C[h^0, h^0, h^0] &= -\frac{3im_{h^0}^2}{v} & C[h^0, G^+, G^-] &= -\frac{im_{h^0}^2}{v} \\
C[h^0, H^0, H^0] &= -i\Lambda_{345}v & C[H^0, G^\mp, H^\pm] &= -\frac{i(m_{H^0}^2 - m_{H^\pm}^2)}{v} \\
C[h^0, A^0, A^0] &= -\frac{i(2m_{A^0}^2 - 2m_{H^0}^2 + \Lambda_{345}v^2)}{v} & C[A^0, G^\mp, H^\pm] &= \pm\frac{m_{H^\pm}^2 - m_{A^0}^2}{v} \\
C[H^0, A^0, G^0] &= \frac{i(m_{A^0}^2 - m_{H^0}^2)}{v} & C[h^0, G^0, G^0] &= -\frac{im_{h^0}^2}{v} \\
C[h^0, H^\pm, H^\mp] &= -\frac{i(2m_{H^\pm}^2 - 2m_{H^0}^2 + \Lambda_{345}v^2)}{v} & &
\end{aligned}$$

Feynman rules for the quartic scalar couplings in the IHDM


$$\begin{aligned}
C[h^0, h^0, h^0, h^0] &= -\frac{3im_{h^0}^2}{v^2} & C[H^0, H^0, H^0, H^0] &= -3i\Lambda_2 \\
C[h^0, h^0, H^0, H^0] &= -i\Lambda_{345} & C[H^0, H^0, A^0, A^0] &= -i\Lambda_2 \\
C[h^0, h^0, A^0, A^0] &= -\frac{i(2m_{A^0}^2 - 2m_{H^0}^2 + \Lambda_{345}v^2)}{v^2} & C[H^0, H^0, H^+, H^-] &= -i\Lambda_2 \\
C[h^0, H^0, A^0, G^0] &= \frac{i(m_{A^0}^2 - m_{H^0}^2)}{v^2} & C[A^0, A^0, A^0, A^0] &= -3i\Lambda_2 \\
C[h^0, H^0, G^\mp, H^\pm] &= -\frac{i(m_{H^0}^2 - m_{H^\pm}^2)}{v^2} & C[A^0, A^0, G^0, G^0] &= -i\Lambda_{345} \\
C[h^0, A^0, G^\mp, H^\pm] &= \pm\frac{m_{H^\pm}^2 - m_{A^0}^2}{v^2} & C[A^0, G^0, G^\mp, H^\pm] &= -\frac{i(m_{H^0}^2 - m_{H^\pm}^2)}{v^2} \\
C[h^0, h^0, H^+, H^-] &= -\frac{i(2m_{H^\pm}^2 - 2m_{H^0}^2 + \Lambda_{345}v^2)}{v^2} & C[A^0, A^0, H^+, H^-] &= -i\Lambda_2 \\
C[H^0, H^0, G^0, G^0] &= -\frac{i(2m_{A^0}^2 - 2m_{H^0}^2 + \Lambda_{345}v^2)}{v^2} & C[G^0, G^0, G^0, G^0] &= -\frac{3im_{h^0}^2}{v^2} \\
C[H^0, H^0, G^+, G^-] &= -\frac{i(2m_{H^\pm}^2 - 2m_{H^0}^2 + \Lambda_{345}v^2)}{v^2} & C[G^0, G^0, G^+, G^-] &= -\frac{im_{h^0}^2}{v^2} \\
C[H^0, G^0, G^\mp, H^\pm] &= \pm\frac{m_{A^0}^2 - m_{H^\pm}^2}{v^2} & C[G^+, G^+, G^-, G^-] &= -\frac{2im_{h^0}^2}{v^2} \\
C[A^0, A^0, G^+, G^-] &= -\frac{i(2m_{H^\pm}^2 - 2m_{H^0}^2 + \Lambda_{345}v^2)}{v^2} & C[G^\pm, G^\pm, H^\mp, H^\mp] &= \frac{2i(m_{A^0}^2 - m_{H^0}^2)}{v^2} \\
C[G^0, G^0, H^+, H^-] &= -\frac{i(2m_{H^\pm}^2 - 2m_{H^0}^2 + \Lambda_{345}v^2)}{v^2} & C[H^+, H^+, H^-, H^-] &= -2i\Lambda_2 \\
C[G^+, G^-, H^+, H^-] &= -\frac{i(m_{A^0}^2 - m_{H^0}^2 + \Lambda_{345}v^2)}{v^2} & C[h^0, h^0, G^0, G^0] &= -\frac{im_{h^0}^2}{v^2} \\
C[G^+, G^-, H^+, H^-] &= -\frac{i(m_{A^0}^2 - m_{H^0}^2 + \Lambda_{345}v^2)}{v^2} & C[h^0, h^0, G^+, G^-] &= -\frac{im_{h^0}^2}{v^2}
\end{aligned}$$

Appendix B

Loop integrals

In this section we present the analytic results for the expansion of the relevant one- and two-loop integrals. The integrals are expanded in

$$\delta = \frac{(D-4)}{2} \quad (\text{B.1})$$

and the divergences appear as poles in δ .

B.1 One-loop integrals

The analytic results for the divergent and finite terms of the scalar one-loop integrals were first derived in [171]. The expansion up to the terms linear in δ , which are needed in two-loop calculations, are given in [174]. The following expressions are taken from [175].

The scalar one-point integral is defined by

$$A_0(m^2) = \int \frac{d^D q}{(2\pi\mu)^{D-4} i\pi^2} \frac{1}{q^2 - m^2}. \quad (\text{B.2})$$

The expansion in δ yields

$$\begin{aligned} A_0(m^2) &= \frac{m^2}{\delta} + m^2 \left(C - \log\left(\frac{m^2}{\mu_D^2}\right) \right) \\ &\quad + \delta \cdot m^2 \left(\frac{\pi^2}{12} + \frac{1}{2} + \frac{1}{2} \left(\log\left(\frac{m^2}{\mu_D^2}\right) - C \right)^2 \right), \end{aligned} \quad (\text{B.3})$$

with

$$C = 1 - \gamma_E + \log(4\pi), \quad (\text{B.4})$$

where γ_E is the Euler-Mascheroni constant. A special case is

$$A_0(0) = 0. \quad (\text{B.5})$$

For the derivatives one obtains

$$\frac{\partial}{\partial m^2} A_0(m^2) = \frac{D/2 - 1}{m^2} A_0(m^2), \quad (\text{B.6})$$

$$\frac{\partial^2}{\partial (m^2)^2} A_0(m^2) = \frac{D/2 - 1}{m^4} \left(\frac{D}{2} - 2 \right) A_0(m^2). \quad (\text{B.7})$$

The scalar two point function is defined as

$$\begin{aligned} B_0(p^2, m_1^2, m_2^2) &= \int \frac{d^D q}{(2\pi\mu)^{D-4} i\pi^2} \frac{1}{[q^2 - m_1^2] [(q+p)^2 - m_2^2]} \\ &= \frac{1}{\delta} + B_0^{\text{fin}}(p^2, m_1^2, m_2^2) + \delta B_0^\delta(p^2, m_1^2, m_2^2). \end{aligned} \quad (\text{B.8})$$

The finite part is given by

$$\begin{aligned}
B_0^{\text{fin}}(p^2, m_1^2, m_2^2) &= \frac{(p^2 + m_1^2 - m_2^2)}{2p^2} \left(1 + C - \log \left(\frac{m_1^2}{\mu_D^2} \right) \right) \\
&+ \frac{(p^2 - m_1^2 + m_2^2)}{2p^2} \left(1 + C - \log \left(\frac{m_2^2}{\mu_D^2} \right) \right) \\
&+ \frac{R_0}{2p^2} \left[\log \left(\frac{1}{m_1^2 + m_2^2 - p^2 - R_0} \right) + \log (m_1^2 + m_2^2 - p^2 + R_0) \right]. \quad (\text{B.9})
\end{aligned}$$

The term linear in δ is

$$\begin{aligned}
B_0^\delta(p^2, m_1^2, m_2^2) &= 2 + \frac{\pi^2}{12} + \frac{1}{4p^2} (p^2 + m_1^2 - m_2^2) \left(1 + C - \log \left(\frac{m_1^2}{\mu_D^2} \right) \right)^2 \\
&+ \frac{1}{4p^2} (p^2 - m_1^2 + m_2^2) \left(1 + C - \log \left(\frac{m_2^2}{\mu_D^2} \right) \right)^2 \\
&+ \frac{R_0}{4p^2} \left[\left(\log (R_0 - m_1^2 + m_2^2 - p^2) - \log (R_0 + m_1^2 - m_2^2 + p^2) \right) \cdot \right. \\
&\quad \cdot \left(1 + C - \log \left(\frac{m_1^2}{\mu_D^2} \right) \right) \\
&\quad + \left(\log (R_0 + m_1^2 - m_2^2 - p^2) - \log (R_0 - m_1^2 + m_2^2 + p^2) \right) \cdot \\
&\quad \cdot \left(1 + C - \log \left(\frac{m_2^2}{\mu_D^2} \right) \right) \\
&\quad + \left(\log \left(\frac{1}{-R_0 + m_1^2 + m_2^2 - p^2} \right) + \log (R_0 + m_1^2 + m_2^2 - p^2) \right) \cdot \\
&\quad \cdot \left(1 + C - 2 \log \left(\frac{R_0}{\mu_D^2} \right) + \log \left(-\frac{p^2}{\mu_D^2} \right) \right) \\
&\quad \left. - 2 \left\{ \text{Li}_2 \left(\frac{R_0 + m_1^2 - m_2^2 + p^2}{2R_0} \right) - \text{Li}_2 \left(\frac{R_0 + m_1^2 - m_2^2 - p^2}{2R_0} \right) \right\} \right. \\
&\quad \left. - 2 \left\{ \text{Li}_2 \left(\frac{R_0 - m_1^2 + m_2^2 + p^2}{2R_0} \right) - \text{Li}_2 \left(\frac{R_0 - m_1^2 + m_2^2 - p^2}{2R_0} \right) \right\} \right]. \quad (\text{B.10})
\end{aligned}$$

For the above expressions the abbreviation

$$R_0 = \sqrt{m_1^4 + m_2^4 + p^4 - 2(m_1^2 p^2 + m_2^2 p^2 + m_2^2 m_1^2)} \quad (\text{B.11})$$

has been introduced.

Special cases for the two-point functions are

$$B_0(0, m_1^2, m_2^2) = \frac{A_0(m_1^2) - A_0(m_2^2)}{m_1^2 - m_2^2}, \quad (\text{B.12})$$

$$B_0(0, m^2, m^2) = \frac{D/2 - 1}{m^2} A_0(m^2). \quad (\text{B.13})$$

For the other scalar functions we have

$$B_1(p^2, m_1^2, m_2^2) = \frac{1}{2p^2} [A_0(m_1^2) - A_0(m_2^2) - (p^2 - m_2^2 + m_1^2) B_0(p^2, m_1^2, m_2^2)], \quad (\text{B.14})$$

$$B_1(0, m_1^2, m_2^2) = \frac{1}{2} B_0(0, m_1^2, m_2^2) - \frac{1}{2} (m_1^2 - m_2^2) \left. \frac{\partial}{\partial p^2} B_0(p^2, m_1^2, m_2^2) \right|_{p^2=0}, \quad (\text{B.15})$$

$$B_{00}(p^2, m_1^2, m_2^2) = \frac{1}{2(D-1)} \left[A_0(m_2^2) + 2m_1^2 B_0(p^2, m_1^2, m_2^2) + (p^2 + m_1^2 - m_2^2) B_1(p^2, m_1^2, m_2^2) \right], \quad (\text{B.16})$$

$$B_{00}(0, m_1^2, m_2^2) = \frac{1}{D} \left[\frac{m_1^2 A_0(m_1^2) - m_2^2 A_0(m_2^2)}{m_1^2 - m_2^2} \right], \quad (\text{B.17})$$

$$B_{00}(0, m^2, m^2) = \frac{A_0(m^2)}{2}. \quad (\text{B.18})$$

B.2 Two-loop integrals

For two-loop self-energy diagrams the reduction of tensor integrals and the definition of the resulting scalar two-loop integrals is given in [169]. As discussed in Chapter 3 the results of the self-energies can be expressed in terms of the scalar integrals given in (3.16). For vanishing external momentum the scalar integrals contain only the internal momenta k_1 , k_3 and k_4 from (3.17) and can be expressed in terms of products of one-loop integrals and the two-loop integral T_{134} from (3.21). Here we review the techniques for the reduction of the scalar integrals and give the analytic expression for the T_{134} integral, following the presentations in [175] and [268].

We introduce the notation

$$I(\nu_1, \nu_2, \nu_3; m_1, m_2, m_3) = T_{\underbrace{1 \dots 3}_{\nu_1} \dots \underbrace{4 \dots}_{\nu_2} \dots}_{\nu_3}(m_1^2, m_2^2, m_3^2) \\ = \int \int \frac{d^D q_1 d^D q_2}{(i\pi^2(2\pi\mu)^{D-4})^2} \frac{1}{[q_1^2 - m_1^2]^{\nu_1} [(q_2 - q_1)^2 - m_2^2]^{\nu_2} [q_2^2 - m_3^2]^{\nu_3}} \quad (\text{B.19})$$

for scalar integrals with vanishing external momentum and three different types of propagators. Relations between these type of scalar integrals can be derived with the integration-by-parts technique [269]. It leads to identities of the form

$$0 = \int d^D q \frac{\partial}{\partial q_\mu} f(q), \quad (\text{B.20})$$

which follow from the translation invariance of dimensionally regularized integrals

$$\int d^D q f(q) = \int d^D q f(q+k). \quad (\text{B.21})$$

For the integrals $I(\nu_1, \nu_2, \nu_3; m_1, m_2, m_3)$ the integration-by-parts method leads to the three independent relations

$$\int \int d^D q_1 d^D q_2 \frac{\partial}{\partial q_1^\mu} \left\{ \frac{q_1^\mu}{[q_1^2 - m_1^2]^{\nu_1} [(q_2 - q_1)^2 - m_2^2]^{\nu_2} [q_2^2 - m_3^2]^{\nu_3}} \right\} = 0, \\ \int \int d^D q_1 d^D q_2 \frac{\partial}{\partial q_2^\mu} \left\{ \frac{q_2^\mu}{[q_1^2 - m_1^2]^{\nu_1} [(q_2 - q_1)^2 - m_2^2]^{\nu_2} [q_2^2 - m_3^2]^{\nu_3}} \right\} = 0, \\ \int \int d^D q_1 d^D q_2 \frac{\partial}{\partial q_2^\mu} \left\{ \frac{q_1^\mu}{[q_1^2 - m_1^2]^{\nu_1} [(q_2 - q_1)^2 - m_2^2]^{\nu_2} [q_2^2 - m_3^2]^{\nu_3}} \right\} = 0. \quad (\text{B.22})$$

These relations result in the following system of equations:¹

$$\begin{aligned} & \begin{pmatrix} -2\nu_1 m_1^2 & -\nu_2(m_1^2 + m_2^2 - m_3^2) & 0 \\ 0 & \nu_2(m_1^2 + m_2^2 - m_3^2) & -\nu_3(m_1^2 - m_2^2 + m_3^2) \\ 0 & \nu_2(m_1^2 - m_2^2 - m_3^2) & -2\nu_3 m_3^2 \end{pmatrix} \cdot \begin{pmatrix} I(\nu_1 + 1, \nu_2, \nu_3) \\ I(\nu_1, \nu_2 + 1, \nu_3) \\ I(\nu_1, \nu_2, \nu_3 + 1) \end{pmatrix} \\ &= \begin{pmatrix} (-D + 2\nu_1 + \nu_2)I(\nu_1, \nu_2, \nu_3) - \nu_2 I(\nu_1, \nu_2 + 1, \nu_3 - 1) + \nu_2 I(\nu_1 - 1, \nu_2 + 1, \nu_3) \\ (\nu_3 - \nu_2)I(\nu_1, \nu_2, \nu_3) + \nu_3 I(\nu_1 - 1, \nu_2, \nu_3 + 1) - \nu_3 I(\nu_1, \nu_2 - 1, \nu_3 + 1) + F \\ (-D + 2\nu_3 + \nu_2)I(\nu_1, \nu_2, \nu_3) + \nu_2 I(\nu_1, \nu_2 + 1, \nu_3 - 1) - \nu_2 I(\nu_1 - 1, \nu_2 + 1, \nu_3) \end{pmatrix} \end{aligned} \quad (\text{B.23})$$

with

$$F = \nu_2 I(\nu_1, \nu_2 + 1, \nu_3 - 1) - \nu_2 I(\nu_1 - 1, \nu_2 + 1, \nu_3). \quad (\text{B.24})$$

The solution of these equations expresses integrals with $\nu_1 + \nu_2 + \nu_3 = s + 1$ in terms of integrals with $\nu_1 + \nu_2 + \nu_3 = s$.

For scalar two-loop integrals which contain only powers of two different propagators, additional relations can be obtained by taking the derivative of the integrals of lower rank with respect to the masses. The resulting expressions

$$T_{a^x b^y}(\underbrace{m_1^2, \dots, m_1^2}_x, \underbrace{m_2^2, \dots, m_2^2}_y) = \frac{x - 3 + \delta}{(1 - x)m_1^2} T_{a^{x-1} b^y}(\underbrace{m_1^2, \dots, m_1^2}_{x-1}, \underbrace{m_2^2, \dots, m_2^2}_y) \quad (\text{B.25})$$

for $x > 1, y \geq 1$,

$$T_{a^x b^y}(\underbrace{m_1^2, \dots, m_1^2}_x, \underbrace{m_2^2, \dots, m_2^2}_y) = \frac{y - 3 + \delta}{(1 - y)m_2^2} T_{a^x b^{y-1}}(\underbrace{m_1^2, \dots, m_1^2}_x, \underbrace{m_2^2, \dots, m_2^2}_{y-1}) \quad (\text{B.26})$$

for $x \geq 1, y > 1$,

with $a, b \in \{1, 3, 4\}$, can be applied iteratively until

$$T_{ab}(m_1^2, m_2^2) = A_0(m_1^2) A_0(m_2^2) \quad (\text{B.27})$$

is reached.

Partial fraction can be used to simplify integrals with propagators with the same loop-momentum but different masses, such that

$$T_{aa\dots}(m_1^2, m_2^2, \dots) = \frac{1}{m_1^2 - m_2^2} [T_{a\dots}(m_1^2, \dots) - T_{a\dots}(m_2^2, \dots)] \quad (\text{B.28})$$

for $m_1^2 \neq m_2^2$ and $a \in \{1, 3, 4\}$.

If the external momentum is equal to zero, the techniques described above reduce all the two-loop integrals to the scalar integral T_{134} from (3.21), which can be calculated analytically [177, 178]. The following compact expression is taken from [175]:

$$\begin{aligned} T_{134}(m_1^2, m_2^2, m_3^2) &= \frac{1 - \delta}{2(1 - 2\delta)} \left\{ \frac{[A_0(m_1^2)]^2}{m_1^2} + \frac{[A_0(m_2^2)]^2}{m_2^2} + \frac{[A_0(m_3^2)]^2}{m_3^2} \right\} \\ &\quad + \Phi^{\text{cyc}}(m_1^2, m_2^2, m_3^2). \end{aligned} \quad (\text{B.29})$$

¹The masses are omitted in the arguments.

The function Φ^{cyc} is defined by

$$\Phi^{\text{cyc}}(m^2, 0, 0) = m^2 \frac{\pi}{6}, \quad (\text{B.30})$$

$$\Phi^{\text{cyc}}(m_1^2, m_2^2, 0) = m_1^2 \text{Li}_2\left(\frac{m_1^2 - m_2^2}{m_1^2}\right) + m_2^2 \text{Li}_2\left(\frac{m_2^2 - m_1^2}{m_2^2}\right), \quad (\text{B.31})$$

$$\begin{aligned} \Phi^{\text{cyc}}(m_1^2, m_2^2, m_3^2) = & -\frac{m_1^2}{2} \log\left(\frac{m_1^2}{m_2^2}\right) \log\left(\frac{m_1^2}{m_2^2}\right) - \frac{m_2^2}{2} \log\left(\frac{m_2^2}{m_3^2}\right) \log\left(\frac{m_2^2}{m_1^2}\right) \\ & - m_3^2 \log\left(\frac{m_3^2}{m_1^2}\right) \log\left(\frac{m_3^2}{m_1^2}\right) \\ & + R \left[\frac{\pi^2}{6} - \frac{1}{2} \log\left(\frac{m_1^2}{m_2^2}\right) \log\left(\frac{m_2^2}{m_3^2}\right) \right. \\ & + \log\left(\frac{m_1^2 - m_2^2 + m_3^2 - R}{2m_3^2}\right) \log\left(\frac{m_2^2 - m_1^2 + m_3^2 - R}{2m_3^2}\right) \\ & \left. - \text{Li}_2\left(\frac{m_1^2 - m_2^2 + m_3^2 - R}{2m_3^2}\right) - \text{Li}_2\left(\frac{m_2^2 - m_1^2 + m_3^2 - R}{2m_3^2}\right) \right], \quad (\text{B.32}) \end{aligned}$$

with

$$R = \sqrt{m_1^4 + m_2^4 + m_3^4 - 2m_1^2 m_2^2 - 2m_2^2 m_3^2 - 2m_3^2 m_1^2}. \quad (\text{B.33})$$

Appendix C

Analytic results

The explicit results for the different non-standard corrections are presented in this appendix. The results are presented for a THDM in the alignment limit without Z_2 -violating terms of mass dimension four in the potential.

C.1 Non-standard one-loop corrections to the gauge boson selfenergies

The one-loop contributions to the gauge boson self-energies from the nonstandard scalars in the aligned THDM are presented in the following. The corresponding diagrams are shown in Figure 5.1 and Figure 6.1. The resulting expressions are

$$\Sigma_{W,NS}^{(1)}(p^2) = \frac{\alpha_{em}}{16\pi s_W^2} [2A_0(m_{H^\pm}^2) + A_0(m_{H^0}^2) + A_0(m_{A^0}^2) - 4B_{00}(p^2, m_{A^0}^2, m_{H^\pm}^2) - 4B_{00}(p^2, m_{H^0}^2, m_{H^\pm}^2)] \quad (C.1)$$

$$\Sigma_{Z,NS}^{(1)}(p^2) = \frac{\alpha_{em}}{16\pi c_W^2 s_W^2} [2(c_W^2 - s_W^2)^2 A_0(m_{H^\pm}^2) + A_0(m_{H^0}^2) + A_0(m_{A^0}^2) - 4((c_W^2 - s_W^2)^2 B_{00}(p^2, m_{H^\pm}^2, m_{H^\pm}^2) + B_{00}(p^2, m_{A^0}^2, m_{H^0}^2))] \quad (C.2)$$

$$\Sigma_{\gamma,NS}^{(1)}(p^2) = \frac{\alpha_{em}}{2\pi} [A_0(m_{H^\pm}^2) - 2B_{00}(p^2, m_{H^\pm}^2, m_{H^\pm}^2)] \quad (C.3)$$

$$\Sigma_{\gamma Z,NS}^{(1)}(p^2) = \frac{\alpha_{em} (c_W^2 - s_W^2)}{4\pi c_W s_W} [A_0(m_{H^\pm}^2) - 2B_{00}(p^2, m_{H^\pm}^2, m_{H^\pm}^2)] \quad (C.4)$$

From the result for the photon- Z -mixing we see that the additional non-standard contribution vanishes for $p^2 = 0$ since

$$B_{00}(0, m^2, m^2) = \frac{1}{2} A_0(m^2). \quad (C.5)$$

C.2 Two-loop corrections to the ρ parameter

In this appendix we give the full result for the non-standard two-loop corrections to the ρ parameter. The results are given for arbitrary space-time dimension D in terms of the scalar integrals $A_0(m^2)$ and $T_{134}(m_1^2, m_2^2, m_3^2)$. Following [118] we use the shorthand notation

$$\Delta_{i,j,k,l} = i + jD + kD^2 + lD^3, \quad \Delta_{i,j,k} = i + jD + kD^2. \quad (\text{C.6})$$

C.2.1 Non-standard corrections from the top-Yukawa coupling

The two-loop diagrams from Figure 5.9 with all possible insertions of the non-standard scalars for S and S' give the following contribution:

$$\begin{aligned} \delta\rho_{t,\text{NS}}^{(2\text{Loop})} &= \frac{\alpha_{em}^2}{128\pi^2 DM_W^4 s_W^4 t_\beta^2} \times \\ &\times \left[6(D-2)m_{H^\pm}^2 T_{134}(m_{H^\pm}^2, 0, 0) \right. \\ &+ \frac{3T_{134}(m_t^2, m_{A^0}^2, 0)}{(m_{A^0}^2 - m_{H^\pm}^2)^2} (m_{A^0}^2 - m_t^2) [(D-2)m_{H^\pm}^4 - 2m_{A^0}^2 (Dm_{H^\pm}^2 + 2m_t^2) + (D+2)m_{A^0}^4] \\ &+ \frac{3T_{134}(m_t^2, m_{H^0}^2, 0)}{(m_{H^0}^2 - m_{H^\pm}^2)^2} (m_{H^0}^2 - m_t^2) \times \\ &\times [(D+2)m_{H^0}^4 - 2m_{H^0}^2 (Dm_{H^\pm}^2 + 6m_t^2) + m_{H^\pm}^2 ((D-2)m_{H^\pm}^2 + 8m_t^2)] \\ &- 6T_{134}(m_t^2, m_t^2, m_{H^\pm}^2) \left(\frac{2m_t^2 m_{H^\pm}^2 (m_{H^\pm}^2 - 4m_t^2)}{(m_{H^0}^2 - m_{H^\pm}^2)^2} - \frac{2m_{H^\pm}^2 (m_{H^\pm}^2 - 4m_t^2)}{m_{H^0}^2 - m_{H^\pm}^2} \right. \\ &\quad \left. + \frac{2m_t^2 m_{H^\pm}^4}{(m_{A^0}^2 - m_{H^\pm}^2)^2} - \frac{2m_{H^\pm}^2 (m_{H^\pm}^2 - 2m_t^2)}{m_{A^0}^2 - m_{H^\pm}^2} \right. \\ &\quad \left. - (D-2)(m_{H^\pm}^2 - 2m_t^2) \right) \\ &- 3A_0(m_t^2)^2 \left(\frac{4(D-2)m_t^2 m_{A^0}^2}{(m_{A^0}^2 - 4m_t^2)(m_{A^0}^2 - m_{H^\pm}^2)} + \frac{(D-2)(m_{A^0}^2 + 4(D-3)m_t^2)}{m_{A^0}^2 - 4m_t^2} \right. \\ &\quad \left. - \frac{16(D-2)m_t^4}{(m_{A^0}^2 - m_{H^0}^2)(m_{A^0}^2 - 4m_t^2)} - \frac{(D-2)^2 m_t^2}{m_{A^0}^2 - 4m_t^2} \right. \\ &\quad \left. + \frac{(D-2)^2(D-1)m_t^2}{m_{H^0}^2 - 4m_t^2} + \frac{4(D-2)m_t^2}{m_{H^0}^2 - m_{H^\pm}^2} - D + 10 \right) \\ &- 3T_{134}(m_t^2, m_{H^\pm}^2, 0) \left(\frac{(D-2)(\Delta_{14,-5,1}m_t^4 - 12m_t^2 m_{H^\pm}^2 + 4m_{H^\pm}^4)}{m_{H^\pm}^2 - m_t^2} \right. \\ &\quad \left. + \frac{4}{(m_{A^0}^2 - m_{H^\pm}^2)^2} [m_{A^0}^2 (-Dm_t^2 m_{H^\pm}^2 + m_{H^\pm}^4 + m_t^4) \right. \\ &\quad \left. - m_{H^\pm}^4 (-Dm_t^2 + m_{H^\pm}^2 + m_t^2)] \right. \\ &\quad \left. + \frac{4}{(m_{H^0}^2 - m_{H^\pm}^2)^2} [m_{H^0}^2 (-(D+2)m_t^2 m_{H^\pm}^2 + m_{H^\pm}^4 + 3m_t^4) \right. \\ &\quad \left. + m_{H^\pm}^2 ((D+1)m_t^2 m_{H^\pm}^2 - m_{H^\pm}^4 - 2m_t^4)] \right) \\ &- 3T_{134}(m_t^2, m_t^2, m_{H^0}^2) \left(\frac{(D-2)m_t^2 (2\Delta_{-1,-2,1}m_t^2 - (D-2)m_{H^0}^2)}{m_{H^0}^2 - 4m_t^2} \right. \\ &\quad \left. + (D-2)(2(D-3)m_t^2 + m_{H^0}^2) + \frac{4m_{H^0}^2 (m_{H^0}^2 - 4m_t^2)}{m_{H^0}^2 - m_{H^\pm}^2} \right. \\ &\quad \left. - \frac{4m_t^2 (m_{H^0}^2 (m_{H^0}^2 - 2(D-3)m_t^2) - m_{A^0}^2 (m_{H^0}^2 - 2(D-1)m_t^2))}{(m_{A^0}^2 - m_{H^0}^2)^2} \right) \end{aligned}$$

$$\begin{aligned}
 & + \frac{4m_t^2}{(m_{H^0}^2 - m_{H^\pm}^2)^2} \left[m_{H^0}^2 (-Dm_{H^\pm}^2 - 2(D-3)m_t^2 + m_{H^\pm}^2) \right. \\
 & \quad \left. + 2(D-1)m_t^2 m_{H^\pm}^2 + (D-2)m_{H^0}^4 \right] \\
 - 3A_0(m_{A^0}^2) A_0(m_t^2) & \left(-\frac{4m_{A^0}^2(m_{A^0}^2 - m_{H^\pm}^2 + m_t^2)}{(m_{A^0}^2 - m_{H^\pm}^2)^2} - \frac{8m_t^2(-Dm_{A^0}^2 + m_{A^0}^2 + 2Dm_t^2)}{(m_{A^0}^2 - m_{H^0}^2)(m_{A^0}^2 - 4m_t^2)} \right. \\
 & + \frac{(D-2)^2 m_t^2}{m_{A^0}^2 - 4m_t^2} - \frac{(D-2)(m_{A^0}^2 + 4(D-3)m_t^2)}{m_{A^0}^2 - 4m_t^2} \\
 & - \frac{8m_t^2}{(m_{A^0}^2 - 4m_t^2)(m_{A^0}^2 - m_{H^\pm}^2)^2} \times \\
 & \times \left[m_{A^0}^2 (-Dm_{H^\pm}^2 - 2(D-2)m_t^2 + m_{H^\pm}^2) \right. \\
 & \quad \left. + (D-2)m_{A^0}^4 + 2Dm_t^2 m_{H^\pm}^2 \right] \\
 - 3T_{134}(m_t^2, m_t^2, m_{A^0}^2) & \left(\frac{(D-2)m_t^2(2(D-1)m_t^2 - (D-2)m_{A^0}^2)}{m_{A^0}^2 - 4m_t^2} \right. \\
 & + \frac{(D-2)m_{A^0}^2(m_{A^0}^2 + 2(D-5)m_t^2)}{m_{A^0}^2 - 4m_t^2} + \frac{4m_{A^0}^2(m_{A^0}^2 - 2m_t^2)}{m_{A^0}^2 - m_{H^\pm}^2} \\
 & + \frac{4m_t^2 m_{A^0}^2}{(m_{A^0}^2 - 4m_t^2)(m_{A^0}^2 - m_{H^\pm}^2)^2} \times \\
 & \times \left[-(D-1)m_{A^0}^2(m_{H^\pm}^2 + 2m_t^2) \right. \\
 & \quad \left. + (D-2)m_{A^0}^4 + 2(D+1)m_t^2 m_{H^\pm}^2 \right] \\
 & - \frac{4m_t^2 m_{A^0}^2}{(m_{A^0}^2 - m_{H^0}^2)^2(m_{A^0}^2 - 4m_t^2)} \times \\
 & \times \left[-m_{A^0}^2(m_{H^0}^2 - 2(D-7)m_t^2) + m_{A^0}^4 \right. \\
 & \quad \left. + 2m_t^2(8m_t^2 - (D-5)m_{H^0}^2) \right] \\
 - 3A_0(m_{H^0}^2) A_0(m_t^2) & \left(-\frac{8m_t^2((D-2)m_{H^0}^2 - Dm_{H^\pm}^2 + m_{H^\pm}^2)}{(m_{H^0}^2 - m_{H^\pm}^2)^2} \right. \\
 & - \frac{4(-m_{H^0}^2(m_{H^\pm}^2 + m_t^2) + 2m_t^2 m_{H^\pm}^2 + m_{H^0}^4)}{(m_{H^0}^2 - m_{H^\pm}^2)^2} \\
 & - \frac{8(D-1)m_t^2}{m_{A^0}^2 - m_{H^0}^2} - \frac{(D-2)^2(D-1)m_t^2}{m_{H^0}^2 - 4m_t^2} - D + 2 \Big) \\
 - \frac{3}{2}A_0(m_{H^\pm}^2) A_0(m_t^2) & \left(\frac{(2-D)m_t^2(\Delta_{4,-8,1}m_{H^\pm}^2 + 4Dm_t^2)}{m_{H^\pm}^2(m_{H^\pm} - m_t)(m_{H^\pm} + m_t)} \right. \\
 & - \frac{16m_t^2 m_{H^\pm}^2}{(m_{A^0}^2 - m_{H^\pm}^2)^2} - \frac{16m_t^2 m_{H^\pm}^2}{(m_{H^0}^2 - m_{H^\pm}^2)^2} \\
 & + \frac{8(m_{H^0}^2((D-3)m_t^2 + m_{H^\pm}^2) - m_{H^\pm}^2((D-4)m_t^2 + m_{H^\pm}^2))}{(m_{H^0}^2 - m_{H^\pm}^2)^2} \\
 & \left. + \frac{8(m_{A^0}^2((D-1)m_t^2 + m_{H^\pm}^2) - m_{H^\pm}^2((D-2)m_t^2 + m_{H^\pm}^2))}{(m_{A^0}^2 - m_{H^\pm}^2)^2} \right) \Big] \\
 & \tag{C.7}
 \end{aligned}$$

To obtain the finite result we need also the subloop renormalization from the diagrams in Figure 5.2 and Figure 5.3 with the counterterms calculated from the self-energies in Figure 5.5 and Figure 5.6. The corresponding result are given by

$$\delta\rho_{t,\text{NS}}^{(\text{CT})} = \frac{3\alpha_{em}^2 m_t^2}{16\pi^2 DM_W^4 s_W^4 t_\beta^2} \left[-\frac{1}{16} (D-4)(D-2)^2 A_0(m_t^2) \left(\text{Re}(B_1(m_t^2, m_{A_0}^2, m_t^2)) \right. \right. \\ \left. \left. + 2 \text{Re}(B_0(m_t^2, m_{H^0}^2, m_t^2)) + \text{Re}(B_1(m_t^2, m_{H^0}^2, m_t^2)) - \text{Re}(B_1(m_t^2, 0, m_{H^\pm}^2)) \right) \right] \quad (\text{C.8})$$

and

$$\delta\rho_{H,t}^{(\text{CT})} = \frac{3\alpha_{em}^2 m_t^2}{16\pi^2 DM_W^4 s_W^4 t_\beta^2} \times \\ \times \left[-\frac{1}{2} \left(\frac{A_0(m_{A_0}^2) (Dm_{H^0}^2 - (D-2)m_{A_0}^2) - 2m_{H^0}^2 A_0(m_{H^0}^2)}{(m_{A_0}^2 - m_{H^0}^2)^2} \right. \right. \\ \left. \left. + \frac{A_0(m_{A_0}^2) ((D-2)m_{A_0}^2 - Dm_{H^\pm}^2) + 2m_{H^\pm}^2 A_0(m_{H^\pm}^2)}{(m_{A_0}^2 - m_{H^\pm}^2)^2} \right) \times \right. \\ \left. [m_{A_0}^2 \text{Re}(B_1(m_{A_0}^2, m_t^2, m_t^2)) + \text{Re}(A_0(m_t^2))] \right. \\ \left. - \frac{1}{2} \left(\frac{A_0(m_{H^0}^2) (Dm_{A_0}^2 - (D-2)m_{H^0}^2) - 2m_{A_0}^2 A_0(m_{A_0}^2)}{(m_{A_0}^2 - m_{H^0}^2)^2} \right. \right. \\ \left. \left. + \frac{A_0(m_{H^0}^2) ((D-2)m_{H^0}^2 - Dm_{H^\pm}^2) + 2m_{H^\pm}^2 A_0(m_{H^\pm}^2)}{(m_{H^0}^2 - m_{H^\pm}^2)^2} \right) \times \right. \\ \left. \times [2m_t^2 \text{Re}(B_0(m_{H^0}^2, m_t^2, m_t^2)) + m_{H^0}^2 \text{Re}(B_1(m_{H^0}^2, m_t^2, m_t^2)) + \text{Re}(A_0(m_t^2))] \right. \\ \left. + \frac{D}{4} \left(\frac{2A_0(m_{H^\pm}^2) ((D-2)m_{H^\pm}^2 - Dm_{A_0}^2) + 4A_0(m_{A_0}^2) m_{A_0}^2}{D(m_{A_0}^2 - m_{H^\pm}^2)^2} \right. \right. \\ \left. \left. + \frac{2A_0(m_{H^\pm}^2) ((D-2)m_{H^\pm}^2 - Dm_{H^0}^2) + 4m_{H^0}^2 A_0(m_{H^0}^2) - (D-2)A_0(m_{H^\pm}^2)}{D(m_{H^0}^2 - m_{H^\pm}^2)^2} - \frac{(D-2)A_0(m_{H^\pm}^2)}{m_{H^\pm}^2} \right) \times \right. \\ \left. \times [m_{H^\pm}^2 \text{Re}(B_1(m_{H^\pm}^2, 0, m_t^2)) + (m_{H^\pm}^2 - m_t^2) \text{Re}(B_0(m_{H^\pm}^2, 0, m_t^2))] \right]. \quad (\text{C.9})$$

C.2.2 Scalar corrections from the interaction of the non-standard scalars

For the interaction between the non-standard scalars the result from the two-loop diagrams in Figure 5.12 reads

$$\delta\rho_{H,\text{NS}}^{(2\text{Loop})} = \frac{\alpha_{em}^2 \left(2m_{H^0}^2 - \frac{\lambda_5 M_W^2 s_W^2}{\pi\alpha} \right)^2}{64\pi^2 DM_W^4 s_W^4 t_\beta^2} \times \\ \times \left[\frac{m_{A_0}^2 T_{134}(m_{H^\pm}^2, m_{H^\pm}^2, m_{A_0}^2)}{(m_{A_0}^2 - m_{H^0}^2)^2} + \frac{2m_{A_0}^2 T_{134}(m_{H^0}^2, m_{H^0}^2, m_{A_0}^2)}{(m_{A_0}^2 - m_{H^0}^2)^2} \right. \\ \left. - \frac{2m_{H^\pm}^2 T_{134}(m_{H^\pm}^2, m_{H^0}^2, m_{H^0}^2)}{(m_{H^0}^2 - m_{H^\pm}^2)^2} - \frac{m_{H^0}^2 T_{134}(m_{H^\pm}^2, m_{H^0}^2, m_{A_0}^2)}{(m_{A_0}^2 - m_{H^\pm}^2)^2} \right. \\ \left. - \frac{m_{H^\pm}^2 T_{134}(m_{H^\pm}^2, m_{A_0}^2, m_{A_0}^2)}{2(m_{H^0}^2 - m_{H^\pm}^2)^2} - \frac{m_{H^\pm}^2 T_{134}(m_{H^\pm}^2, m_{H^\pm}^2, m_{H^\pm}^2)}{2(m_{H^0}^2 - m_{H^\pm}^2)^2} \right. \\ \left. + A_0(m_{H^0}^2)^2 \left(\frac{1}{(m_{H^0}^2 - m_{H^\pm}^2)^2} - \frac{1}{(m_{A_0}^2 - m_{H^0}^2)^2} \right) - \frac{A_0(m_{A_0}^2) A_0(m_{H^\pm}^2)}{(m_{A_0}^2 - m_{H^\pm}^2)^2} \right. \\ \left. + T_{134}(m_{H^0}^2, m_{H^0}^2, m_{H^0}^2) \left(-\frac{3(Dm_{A_0}^2 - (D-2)m_{H^0}^2)}{2(m_{A_0}^2 - m_{H^0}^2)^2} + \frac{3(Dm_{H^\pm}^2 - (D-2)m_{H^0}^2)}{2(m_{H^0}^2 - m_{H^\pm}^2)^2} \right) \right]$$

$$\begin{aligned}
 & + \frac{A_0(m_{H^0}^2)A_0(m_{A^0}^2)}{4m_{A^0}^2 - m_{H^0}^2} \left(\frac{(D-4)m_{H^0}^2 - (D-10)m_{A^0}^2}{(m_{A^0}^2 - m_{H^0}^2)^2} - \frac{(D-2)(m_{A^0}^2 - m_{H^0}^2)}{2(m_{H^0}^2 - m_{H^\pm}^2)(m_{A^0}^2 - m_{H^\pm}^2)} \right) \\
 & + \frac{A_0(m_{H^0}^2)A_0(m_{H^\pm}^2)}{m_{H^0}^2 - 4m_{H^\pm}^2} \left(\frac{(D-2)(3m_{A^0}^2 - m_{H^0}^2 - 2m_{H^\pm}^2)}{2(m_{A^0}^2 - m_{H^0}^2)(m_{A^0}^2 - m_{H^\pm}^2)} \right. \\
 & \quad \left. + \frac{((D-2)Dm_{H^0}^4 - 2\Delta_{10,-5,1}m_{H^0}^2m_{H^\pm}^2 + \Delta_{44,-8,1}m_{H^\pm}^4)}{4m_{H^\pm}^2(m_{H^0}^2 - m_{H^\pm}^2)^2} \right) \\
 & + \frac{A_0(m_{A^0}^2)^2}{4m_{A^0}^2 - m_{H^0}^2} \left(\frac{(D-6)m_{A^0}^2 - (D-3)m_{H^0}^2}{(m_{A^0}^2 - m_{H^0}^2)^2} \right. \\
 & \quad - \frac{1}{2(m_{H^0}^2 - m_{H^\pm}^2)(m_{A^0}^2 - m_{H^\pm}^2)^2} \times \\
 & \quad \times [m_{H^0}^2(-Dm_{H^\pm}^2 + m_{H^0}^2 + m_{H^\pm}^2) \\
 & \quad \quad \left. + m_{A^0}^2((D-6)m_{H^0}^2 + (D+2)m_{H^\pm}^2) - (D-2)m_{A^0}^4 \right] \\
 & + \frac{A_0(m_{H^\pm}^2)^2}{m_{H^0}^2 - 4m_{H^\pm}^2} \left(- \frac{(-2\Delta_{8,-5,1}m_{H^0}^2m_{H^\pm}^2 + \Delta_{28,-8,1}m_{H^\pm}^4 + (D-2)Dm_{H^0}^4)}{4m_{H^\pm}^2(m_{H^0}^2 - m_{H^\pm}^2)^2} \right. \\
 & \quad - \frac{1}{2(m_{A^0}^2 - m_{H^0}^2)(m_{A^0}^2 - m_{H^\pm}^2)^2} \times \\
 & \quad \times [m_{A^0}^2(-D(m_{H^0}^2 + 5m_{H^\pm}^2) + m_{H^0}^2 + 14m_{H^\pm}^2) \\
 & \quad \quad \left. + (D-2)(3m_{A^0}^4 + 2m_{H^\pm}^4) + (D-6)m_{H^0}^2m_{H^\pm}^2 + m_{H^0}^4 \right] \\
 & + \frac{T_{134}(m_{H^0}^2, m_{A^0}^2, m_{A^0}^2)}{2(4m_{A^0}^2 - m_{H^0}^2)} \left(\frac{(D-20)m_{A^0}^2m_{H^0}^2 + 20m_{A^0}^4 - (D-6)m_{H^0}^4}{(m_{A^0}^2 - m_{H^0}^2)^2} \right. \\
 & \quad + \frac{1}{(m_{H^0}^2 - m_{H^\pm}^2)^2(m_{A^0}^2 - m_{H^\pm}^2)^2} \times \\
 & \quad \times [4m_{A^0}^2m_{H^0}^2m_{H^\pm}^4 - 4m_{A^0}^2m_{H^0}^4m_{H^\pm}^2 + 6m_{A^0}^6m_{H^0}^2 \\
 & \quad \quad - 5m_{A^0}^4m_{H^0}^4 - 6m_{A^0}^4m_{H^0}^2m_{H^\pm}^2 + 6m_{A^0}^2m_{H^0}^6 + 2m_{A^0}^4m_{H^\pm}^4 \\
 & \quad \quad \left. - 2m_{A^0}^6m_{H^\pm}^2 - m_{H^0}^8 \right] \\
 & \quad \left. + \frac{D(m_{A^0}^2(m_{H^0}^2 - 4m_{H^\pm}^2) + 2m_{A^0}^4 + m_{H^0}^2m_{H^\pm}^2)}{(m_{H^\pm}^2 - m_{H^0}^2)(m_{A^0}^2 - m_{H^\pm}^2)} \right) \\
 & + \frac{T_{134}(m_{H^\pm}^2, m_{H^\pm}^2, m_{H^0}^2)}{2(m_{H^0}^2 - 4m_{H^\pm}^2)} \left(\frac{(\Delta_{9,1,-1}m_{H^0}^4 - 2\Delta_{14,1,-1}m_{H^0}^2m_{H^\pm}^2 + \Delta_{22,1,-1}m_{H^\pm}^4)}{(m_{H^0}^2 - m_{H^\pm}^2)^2} \right. \\
 & \quad + \frac{1}{(m_{A^0}^2 - m_{H^0}^2)^2(m_{A^0}^2 - m_{H^\pm}^2)^2} \times \\
 & \quad \times [2m_{A^0}^4m_{H^0}^2m_{H^\pm}^2 + 22m_{A^0}^2m_{H^0}^4m_{H^\pm}^2 + 6m_{A^0}^6m_{H^0}^2 \\
 & \quad \quad - 9m_{A^0}^4m_{H^0}^4 - 6m_{A^0}^6m_{H^\pm}^2 - 4m_{A^0}^2m_{H^\pm}^6 + m_{H^0}^8 \\
 & \quad \quad - 4m_{H^0}^4m_{H^\pm}^4 + 12m_{H^0}^2m_{H^\pm}^6 - 24m_{A^0}^2m_{H^0}^2m_{H^\pm}^4 \\
 & \quad \quad \left. + 10m_{A^0}^4m_{H^\pm}^4 - 6m_{H^0}^6m_{H^\pm}^2 \right] \\
 & \quad \left. - \frac{2D(m_{H^0}^2 - m_{H^\pm}^2)(-3m_{A^0}^2m_{H^\pm}^2 + m_{A^0}^4 + 2m_{H^\pm}^4)}{(m_{A^0}^2 - m_{H^0}^2)(m_{A^0}^2 - m_{H^\pm}^2)^2} \right) \Big].
 \end{aligned} \tag{C.10}$$

For the subloop renormalization the result from the diagrams in Figure 5.3 with the counterterms calculated from the diagrams in Figure 5.7 reads

$$\begin{aligned}
 \delta\rho_{\text{H,NS}}^{(\text{CT})} = & \frac{\alpha_{em}^2 \left(2m_{H^0}^2 - \frac{\lambda_5 M_W^2 s_W^2}{\pi\alpha} \right)^2}{256\pi^2 D M_W^4 s_W^4 t_{2\beta}^2} \times \\
 & \times \left[\frac{2 \operatorname{Re} \left(B_0 \left(m_{A^0}^2, m_{A^0}^2, m_{H^0}^2 \right) \right)}{\left(m_{A^0}^2 - m_{H^0}^2 \right)^2 \left(m_{A^0}^2 - m_{H^\pm}^2 \right)^2} \times \right. \\
 & \times \left[2 \left(m_{A^0}^2 - m_{H^0}^2 \right)^2 m_{H^\pm}^2 A_0 \left(m_{H^\pm}^2 \right) - 2m_{H^0}^2 A_0 \left(m_{H^0}^2 \right) \left(m_{A^0}^2 - m_{H^\pm}^2 \right)^2 \right. \\
 & \left. \left. + A_0 \left(m_{A^0}^2 \right) \left(m_{H^\pm}^2 - m_{H^0}^2 \right) \left(-(D-2)m_{A^0}^2 \left(m_{H^0}^2 + m_{H^\pm}^2 \right) + (D-4)m_{A^0}^4 + Dm_{H^0}^2 m_{H^\pm}^2 \right) \right] \right. \\
 & + \left(\frac{A_0 \left(m_{H^0}^2 \right) \left(Dm_{A^0}^2 - (D-2)m_{H^0}^2 \right) - 2m_{A^0}^2 A_0 \left(m_{A^0}^2 \right)}{\left(m_{A^0}^2 - m_{H^0}^2 \right)^2} \right. \\
 & \left. + \frac{A_0 \left(m_{H^0}^2 \right) \left((D-2)m_{H^0}^2 - Dm_{H^\pm}^2 \right) + 2m_{H^\pm}^2 A_0 \left(m_{H^\pm}^2 \right)}{\left(m_{H^0}^2 - m_{H^\pm}^2 \right)^2} \right) \times \\
 & \times \left[\operatorname{Re} \left(B_0 \left(m_{H^0}^2, m_{A^0}^2, m_{A^0}^2 \right) \right) + 9 \operatorname{Re} \left(B_0 \left(m_{H^0}^2, m_{H^0}^2, m_{H^0}^2 \right) \right) \right. \\
 & \left. + 2 \operatorname{Re} \left(B_0 \left(m_{H^0}^2, m_{H^\pm}^2, m_{H^\pm}^2 \right) \right) \right] \\
 & + \left(\frac{2A_0 \left(m_{H^\pm}^2 \right) \left((D-2)m_{H^\pm}^2 - Dm_{A^0}^2 \right) + 4A_0 \left(m_{A^0}^2 \right) m_{A^0}^2}{D \left(m_{A^0}^2 - m_{H^\pm}^2 \right)^2} \right. \\
 & \left. + \frac{2A_0 \left(m_{H^\pm}^2 \right) \left((D-2)m_{H^\pm}^2 - Dm_{H^0}^2 \right) + 4m_{H^0}^2 A_0 \left(m_{H^0}^2 \right)}{D \left(m_{H^0}^2 - m_{H^\pm}^2 \right)^2} \right. \\
 & \left. - \frac{(D-2)A_0 \left(m_{H^\pm}^2 \right)}{m_{H^\pm}^2} \right) D \operatorname{Re} \left(B_0 \left(m_{H^\pm}^2, m_{H^0}^2, m_{H^\pm}^2 \right) \right) \Big]. \tag{C.11}
 \end{aligned}$$

C.2.3 Scalar corrections from the interactions of the SM scalars with the non-standard scalars

The two-loop diagrams from Figure 5.13 result in the following expression

$$\begin{aligned}
 \delta\rho_{\text{H,Mix}}^{(2\text{Loop})} &= \frac{\alpha_{em}^2}{64\pi^2 DM_W^4 s_W^4} \times \\
 &\times \left[A_0(m_{A^0}^2) A_0(m_{H^0}^2) \left(3 - 2D + \frac{(2m_{A^0}^2 + m_{h^0}^2 - \lambda_5 v^2)(m_{h^0}^2 + 2m_{H^0}^2 - \lambda_5 v^2)}{(m_{A^0}^2 - m_{H^0}^2)^2} \right. \right. \\
 &\quad \left. \left. + \frac{1}{2(m_{H^0}^2 - m_{H^\pm}^2)(m_{A^0}^2 - m_{H^\pm}^2)} \times \right. \right. \\
 &\quad \times [-m_{A^0}^2(-D(2m_{H^0}^2 - 4m_{H^\pm}^2) + 2m_{H^0}^2 - 6m_{H^\pm}^2) \\
 &\quad \left. \left. + (3 - 2D)(2m_{H^0}^2 m_{H^\pm}^2 - 2m_{H^\pm}^4) - (2 - D)(m_{A^0}^4 + m_{H^0}^4) \right] \right) \\
 &+ T_{134}(m_{H^\pm}^2, m_{A^0}^2, 0) \left(\Delta_{3,2,-1} m_{A^0}^2 + \frac{3(m_{A^0}^2 - m_{H^\pm}^2)^2}{m_{h^0}^2} + m_{H^\pm}^2 \right. \\
 &\quad \left. - \frac{1}{(m_{A^0}^2 - m_{H^0}^2)(m_{H^0}^2 - m_{H^\pm}^2)} \times \right. \\
 &\quad \times [2m_{A^0}^4(m_{H^0}^2 - (2 - D)m_{H^\pm}^2) + (1 - D)m_{A^0}^6 \\
 &\quad - m_{H^\pm}^2(m_{H^0}^2 - m_{H^\pm}^2)(2m_{H^\pm}^2 - (4 - D)m_{H^0}^2) \\
 &\quad \left. + m_{A^0}^2((5 - D)m_{H^0}^4 - (14 - 3D)m_{H^0}^2 m_{H^\pm}^2 \right. \\
 &\quad \left. + (10 - 3D)m_{H^\pm}^4) \right] \Big) \\
 &+ T_{134}(m_{H^\pm}^2, m_{H^0}^2, 0) \left(\Delta_{3,2,-1} m_{H^0}^2 + \frac{3(m_{H^0}^2 - m_{H^\pm}^2)^2}{m_{h^0}^2} + m_{H^\pm}^2 \right. \\
 &\quad \left. + \frac{1}{(m_{A^0}^2 - m_{H^0}^2)(m_{A^0}^2 - m_{H^\pm}^2)} \times \right. \\
 &\quad \times [m_{A^0}^4((5 - D)m_{H^0}^2 + (4 - D)m_{H^\pm}^2) \\
 &\quad + m_{A^0}^2(-14 - 3D)m_{H^0}^2 m_{H^\pm}^2 - (6 - D)m_{H^\pm}^4 + 2m_{H^0}^4 \\
 &\quad + (1 - D)m_{H^0}^6 - 2(2 - D)m_{H^0}^4 m_{H^\pm}^2 \\
 &\quad \left. + (10 - 3D)m_{H^0}^2 m_{H^\pm}^4 + 2m_{H^\pm}^6] \right) \\
 &+ T_{134}(m_{H^\pm}^2, m_{H^0}^2, m_{h^0}^2) \left(-\frac{1}{m_{h^0}^2} [3(m_{H^0}^2 - m_{H^\pm}^2)^2 \right. \\
 &\quad \left. - 2(m_{h^0}^2(m_{H^0}^2 + m_{H^\pm}^2 - \lambda_5 v^2) + m_{h^0}^4)] \right. \\
 &\quad \left. - \frac{1}{(m_{H^0}^2 - m_{H^\pm}^2)^2} \times \right. \\
 &\quad \times [2(m_{h^0}^4(m_{H^0}^2 + m_{H^\pm}^2 - \lambda_5 v^2) + \lambda_5 v^2(m_{H^0}^2 - m_{H^\pm}^2)^2) + m_{h^0}^6 \\
 &\quad + m_{h^0}^2(-2(\lambda_5 v^2(m_{H^0}^2 + m_{H^\pm}^2) + m_{H^0}^4 + m_{H^\pm}^4) \\
 &\quad \left. + 8m_{H^0}^2 m_{H^\pm}^2 + \lambda_5^2 v^4)] \right) \\
 &+ T_{134}(m_{H^\pm}^2, m_{h^0}^2, m_{A^0}^2) \left(-\frac{1}{m_{h^0}^2} [3m_{A^0}^4 - 2m_{h^0}^4 + 3m_{H^\pm}^4 \right. \\
 &\quad \left. - 2(m_{A^0}^2(m_{h^0}^2 + 3m_{H^\pm}^2) + m_{h^0}^2(m_{H^\pm}^2 - \lambda_5 v^2))] \right. \\
 &\quad \left. - \frac{1}{(m_{A^0}^2 - m_{H^\pm}^2)^2} \times \right. \\
 &\quad \times [2m_{A^0}^2(m_{h^0}^2(4m_{H^\pm}^2 - \lambda_5 v^2) + m_{h^0}^4 - 2\lambda_5 v^2 m_{H^\pm}^2) \\
 &\quad + (m_{h^0}^2 - \lambda_5 v^2) \times \\
 &\quad \left. \times (-2(m_{A^0}^4 + m_{H^\pm}^4) + m_{h^0}^2(2m_{H^\pm}^2 - \lambda_5 v^2) + m_{h^0}^4) \right] \Big)
 \end{aligned}$$

$$\begin{aligned}
 & + T_{134} (m_{H^0}^2, m_{h^0}^2, m_{A^0}^2) \left(\frac{1}{m_{h^0}^2} [3 (m_{A^0}^4 + m_{H^0}^4) + 2\lambda_5 v^2 m_{h^0}^2 \right. \\
 & \quad \left. - 2 (m_{A^0}^2 (m_{h^0}^2 + 3m_{H^0}^2) + m_{h^0}^2 m_{H^0}^2 + m_{h^0}^4) \right] \\
 & \quad + \frac{1}{(m_{A^0}^2 - m_{H^0}^2)^2} \times \\
 & \quad \times [2m_{A^0}^2 (m_{h^0}^2 (4m_{H^0}^2 - \lambda_5 v^2) + m_{h^0}^4 - 2\lambda_5 v^2 m_{H^0}^2) \\
 & \quad + (m_{h^0}^2 - \lambda_5 v^2) \times \\
 & \quad \times (-2 (m_{A^0}^4 + m_{H^0}^4) + m_{h^0}^2 (2m_{H^0}^2 - \lambda_5 v^2) + m_{h^0}^4) \left. \right] \\
 & + T_{134} (m_{H^0}^2, m_{A^0}^2, 0) \left(2(3-D) (-m_{A^0}^2 - m_{H^0}^2) - \frac{3 (m_{A^0}^2 - m_{H^0}^2)^2}{m_{h^0}^2} \right. \\
 & \quad + \frac{1}{(m_{H^0}^2 - m_{H^\pm}^2) (m_{A^0}^2 - m_{H^\pm}^2)} \times \\
 & \quad \times [(1-D)m_{A^0}^6 - m_{A^0}^4 ((5-3D)m_{H^\pm}^2 - (3-D)m_{H^0}^2) \\
 & \quad + m_{A^0}^2 (2(2-D)m_{H^\pm}^4 + (3-D)(m_{H^0}^4 - 2m_{H^0}^2 m_{H^\pm}^2)) \\
 & \quad \left. + m_{H^0}^2 (m_{H^0}^2 - m_{H^\pm}^2) ((1-D)m_{H^0}^2 - 2(2-D)m_{H^\pm}^2) \right] \\
 & + A_0 (m_{H^0}^2)^2 \left(\frac{1}{2} (m_{h^0}^2 + 2m_{H^0}^2 - \lambda_5 v^2) \times \right. \\
 & \quad \times \left[\frac{-2m_{A^0}^2 - m_{h^0}^2 + \lambda_5 v^2}{(m_{A^0}^2 - m_{H^0}^2)^2} + \frac{m_{h^0}^2 + 2m_{H^\pm}^2 - \lambda_5 v^2}{(m_{H^0}^2 - m_{H^\pm}^2)^2} \right] \\
 & \quad - \frac{(D-2) (m_{A^0}^2 - m_{H^\pm}^2) (m_{h^0}^2 + 2m_{H^0}^2 - \lambda_5 v^2)^2}{2 (m_{H^0}^2 - m_{A^0}^2) (m_{h^0}^2 - 4m_{H^0}^2) (m_{H^0}^2 - m_{H^\pm}^2)} \\
 & + A_0 (m_{A^0}^2)^2 \left(\frac{(D-2) (m_{H^0}^2 - m_{H^\pm}^2) (2m_{A^0}^2 + m_{h^0}^2 - \lambda_5 v^2)^2}{2 (4m_{A^0}^2 - m_{h^0}^2) (m_{A^0}^2 - m_{H^0}^2) (m_{A^0}^2 - m_{H^\pm}^2)} \right. \\
 & \quad + \frac{1}{2} (2m_{A^0}^2 + m_{h^0}^2 - \lambda_5 v^2) \times \\
 & \quad \left. \left(\frac{-m_{h^0}^2 - 2m_{H^0}^2 + \lambda_5 v^2}{(m_{A^0}^2 - m_{H^0}^2)^2} + \frac{m_{h^0}^2 + 2m_{H^\pm}^2 - \lambda_5 v^2}{(m_{A^0}^2 - m_{H^\pm}^2)^2} \right) \right) \\
 & + A_0 (m_{H^\pm}^2)^2 \left(- \frac{(D-2) (m_{A^0}^2 + m_{H^0}^2 - 2m_{H^\pm}^2) (m_{h^0}^2 + 2m_{H^\pm}^2 - \lambda_5 v^2)^2}{2 (m_{H^\pm}^2 - m_{H^0}^2) (m_{H^\pm}^2 - m_{A^0}^2) (m_{h^0}^2 - 4m_{H^\pm}^2)} \right. \\
 & \quad + \frac{1}{2} (m_{h^0}^2 + 2m_{H^\pm}^2 - \lambda_5 v^2) \left(\frac{2m_{A^0}^2 + m_{h^0}^2 - \lambda_5 v^2}{(m_{A^0}^2 - m_{H^\pm}^2)^2} + \frac{m_{h^0}^2 + 2m_{H^0}^2 - \lambda_5 v^2}{(m_{H^0}^2 - m_{H^\pm}^2)^2} \right) \\
 & \quad - \frac{(D-2)D (m_{h^0}^2 - \lambda_5 v^2)^2}{4m_{H^\pm}^2 (m_{h^0}^2 - 4m_{H^\pm}^2)} - \frac{(D-2)D (m_{h^0}^2 + m_{H^\pm}^2 - \lambda_5 v^2)}{m_{h^0}^2 - 4m_{H^\pm}^2} + \frac{2D-4}{3-D} \\
 & + T_{134} (m_{H^0}^2, m_{H^0}^2, m_{h^0}^2) \left(\frac{(m_{h^0}^2 + 2m_{H^0}^2 - \lambda_5 v^2)^2}{m_{h^0}^2 - 4m_{H^0}^2} \times \right. \\
 & \quad \times \left[\frac{(D-3)m_{H^0}^4 - (D+1)m_{H^0}^2 m_{H^\pm}^2 + m_{h^0}^2 m_{H^\pm}^2}{(m_{H^0}^2 - m_{H^\pm}^2)^2} \right. \\
 & \quad \left. - \frac{m_{A^0}^2 (m_{h^0}^2 - (D+1)m_{H^0}^2) + (D-3)m_{H^0}^4}{(m_{A^0}^2 - m_{H^0}^2)^2} \right] \\
 & \quad + \frac{1}{2} (m_{h^0}^2 + 2m_{H^0}^2 - \lambda_5 v^2) \times \\
 & \quad \times \left[\frac{(2m_{H^0}^2 - m_{h^0}^2) (2m_{A^0}^2 + m_{h^0}^2 - \lambda_5 v^2)}{(m_{A^0}^2 - m_{H^0}^2)^2} \right]
 \end{aligned}$$

$$\begin{aligned}
 & + \frac{(m_{h^0}^2 - 2m_{H^0}^2)(m_{h^0}^2 + 2m_{H^\pm}^2 - \lambda_5 v^2)}{(m_{H^0}^2 - m_{H^\pm}^2)^2} \Big] \Big) \\
 + T_{134}(m_{h^0}^2, m_{A^0}^2, m_{A^0}^2) & \left(\frac{(m_{H^0}^2 - m_{H^\pm}^2)(2m_{A^0}^2 + m_{h^0}^2 - \lambda_5 v^2)^2}{(4m_{A^0}^2 - m_{h^0}^2)(m_{A^0}^2 - m_{H^0}^2)^2(m_{A^0}^2 - m_{H^\pm}^2)^2} \times \right. \\
 & \times [m_{A^0}^4(m_{h^0}^2 - (D-3)(m_{H^0}^2 + m_{H^\pm}^2)) + (D+1)m_{A^0}^2 m_{H^0}^2 m_{H^\pm}^2 \\
 & \quad + (D-7)m_{A^0}^6 - m_{h^0}^2 m_{H^0}^2 m_{H^\pm}^2] \\
 & + \frac{1}{2}(2m_{A^0}^2 + m_{h^0}^2 - \lambda_5 v^2) \times \\
 & \times \left[\frac{(2m_{A^0}^2 - m_{h^0}^2)(m_{h^0}^2 + 2m_{H^0}^2 - \lambda_5 v^2)}{(m_{A^0}^2 - m_{H^0}^2)^2} \right. \\
 & \quad \left. + \frac{(m_{h^0}^2 - 2m_{A^0}^2)(m_{h^0}^2 + 2m_{H^\pm}^2 - \lambda_5 v^2)}{(m_{A^0}^2 - m_{H^\pm}^2)^2} \right] \Big) \\
 + T_{134}(m_{H^\pm}^2, m_{H^\pm}^2, m_{h^0}^2) & \left(\frac{(m_{h^0}^2 + 2m_{H^\pm}^2 - \lambda_5 v^2)^2}{2(m_{h^0}^2 - 4m_{H^\pm}^2)} \times \right. \\
 & \times \left[\frac{2(m_{A^0}^2(m_{h^0}^2 - (D+1)m_{H^\pm}^2) + (D-3)m_{H^\pm}^4)}{(m_{A^0}^2 - m_{H^\pm}^2)^2} - (D-3)D \right. \\
 & \quad \left. + \frac{2(m_{H^\pm}^2((D-3)m_{H^\pm}^2 - (D+1)m_{H^0}^2) + m_{h^0}^2 m_{H^0}^2)}{(m_{H^0}^2 - m_{H^\pm}^2)^2} \right] \\
 & + \frac{1}{2}(m_{h^0}^2 + 2m_{H^\pm}^2 - \lambda_5 v^2) \times \\
 & \times \left[\frac{(m_{h^0}^2 - 2m_{H^\pm}^2)(2m_{A^0}^2 + m_{h^0}^2 - \lambda_5 v^2)}{(m_{A^0}^2 - m_{H^\pm}^2)^2} \right. \\
 & \quad \left. + \frac{(m_{h^0}^2 - 2m_{H^\pm}^2)(m_{h^0}^2 + 2m_{H^0}^2 - \lambda_5 v^2)}{(m_{H^0}^2 - m_{H^\pm}^2)^2} - 4 \right] \Big) \\
 + A_0(m_{A^0}^2) A_0(m_{H^\pm}^2) & \left(- \frac{D((2-D)m_{A^0}^2 - Dm_{H^\pm}^2)}{4m_{H^\pm}^2} \right. \\
 & - \frac{(2m_{A^0}^2 + m_{h^0}^2 - \lambda_5 v^2)(m_{h^0}^2 + 2m_{H^\pm}^2 - \lambda_5 v^2)}{(m_{A^0}^2 - m_{H^\pm}^2)^2} \\
 & - \frac{1}{2(m_{A^0}^2 - m_{H^0}^2)(m_{H^0}^2 - m_{H^\pm}^2)} \times \\
 & \times [m_{A^0}^2((4-D)m_{H^0}^2 - Dm_{H^\pm}^2) - (2-D)(m_{A^0}^4 + 2m_{H^\pm}^4) \\
 & \quad \left. - 2(3-D)m_{H^0}^4 + (8-3D)m_{H^0}^2 m_{H^\pm}^2] \right) \\
 + A_0(m_{H^0}^2) A_0(m_{H^\pm}^2) & \left(- \frac{D((2-D)m_{H^0}^2 - Dm_{H^\pm}^2)}{4m_{H^\pm}^2} \right. \\
 & - \frac{(m_{h^0}^2 + 2m_{H^0}^2 - \lambda_5 v^2)(m_{h^0}^2 + 2m_{H^\pm}^2 - \lambda_5 v^2)}{(m_{H^0}^2 - m_{H^\pm}^2)^2} \\
 & + \frac{1}{2(m_{A^0}^2 - m_{H^0}^2)(m_{A^0}^2 - m_{H^\pm}^2)} \times \\
 & \times [m_{A^0}^2((4-D)m_{H^0}^2 + (8-3D)m_{H^\pm}^2) \\
 & \quad \left. - 2(3-D)m_{A^0}^4 - Dm_{H^0}^2 m_{H^\pm}^2 \right. \\
 & \quad \left. - (2-D)(m_{H^0}^4 + 2m_{H^\pm}^4) \right] \Big) \\
 + A_0(m_{A^0}^2) A_0(m_{h^0}^2) & \left(\frac{-2(m_{A^0}^2 - m_{H^0}^2) + 2(m_{A^0}^2 - m_{H^\pm}^2) + m_{H^0}^2 - m_{H^\pm}^2}{m_{h^0}^2} \right)
 \end{aligned}$$

$$\begin{aligned}
 & + \frac{1}{4(4m_{A^0}^2 - m_{h^0}^2)(m_{A^0}^2 - m_{H^0}^2)} \times \\
 & \times [m_{A^0}^2((20 - 6D)m_{h^0}^2 - 4(4 - D)\lambda_5 v^2) \\
 & \quad + (m_{h^0}^2 - \lambda_5 v^2)((4 - 3D)m_{h^0}^2 - 2(2 - D)\lambda_5 v^2)] \\
 & - \frac{1}{4(4m_{A^0}^2 - m_{h^0}^2)(m_{A^0}^2 - m_{H^\pm}^2)} \times \\
 & \times [2m_{A^0}^2((10 - 3D)m_{h^0}^2 - 2(4 - D)\lambda_5 v^2) \\
 & \quad + (m_{h^0}^2 - \lambda_5 v^2)((4 - 3D)m_{h^0}^2 - 2(2 - D)\lambda_5 v^2)] \\
 & + A_0(m_{H^0}^2) A_0(m_{h^0}^2) \left(\frac{2(m_{A^0}^2 - m_{H^0}^2) + m_{A^0}^2 - m_{H^\pm}^2 + 2(m_{H^0}^2 - m_{H^\pm}^2)}{m_{h^0}^2} \right. \\
 & \quad + \frac{1}{4(m_{A^0}^2 - m_{H^0}^2)(m_{h^0}^2 - 4m_{H^0}^2)} \times \\
 & \quad \times [m_{h^0}^2((20 - 6D)m_{H^0}^2 - (8 - 5D)\lambda_5 v^2) \\
 & \quad \quad + (4 - 3D)m_{h^0}^4 + 2\lambda_5 v^2((2 - D)\lambda_5 v^2 - 2(4 - D)m_{H^0}^2)] \\
 & \quad + \frac{1}{4(m_{h^0}^2 - 4m_{H^0}^2)(m_{H^0}^2 - m_{H^\pm}^2)} \times \\
 & \quad \times [m_{h^0}^2((20 - 6D)m_{H^0}^2 - (8 - 5D)\lambda_5 v^2) \\
 & \quad \quad + (4 - 3D)m_{h^0}^4 + 2\lambda_5 v^2((2 - D)\lambda_5 v^2 - 2(4 - D)m_{H^0}^2)] \Big) \\
 & + A_0(m_{H^\pm}^2) A_0(m_{h^0}^2) \left(\frac{1}{m_{h^0}^2} [-2(m_{A^0}^2 - m_{H^\pm}^2) - m_{A^0}^2 - m_{H^0}^2 \right. \\
 & \quad \quad \left. + 2m_{H^\pm}^2 - 2(m_{H^0}^2 - m_{H^\pm}^2)] \right. \\
 & \quad - \frac{D(2 - D)}{8m_{H^\pm}^2(m_{h^0}^2 - 4m_{H^\pm}^2)} (3m_{h^0}^2 - 2\lambda_5 v^2)(m_{h^0}^2 + 2m_{H^\pm}^2 - \lambda_5 v^2) \\
 & \quad - \frac{1}{4(m_{A^0}^2 - m_{H^\pm}^2)(m_{h^0}^2 - 4m_{H^\pm}^2)} \times \\
 & \quad \times [m_{h^0}^2((20 - 6D)m_{H^\pm}^2 - (8 - 5D)\lambda_5 v^2) \\
 & \quad \quad + (4 - 3D)m_{h^0}^4 + 2\lambda_5 v^2((2 - D)\lambda_5 v^2 - 2(4 - D)m_{H^\pm}^2)] \\
 & \quad - \frac{1}{4(m_{H^0}^2 - m_{H^\pm}^2)(m_{h^0}^2 - 4m_{H^\pm}^2)} \times \\
 & \quad \times [m_{h^0}^2((20 - 6D)m_{H^\pm}^2 - (8 - 5D)\lambda_5 v^2) + (4 - 3D)m_{h^0}^4 \\
 & \quad \quad \left. + 2\lambda_5 v^2((2 - D)\lambda_5 v^2 - 2(4 - D)m_{H^\pm}^2)] \Big) \right]. \tag{C.12}
 \end{aligned}$$

The diagrams from Figure 5.3 with the counterterms calculated from Figure 5.8 leads to

$$\begin{aligned}
 \delta\rho_{\text{H,Mix}}^{(\text{CT})} = & \frac{\alpha_{em}^2}{256\pi^2 M_W^4 s_W^4} \times \\
 & \times \left[\frac{1}{D} \left(\frac{A_0(m_{A^0}^2) (Dm_{H^0}^2 - (D-2)m_{A^0}^2) - 2m_{H^0}^2 A_0(m_{H^0}^2)}{(m_{A^0}^2 - m_{H^0}^2)^2} \right. \right. \\
 & \quad \left. \left. + \frac{A_0(m_{A^0}^2) ((D-2)m_{A^0}^2 - Dm_{H^\pm}^2) + 2m_{H^\pm}^2 A_0(m_{H^\pm}^2)}{(m_{A^0}^2 - m_{H^\pm}^2)^2} \right) \times \right. \\
 & \times \left[\text{Re}(A_0(m_{h^0}^2)) (2m_{A^0}^2 + m_{h^0}^2 - \lambda_5 v^2) \right. \\
 & \quad + 2((2m_{A^0}^2 + m_{h^0}^2 - \lambda_5 v^2)^2 \text{Re}(B_0(m_{A^0}^2, m_{A^0}^2, m_{h^0}^2))) \\
 & \quad \left. + (m_{A^0}^2 - m_{H^0}^2)^2 \text{Re}(B_0(m_{A^0}^2, 0, m_{H^0}^2)) + 2(m_{A^0}^2 - m_{H^\pm}^2)^2 \text{Re}(B_0(m_{A^0}^2, 0, m_{H^\pm}^2)) \right] \\
 & + \frac{1}{D} \left(\frac{A_0(m_{H^0}^2) (Dm_{A^0}^2 - (D-2)m_{H^0}^2) - 2m_{A^0}^2 A_0(m_{A^0}^2)}{(m_{A^0}^2 - m_{H^0}^2)^2} \right. \\
 & \quad \left. + \frac{A_0(m_{H^0}^2) ((D-2)m_{H^0}^2 - Dm_{H^\pm}^2) + 2m_{H^\pm}^2 A_0(m_{H^\pm}^2)}{(m_{H^0}^2 - m_{H^\pm}^2)^2} \right) \times \\
 & \times \left[\text{Re}(A_0(m_{h^0}^2)) (m_{h^0}^2 + 2m_{H^0}^2 - \lambda_5 v^2) + 2((m_{A^0}^2 - m_{H^0}^2)^2 \text{Re}(B_0(m_{H^0}^2, 0, m_{A^0}^2))) \right. \\
 & \quad + (m_{h^0}^2 + 2m_{H^0}^2 - \lambda_5 v^2)^2 \text{Re}(B_0(m_{H^0}^2, m_{h^0}^2, m_{H^0}^2)) \\
 & \quad \left. + 2(m_{H^0}^2 - m_{H^\pm}^2)^2 \text{Re}(B_0(m_{H^0}^2, 0, m_{H^\pm}^2)) \right] \\
 & + \frac{1}{2} \left(\frac{2A_0(m_{H^\pm}^2) ((D-2)m_{H^\pm}^2 - Dm_{A^0}^2) + 4A_0(m_{A^0}^2) m_{A^0}^2}{D(m_{A^0}^2 - m_{H^\pm}^2)^2} \right. \\
 & \quad \left. + \frac{2A_0(m_{H^\pm}^2) ((D-2)m_{H^\pm}^2 - Dm_{H^0}^2) + 4m_{H^0}^2 A_0(m_{H^0}^2)}{D(m_{H^0}^2 - m_{H^\pm}^2)^2} - \frac{(D-2)A_0(m_{H^\pm}^2)}{m_{H^\pm}^2} \right) \times \\
 & \times \left[\text{Re}(A_0(m_{h^0}^2)) (m_{h^0}^2 + 2m_{H^\pm}^2 - \lambda_5 v^2) + 2((m_{A^0}^2 - m_{H^\pm}^2)^2 \text{Re}(B_0(m_{H^\pm}^2, 0, m_{A^0}^2))) \right. \\
 & \quad + (m_{h^0}^2 + 2m_{H^\pm}^2 - \lambda_5 v^2)^2 \text{Re}(B_0(m_{H^\pm}^2, m_{h^0}^2, m_{H^\pm}^2)) \\
 & \quad \left. + (m_{H^0}^2 - m_{H^\pm}^2)^2 \text{Re}(B_0(m_{H^\pm}^2, 0, m_{H^0}^2)) \right] \Big]. \tag{C.13}
 \end{aligned}$$

List of Figures

3.1	Topologies for the two-loop self-energy diagrams	23
4.1	Generic diagrams of the gauge-boson self-energies with vertex counterterm insertions for internal scalars or fermions.	31
5.1	Non-standard contributions from the THDM scalars to the Z and W boson self-energies in the alignment limit at the one-loop level.	46
5.2	Generic diagrams for the gauge-boson self-energies containing quarks with counterterm insertions.	49
5.3	Generic diagrams for the gauge-boson self-energies containing scalars with counterterm insertions.	50
5.4	One-loop diagrams for the standard contribution to the quark mass counterterms.	51
5.5	One-loop diagrams for the non-standard contribution to the quark mass counterterms.	51
5.6	One-loop diagrams for the Yukawa contribution to the non-standard scalar mass counterterms.	52
5.7	One-loop diagrams for the non-standard scalar mass counterterms from the interaction between the non-standard scalars.	52
5.8	One-loop diagrams for the non-standard scalar mass counterterms from the interaction between the SM-like scalars and the non-standard scalars.	53
5.9	Generic two-loop diagrams for the top-Yukawa corrections to the vector boson self-energies.	53
5.10	Generic two-loop diagrams for the top-Yukawa contribution to the Goldstone boson self-energies.	54
5.11	Corrections from the quartic couplings between four non-standard scalars.	55
5.12	Generic two-loop diagrams for the vector-boson self-energies from the interaction between the non-standard scalars.	55
5.13	Generic two-loop diagrams from the interaction between the SM-like scalars and the non-standard scalars.	56
5.14	Analysis of $\delta\rho_{t,\text{NS}}^{(2)}$	58
5.15	Comparison between $\delta\rho_{t,\text{NS}}^{(2)}$ and $\delta\rho_{tb,\text{NS}}^{(2)}$ in the THDM of type-II and type-Y.	59
5.16	Effect of mass differences between neutral and charged scalars on $\delta\rho_{H,\text{NS}}^{(2)}$	59
5.17	Influence of a variation of t_β on $\delta\rho_{H,\text{NS}}^{(2)}$	60
5.18	Influence of mass splitting between charged and neutral scalars on $\delta\rho_{H,\text{Mix}}^{(2)}$	61
5.19	Results for the two-loop corrections to the ρ parameter in the IHDM.	62
6.1	Non-standard contributions to the photon self-energy and $\gamma - Z$ mixing from the charged scalars in the alignment limit	67
7.1	Feynman diagrams for the process $e^+e^- \rightarrow f\bar{f}$ at the tree-level.	72
7.2	Higher-order corrections to the $Z \rightarrow f\bar{f}$ decay.	75
8.1	Influence of the reducible two-loop corrections on M_W	87
8.2	Influence of the reducible two-loop corrections on s_l^2 and Γ_Z	88
8.3	Results of M_W (upper row), s_l^2 (middle row) and Γ_Z (lower row) for a variation of m_{H^\pm}	89

8.4	Influence of t_β and λ_5 on the theoretical prediction of M_W , s_l^2 and Γ_Z	91
8.5	Influence of m_{H^\pm} and t_β on the theoretical prediction of M_W , s_l^2 and Γ_Z	93
8.6	Results of M_W (upper row), s_l^2 (middle row) and Γ_Z (lower row) for a light A^0 . . .	94
8.7	Prediction of M_W , s_l^2 and Γ_Z for a light A^0 in the t_β - λ_5 -plane and the m_{H^\pm} - t_β -plane.	96
8.8	Prediction of M_W , s_l^2 and Γ_Z for a variation of t_β in the CP -overlap benchmark scenario	97
8.9	Results of M_W , s_l^2 and Γ_Z for a variation of m_{A^0} with $m_{H^0} = m_{H^\pm} = 350$ GeV and $t_\beta = 1.5$	99
8.10	Prediction of M_W , s_l^2 and Γ_Z in the IHDM in dependence of the charged Higgs mass.	101
8.11	Results in the IHDM in the m_{H^\pm} - Λ_{345} -plane.	102
8.12	Two-loop corrections to precision observables in the IHDM for a light dark matter candidate	103
8.13	Precision observables in the IHDM for $m_{H^0} = 70$ GeV and $m_{A^0} = 200$ GeV . . .	104

List of Tables

2.1	Quantum numbers of the fermion fields	6
2.2	Transformations of the right-handed fermion singlets under the discrete Z_2 symmetry in the different versions of the THDM	13
2.3	Doublet-assignment in the different Z_2 symmetric versions of the THDM	13
2.4	Proportionality factors of the couplings of the fermions to the scalars in the different versions of the Z_2 symmetric THDM	15
7.1	Coefficients for the parameterisation formula (7.59) of the partial widths in the SM.	78
A.1	Counterterms from the proportionality factors ξ_S^f in the different versions of the THDM	118

Bibliography

- [1] S. Hossenberger and W. Hollik. „Two-loop corrections to the ρ parameter in Two-Higgs-Doublet Models“. Eur. Phys. J. C77.3 (2017), p. 178. DOI: 10.1140/epjc/s10052-017-4734-8. arXiv: 1607.04610 [hep-ph].
- [2] S. Hossenberger and W. Hollik. „Two-loop improved predictions of the W boson mass and the effective leptonic mixing angle in Two-Higgs-Doublet Models“. in preparation (2017).
- [3] S. L. Glashow. „Partial Symmetries of Weak Interactions“. Nucl. Phys. 22 (1961), pp. 579–588. DOI: 10.1016/0029-5582(61)90469-2.
- [4] S. Weinberg. „A Model of Leptons“. Phys. Rev. Lett. 19 (1967), pp. 1264–1266. DOI: 10.1103/PhysRevLett.19.1264.
- [5] A. Salam. „Elementary Particle Theory“. In: „Proceedings of the 8th Nobel Symposium“. Ed. by N. Svartholm. Stockholm: Almqvist and Wiksell, 1968, p. 367.
- [6] G. Aad et al. „Observation of a new particle in the search for the Standard Model Higgs boson with the ATLAS detector at the LHC“. Phys. Lett. B716 (2012), pp. 1–29. DOI: 10.1016/j.physletb.2012.08.020. arXiv: 1207.7214 [hep-ex].
- [7] S. Chatrchyan et al. „Observation of a new boson at a mass of 125 GeV with the CMS experiment at the LHC“. Phys. Lett. B716 (2012), pp. 30–61. DOI: 10.1016/j.physletb.2012.08.021. arXiv: 1207.7235 [hep-ex].
- [8] P. W. Higgs. „Broken symmetries, massless particles and gauge fields“. Phys. Lett. 12 (1964), pp. 132–133. DOI: 10.1016/0031-9163(64)91136-9.
- [9] P. W. Higgs. „Broken Symmetries and the Masses of Gauge Bosons“. Phys. Rev. Lett. 13 (1964), pp. 508–509. DOI: 10.1103/PhysRevLett.13.508.
- [10] P. W. Higgs. „Spontaneous Symmetry Breakdown without Massless Bosons“. Phys. Rev. 145 (1966), pp. 1156–1163. DOI: 10.1103/PhysRev.145.1156.
- [11] F. Englert and R. Brout. „Broken Symmetry and the Mass of Gauge Vector Mesons“. Phys. Rev. Lett. 13 (1964), pp. 321–323. DOI: 10.1103/PhysRevLett.13.321.
- [12] T. W. B. Kibble. „Symmetry breaking in non-Abelian gauge theories“. Phys. Rev. 155 (1967), pp. 1554–1561. DOI: 10.1103/PhysRev.155.1554.
- [13] G. Aad et al. „Combined Measurement of the Higgs Boson Mass in pp Collisions at $\sqrt{s} = 7$ and 8 TeV with the ATLAS and CMS Experiments“. Phys. Rev. Lett. 114 (2015), p. 191803. DOI: 10.1103/PhysRevLett.114.191803. arXiv: 1503.07589 [hep-ex].
- [14] CDF collaboration, DELPHI collaboration, ALEPH collaboration, SLD collaboration, OPAL collaboration, D0 collaboration, L3 collaboration, the Tevatron Electroweak Working Group, the SLD Electroweak and Heavy Flavour Groups, the LEP Electroweak Working Group. *Precision Electroweak Measurements and Constraints on the Standard Model*. <http://www.cern.ch/LEPEWWG>. 2010. arXiv: 1012.2367 [hep-ex].
- [15] G. W. Bennett et al. „Final Report of the Muon E821 Anomalous Magnetic Moment Measurement at BNL“. Phys. Rev. D73 (2006), p. 072003. DOI: 10.1103/PhysRevD.73.072003. arXiv: hep-ex/0602035 [hep-ex].
- [16] M. Baak et al. „The global electroweak fit at NNLO and prospects for the LHC and ILC“. Eur. Phys. J. C74 (2014), p. 3046. DOI: 10.1140/epjc/s10052-014-3046-5. arXiv: 1407.3792 [hep-ph].

- [17] J. de Blas et al. „*Electroweak precision observables and Higgs-boson signal strengths in the Standard Model and beyond: present and future*“. JHEP 12 (2016), p. 135. DOI: 10.1007/JHEP12(2016)135. arXiv: 1608.01509 [hep-ph].
- [18] S. Weinberg. „*Implications of Dynamical Symmetry Breaking: An Addendum*“. Phys. Rev. D19 (1979), pp. 1277–1280. DOI: 10.1103/PhysRevD.19.1277.
- [19] L. Susskind. „*Dynamics of Spontaneous Symmetry Breaking in the Weinberg-Salam Theory*“. Phys. Rev. D20 (1979), pp. 2619–2625. DOI: 10.1103/PhysRevD.20.2619.
- [20] P. Sikivie et al. „*Isospin Breaking in Technicolor Models*“. Nucl. Phys. B173 (1980), p. 189. DOI: 10.1016/0550-3213(80)90214-X.
- [21] M. J. G. Veltman. „*Limit on Mass Differences in the Weinberg Model*“. Nucl. Phys. B123 (1977), p. 89. DOI: 10.1016/0550-3213(77)90342-X.
- [22] M. S. Chanowitz, M. A. Furman and I. Hinchliffe. „*Weak Interactions of Ultraheavy Fermions. 2.*“ Nucl. Phys. B153 (1979), p. 402. DOI: 10.1016/0550-3213(79)90606-0.
- [23] M. S. Chanowitz, M. A. Furman and I. Hinchliffe. „*Weak Interactions of Ultraheavy Fermions*“. Phys. Lett. B78 (1978), p. 285. DOI: 10.1016/0370-2693(78)90024-2.
- [24] J. van der Bij and M. J. G. Veltman. „*Two Loop Large Higgs Mass Correction to the rho Parameter*“. Nucl. Phys. B231 (1984), p. 205. DOI: 10.1016/0550-3213(84)90284-0.
- [25] J. J. van der Bij and F. Hoogeveen. „*Two Loop Correction to Weak Interaction Parameters Due to a Heavy Fermion Doublet*“. Nucl. Phys. B283 (1987), p. 477. DOI: 10.1016/0550-3213(87)90284-7.
- [26] R. Barbieri et al. „*Two loop heavy top effects in the Standard Model*“. Nucl. Phys. B409 (1993), pp. 105–127. DOI: 10.1016/0550-3213(93)90448-X.
- [27] J. Fleischer, O. V. Tarasov and F. Jegerlehner. „*Two-loop heavy top corrections to the rho parameter: A Simple formula valid for arbitrary Higgs mass*“. Phys. Lett. B319 (1993), pp. 249–256. DOI: 10.1016/0370-2693(93)90810-5.
- [28] J. Fleischer, O. V. Tarasov and F. Jegerlehner. „*Two-loop large top mass corrections to electroweak parameters: Analytic results valid for arbitrary Higgs mass*“. Phys. Rev. D51 (1995), pp. 3820–3837. DOI: 10.1103/PhysRevD.51.3820.
- [29] A. Djouadi and C. Verzegnassi. „*Virtual very heavy top effects in LEP/SLC precision measurements*“. Phys. Lett. B195 (1987), pp. 265–271. DOI: [http://dx.doi.org/10.1016/0370-2693\(87\)91206-8](http://dx.doi.org/10.1016/0370-2693(87)91206-8).
- [30] A. Djouadi. „*O(α_S) vacuum polarization functions of the standard-model gauge bosons*“. Nuovo Cim. A100 (1988), pp. 357–371. DOI: 10.1007/BF02812964.
- [31] B. A. Kniehl. „*Two-loop corrections to the vacuum polarizations in perturbative QCD*“. Nucl. Phys. B347 (1990), pp. 86–104. DOI: [http://dx.doi.org/10.1016/0550-3213\(90\)90552-0](http://dx.doi.org/10.1016/0550-3213(90)90552-0).
- [32] L. Avdeev et al. „*O(α_s^2) correction to the electroweak rho parameter*“. Phys. Lett. B336 (1994), pp. 560–566. DOI: 10.1016/0370-2693(94)90573-8. arXiv: hep-ph/9406363 [hep-ph].
- [33] K. G. Chetyrkin, J. H. Kühn and M. Steinhauser. „*Corrections of order $\mathcal{O}(G_F M_t^2 \alpha_s^2)$ to the rho parameter*“. Phys. Lett. B351 (1995), pp. 331–338. DOI: 10.1016/0370-2693(95)00380-4. arXiv: hep-ph/9502291 [hep-ph].
- [34] M. Faisst et al. „*Three loop top quark contributions to the rho parameter*“. Nucl. Phys. B665 (2003), pp. 649–662. DOI: 10.1016/S0550-3213(03)00450-4. arXiv: hep-ph/0302275 [hep-ph].
- [35] J. J. van der Bij et al. „*Three-loop leading top mass contributions to the rho parameter*“. Phys. Lett. B498 (2001), pp. 156–162. DOI: [http://dx.doi.org/10.1016/S0370-2693\(01\)00002-8](http://dx.doi.org/10.1016/S0370-2693(01)00002-8).
- [36] Y. Schröder and M. Steinhauser. „*Four-loop singlet contribution to the rho parameter*“. Phys. Lett. B622 (2005), pp. 124–130. DOI: 10.1016/j.physletb.2005.06.085. arXiv: hep-ph/0504055 [hep-ph].

- [37] K. G. Chetyrkin et al. „*Four-Loop QCD Corrections to the ρ Parameter*“. Phys. Rev. Lett. 97 (2006), p. 102003. DOI: 10.1103/PhysRevLett.97.102003. arXiv: hep-ph/0605201 [hep-ph].
- [38] R. Boughezal and M. Czakon. „*Single scale tadpoles and $\mathcal{O}(G_F m_t^2 \alpha_s^3)$ corrections to the ρ parameter*“. Nucl. Phys. B755 (2006), pp. 221–238. DOI: 10.1016/j.nuclphysb.2006.08.007. arXiv: hep-ph/0606232 [hep-ph].
- [39] P. Langacker. „*Grand Unified Theories and Proton Decay*“. Phys. Rept. 72 (1981), p. 185. DOI: 10.1016/0370-1573(81)90059-4.
- [40] V. Silveira and A. Zee. „*Scalar Phantoms*“. Phys. Lett. B161 (1985), pp. 136–140. DOI: 10.1016/0370-2693(85)90624-0.
- [41] J. McDonald. „*Gauge singlet scalars as cold dark matter*“. Phys. Rev. D50 (1994), pp. 3637–3649. DOI: 10.1103/PhysRevD.50.3637. arXiv: hep-ph/0702143 [HEP-PH].
- [42] R. M. Schabinger and J. D. Wells. „*A Minimal spontaneously broken hidden sector and its impact on Higgs boson physics at the large hadron collider*“. Phys. Rev. D72 (2005), p. 093007. DOI: 10.1103/PhysRevD.72.093007. arXiv: hep-ph/0509209 [hep-ph].
- [43] J. Schechter and J. W. F. Valle. „*Neutrino Masses in $SU(2) \times U(1)$ Theories*“. Phys. Rev. D22 (1980), p. 2227. DOI: 10.1103/PhysRevD.22.2227.
- [44] T. P. Cheng and L.-F. Li. „*Neutrino Masses, Mixings and Oscillations in $SU(2) \times U(1)$ Models of Electroweak Interactions*“. Phys. Rev. D22 (1980), p. 2860. DOI: 10.1103/PhysRevD.22.2860.
- [45] H. Georgi and M. Machacek. „*Doubly charged Higgs Bosons*“. Nucl. Phys. B262 (1985), pp. 463–477. DOI: 10.1016/0550-3213(85)90325-6.
- [46] M. S. Chanowitz and M. Golden. „*Higgs Boson Triplets With $M_W = M_Z \cos \theta_W$* “. Phys. Lett. B165 (1985), pp. 105–108. DOI: 10.1016/0370-2693(85)90700-2.
- [47] I. P. Ivanov. „*Building and testing models with extended Higgs sectors*“. Prog. Part. Nucl. Phys. 95 (2017), pp. 160–208. DOI: 10.1016/j.pnpnp.2017.03.001. arXiv: 1702.03776 [hep-ph].
- [48] H. E. Haber and R. Hempfling. „*The Renormalization group improved Higgs sector of the minimal supersymmetric model*“. Phys. Rev. D48 (1993), pp. 4280–4309. DOI: 10.1103/PhysRevD.48.4280. arXiv: hep-ph/9307201 [hep-ph].
- [49] M. Carena et al. „ *$b \rightarrow s\gamma$ and supersymmetry with large $\tan \beta$* “. Phys. Lett. B499 (2001), pp. 141–146. DOI: 10.1016/S0370-2693(01)00009-0. arXiv: hep-ph/0010003 [hep-ph].
- [50] M. Gorbahn et al. „*The supersymmetric Higgs sector and $B - \bar{B}$ mixing for large $\tan \beta$* “. Phys. Rev. D84 (2011), p. 034030. DOI: 10.1103/PhysRevD.84.034030. arXiv: 0901.2065 [hep-ph].
- [51] G. Lee and C. E. M. Wagner. „*Higgs bosons in heavy supersymmetry with an intermediate m_A* “. Phys. Rev. D92.7 (2015), p. 075032. DOI: 10.1103/PhysRevD.92.075032. arXiv: 1508.00576 [hep-ph].
- [52] E. Bagnaschi et al. „*Vacuum stability and supersymmetry at high scales with two Higgs doublets*“. JHEP 03 (2016), p. 158. DOI: 10.1007/JHEP03(2016)158. arXiv: 1512.07761 [hep-ph].
- [53] T. D. Lee. „*A Theory of Spontaneous T Violation*“. Phys. Rev. D8 (1973), pp. 1226–1239. DOI: 10.1103/PhysRevD.8.1226.
- [54] T. D. Lee. „*CP Nonconservation and Spontaneous Symmetry Breaking*“. Phys. Rept. 9 (1974), pp. 143–177. DOI: 10.1016/0370-1573(74)90020-9.
- [55] A. I. Bochkarev, S. V. Kuzmin and M. E. Shaposhnikov. „*Electroweak baryogenesis and the Higgs boson mass problem*“. Phys. Lett. B244 (1990), pp. 275–278. DOI: 10.1016/0370-2693(90)90069-I.
- [56] N. Turok and J. Zadrozny. „*Phase transitions in the two doublet model*“. Nucl. Phys. B369 (1992), pp. 729–742. DOI: 10.1016/0550-3213(92)90284-I.

- [57] G. C. Dorsch, S. J. Huber and J. M. No. „*A strong electroweak phase transition in the 2HDM after LHC8*“. JHEP 10 (2013), p. 029. DOI: 10.1007/JHEP10(2013)029. arXiv: 1305.6610 [hep-ph].
- [58] G. C. Branco et al. „*Theory and phenomenology of two-Higgs-doublet models*“. Phys. Rept. 516 (2012), pp. 1–102. DOI: 10.1016/j.physrep.2012.02.002. arXiv: 1106.0034 [hep-ph].
- [59] N. G. Deshpande and E. Ma. „*Pattern of Symmetry Breaking with Two Higgs Doublets*“. Phys. Rev. D18 (1978), p. 2574. DOI: 10.1103/PhysRevD.18.2574.
- [60] E. Ma. „*Verifiable radiative seesaw mechanism of neutrino mass and dark matter*“. Phys. Rev. D73 (2006), p. 077301. DOI: 10.1103/PhysRevD.73.077301. arXiv: hep-ph/0601225 [hep-ph].
- [61] R. Barbieri, L. J. Hall and V. S. Rychkov. „*Improved naturalness with a heavy Higgs: An Alternative road to LHC physics*“. Phys. Rev. D74 (2006), p. 015007. DOI: 10.1103/PhysRevD.74.015007. arXiv: hep-ph/0603188 [hep-ph].
- [62] L. Lopez Honorez et al. „*The Inert Doublet Model: An Archetype for Dark Matter*“. JCAP 0702 (2007), p. 028. DOI: 10.1088/1475-7516/2007/02/028. arXiv: hep-ph/0612275 [hep-ph].
- [63] A. Goudelis, B. Herrmann and O. Stål. „*Dark matter in the Inert Doublet Model after the discovery of a Higgs-like boson at the LHC*“. JHEP 09 (2013), p. 106. DOI: 10.1007/JHEP09(2013)106. arXiv: 1303.3010 [hep-ph].
- [64] A. Arhrib et al. „*An Updated Analysis of Inert Higgs Doublet Model in light of the Recent Results from LUX, PLANCK, AMS-02 and LHC*“. JCAP 1406 (2014), p. 030. DOI: 10.1088/1475-7516/2014/06/030. arXiv: 1310.0358 [hep-ph].
- [65] A. Ilnicka, M. Krawczyk and T. Robens. „*Inert Doublet Model in light of LHC Run I and astrophysical data*“. Phys. Rev. D93 (2016), p. 055026. DOI: 10.1103/PhysRevD.93.055026. arXiv: 1508.01671 [hep-ph].
- [66] A. Belyaev et al. „*Anatomy of the Inert Two Higgs Doublet Model in the light of the LHC and non-LHC Dark Matter Searches*“ (2016). arXiv: 1612.00511 [hep-ph].
- [67] J. F. Gunion and H. E. Haber. „*The CP conserving two Higgs doublet model: The Approach to the decoupling limit*“. Phys. Rev. D67 (2003), p. 075019. DOI: 10.1103/PhysRevD.67.075019. arXiv: hep-ph/0207010 [hep-ph].
- [68] M. Carena et al. „*Impersonating the Standard Model Higgs Boson: Alignment without Decoupling*“. JHEP 04 (2014), p. 015. DOI: 10.1007/JHEP04(2014)015. arXiv: 1310.2248 [hep-ph].
- [69] P. S. Bhupal Dev and A. Pilaftsis. „*Maximally Symmetric Two Higgs Doublet Model with Natural Standard Model Alignment*“. JHEP 12 (2014). [Erratum: JHEP11,147(2015)], p. 024. DOI: 10.1007/JHEP11(2015)147, 10.1007/JHEP12(2014)024. arXiv: 1408.3405 [hep-ph].
- [70] G. Abbiendi et al. „*Search for Charged Higgs bosons: Combined Results Using LEP Data*“. Eur. Phys. J. C73 (2013), p. 2463. DOI: 10.1140/epjc/s10052-013-2463-1. arXiv: 1301.6065 [hep-ex].
- [71] C.-Y. Chen, S. Dawson and M. Sher. „*Heavy Higgs Searches and Constraints on Two Higgs Doublet Models*“. Phys. Rev. D88 (2013). [Erratum: Phys. Rev.D88,039901(2013)], p. 015018. DOI: 10.1103/PhysRevD.88.015018, 10.1103/PhysRevD.88.039901. arXiv: 1305.1624 [hep-ph].
- [72] O. Eberhardt, U. Nierste and M. Wiebusch. „*Status of the two-Higgs-doublet model of type II*“. JHEP 07 (2013), p. 118. DOI: 10.1007/JHEP07(2013)118. arXiv: 1305.1649 [hep-ph].
- [73] B. Coleppa, F. Kling and S. Su. „*Constraining Type II 2HDM in Light of LHC Higgs Searches*“. JHEP 01 (2014), p. 161. DOI: 10.1007/JHEP01(2014)161. arXiv: 1305.0002 [hep-ph].
- [74] B. Dumont et al. „*Constraints on and future prospects for Two-Higgs-Doublet Models in light of the LHC Higgs signal*“. Phys. Rev. D90 (2014), p. 035021. DOI: 10.1103/PhysRevD.90.035021. arXiv: 1405.3584 [hep-ph].

- [75] J. Bernon et al. „*Scrutinizing the alignment limit in two-Higgs-doublet models: $m_h = 125$ GeV*“. Phys. Rev. D92 (2015), p. 075004. DOI: 10.1103/PhysRevD.92.075004. arXiv: 1507.00933 [hep-ph].
- [76] J. Bernon et al. „*Scrutinizing the alignment limit in two-Higgs-doublet models. II. $m_H = 125$ GeV*“. Phys. Rev. D93 (2016), p. 035027. DOI: 10.1103/PhysRevD.93.035027. arXiv: 1511.03682 [hep-ph].
- [77] J. Bernon et al. „*Light Higgs bosons in Two-Higgs-Doublet Models*“. Phys. Rev. D91 (2015), p. 075019. DOI: 10.1103/PhysRevD.91.075019. arXiv: 1412.3385 [hep-ph].
- [78] A. Wahab El Kaffas, P. Osland and O. M. Ogreid. „*Constraining the Two-Higgs-Doublet-Model parameter space*“. Phys. Rev. D76 (2007), p. 095001. DOI: 10.1103/PhysRevD.76.095001. arXiv: 0706.2997 [hep-ph].
- [79] F. Mahmoudi and O. Stal. „*Flavor constraints on the two-Higgs-doublet model with general Yukawa couplings*“. Phys. Rev. D81 (2010), p. 035016. DOI: 10.1103/PhysRevD.81.035016. arXiv: 0907.1791 [hep-ph].
- [80] M. Aoki et al. „*Models of Yukawa interaction in the two Higgs doublet model, and their collider phenomenology*“. Phys. Rev. D80 (2009), p. 015017. DOI: 10.1103/PhysRevD.80.015017. arXiv: 0902.4665 [hep-ph].
- [81] O. Deschamps et al. „*The Two Higgs Doublet of Type II facing flavour physics data*“. Phys. Rev. D82 (2010), p. 073012. DOI: 10.1103/PhysRevD.82.073012. arXiv: 0907.5135 [hep-ph].
- [82] T. Enomoto and R. Watanabe. „*Flavor constraints on the Two Higgs Doublet Models of Z_2 symmetric and aligned types*“. JHEP 05 (2016), p. 002. DOI: 10.1007/JHEP05(2016)002. arXiv: 1511.05066 [hep-ph].
- [83] A. Arbey et al. „*Status of the Charged Higgs Boson in Two Higgs Doublet Models*“ (2017). arXiv: 1706.07414 [hep-ph].
- [84] J. M. Frere and J. A. M. Vermaseren. „*Radiative Corrections to Masses in the Standard Model With Two Scalar Doublets*“. Z. Phys. C19 (1983), pp. 63–67. DOI: 10.1007/BF01572337.
- [85] S. Bertolini. „*Quantum Effects in a Two Higgs Doublet Model of the Electroweak Interactions*“. Nucl. Phys. B272 (1986), p. 77. DOI: 10.1016/0550-3213(86)90341-X.
- [86] W. Hollik. „*Non-standard Higgs Bosons in $SU(2) \times U(1)$ Radiative Corrections*“. Z. Phys. C32 (1986), p. 291. DOI: 10.1007/BF01552507.
- [87] W. Hollik. „*Radiative Corrections With Two Higgs Doublets at LEP / SLC and HERA*“. Z. Phys. C37 (1988), p. 569. DOI: 10.1007/BF01549716.
- [88] A. Denner et al. „*The Z width in the two Higgs doublet model*“. Z. Phys. C51 (1991), pp. 695–705. DOI: 10.1007/BF01565598.
- [89] C. D. Froggatt, R. G. Moorhouse and I. G. Knowles. „*Leading radiative corrections in two scalar doublet models*“. Phys. Rev. D45 (1992), pp. 2471–2481. DOI: 10.1103/PhysRevD.45.2471.
- [90] P. H. Chankowski, M. Krawczyk and J. Zochowski. „*Implications of the precision data for very light Higgs boson scenario in 2HDM(II)*“. Eur. Phys. J. C11 (1999), pp. 661–672. DOI: 10.1007/s100529900217, 10.1007/s100520050662. arXiv: hep-ph/9905436 [hep-ph].
- [91] W. Grimus et al. „*A Precision constraint on multi-Higgs-doublet models*“. J. Phys. G35 (2008), p. 075001. DOI: 10.1088/0954-3899/35/7/075001. arXiv: 0711.4022 [hep-ph].
- [92] W. Grimus et al. „*The Oblique parameters in multi-Higgs-doublet models*“. Nucl. Phys. B801 (2008), pp. 81–96. DOI: 10.1016/j.nuclphysb.2008.04.019. arXiv: 0802.4353 [hep-ph].
- [93] D. Lopez-Val and J. Sola. „ *Δr in the Two-Higgs-Doublet Model at full one loop level – and beyond*“. Eur. Phys. J. C73 (2013), p. 2393. DOI: 10.1140/epjc/s10052-013-2393-y. arXiv: 1211.0311 [hep-ph].
- [94] S. Hossenberger. „*Two Higgs doublet models and electroweak precision observables*“. Diploma thesis. Technische Universität München, 2013.

- [95] A. Broggio et al. „*Limiting two-Higgs-doublet models*“. JHEP 11 (2014), p. 058. DOI: 10.1007/JHEP11(2014)058. arXiv: 1409.3199 [hep-ph].
- [96] F. Halzen and B. A. Kniehl. „ *Δr beyond one loop*“. Nucl. Phys. B353.3 (1991), pp. 567–590. DOI: [http://dx.doi.org/10.1016/0550-3213\(91\)90319-S](http://dx.doi.org/10.1016/0550-3213(91)90319-S).
- [97] B. A. Kniehl and A. Sirlin. „*Effect of the $t\bar{t}$ threshold on electroweak parameters*“. Phys. Rev. D 47 (3 1993), pp. 883–893. DOI: 10.1103/PhysRevD.47.883.
- [98] A. Djouadi and P. Gambino. „*Electroweak gauge bosons selfenergies: Complete QCD corrections*“. Phys.Rev. D49 (1994), pp. 3499–3511. DOI: 10.1103/PhysRevD.49.3499, 10.1103/PhysRevD.53.4111. arXiv: hep-ph/9309298 [hep-ph].
- [99] A. Freitas et al. „*Complete fermionic two-loop results for the M_W – M_Z interdependence*“. Phys. Lett. B495 (2000), pp. 338–346. DOI: 10.1016/S0370-2693(00)01263-6. arXiv: hep-ph/0007091 [hep-ph].
- [100] A. Freitas et al. „*Electroweak two-loop corrections to the M_W – M_Z mass correlation in the standard model*“. Nucl. Phys. B632 (2002), pp. 189–218. DOI: 10.1016/S0550-3213(02)00243-2. arXiv: hep-ph/0202131 [hep-ph].
- [101] M. Awramik and M. Czakon. „*Complete two loop electroweak contributions to the muon lifetime in the standard model*“. Phys. Lett. B568 (2003), pp. 48–54. DOI: 10.1016/j.physletb.2003.06.007. arXiv: hep-ph/0305248 [hep-ph].
- [102] M. Awramik and M. Czakon. „*Complete two loop bosonic contributions to the muon lifetime in the standard model*“. Phys. Rev. Lett. 89 (2002), p. 241801. DOI: 10.1103/PhysRevLett.89.241801. arXiv: hep-ph/0208113 [hep-ph].
- [103] M. Awramik and M. Czakon. „*Two loop electroweak bosonic corrections to the muon decay lifetime*“. Nucl. Phys. Proc. Suppl. 116 (2003), pp. 238–242. DOI: 10.1016/S0920-5632(03)80177-9. arXiv: hep-ph/0211041 [hep-ph].
- [104] A. Onishchenko and O. Veretin. „*Two-loop bosonic electroweak corrections to the muon lifetime and M_W – M_Z interdependence*“. Phys. Lett. B551 (2003), pp. 111–114. DOI: 10.1016/S0370-2693(02)03004-6. arXiv: hep-ph/0209010 [hep-ph].
- [105] M. Awramik et al. „*Bosonic corrections to Δr at the two loop level*“. Phys. Rev. D68 (2003), p. 053004. DOI: 10.1103/PhysRevD.68.053004. arXiv: hep-ph/0209084 [hep-ph].
- [106] M. Awramik et al. „*Precise prediction for the W boson mass in the standard model*“. Phys. Rev. D69 (2004), p. 053006. DOI: 10.1103/PhysRevD.69.053006. arXiv: hep-ph/0311148 [hep-ph].
- [107] W. Hollik, U. Meier and S. Uccirati. „*Higgs-mass dependence of the effective electroweak mixing angle $\sin^2 \theta_{\text{eff}}$ at the two-loop level*“. Phys. Lett. B632 (2006), pp. 680–683. DOI: 10.1016/j.physletb.2005.11.032. arXiv: hep-ph/0509302 [hep-ph].
- [108] W. Hollik, U. Meier and S. Uccirati. „*The Effective electroweak mixing angle $\sin^2 \theta_{\text{eff}}$ with two-loop fermionic contributions*“. Nucl. Phys. B731 (2005), pp. 213–224. DOI: 10.1016/j.nuclphysb.2005.10.015. arXiv: hep-ph/0507158 [hep-ph].
- [109] W. Hollik, U. Meier and S. Uccirati. „*The Effective electroweak mixing angle $\sin^2 \theta_{\text{eff}}$ with two-loop bosonic contributions*“. Nucl. Phys. B765 (2007), pp. 154–165. DOI: 10.1016/j.nuclphysb.2006.12.001. arXiv: hep-ph/0610312 [hep-ph].
- [110] M. Awramik, M. Czakon and A. Freitas. „*Electroweak two-loop corrections to the effective weak mixing angle*“. JHEP 0611 (2006), p. 048. DOI: 10.1088/1126-6708/2006/11/048. arXiv: hep-ph/0608099 [hep-ph].
- [111] A. Freitas. „*Two-loop fermionic electroweak corrections to the Z -boson width and production rate*“. Phys. Lett. B730 (2014), pp. 50–52. DOI: 10.1016/j.physletb.2014.01.017. arXiv: 1310.2256 [hep-ph].
- [112] A. Freitas. „*Higher-order electroweak corrections to the partial widths and branching ratios of the Z boson*“. JHEP 04 (2014), p. 070. DOI: 10.1007/JHEP04(2014)070. arXiv: 1401.2447 [hep-ph].

- [113] K. G. Chetyrkin, J. H. Kühn and M. Steinhauser. „*QCD corrections from top quark to relations between electroweak parameters to order α_s^2* “. Phys. Rev. Lett. 75 (1995), pp. 3394–3397. DOI: 10.1103/PhysRevLett.75.3394. arXiv: hep-ph/9504413 [hep-ph].
- [114] K. G. Chetyrkin, J. H. Kühn and M. Steinhauser. „*Three-loop polarization function and $O(\alpha_s^2)$ corrections to the production of heavy quarks*“. Nucl. Phys. B482 (1996), pp. 213–240. DOI: 10.1016/S0550-3213(96)00534-2. arXiv: hep-ph/9606230 [hep-ph].
- [115] R. Boughezal, J. B. Tausk and J. J. van der Bij. „*Three-loop electroweak correction to the ρ parameter in the large Higgs mass limit*“. Nucl. Phys. B713 (2005), pp. 278–290. DOI: <http://dx.doi.org/10.1016/j.nuclphysb.2005.02.020>.
- [116] A. Djouadi et al. „*Supersymmetric contributions to electroweak precision observables: QCD corrections*“. Phys. Rev. Lett. 78 (1997), pp. 3626–3629. DOI: 10.1103/PhysRevLett.78.3626. arXiv: hep-ph/9612363 [hep-ph].
- [117] A. Djouadi et al. „*Leading QCD corrections to scalar quark contributions to electroweak precision observables*“. Phys. Rev. D57 (1998), pp. 4179–4196. DOI: 10.1103/PhysRevD.57.4179. arXiv: hep-ph/9710438 [hep-ph].
- [118] S. Heinemeyer and G. Weiglein. „*Leading electroweak two-loop corrections to precision observables in the MSSM*“. JHEP 10 (2002), p. 072. DOI: 10.1088/1126-6708/2002/10/072. arXiv: hep-ph/0209305 [hep-ph].
- [119] J. Haestier et al. „*Electroweak precision observables: Two-loop Yukawa corrections of supersymmetric particles*“. JHEP 12 (2005), p. 027. DOI: 10.1088/1126-6708/2005/12/027. arXiv: hep-ph/0508139 [hep-ph].
- [120] J. F. Donoghue and L. F. Li. „*Properties of Charged Higgs Bosons*“. Phys. Rev. D19 (1979), p. 945. DOI: 10.1103/PhysRevD.19.945.
- [121] H. E. Haber, G. L. Kane and T. Sterling. „*The Fermion Mass Scale and Possible Effects of Higgs Bosons on Experimental Observables*“. Nucl. Phys. B161 (1979), pp. 493–532. DOI: 10.1016/0550-3213(79)90225-6.
- [122] B. McWilliams and L.-F. Li. „*Virtual Effects of Higgs Particles*“. Nucl. Phys. B179 (1981), pp. 62–84. DOI: 10.1016/0550-3213(81)90249-2.
- [123] L. J. Hall and M. B. Wise. „*Flavor Changing Higgs Boson Couplings*“. Nucl. Phys. B187 (1981), pp. 397–408. DOI: 10.1016/0550-3213(81)90469-7.
- [124] R. A. Flores and M. Sher. „*Higgs Masses in the Standard, Multi-Higgs and Supersymmetric Models*“. Annals Phys. 148 (1983), p. 95. DOI: 10.1016/0003-4916(83)90331-7.
- [125] Y. Fukuda et al. „*Evidence for oscillation of atmospheric neutrinos*“. Phys. Rev. Lett. 81 (1998), pp. 1562–1567. DOI: 10.1103/PhysRevLett.81.1562. arXiv: hep-ex/9807003 [hep-ex].
- [126] Q. R. Ahmad et al. „*Measurement of the rate of $\nu_e + d \rightarrow p + p + e^-$ interactions produced by 8B solar neutrinos at the Sudbury Neutrino Observatory*“. Phys. Rev. Lett. 87 (2001), p. 071301. DOI: 10.1103/PhysRevLett.87.071301. arXiv: nucl-ex/0106015 [nucl-ex].
- [127] Q. R. Ahmad et al. „*Direct evidence for neutrino flavor transformation from neutral current interactions in the Sudbury Neutrino Observatory*“. Phys. Rev. Lett. 89 (2002), p. 011301. DOI: 10.1103/PhysRevLett.89.011301. arXiv: nucl-ex/0204008 [nucl-ex].
- [128] S. Davidson and H. E. Haber. „*Basis-independent methods for the two-Higgs-doublet model*“. Phys. Rev. D72 (2005). [Erratum: Phys. Rev. D72,099902(2005)], p. 035004. DOI: 10.1103/PhysRevD.72.099902, 10.1103/PhysRevD.72.035004. arXiv: hep-ph/0504050 [hep-ph].
- [129] I. F. Ginzburg and M. Krawczyk. „*Symmetries of two Higgs doublet model and CP violation*“. Phys. Rev. D72 (2005), p. 115013. DOI: 10.1103/PhysRevD.72.115013. arXiv: hep-ph/0408011 [hep-ph].
- [130] T. Hahn. „*Generating Feynman diagrams and amplitudes with FeynArts 3*“. Comput. Phys. Commun. 140 (2001), pp. 418–431. DOI: 10.1016/S0010-4655(01)00290-9. arXiv: hep-ph/0012260 [hep-ph].

- [131] J. F. Gunion, H. E. Haber, G. L. Kane and S. Dawson. „*The Higgs hunter’s guide*“. Cambridge, Mass.: Perseus Publishing, 1990.
- [132] S. L. Glashow and S. Weinberg. „*Natural Conservation Laws for Neutral Currents*“. Phys. Rev. D15 (1977), p. 1958. DOI: 10.1103/PhysRevD.15.1958.
- [133] E. A. Paschos. „*Diagonal Neutral Currents*“. Phys. Rev. D15 (1977), p. 1966. DOI: 10.1103/PhysRevD.15.1966.
- [134] A. Pich and P. Tuzon. „*Yukawa Alignment in the Two-Higgs-Doublet Model*“. Phys. Rev. D80 (2009), p. 091702. DOI: 10.1103/PhysRevD.80.091702. arXiv: 0908.1554 [hep-ph].
- [135] P. Tuzon and A. Pich. „*The Aligned two-Higgs Doublet model*“. Acta Phys. Polon. Supp. 3 (2010), pp. 215–220. arXiv: 1001.0293 [hep-ph].
- [136] T. P. Cheng and M. Sher. „*Mass Matrix Ansatz and Flavor Nonconservation in Models with Multiple Higgs Doublets*“. Phys. Rev. D35 (1987), p. 3484. DOI: 10.1103/PhysRevD.35.3484.
- [137] W.-S. Hou. „*Tree level $t \rightarrow ch^0$ or $h \rightarrow t\bar{c}$ decays*“. Phys. Lett. B296 (1992), pp. 179–184. DOI: 10.1016/0370-2693(92)90823-M.
- [138] D. Chang, W. S. Hou and W.-Y. Keung. „*Two-loop contributions of flavor changing neutral Higgs bosons to $\mu \rightarrow e\gamma$* “. Phys. Rev. D48 (1993), pp. 217–224. DOI: 10.1103/PhysRevD.48.217. arXiv: hep-ph/9302267 [hep-ph].
- [139] D. Atwood, L. Reina and A. Soni. „*Phenomenology of two Higgs doublet models with flavor changing neutral currents*“. Phys. Rev. D55 (1997), pp. 3156–3176. DOI: 10.1103/PhysRevD.55.3156. arXiv: hep-ph/9609279 [hep-ph].
- [140] G. Aad et al. „*Measurements of the Higgs boson production and decay rates and coupling strengths using pp collision data at $\sqrt{s} = 7$ and 8 TeV in the ATLAS experiment*“. Eur. Phys. J. C76.1 (2016), p. 6. DOI: 10.1140/epjc/s10052-015-3769-y. arXiv: 1507.04548 [hep-ex].
- [141] V. Khachatryan et al. „*Precise determination of the mass of the Higgs boson and tests of compatibility of its couplings with the standard model predictions using proton collisions at 7 and 8 TeV*“. Eur. Phys. J. C75.5 (2015), p. 212. DOI: 10.1140/epjc/s10052-015-3351-7. arXiv: 1412.8662 [hep-ex].
- [142] K. G. Klimenko. „*On Necessary and Sufficient Conditions for Some Higgs Potentials to Be Bounded From Below*“. Theor. Math. Phys. 62 (1985). [Teor. Mat. Fiz.62,87(1985)], pp. 58–65. DOI: 10.1007/BF01034825.
- [143] M. Maniatis et al. „*Stability and symmetry breaking in the general two-Higgs-doublet model*“. Eur. Phys. J. C48 (2006), pp. 805–823. DOI: 10.1140/epjc/s10052-006-0016-6. arXiv: hep-ph/0605184 [hep-ph].
- [144] F. Staub. „*Reopen parameter regions in Two-Higgs Doublet Models*“ (2017). arXiv: 1705.03677 [hep-ph].
- [145] B. W. Lee, C. Quigg and H. B. Thacker. „*Weak Interactions at Very High-Energies: The Role of the Higgs Boson Mass*“. Phys. Rev. D16 (1977), p. 1519. DOI: 10.1103/PhysRevD.16.1519.
- [146] B. W. Lee, C. Quigg and H. B. Thacker. „*The Strength of Weak Interactions at Very High-Energies and the Higgs Boson Mass*“. Phys. Rev. Lett. 38 (1977), pp. 883–885. DOI: 10.1103/PhysRevLett.38.883.
- [147] R. Casalbuoni et al. „*Strong Interacting Two Doublet and Doublet Singlet Higgs Models*“. Phys. Lett. B178 (1986), p. 235. DOI: 10.1016/0370-2693(86)91502-9.
- [148] R. Casalbuoni et al. „*Tree-Level Unitarity Violation for Large Scalar Mass in Multi-Higgs Extensions of the Standard Model*“. Nucl. Phys. B299 (1988), pp. 117–150. DOI: 10.1016/0550-3213(88)90469-5.
- [149] J. Maalampi, J. Sirkka and I. Vilja. „*Tree level unitarity and triviality bounds for two Higgs models*“. Phys. Lett. B265 (1991), pp. 371–376. DOI: 10.1016/0370-2693(91)90068-2.

- [150] S. Kanemura, T. Kubota and E. Takasugi. „*Lee-Quigg-Thacker bounds for Higgs boson masses in a two doublet model*“. Phys. Lett. B313 (1993), pp. 155–160. DOI: 10.1016/0370-2693(93)91205-2. arXiv: hep-ph/9303263 [hep-ph].
- [151] A. G. Akeroyd, A. Arhrib and E.-M. Naimi. „*Note on tree-level unitarity in the general two Higgs doublet model*“. Phys. Lett. B490 (2000), pp. 119–124. DOI: 10.1016/S0370-2693(00)00962-X. arXiv: hep-ph/0006035 [hep-ph].
- [152] J. Horejsi and M. Kladiva. „*Tree-unitarity bounds for THDM Higgs masses revisited*“. Eur. Phys. J. C46 (2006), pp. 81–91. DOI: 10.1140/epjc/s2006-02472-3. arXiv: hep-ph/0510154 [hep-ph].
- [153] I. F. Ginzburg and I. P. Ivanov. „*Tree-level unitarity constraints in the most general 2HDM*“. Phys. Rev. D72 (2005), p. 115010. DOI: 10.1103/PhysRevD.72.115010. arXiv: hep-ph/0508020 [hep-ph].
- [154] B. Grinstein, C. W. Murphy and P. Uttayarat. „*One-loop corrections to the perturbative unitarity bounds in the CP-conserving two-Higgs doublet model with a softly broken \mathbb{Z}_2 symmetry*“. JHEP 06 (2016), p. 070. DOI: 10.1007/JHEP06(2016)070. arXiv: 1512.04567 [hep-ph].
- [155] V. Cacchio et al. „*Next-to-leading order unitarity fits in Two-Higgs-Doublet models with soft \mathbb{Z}_2 breaking*“. JHEP 11 (2016), p. 026. DOI: 10.1007/JHEP11(2016)026. arXiv: 1609.01290 [hep-ph].
- [156] P. M. Ferreira, R. Santos and A. Barroso. „*Stability of the tree-level vacuum in two Higgs doublet models against charge or CP spontaneous violation*“. Phys. Lett. B603 (2004). [Erratum: Phys. Lett. B629,114(2005)], pp. 219–229. DOI: 10.1016/j.physletb.2004.10.022, 10.1016/j.physletb.2005.09.074. arXiv: hep-ph/0406231 [hep-ph].
- [157] A. Barroso, P. M. Ferreira and R. Santos. „*Charge and CP symmetry breaking in two Higgs doublet models*“. Phys. Lett. B632 (2006), pp. 684–687. DOI: 10.1016/j.physletb.2005.11.031. arXiv: hep-ph/0507224 [hep-ph].
- [158] A. Barroso, P. M. Ferreira and R. Santos. „*Neutral minima in two-Higgs doublet models*“. Phys. Lett. B652 (2007), pp. 181–193. DOI: 10.1016/j.physletb.2007.07.010. arXiv: hep-ph/0702098 [HEP-PH].
- [159] I. P. Ivanov. „*Minkowski space structure of the Higgs potential in 2HDM. II. Minima, symmetries, and topology*“. Phys. Rev. D77 (2008), p. 015017. DOI: 10.1103/PhysRevD.77.015017. arXiv: 0710.3490 [hep-ph].
- [160] A. Barroso et al. „*Evading death by vacuum*“. Eur. Phys. J. C73 (2013), p. 2537. DOI: 10.1140/epjc/s10052-013-2537-0. arXiv: 1211.6119 [hep-ph].
- [161] A. Barroso et al. „*Metastability bounds on the two Higgs doublet model*“. JHEP 06 (2013), p. 045. DOI: 10.1007/JHEP06(2013)045. arXiv: 1303.5098 [hep-ph].
- [162] I. P. Ivanov and J. P. Silva. „*Tree-level metastability bounds for the most general two Higgs doublet model*“. Phys. Rev. D92 (2015), p. 055017. DOI: 10.1103/PhysRevD.92.055017. arXiv: 1507.05100 [hep-ph].
- [163] I. F. Ginzburg et al. „*Evolution of Universe to the present inert phase*“. Phys. Rev. D82 (2010), p. 123533. DOI: 10.1103/PhysRevD.82.123533. arXiv: 1009.4593 [hep-ph].
- [164] G. 't Hooft and M. J. G. Veltman. „*Regularization and Renormalization of Gauge Fields*“. Nucl. Phys. B44 (1972), pp. 189–213. DOI: 10.1016/0550-3213(72)90279-9.
- [165] C. G. Bollini and J. J. Giambiagi. „*Dimensional Renormalization: The Number of Dimensions as a Regularizing Parameter*“. Nuovo Cim. B12 (1972), pp. 20–26. DOI: 10.1007/BF02895558.
- [166] J. F. Ashmore. „*A Method of Gauge Invariant Regularization*“. Lett. Nuovo Cim. 4 (1972), pp. 289–290. DOI: 10.1007/BF02824407.
- [167] G. M. Cicuta and E. Montaldi. „*Analytic renormalization via continuous space dimension*“. Lett. Nuovo Cim. 4 (1972), pp. 329–332. DOI: 10.1007/BF02756527.
- [168] G. Passarino and M. J. G. Veltman. „*One Loop Corrections for e^+e^- Annihilation Into $\mu^+\mu^-$ in the Weinberg Model*“. Nucl. Phys. B160 (1979), p. 151. DOI: 10.1016/0550-3213(79)90234-7.

- [169] G. Weiglein, R. Scharf and M. Böhm. „Reduction of general two loop selfenergies to standard scalar integrals“. Nucl. Phys. B416 (1994), pp. 606–644. DOI: 10.1016/0550-3213(94)90325-5. arXiv: hep-ph/9310358 [hep-ph].
- [170] D. B. Melrose. „Reduction of Feynman diagrams“. Nuovo Cim. 40 (1965), pp. 181–213. DOI: 10.1007/BF02832919.
- [171] G. 't Hooft and M. J. G. Veltman. „Scalar One Loop Integrals“. Nucl. Phys. B153 (1979), pp. 365–401. DOI: 10.1016/0550-3213(79)90605-9.
- [172] A. Denner. „Techniques for calculation of electroweak radiative corrections at the one loop level and results for W physics at LEP-200“. Fortsch. Phys. 41 (1993), pp. 307–420. arXiv: 0709.1075 [hep-ph].
- [173] M. Böhm, A. Denner and H. Joos. „Gauge Theories of the Strong and Electroweak Interaction“. Wiesbaden: Vieweg+Teubner Verlag, 2001.
- [174] U. Nierste, D. Müller and M. Böhm. „Two-loop relevant parts of D -dimensional massive scalar one loop integrals“. Z. Phys. C57 (1993), pp. 605–614. DOI: 10.1007/BF01561479.
- [175] W. Hollik and S. Paßehr. „Higgs boson masses and mixings in the complex MSSM with two-loop top-Yukawa-coupling corrections“. JHEP 10 (2014), p. 171. DOI: 10.1007/JHEP10(2014)171. arXiv: 1409.1687 [hep-ph].
- [176] G. Weiglein et al. „Computer algebraic calculation of two-loop self-energies in the electroweak standard model“. In: „New computing techniques in physics research II. Proceedings, 2nd International Workshop on Software Engineering, Artificial Intelligence and Expert Systems in High-Energy and Nuclear Physics, La Londe les Maures, France, January 13-18, 1992“. Ed. by D. Perret-Gallix. 1992, pp. 617–623.
- [177] A. I. Davydychev and J. B. Tausk. „Two-loop selfenergy diagrams with different masses and the momentum expansion“. Nucl. Phys. B397 (1993), pp. 123–142. DOI: 10.1016/0550-3213(93)90338-P.
- [178] F. A. Berends and J. B. Tausk. „On the numerical evaluation of scalar two-loop selfenergy diagrams“. Nucl. Phys. B421 (1994), pp. 456–470. DOI: 10.1016/0550-3213(94)90336-0.
- [179] R. Scharf. Diploma thesis. University of Würzburg, 1991.
- [180] T. Hahn and M. Perez-Victoria. „Automatized one loop calculations in four-dimensions and D -dimensions“. Comput. Phys. Commun. 118 (1999), pp. 153–165. DOI: 10.1016/S0010-4655(98)00173-8. arXiv: hep-ph/9807565 [hep-ph].
- [181] T. Hahn and S. Paßehr. „Implementation of the $\mathcal{O}(\alpha_t^2)$ MSSM Higgs-mass corrections in FeynHiggs“. Comput. Phys. Commun. 214 (2017), pp. 91–97. DOI: 10.1016/j.cpc.2017.01.026. arXiv: 1508.00562 [hep-ph].
- [182] T. Hahn and J. I. Illana. „Excursions into FeynArts and FormCalc“. Nucl. Phys. Proc. Suppl. 160 (2006), pp. 101–105. DOI: 10.1016/j.nuclphysbps.2006.09.035. arXiv: hep-ph/0607049 [hep-ph].
- [183] S. Heinemeyer, W. Hollik and G. Weiglein. „FeynHiggs: A Program for the calculation of the masses of the neutral CP even Higgs bosons in the MSSM“. Comput. Phys. Commun. 124 (2000), pp. 76–89. DOI: 10.1016/S0010-4655(99)00364-1. arXiv: hep-ph/9812320 [hep-ph].
- [184] T. Hahn et al. „FeynHiggs: A program for the calculation of MSSM Higgs-boson observables - Version 2.6.5“. Comput. Phys. Commun. 180 (2009), pp. 1426–1427. DOI: 10.1016/j.cpc.2009.02.014.
- [185] N. N. Bogoliubov and O. S. Parasiuk. „On the Multiplication of the causal function in the quantum theory of fields“. Acta Math. 97 (1957), pp. 227–266. DOI: 10.1007/BF02392399.
- [186] K. Hepp. „Proof of the Bogolyubov-Parasiuk theorem on renormalization“. Commun. Math. Phys. 2 (1966), pp. 301–326. DOI: 10.1007/BF01773358.
- [187] W. Zimmermann. „Convergence of Bogolyubov’s method of renormalization in momentum space“. Commun. Math. Phys. 15 (1969). [Lect. Notes Phys.558,217(2000)], pp. 208–234. DOI: 10.1007/BF01645676.

- [188] G. 't Hooft. „Renormalization of Massless Yang-Mills Fields“. Nucl. Phys. B33 (1971), pp. 173–199. DOI: 10.1016/0550-3213(71)90395-6.
- [189] G. 't Hooft. „Renormalizable Lagrangians for Massive Yang-Mills Fields“. Nucl. Phys. B35 (1971), pp. 167–188. DOI: 10.1016/0550-3213(71)90139-8.
- [190] D. A. Ross and J. C. Taylor. „Renormalization of a unified theory of weak and electromagnetic interactions“. Nucl. Phys. B51 (1973). [Erratum: Nucl. Phys. B58,643(1973)], pp. 125–144. DOI: 10.1016/0550-3213(73)90608-1, 10.1016/0550-3213(73)90505-1.
- [191] R. Santos and A. Barroso. „On the renormalization of two Higgs doublet models“. Phys. Rev. D56 (1997), pp. 5366–5385. DOI: 10.1103/PhysRevD.56.5366. arXiv: hep-ph/9701257 [hep-ph].
- [192] D. Lopez-Val and J. Sola. „Neutral Higgs-pair production at Linear Colliders within the general 2HDM: Quantum effects and triple Higgs boson self-interactions“. Phys. Rev. D81 (2010), p. 033003. DOI: 10.1103/PhysRevD.81.033003. arXiv: 0908.2898 [hep-ph].
- [193] S. Kanemura et al. „Fingerprinting nonminimal Higgs sectors“. Phys. Rev. D90 (2014), p. 075001. DOI: 10.1103/PhysRevD.90.075001. arXiv: 1406.3294 [hep-ph].
- [194] S. Kanemura, M. Kikuchi and K. Yagyu. „Fingerprinting the extended Higgs sector using one-loop corrected Higgs boson couplings and future precision measurements“. Nucl. Phys. B896 (2015), pp. 80–137. DOI: 10.1016/j.nuclphysb.2015.04.015. arXiv: 1502.07716 [hep-ph].
- [195] M. Krause et al. „Gauge-independent Renormalization of the 2-Higgs-Doublet Model“. JHEP 09 (2016), p. 143. DOI: 10.1007/JHEP09(2016)143. arXiv: 1605.04853 [hep-ph].
- [196] A. Denner et al. „Gauge-independent \overline{MS} renormalization in the 2HDM“. JHEP 09 (2016), p. 115. DOI: 10.1007/JHEP09(2016)115. arXiv: 1607.07352 [hep-ph].
- [197] L. Altenkamp, S. Dittmaier and H. Rzehak. „Renormalization schemes for the Two-Higgs-Doublet Model and applications to $h \rightarrow WW/ZZ \rightarrow 4\text{fermions}$ “ (2017). arXiv: 1704.02645 [hep-ph].
- [198] M. Böhm, H. Spiesberger and W. Hollik. „On the One-Loop Renormalization of the Electroweak Standard Model and Its Application to Leptonic Processes“. Fortsch. Phys. 34 (1986), pp. 687–751. DOI: 10.1002/prop.19860341102.
- [199] A. Sirlin. „Theoretical considerations concerning the Z^0 mass“. Phys. Rev. Lett. 67 (1991), pp. 2127–2130. DOI: 10.1103/PhysRevLett.67.2127.
- [200] A. Arhrib et al. „Higgs decays in the two Higgs doublet model: Large quantum effects in the decoupling regime“. Phys. Lett. B579 (2004), pp. 361–370. DOI: 10.1016/j.physletb.2003.10.006. arXiv: hep-ph/0307391 [hep-ph].
- [201] P. H. Chankowski, S. Pokorski and J. Rosiek. „Complete on-shell renormalization scheme for the minimal supersymmetric Higgs sector“. Nucl. Phys. B423 (1994), pp. 437–496. DOI: 10.1016/0550-3213(94)90141-4. arXiv: hep-ph/9303309 [hep-ph].
- [202] A. Dabelstein. „The One loop renormalization of the MSSM Higgs sector and its application to the neutral scalar Higgs masses“. Z. Phys. C67 (1995), pp. 495–512. DOI: 10.1007/BF01624592. arXiv: hep-ph/9409375 [hep-ph].
- [203] S. Willenbrock. „Symmetries of the standard model“. In: „Physics in $D \geq 4$. Proceedings, Theoretical Advanced Study Institute in elementary particle physics, TASI 2004, Boulder, USA, June 6-July 2, 2004“. 2004, pp. 3–38. arXiv: hep-ph/0410370 [hep-ph].
- [204] H. E. Haber and A. Pomarol. „Constraints from global symmetries on radiative corrections to the Higgs sector“. Phys. Lett. B302 (1993), pp. 435–441. DOI: 10.1016/0370-2693(93)90423-F. arXiv: hep-ph/9207267 [hep-ph].
- [205] A. Pomarol and R. Vega. „Constraints on CP violation in the Higgs sector from the ρ parameter“. Nucl. Phys. B413 (1994), pp. 3–15. DOI: 10.1016/0550-3213(94)90611-4. arXiv: hep-ph/9305272 [hep-ph].
- [206] J.-M. Gerard and M. Herquet. „A Twisted custodial symmetry in the two-Higgs-doublet model“. Phys. Rev. Lett. 98 (2007), p. 251802. DOI: 10.1103/PhysRevLett.98.251802. arXiv: hep-ph/0703051 [HEP-PH].

- [207] B. Grzadkowski, M. Maniatis and J. Wudka. „*Note on Custodial Symmetry in the Two-Higgs-Doublet model*“. JHEP 1111 (2011), p. 030. DOI: 10.1007/JHEP11(2011)030. arXiv: 1011.5228 [hep-ph].
- [208] H. E. Haber and D. O’Neil. „*Basis-independent methods for the two-Higgs-doublet model III: The CP-conserving limit, custodial symmetry, and the oblique parameters S, T, U*“. Phys. Rev. D83 (2011), p. 055017. DOI: 10.1103/PhysRevD.83.055017. arXiv: 1011.6188 [hep-ph].
- [209] C. Nishi. „*Custodial $SO(4)$ symmetry and CP violation in N-Higgs-doublet potentials*“. Phys. Rev. D83 (2011), p. 095005. DOI: 10.1103/PhysRevD.83.095005. arXiv: 1103.0252 [hep-ph].
- [210] F. J. Botella and J. P. Silva. „*Jarlskog - like invariants for theories with scalars and fermions*“. Phys. Rev. D51 (1995), pp. 3870–3875. DOI: 10.1103/PhysRevD.51.3870. arXiv: hep-ph/9411288 [hep-ph].
- [211] D. A. Ross and M. J. G. Veltman. „*Neutral Currents in Neutrino Experiments*“. Nucl. Phys. B95 (1975), p. 135. DOI: 10.1016/0550-3213(75)90485-X.
- [212] M. Consoli, W. Hollik and F. Jegerlehner. „*The Effect of the Top Quark on the M_W – M_Z Interdependence and Possible Decoupling of Heavy Fermions from Low-Energy Physics*“. Phys. Lett. B227 (1989), p. 167. DOI: 10.1016/0370-2693(89)91301-4.
- [213] C. Patrignani et al. „*Review of Particle Physics*“. Chin. Phys. C40.10 (2016), p. 100001. DOI: 10.1088/1674-1137/40/10/100001.
- [214] M. E. Peskin and T. Takeuchi. „*A New constraint on a strongly interacting Higgs sector*“. Phys. Rev. Lett. 65 (1990), pp. 964–967. DOI: 10.1103/PhysRevLett.65.964.
- [215] M. E. Peskin and T. Takeuchi. „*Estimation of oblique electroweak corrections*“. Phys. Rev. D46 (1992), pp. 381–409. DOI: 10.1103/PhysRevD.46.381.
- [216] D. Das. „*New limits on $\tan \beta$ for 2HDMs with Z_2 symmetry*“. Int. J. Mod. Phys. A30.26 (2015), p. 1550158. DOI: 10.1142/S0217751X15501584. arXiv: 1501.02610 [hep-ph].
- [217] R. E. Behrends, R. J. Finkelstein and A. Sirlin. „*Radiative corrections to decay processes*“. Phys. Rev. 101 (1956), pp. 866–873. DOI: 10.1103/PhysRev.101.866.
- [218] S. M. Berman. „*Radiative corrections to muon and neutron decay*“. Phys. Rev. 112 (1958), pp. 267–270. DOI: 10.1103/PhysRev.112.267.
- [219] T. Kinoshita and A. Sirlin. „*Radiative corrections to Fermi interactions*“. Phys. Rev. 113 (1959), pp. 1652–1660. DOI: 10.1103/PhysRev.113.1652.
- [220] T. van Ritbergen and R. G. Stuart. „*Complete 2-loop quantum electrodynamic contributions to the muon lifetime in the Fermi model*“. Phys. Rev. Lett. 82 (1999), pp. 488–491. DOI: 10.1103/PhysRevLett.82.488. arXiv: hep-ph/9808283 [hep-ph].
- [221] T. van Ritbergen and R. G. Stuart. „*On the precise determination of the Fermi coupling constant from the muon lifetime*“. Nucl. Phys. B564 (2000), pp. 343–390. DOI: 10.1016/S0550-3213(99)00572-6. arXiv: hep-ph/9904240 [hep-ph].
- [222] M. Steinhauser and T. Seidensticker. „*Second order corrections to the muon lifetime and the semileptonic B decay*“. Phys. Lett. B467 (1999), pp. 271–278. DOI: 10.1016/S0370-2693(99)01168-5. arXiv: hep-ph/9909436 [hep-ph].
- [223] W. Hollik. „*Electroweak theory*“. In: „*5th Hellenic School and Workshops on Elementary Particle Physics (CORFU 1995) Corfu, Greece, September 3-24, 1995*“. 1995. arXiv: hep-ph/9602380 [hep-ph].
- [224] W. J. Marciano. „*The Weak Mixing Angle and Grand Unified Gauge Theories*“. Phys. Rev. D20 (1979), p. 274. DOI: 10.1103/PhysRevD.20.274.
- [225] A. Sirlin. „*On the $O(\alpha^2)$ Corrections to τ_μ , m_W , m_Z in the $SU(2)_L \times U(1)$ Theory*“. Phys. Rev. D29 (1984), p. 89. DOI: 10.1103/PhysRevD.29.89.
- [226] B. A. Kniehl and A. Sirlin. „*Dispersion relations for vacuum-polarization functions in electroweak physics*“. Nucl. Phys. B371 (1992), pp. 141–148. DOI: [http://dx.doi.org/10.1016/0550-3213\(92\)90232-Z](http://dx.doi.org/10.1016/0550-3213(92)90232-Z).

- [227] R. Boughezal, J. Tausk and J. van der Bij. „Three-loop electroweak corrections to the W -boson mass and $\sin^2 \theta_{\text{eff}}^{\text{lept}}$ in the large Higgs mass limit“. Nuclear Physics B 725.1–2 (2005), pp. 3–14. DOI: <http://dx.doi.org/10.1016/j.nuclphysb.2005.07.013>.
- [228] G. Weiglein. „Results for precision observables in the electroweak standard model at two-loop order and beyond“. Acta Phys. Polon. B29 (1998), pp. 2735–2741. arXiv: [hep-ph/9807222](https://arxiv.org/abs/hep-ph/9807222) [hep-ph].
- [229] A. Stremplatt. Diploma thesis. Univ. of Karlsruhe, 1998.
- [230] The ALEPH, DELPHI, L3, OPAL, SLD Collaborations, the LEP Electroweak Working Group, the SLD Electroweak and Heavy Flavour Groups. „Precision Electroweak Measurements on the Z Resonance“. Phys. Rept. 427 (2006), p. 257. arXiv: [hep-ex/0509008](https://arxiv.org/abs/hep-ex/0509008).
- [231] D. Bardin et al. „Electroweak working group report“. In: „Reports of the Working Group on precision calculations for the Z resonance“. Ed. by D. Y. Bardin, W. Hollik and G. Passarino. Geneva: CERN-95-03A, 1995, p. 7. arXiv: [hep-ph/9709229](https://arxiv.org/abs/hep-ph/9709229) [hep-ph].
- [232] D. Y. Bardin et al. „ZFITTER v.6.21: A Semianalytical program for fermion pair production in e^+e^- annihilation“. Comput. Phys. Commun. 133 (2001), pp. 229–395. DOI: [10.1016/S0010-4655\(00\)00152-1](https://doi.org/10.1016/S0010-4655(00)00152-1). arXiv: [hep-ph/9908433](https://arxiv.org/abs/hep-ph/9908433) [hep-ph].
- [233] A. B. Arbuzov et al. „ZFITTER: A Semi-analytical program for fermion pair production in e^+e^- annihilation, from version 6.21 to version 6.42“. Comput. Phys. Commun. 174 (2006), pp. 728–758. DOI: [10.1016/j.cpc.2005.12.009](https://doi.org/10.1016/j.cpc.2005.12.009). arXiv: [hep-ph/0507146](https://arxiv.org/abs/hep-ph/0507146) [hep-ph].
- [234] G. Montagna et al. „TOPAZ0 4.0: A New version of a computer program for evaluation of deconvoluted and realistic observables at LEP-1 and LEP-2“. Comput. Phys. Commun. 117 (1999), pp. 278–289. DOI: [10.1016/S0010-4655\(98\)00080-0](https://doi.org/10.1016/S0010-4655(98)00080-0). arXiv: [hep-ph/9804211](https://arxiv.org/abs/hep-ph/9804211) [hep-ph].
- [235] K. G. Chetyrkin, J. H. Kühn and A. Kwiatkowski. „QCD corrections to the e^+e^- cross-section and the Z boson decay rate“ (1996). [Phys. Rept.277,189(1996)]. DOI: [10.1016/S0370-1573\(96\)00012-9](https://doi.org/10.1016/S0370-1573(96)00012-9). arXiv: [hep-ph/9503396](https://arxiv.org/abs/hep-ph/9503396) [hep-ph].
- [236] A. L. Kataev. „Higher-order $O(\alpha^2)$ and $O(\alpha\alpha_s)$ corrections to $\sigma_{\text{tot}}(e^+e^- \rightarrow \text{hadrons})$ and Z -boson decay rate“. Physics Letters B 287.1–3 (1992), pp. 209–212. DOI: [http://dx.doi.org/10.1016/0370-2693\(92\)91901-K](http://dx.doi.org/10.1016/0370-2693(92)91901-K).
- [237] P. A. Baikov, K. G. Chetyrkin and J. H. Kühn. „Order α_s^4 QCD Corrections to Z and tau Decays“. Phys. Rev. Lett. 101 (2008), p. 012002. DOI: [10.1103/PhysRevLett.101.012002](https://doi.org/10.1103/PhysRevLett.101.012002). arXiv: [0801.1821](https://arxiv.org/abs/0801.1821) [hep-ph].
- [238] P. A. Baikov et al. „Complete $\mathcal{O}(\alpha_s^4)$ QCD Corrections to Hadronic Z -Decays“. Phys. Rev. Lett. 108 (2012), p. 222003. DOI: [10.1103/PhysRevLett.108.222003](https://doi.org/10.1103/PhysRevLett.108.222003). arXiv: [1201.5804](https://arxiv.org/abs/1201.5804) [hep-ph].
- [239] K. G. Chetyrkin, J. H. Kühn and M. Steinhauser. „RunDec: A Mathematica package for running and decoupling of the strong coupling and quark masses“. Comput. Phys. Commun. 133 (2000), pp. 43–65. DOI: [10.1016/S0010-4655\(00\)00155-7](https://doi.org/10.1016/S0010-4655(00)00155-7). arXiv: [hep-ph/0004189](https://arxiv.org/abs/hep-ph/0004189) [hep-ph].
- [240] M. Consoli, W. Hollik and F. Jegerlehner. „Electroweak Radiative Corrections for Z Physics“. In: „LEP Physics Workshop Geneva, Switzerland, February 20, 1989“. 1989, pp. 7–54.
- [241] A. Czarnecki and J. H. Kühn. „Nonfactorizable QCD and electroweak corrections to the hadronic Z boson decay rate“. Phys. Rev. Lett. 77 (1996), pp. 3955–3958. DOI: [10.1103/PhysRevLett.77.3955](https://doi.org/10.1103/PhysRevLett.77.3955). arXiv: [hep-ph/9608366](https://arxiv.org/abs/hep-ph/9608366) [hep-ph].
- [242] R. Harlander, T. Seidensticker and M. Steinhauser. „Complete corrections of $\mathcal{O}(\alpha\alpha_s)$ to the decay of the Z boson into bottom quarks“. Phys. Lett. B426 (1998), pp. 125–132. DOI: [10.1016/S0370-2693\(98\)00220-2](https://doi.org/10.1016/S0370-2693(98)00220-2). arXiv: [hep-ph/9712228](https://arxiv.org/abs/hep-ph/9712228) [hep-ph].
- [243] J. Fleischer et al. „Two-loop $O(\alpha_s G_\mu m_t^2)$ corrections to the partial decay width of the Z^0 into $b\bar{b}$ final states in the large top mass limit“. Phys. Lett. B293 (1992), pp. 437–444. DOI: [10.1016/0370-2693\(92\)90909-N](https://doi.org/10.1016/0370-2693(92)90909-N).

- [244] G. Buchalla and A. J. Buras. „*QCD corrections to the $\bar{s}dZ$ vertex for arbitrary top quark mass*“. Nucl. Phys. B398 (1993), pp. 285–300. DOI: 10.1016/0550-3213(93)90110-B.
- [245] G. Degrossi. „*Current algebra approach to heavy top effects in $Z \rightarrow b + \bar{b}$* “. Nucl. Phys. B407 (1993), pp. 271–289. DOI: 10.1016/0550-3213(93)90058-W. arXiv: hep-ph/9302288 [hep-ph].
- [246] K. G. Chetyrkin, A. Kwiatkowski and M. Steinhauser. „*Leading top mass corrections of order $O(\alpha_s m_t^2/M_W^2)$ to partial decay rate $\Gamma(Z \rightarrow b\bar{b})$* “. Mod. Phys. Lett. A8 (1993), pp. 2785–2792. DOI: 10.1142/S0217732393003172.
- [247] A. Sirlin. „*Radiative corrections in the $SU(2)_L \times U(1)$ theory: A simple renormalization framework*“. Phys. Rev. D 22 (4 1980), pp. 971–981. DOI: 10.1103/PhysRevD.22.971.
- [248] W. J. Marciano and A. Sirlin. „*Radiative corrections to neutrino-induced neutral-current phenomena in the $SU(2)_L \times U(1)$ theory*“. Phys. Rev. D 22 (11 1980), pp. 2695–2717. DOI: 10.1103/PhysRevD.22.2695.
- [249] P. Gambino and A. Sirlin. „*Relation between $\sin^2 \hat{\theta}_W(m_Z)$ and $\sin^2 \theta_{\text{eff}}^{\text{lept}}$* “. Phys. Rev. D 49 (3 1994), R1160–R1162. DOI: 10.1103/PhysRevD.49.R1160.
- [250] G. Degrossi and A. Sirlin. „*Comparative analysis of electroweak corrections to $e^+ + e^- \rightarrow f + \bar{f}$ in on-shell and \overline{MS} frameworks*“. Nuclear Physics B 352.2 (1991), pp. 342–366. DOI: [http://dx.doi.org/10.1016/0550-3213\(91\)90446-5](http://dx.doi.org/10.1016/0550-3213(91)90446-5).
- [251] M. Steinhauser. „*Leptonic contribution to the effective electromagnetic coupling constant up to three loops*“. Phys.Lett. B429 (1998), pp. 158–161. DOI: 10.1016/S0370-2693(98)00503-6. arXiv: hep-ph/9803313 [hep-ph].
- [252] F. Jegerlehner. „*Hadronic contributions to the photon vacuum polarization and their role in precision physics*“. J.Phys. G29 (2003), pp. 101–110. DOI: 10.1088/0954-3899/29/1/311. arXiv: hep-ph/0104304 [hep-ph].
- [253] D. de Florian et al. „*Handbook of LHC Higgs Cross Sections: 4. Deciphering the Nature of the Higgs Sector*“ (2016). DOI: 10.23731/CYRM-2017-002. arXiv: 1610.07922 [hep-ph].
- [254] D. Chang et al. „*Large two loop contributions to $g-2$ from a generic pseudoscalar boson*“. Phys. Rev. D63 (2001), p. 091301. DOI: 10.1103/PhysRevD.63.091301. arXiv: hep-ph/0009292 [hep-ph].
- [255] E. J. Chun and J. Kim. „*Leptonic Precision Test of Leptophilic Two-Higgs-Doublet Model*“. JHEP 07 (2016), p. 110. DOI: 10.1007/JHEP07(2016)110. arXiv: 1605.06298 [hep-ph].
- [256] H. E. Haber and O. Stål. „*New LHC benchmarks for the CP -conserving two-Higgs-doublet model*“. Eur. Phys. J. C75.10 (2015). [Erratum: Eur. Phys. J.C76,no.6,312(2016)], p. 491. DOI: 10.1140/epjc/s10052-015-3697-x, 10.1140/epjc/s10052-016-4151-4. arXiv: 1507.04281 [hep-ph].
- [257] F. Kling, J. M. No and S. Su. „*Anatomy of Exotic Higgs Decays in 2HDM*“. JHEP 09 (2016), p. 093. DOI: 10.1007/JHEP09(2016)093. arXiv: 1604.01406 [hep-ph].
- [258] V. Khachatryan et al. „*Search for neutral resonances decaying into a Z boson and a pair of b jets or τ leptons*“. Phys. Lett. B759 (2016), pp. 369–394. DOI: 10.1016/j.physletb.2016.05.087. arXiv: 1603.02991 [hep-ex].
- [259] P. A. R. Ade et al. „*Planck 2013 results. XVI. Cosmological parameters*“. Astron. Astrophys. 571 (2014), A16. DOI: 10.1051/0004-6361/201321591. arXiv: 1303.5076 [astro-ph.CO].
- [260] P. A. R. Ade et al. „*Planck 2015 results. XIII. Cosmological parameters*“. Astron. Astrophys. 594 (2016), A13. DOI: 10.1051/0004-6361/201525830. arXiv: 1502.01589 [astro-ph.CO].
- [261] A. Pierce and J. Thaler. „*Natural Dark Matter from an Unnatural Higgs Boson and New Colored Particles at the TeV Scale*“. JHEP 08 (2007), p. 026. DOI: 10.1088/1126-6708/2007/08/026. arXiv: hep-ph/0703056 [HEP-PH].

-
- [262] G. Aad et al. „Search for invisible decays of a Higgs boson using vector-boson fusion in pp collisions at $\sqrt{s} = 8$ TeV with the ATLAS detector“. JHEP 01 (2016), p. 172. DOI: 10.1007/JHEP01(2016)172. arXiv: 1508.07869 [hep-ex].
- [263] D. S. Akerib et al. „First results from the LUX dark matter experiment at the Sanford Underground Research Facility“. Phys. Rev. Lett. 112 (2014), p. 091303. DOI: 10.1103/PhysRevLett.112.091303. arXiv: 1310.8214 [astro-ph.CO].
- [264] M. Aaboud et al. „Measurement of the W -boson mass in pp collisions at $\sqrt{s} = 7$ TeV with the ATLAS detector“ (2017). arXiv: 1701.07240 [hep-ex].
- [265] R. Hawkings and K. Mönig. „Electroweak and CP violation physics at a linear collider Z factory“. Eur. Phys. J.direct 1 (1999), p. 8. DOI: 10.1007/s1010599c0008. arXiv: hep-ex/9910022 [hep-ex].
- [266] M. Baak et al. „Working Group Report: Precision Study of Electroweak Interactions“. In: „Proceedings, 2013 Community Summer Study on the Future of U.S. Particle Physics: Snowmass on the Mississippi (CSS2013): Minneapolis, MN, USA, July 29-August 6, 2013“. 2013. arXiv: 1310.6708 [hep-ph].
- [267] A. Arbey et al. „Physics at the e^+e^- Linear Collider“. Eur. Phys. J. C75 (2015). Ed. by G. Moortgat-Pick et al., p. 371. DOI: 10.1140/epjc/s10052-015-3511-9. arXiv: 1504.01726 [hep-ph].
- [268] S. Heinemeyer. „Zwei-Schleifen-Rechnungen im MSSM“. PhD thesis. Universität Karlsruhe, 1998.
- [269] K. G. Chetyrkin and F. V. Tkachov. „Integration by Parts: The Algorithm to Calculate beta Functions in 4 Loops“. Nucl. Phys. B192 (1981), pp. 159–204. DOI: 10.1016/0550-3213(81)90199-1.

Acknowledgements

First of all, I want to thank my supervisor Professor Hollik for his inestimable support. I am extremely grateful that he offered me the possibility to work on such an interesting topic in this prestigious institute. He left me plenty of freedom to conduct the research in my own way and has always been ready to give me an useful advice if I ran into problems. Furthermore, he gave me the opportunity to attend several schools and conferences, which I appreciated a lot.

I also want to thank Professor Ibarra, who agreed to be the second corrector, especially since he is currently on a sabbatical.

Furthermore, I am most grateful for the financial support from the Excellence Cluster *Structure and Origin of the Universe*.

There are several other people, which helped me in multiple ways.

I profited a lot from Thomas Hahn and his knowledge of computing. All of the results in this thesis were achieved with the help of his excellent tools. He advised me on the automation of my calculation and answered each of my numerous questions. His technical support of the IT system at the institute has also been indispensable. In addition, I have enjoyed all of the nice evenings he organized at his home.

Sebastain Paßehr helped me in various ways in the early stage of my thesis. He introduced me into the program `TwoCalc` and provided me with the analytic expressions for the loop integrals. He was always helpful when I had a question and invited me to his place when I was visiting Hamburg.

I benefited a lot from the discussions with Abdesslam Arhrib, especially from those about the Inert-Higgs-Doublet model. Furthermore, I want to thank him for proof-reading parts of this thesis.

I had always a nice time during the multiple visits of Castle Ringberg. It would have not been possible without the organization from Frank Steffen. I want to thank him furthermore for all the time he spends with the coordination of the IMPRS.

Cyril Pietsch and Henning Bahl provided a nice working atmosphere and many interesting discussions. I cannot think of any better office mates. My special thanks goes also to Henning for proof-reading this thesis.

Gudrun Heinrich helped me with the application at the institute for which I am very grateful, to.

I really enjoyed the lunch breaks and the interesting discussions with the various members of the Phenomenology group, that I have met during my stay at the institute. Therefore, I want to thank Johann-Felix, Uli, Johannes, Viktor, Stephen, Stefan, Gionata, Tom, Sophia, Nico, Jan, Anton, Matteo, Joao and Matthias.

The institute would not be the same place without the many people who work in the administration and were always helpful if I had any organizational problems. A special thank you goes to the secretaries of the theory department Anette Sturm, Sarah Fischer, Rosita Jurgeleit and Monika Goldammer. Moreover, I am very thankful to Jördis Scholz for all the help concerning my flat.

My last thanks go to my friends and family, who always reminded me of what is really important.